Université de Pau et des Pays de l'Adour

Faculté des Sciences et Techniques

Thèse

pour obtenir le grade de :

Docteur de l'Université de Pau et Pays de l'Adour

Discipline : Chimie-Physique

Spécialité : Chimie des Polymères

Présentée par :

Huda SFEIR

Macromolecular engineering to design latex particles by miniemulsion polymerization

Soutenue le 5 Mars 2014 à l'IPREM

Devant le jury composé de :

Pr. Alain DURAND	Université Nancy - INPL	Rapporteur
Pr. Daniel TATON	Université Bordeaux	Rapporteur
Dr. Muriel LANSALOT	CNRS, Université Claude Bernard Lyon	Examinateur
Dr. Maud SAVE	CNRS, Université de Pau et Pays de l'Adour	Co-directrice
Pr. Laurent BILLON	Université de Pau et Pays de l'Adour	Co-directeur
Dr. Leila GHANNAM	Université Libanaise	Co-encadrante

Acknowledgments

The work presented in this PhD was performed within the team “Equipe de Physique et de Chimie des Polymères” (EPCP) in the laboratory “Institut des Sciences Analytiques et de Physico-chimie pour l'Environnement et les Matériaux” (IPREM) of “Université de Pau et des Pays de l’Adour” (UPPA). First, I would like to thank Mr. Olivier Donard, director of the IPREM for hosting me in the laboratory within the three years of my PhD. I also thank the CNRS for making this PhD possible by the funding they provided.

My deepest gratitude and thanks for Dr. Maud Save, first for making this PhD possible by applying for the finance after my Master and believing in me to do the work. Second for her direction throughout the three years of my PhD. In know it was not easy, but for all the ups and downs you were always there for advices and direction. So thank you Maud for all the time you gave me, for all what you taught me and for not losing faith in my potentials.

I extend my thanks to Professor Laurent Billon, the co-director of my PhD, he was a great mentor and it was my honor to work under his supervision and acquire some of his wide knowledge. Thank you again Laurent for this chance and all the knowledge you gave me.

Another member who participated in supervising my work and I would like to thank is Leila Ghannam. Leila, you taught me before I embarked on the journey of earning a PhD, and ever since you were a great mentor whom I appreciate and will always respect. You always encouraged me when I was about to give up, so many thanks for you.

I also thank Professors Alain Durand and Daniel Taton for agreeing to judge this PhD work as reviewers, and Dr. Muriel Lansalot for her experts as an examiner during my defense.

My thanks to all the permanents of the EPCP team, for their help and support in the times when where needed some advices. Special thanks for Virginie Pellerin for all the microscopic analysis, and Abdel Khouh for his expert in NMR method. Thanks to Laura Etchenausia and M.H Alves for the help they offered during the last part of my PhD work.

A PhD is not just a work you do for three years, but it extends to become a life you live with certain people in the environment called “work place”. There you create many memories with colleagues and friends that will remain forever engraved in your memory. Being a stranger who came from a completely different country with different language and habits, I became quite well acquainted with all the people I met in my working area. I would like to thank the

people who made the working place a fun zone, and showed me the possibility of having fun even while performing a job. Thanks for all my friends in the laboratory, Hussein A., Laurence, Aurélie, Laura, Momo, Malu, and special thanks for Julien for being the friend who always made me laugh and who was always ready for any help. For the friends who left, Hussein M, Pierre E., Damien, thank you all.

I extend my thanks to my second Lebanese family in Pau, my friends who were always helpful when I needed, who reminded me of home and stood by my side. For all their support and help, I thank Hussein A, Mohamad A., Zeina, Nelly, Georgio. For the friends who stood by my side mentally despite of the distance, Ana, Oana, Ali S. Ali M.

To all the members of my family, thank you for having faith in me, and always supporting me to continue for higher degrees. Dad you were my inspiration, you were the person who always wanted me to my best, ever since I was a little girl you always pushed me to do better and pursue my dreams. Thank you for being my dad, for trusting that I can be a successful person.

Again Thank you all…

Abbreviations

AIBN	2,2’-azobis(isobutyronitrile)
APTMS	Aminopropyltrimethoxysilane
AGET	Activators generated by electron transfer
ATRA	Atom transfer radical addition
ATRP	Atom transfer radical polymerization
AFM	Atomic force microscopy
AA	Acrylic acid
ACPA	4,4’-azobis(4-cyanopentanoic acid)
BA	*n*-butyl acrylate
BB	Blocbuilder® alkoxyamine (Arkema)
CoMRP	Cobalt-mediated radical polymerization
CRP	Controlled radical polymerization
DMF	*N*,*N*-dimethylformamide
DLS	Dynamic light scattering
Dowfax	Mono- and dihexadecyl disulfonated diphenyloxide disodium salts
D_h	Hydrodynamic diameter
DBTTC	Dibenzyltrithio carbonate
DHM	6-Dimethyloct-7-ene-2-ol (dihydromyrcenol)
DCC	*N*-dicyclocarbodiimide
DMSO	Dimethyl sulfoxide
DPC	Dead polymer chains
EtOH	Ethanol

E_A	Activation energy
FT-IR	Fourier transform infrared
G_A	Grafting density of alkoxyamine onto silica surface
HF	Hydrofluoric acid
K_{eq}	Equilibrium rate constant
k_p	Propagation rate constant
MONAMS	*N*-tert-butyl-*N*-(1-diethylphosphono-2,2-dimethylpropyl) methyl propionate
$M_{n,\ exp}$	Experimental number-average molar mass
$M_{n,\ theo}$	Theoretical number-average molar mass
NMR	Nuclear magnetic resonance
NMP	Nitroxide mediated polymerization
NH_4OH	Ammonium hydroxide
N_p	Number of particles
$NaHCO_3$	Sodium hydrogen carbonate
PTSA	*para*-toluene sulfonic acid monohydrate
PS	Polystyrene
PBA	Poly(*n*-butyl acrylate)
PAA	Poly(acrylic acid)
PRE	Persistent radical effect
$P^{\bullet}$	Propagating radical
RAFT	Reversible addition-fragmentation chain transfer
RDRP	Reversible-deactivation radical polymerization
SEC	Size exclusion chromatography

S	Styrene
SG1	*N*-tert-butyl-*N*-(1-diethylphosphono-2,2-dimethylpropyl) nitroxide
SDS	Sodium dodecyl sulfate
SI-NMP	Surface initiated nitroxide mediated polymerization
SI-ATRP	Surface initiated atom transfer radical polymerization
SI-RAFT	Surface initiated reversible addition-fragmentation chain transfer
SI-CRP	Surface initiated controlled radical polymerization
S_{spe}	Specific surface area
TMS	Trimethylsilyl diazomethane
TMSPA	3-(Trimethoxysilyl)propyl acrylate
THG	Tetrahydrogeraniol
THF	Tetrahydrofuran
TGA	Theromogravemetric analysis
TEM	Transmission electron microscopy
TEOS	Tetraethyl orthosilicate
T	Temperature

Table of contents

General Introduction 01

Chapter 1 Bibiliographic section 04

Chapter 2 Synthesis of high molar mass polymer by NMP in mini(micro)emulsion 70

Chapter 3 Surface-initiated NMP in miniemulsion for the design of silica@core polymer shell nanoparticles 100

Chapter 4 Terpene based amphiphilic copolymers as stabilizers for Latex functionalization *via* styrene miniemulsion polymerization 134

General Conclusion 170

Analytical techniques 173

GENERAL INTRODUCTION

Radical polymerization in aqueous dispersed media is one of the most widely used industrial processes for the production of polymers as colloidal particles, so-called latex. From an engineering viewpoint, a water-based continuous phase favors heat transfer of the exothermic polymerization reaction and facilitates polymer recovery from the reactor as a fluid aqueous colloidal dispersion. Moreover, polymerization in aqueous dispersed media is an environmentally safe process, which fulfills one of the green chemistry principles by limiting the organic volatile compounds (VOC) inside the final product. Emulsion polymerization process, which starts in monomer-in-water emulsion containing a water-soluble radical initiator and a surfactant, is the most common process. In parallel, miniemulsion polymerization is another process performed in aqueous dispersed media with the monomer droplets acting as nanoreactors where the polymerization takes place. The interest of such droplet nucleation lies in the possibility to encapsulate hydrophobic species inside the latex particles by controlling its initial location in the organic phase during the emulsification step. The general purpose of this PhD work is to synthesize latex particles (= colloidal polymeric particles dispersed in water) by miniemulsion polymerization. The first part of this work will target the core of the latex particles by designing silica core @ polymer shell hybrid particles. The second part of this work is dedicated to the surface functionalization of the latex particles *via* amphiphilic polymeric stabilizers synthesized from renewable resources.

Organic/inorganic nanocomposites materials have been extensively studied for a long time, especially when they are composed of polymer composites with inorganic nanoscale building blocks. The interest in studying such materials is due to the new properties they exhibit allowing them to be used in diverse areas such as pharmaceuticals, cosmetics, optics, textiles coatings…. These new properties they exhibit are because of the combination between the advantages of the inorganic material (e.g. rigidity, thermal stability…) and those of the organic polymer (e.g. flexibility, dielectric, ductility…). Inorganic nanoscale building blocks include nanotubes, layered silicates (e.g., montmorillonite, saponite), nanoparticles of metals (e.g., Au, Ag), metal oxides (e.g., TiO_2, Al_2O_3), semiconductors (e.g., PbS, CdS), and so forth, among which SiO_2 is viewed as being very important. Among the inorganic materials, silica has proven to be of great interest due to its cheap, chemically inert and reinforcement properties, and the extensive applications in plastics, rubbers, coatings, etc. The synthesis of polymer/silica nanocomposites has attracted substantial academic and industrial interest and

more recently, several studies have been dedicated to the synthesis of such nanocomposites in aqueous dispersed media. Colloidal silica is a type of silica spherical in shape which can be synthesized on a wide range of size. Two methods can be used to graft polymer chains on silica particles. The first method is the 'grafting onto' method, where end-functionalized polymers react with the silica surface; the main drawback of this method is the final limited grafting densities. The second method is the 'grafting from' method, where chains grow up *in situ* from the surface. One of the main advantages of this method is that the initiator density at the surface can be controlled. The combination of this technique with a simultaneous growth of polymer chains by controlled radical polymerization (CRP) is able to produce dense polymeric layer (*ie*, high polymer grafting density) with controlled structural features. Nevertheless, it is worth noting that surface-initiated CRP has been mainly implemented in bulk or in organic solvent. Some issues are related to bulk polymerization such as a limited content of inorganic nanoparticles or to solvent polymerization to avoid inter-particles termination reactions but also difficulty to recover a highly viscous solution after polymerization. As mentioned above, polymerization in aqueous dispersed media has been a preferred polymerization process to produce industrially polymers by free radical polymerization.

Consequently, the first challenge of the present work was to transpose the synthesis of hybrid core@shell nanoparticles by surface-initiated CRP polymerization from bulk to aqueous dispersed media. Very few studies had previously reported such strategy and these syntheses involved Atom Transfer Radical Polymerization, mainly. The objective of the first part of this research work was to investigate the synthesis of core@shell nanoparticles in miniemulsion by surface-initiated Nitroxide-Mediated Polymerization (SI-NMP), a metal-free controlled radical polymerization method.

The second objective of the present work concerns the stabilization of the latex particles synthesized by miniemulsion polymerization using novel macromolecular stabilizers synthesized from renewable resources. Two issues are addressed by this part of the work: i) the replacement of conventional molecular surfactants by polymeric stabilizer can limit their diffusion in the environment while allowing the functionalization of the latex particle by surface coverage, ii) the reduction of fossil resources stimulate the increasing demand of renewable products. Surface-active products and amphiphilic polymers represent a class of materials with a wide range of applications, such as the stabilizing properties investigated in the present work.

The present manuscript will be divided into 4 chapters. The first chapter focuses on the bibliographic study concerning the aspects of controlled radical polymerization techniques, especially NMP, and the implementation of NMP in miniemulsion. We also summarized studies focusing on the synthesis of different organic/inorganic nanocomposite latexes synthesized *via* miniemulsion polymerization. Chapter 2 is dedicated to studying the kinetics of NMP miniemulsion upon targeting a high degree of polymerization under the experimental conditions imposed by the subsequent synthesis of core@shell particles by miniemulsion. In addition to the targeted high molar mass of the polymer, the novelty of chapter 2 in regards to the literature concerns the use of a different alkoxyamine containing both a hydrophilic carboxylic acid group and a C4 hydrophobic alkyl chain. Chapter 3 is first dedicated to the synthesis and initiator functionalization of silica particles of diameters in the range of 20-80 nm. The synthesis of both silica@PolyStyrene and silica@PolyButylAcrylate core@shell particles *via* SI-NMP miniemulsion was investigated by studying polymerization kinetics, features of the grafted polymer chains and location of silica particles. Chapter 4 focuses on the surface functionalization of polystyrene latex particles synthesized by miniemulsion polymerization using novel macromolecular stabilizers. The synthesis of the novel amphiphilic polymers involving renewable resources (dextran or poly(acrylic acid) as hydrophilic part and terpene units as hydrophobic part) will be described before to assess the stabilizing properties of these copolymers towards miniemulsion polymerization.

Chapter 1
Bibliographic section

1 Controlled radical polymerization (CRP) 5
1.1 Introduction 5
1.2 CRP (or) RDRP methods 6
1.2.1 Nitroxide mediated polymerization (NMP) 10
1.2.2 Atom transfer radical polymerization (ATRP) 11
1.2.3 Reversible addition-fragmentation chain transfer polymerization (RAFT) 12
1.2.4 Cobalt-mediated radical polymerization 13
1.3 Nitroxide mediated polymerization (NMP) 14
1.3.1 Nitroxides 15
1.3.2 Alkoxyamines 17
1.3.3 Persistent radical effect (PRE) 21
2 Miniemulsion polymerization 23
2.1 Generalities and mechanism 23
2.2 NMP in miniemulsion 27
2.3 Synthesis of composite latex by miniemulsion polymerization 34
3 Surface-initiated CRP from silica nanoparticles 40
3.1 Surface modification techniques 40
3.1.1 Grafting onto 41
3.1.2 Grafting through 41
3.1.3 Grafting from 42
3.2 SI-ATRP from silica nanoparticles 43
3.3 SI-RAFT from silica nanoparticles 46
3.4 SI-NMP from inorganic surfaces 49
3.4.1 Bi-component initiating system 50
3.4.2 In-situ synthesis of alkoxyamine at the surface of the silica 52
3.4.3 Mono-component initiating system 53
4 Conclusion 54
References 56

1 Controlled radical polymerization (CRP)

1.1 Introduction

Among all the different techniques of polymerization, conventional radical polymerization was the most widely used chain growth polymerization method at the industrial level, and academically studied due to the new techniques emerged during the last 20 years. Radical polymerization (RP) [1] as its name suggests is a method of polymerization by which a polymer is formed by successive addition of free radical chains onto a vinylic monomer. The life duration of the propagating radical is very short in comparison to the total duration of the polymerization process. RP consists of several simultaneous steps: initiation, propagation, termination and transfer (Scheme 1. 1). Such a situation inevitably leads to a large disparity in degrees of polymerization of different chains constituting a sample.

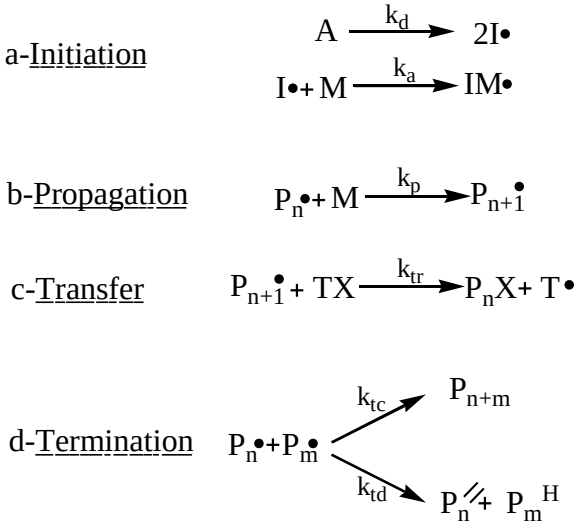

Scheme 1. 1: General mechanism of radical polymerization

Initiation, a key step of RP, allows the activation process by creating the necessary initiating radicals, that is the initial radical fragment. Although thermal initiation is most commonly used, one distinguishes also non-exhaustive ways, the redox or photochemical activation. The radical formed by decomposition of the initiator $I^{\bullet}$ (with decomposition rate constant k_d, Scheme 1. 1) is then capable of reacting with the double bond of a first monomer unit M to create the active center $IM^{\bullet}$ (with activation rate constant k_a, Scheme 1. 1). The propagation step is to ensure the growth of the polymer chains by successive addition of the active center $P_n^{\bullet}$ onto monomeric units (with propagation rate constant k_p Scheme 1. 1). In theory,

propagation is governed by the consumption of all monomer units available in the medium. In reality, it is not. In fact, due the high reactivity of the radicals, side reactions disrupt the propagation process: transfer and termination reactions. The disappearance of active centers is the step of termination. This reaction is produced by reaction between two radical chains $P_n^{\bullet}$ and $P_m^{\bullet}$, leading to the production of one or two dead chains. Indeed there are two types of termination reactions: combination or disproportionation (Scheme 1. 1). From a kinetic viewpoint, radical polymerization follows a steady-state, in that the concentration of radicals increases initially, but almost instantaneously reaches a constant, steady-state value. The rate of change of the concentration of radicals quickly becomes and remains zero during the course of the polymerization. This is equivalent to stating that the rates of initiation R_i and termination R_t of radicals are equal. One considers a transfer reaction with an active center $P_n^{\bullet}$ and another species of the reaction medium TX, on which the radical can be transferred (monomer, solvent, polymer, impurity ...). Growth of P_nX chain is then stopped, and the new active center $T^{\bullet}$ eventually leads to the growth of a new chain, depending on its ability to reinitiate.

RP is considered to present some valuable advantages, such as the ability to tolerate and adapt with the impurities presence in reagents and solvents unlike the ionic polymerization. Also, the range of reaction temperatures and the diversity of the monomers that can be used are quite large. Nevertheless, RP exhibits some limits, of which we can mention some considered the most noticed. The extreme reactivity of the carbon radicals result in many side termination or transfer reactions. The initiating radicals continuously formed throughout the reaction, and the very short lifetime of the propagating radicals (<1s) do not allow the control of polymer architecture and of molar mass distribution (no pure block copolymers can be obtained in RP).

Thus, due to the limits that RP showed, research studies evolved towards the techniques of controlled radical polymerization (CRP), now known as reversible-deactivation radical polymerization (RDRP) [2] as the IUPAC terminology recently recommended this term instead of CRP.

1.2 CRP (or) RDRP methods

The techniques of RDRP also known by “controlled living radical polymerization” rely completely on the small amount of termination reactions, which allows the control of molar mass and dispersity. Following developments in anionic polymerization by Michael Szwarc,[3]

precise control over polymeric structural parameters prepared by RDRP has given rise to a virtually unlimited number of new polymeric materials. [4]

The different techniques of RDRP are based on the same principle, the reversible-deactivation equilibrium established between the dormant and active propagating species (propagating radicals) (Scheme 1. 2). The equilibrium strongly shifts toward the dormant species, which allows them to promote their concentration (between 10^{-3} and 10^{-1} mol.L^{-1}) and to minimize the instantaneous concentration of radicals (between 10^{-9} and 10^{-7} mol.L^{-1}). Active species retain their reactivity in relation to monomer units, so that to provide successive chain growth. At the same time, the impact of secondary reactions of termination and/or transfer is considerably limited. [5-7]

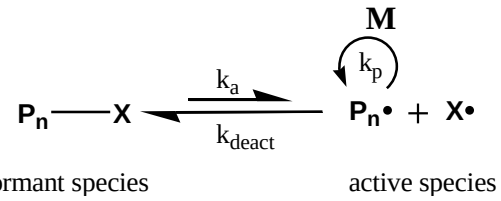

Scheme 1. 2: Reversible-deactivation equilibrium between active and dormant species in RDRP

When it first emerged RDRP had the term of living polymerization, which was first introduced by Szwarc, based on the fact that a living polymerization does not contain any irreversible reactions of transfer and/or termination. However, as the techniques of RDRP do not exclude completely the termination and irreversible reactions, IUPAC recommended not to use the term "living" anymore. Moreover, the strict definition of a living polymerization does not necessarily imply control of molar mass or a narrow molar mass distribution. To respect these last two conditions, two other criteria are considered:

- The initiation of the polymerization must be fast compared to propagation
- Exchange in the reversible-deactivation must be fast against the propagation.

A polymerization satisfying all these characteristics is considered "controlled".

-*Constant concentration of propagating radicals*

For a first order reaction, the logarithmic concentration of monomer should increase linearly with time. This is due to the negligible contribution of non-reversible termination, so that the concentration of the active propagating radical ([P$^{\cdot}$]) is constant (Scheme 1. 2).

$$R_p = \frac{-d[M]}{dt} = k_p[P^\bullet][M]$$

$$ln\frac{[M]_0}{[M]} = k_p[P^\bullet]t$$

With R_p the rate of propagation, k_p the propagation constant, [P·] the concentration of propagating radicals and [M] the concentration of the monomer.

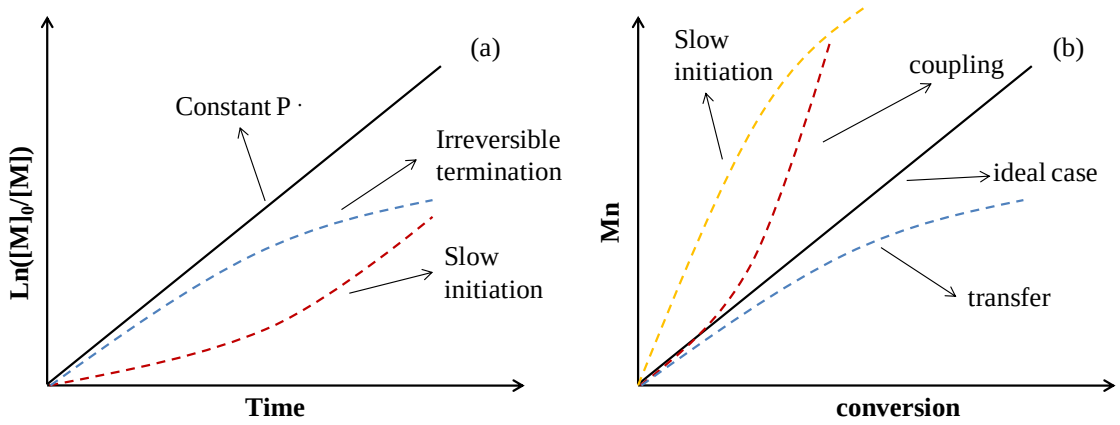

Figure 1. 1: Schematic representation of the effect of slow initiation and irreversible termination on the kinetics (a) and the number average molar mass with conversion (b) for CRP methods

An upward curvature in ln $[M]_0/[M]$ = f(t) curve indicates an increase in $[P^\bullet]$ with time, which occurs in case of slow initiation. Whereas a downward curvature suggests a decrease in $[P^\bullet]$ with time, which may result from termination reactions (Figure 1. 1a).

-Linear evolution of molar mass

In RDRP the number-average molar mass (M_n) is a linear function of monomer conversion. This result comes from maintaining a constant number of chains throughout the polymerization which requires the following two conditions (Figure 1. 1b):

1) Initiation should be sufficiently fast so that essentially all chains are propagating before the reaction is stopped.
2) An absence of irreversible chain transfer reactions that increases the total number of chains.

$$DP_n = \frac{M_n}{M_0} = \frac{\Delta[M]}{[I]_0} = \frac{[M]_0}{[I]_0} \times conversion$$

With DP_n the degree of polymerization, M_n the number-average molar mass, M_0 the molar mass of the monomer unit, $[I]_0$ the initial concentration of the initiator and $[M]_0$ the initial monomer concentration.

-Narrow molar mass distribution

In order to obtain a polymer with a narrow molar mass distribution, each of the following requirements should be fulfilled.

1) The rate of initiation is fast in comparison to the rate of propagation, allowing simultaneous growth of all the polymer chains.
2) The exchange between species involved in the equilibirum is fast in comparison with the rate of propagation.
3) Negligible irreversible chain transfer or termination.
4) The rate of depropagation is substantially lower than propagation which guarantees that the polymerization is essentially irreversible.

This distribution is characterized by the dispersity ($Đ=M_w/M_n$), with M_n the number-average molar mass and M_w the mass-average molar mass.

The evolution of Đ value obeys a Poisson law:

$$\frac{M_w}{M_n} = 1 + \frac{DP_n}{(1+DP_n)^2} \xrightarrow[DP_n \to \infty]{} 1$$

-Termination reactions

In RDRP the lifetime of a growing chain may exceed several hours, in contrast to less than 1 second for the propagating radicals in RP. Less than 10 % of the chains are terminated generally in an irreversible manner. This allows good control over the nature of the chain ends and possible re-initiation for synthesis of block copolymers.

Thus, for establishing an equilibrium between the dormant and active species, two strategies have been developed: reversible termination and reversible chain transfer. Among several techniques of RDRP, Nitroxide Mediated Polymerization (NMP) and Atom Transfer Radical Polymerization (ATRP) achieve control of polymerization through reversible termination reactions. In Reversible Addition-Fragmentation Chain Transfer (RAFT) the control of the polymerization is achieved through reversible chain transfer. Next to RAFT, once can also cite Iodine Transfer Polymerization (ITP) and Reversible Iodine Transfer Polymerization (RITP) as control is achieved by reversible chain transfer. [4]

1.2.1 Nitroxide mediated polymerization (NMP)

NMP first introduced by Georges et al. in 1993 [8] involves a nitroxide radical to establish the reversible deactivation equilibrium known in RDRP.

NMP is based on a reversible termination reaction established between the propagating radical of the growing chain and the nitroxide radical to form an alkoxyamine (dormant species) Scheme 1. 3. [9] The nitroxides $(R_1)(R_2)(N\text{-}O^{\cdot})$ are stable radicals, due to the relocation of the free electrons on the nitrogen and oxygen. The nitroxides are then well too stable to be able to couple each other or initiate polymerization. However, they are capable of coupling with much more reactive carbon radicals to form alkoxyamines. The C-O bond of the alkoxyamine may dissociate under the effect of temperature.

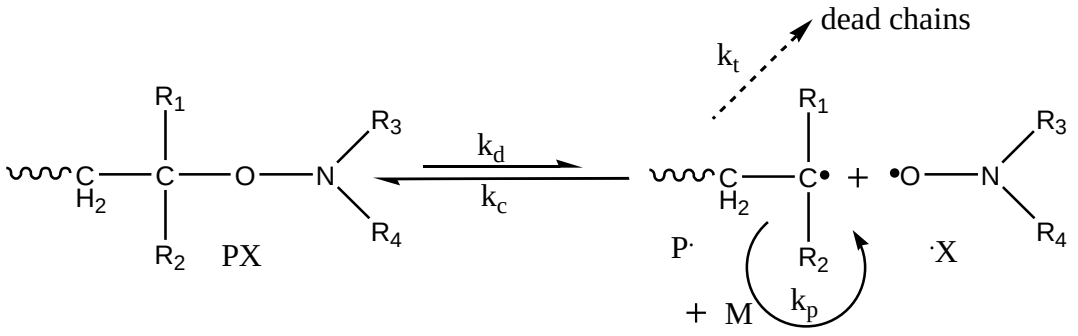

Scheme 1. 3: reversible-deactivation equilibrium in nitroxide mediated polymerization, with k_d dissociation rate constant, k_c recombination rate constant, k_p propagation rate constant and k_t termination rate constant

The reversible-deactivation equilibrium is characterized by the equilibrium constant K_{eq} (Equation 1. 1) represented as a function of concentration of deactivating nitroxide $[X^{\bullet}]$, the propagating radical $[P^{\bullet}]$ and the dormant alkoxyamine [PX] or as a function of rate constants k_d and k_c.

$$Keq = \frac{[P^{\bullet}][X^{\bullet}]}{[PX]} = \frac{k_d}{k_c}$$

Equation 1. 1: Equilibrium constant expression

More details about NMP concerning nitroxides, alkoxyamines will be discussed later in part 1.3.

1.2.2 Atom transfer radical polymerization (ATRP)

ATRP was first introduced in 1995 by Matyjaszewski [10] and Sawamoto [11], it is originally derived from the reaction of organic chemistry reaction called atom transfer radical addition (ATRA)[12]. It is based on the reversible redox equilibrium between organometallic complexes in the presence of radicals. Like NMP, ATRP is based on a reversible termination process (Scheme 1. 4).

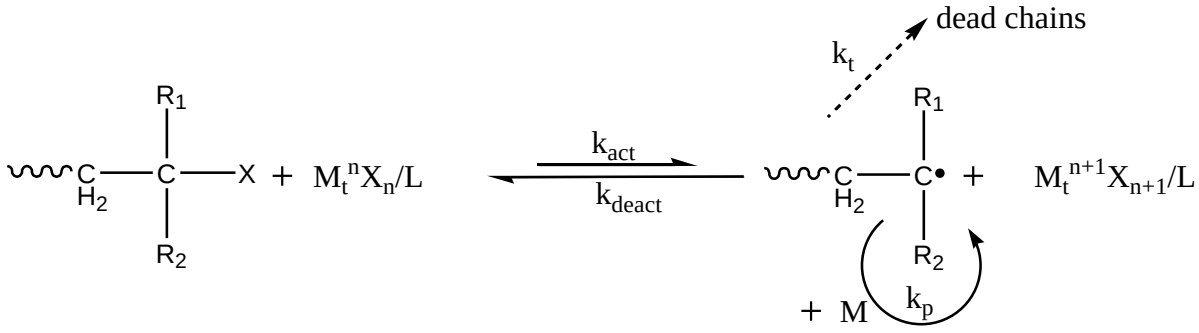

Scheme 1. 4: Principle of ATRP

ATRP relies on the transfer of a halide atom from a catalyst/ligand complex to a propagating macroradical. The initiation of this polymerization is carried out by reacting a halogenated derivative with the metal complex. This results in a transfer of the halogen of the first to the second. This leads to the formation of a carbon radical which can then react with a few monomer units (active species) and form a propagating radical, which quickly recovers its halogen (dormant species). At the same time, the metal (M_t) complex receiving halogen passes temporarily to higher oxidation level, "n+1" in Scheme 1. 4, before returning to its initial oxidation degree "n" when the halogen is recovered by the carbon radical.

A wide variety of monomers can be polymerized in ATRP [13] (styrene, (meth) acrylates, acrylonitrile …). Like any experimental technique, ATRP has a disadvantage in the presence of metal catalyst or amine-based ligands, which should be removed to approach certain areas of application.

Three types of ATRP are known [4]. The first called "direct ATRP" provides the initiation of the polymerization by an alkyl halide and catalyst in the form M^n/L, while the second, the "reverse ATRP" uses a conventional radical polymerization initiator and catalyst in its oxidized highest state M^{n+1}/L. The advantage of reverse ATRP is the use of M^{n+1}/L complex,

less sensitive to oxidation, but the advantage of direct ATRP is the better control of initiator efficiency. Finally, a third technique takes advantage of the previous two as observed recently: the AGET-ATRP (ATRP Using Activators Generated by Electron Transfer) based on the in-situ creation of activating complex (M_t^n/L) starting from a reducing complex M_t^{n+1}/ligand complex and a reducing agent (Tin(II)2-ethyl hexanoate ascorbic acid) in combination with a halogen (Scheme 1. 5). This technique (AGET-ATRP) allows to drastically reduce the amount of copper catalyst. [14, 15]

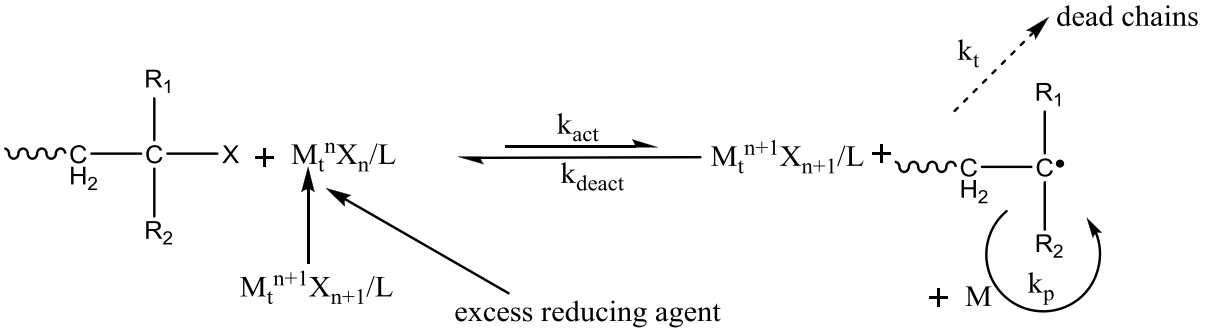

Scheme 1. 5: Principle of AGET-ATRP[14]

1.2.3 Reversible addition-fragmentation chain transfer polymerization (RAFT)

Unlike the previous two RDRP techniques, NMP and ATRP that depend on reversible-deactivation equilibrium provided by reversible termination, RAFT depends on an reversible-deactivation equilibrium provided by reversible chain transfer. It was first reported by in 1998. [16, 17] It requires the use of a conventional radical initiator continuously generating new radicals in the reaction medium and a steady state is established as in conventional radical polymerization.

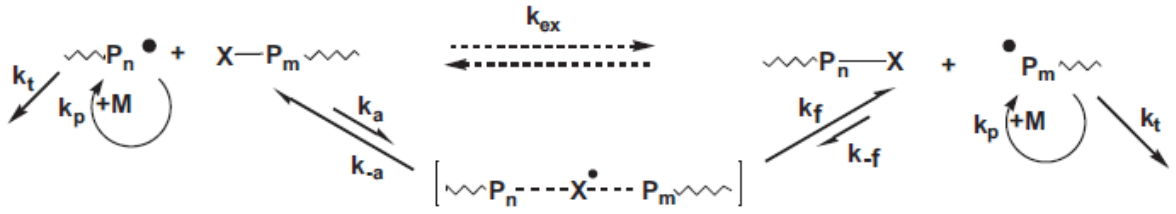

Scheme 1. 6: Principle scheme of RAFT [4]

RAFT is based on addition-fragmentation reaction using a thiocarbonylthio transfer agent (or RAFT agent) by bimolecular reaction between dormant chains and active chains (Scheme 1. 6). [18, 19] This technique allows to control the polymerization of a wide range of monomers as

styrene, acrylates, methacrylates, (meth)acrylic acid, (meth)acrylamide, vinylic ester, and vinylpyridine obtaining various systems: homopolymers, copolymers (diblock, triblock, gradient, star ...).

1.2.4 Cobalt-mediated radical polymerization

The first controlled radical polymerization using cobalt complexes was reported by Wayland et al.[20] and Harwood et al. [21]. Most notably it allows CRP of a broad substrate scope (among others acrylates, acrylic acid, vinyl esters, vinyl acetate, acrylonitrile, vinylamides (vinylpyrrolidone, vinylcaprolactam)) under various reaction conditions, and gives access to very fast RDRP reactions with rates approaching those of conventional uncontrolled free radical polymerization reactions. CMRP [22] offers an advantage over the other RDRP methods in the controlled polymerization of vinyl acetate. Indeed the control of this class of monomer is not straight forward by RDRP techniques which has long been a challenge for RDRP because of the high reactivity of the propagating radical, resulting from the lack of stabilizing groups. Before the first example of CMRP of vinyl acetate which was reported in 2005 by Jérome et al.[23], very few systems proved able to mediate the radical polymerization of this monomer RAFT using dithiocarbamates [24] or xanthates. [25, 26] Most commonly applied cobalt compounds are cobaloximes, cobalt porphyrins and cobalt(II) acetylacetonate $Co(acac)_2$ derivatives, used in combination with various radical initiators.

In many cases, CMRP exploits the weak cobalt(III)-carbon bond to control the radical polymerization reaction. The Co-C bond containing radical initiator easily breaks up (by heat or by light) in a carbon free radical and a cobalt(II) radical species. The carbon radical starts the growth of a polymer chain from the CH_2=CHX monomer as in a free radical polymerization reaction. Cobalt is unusual in that it can reversibly reform a covalent bond with the carbon radical terminus of the growing chain. This reduces the concentration of radicals to a minimum and thereby minimizes undesirable termination reactions by recombination of two carbon radicals. The cobalt trapping reagent is called a persistent radical and the cobalt-capped polymer chain is said to be dormant. This mechanism is called reversible termination (Scheme 1. 7) and is said to operate via the "persistent radical effect".[22] When the monomer lacks protons that can be easily abstracted by the cobalt radical, catalytic chain transfer is also limited and the RP reaction becomes close to ‘living’.

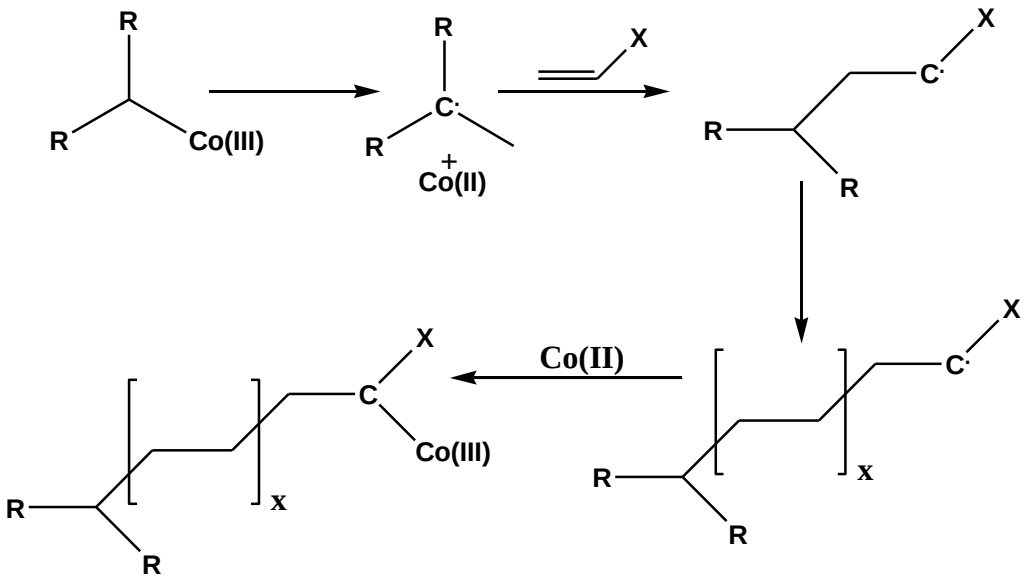

Scheme 1. 7: CMRP via reversible termination

A recent review about CMRP including the recent achievements using this technique of RDRP, was done by Debuigne et al.[27].

In conclusion most of previously mentioned techniques (NMP, ATRP, RAFT and CMRP) have been carried out in homogeneous media (bulk, solvent) but we should mention that the implementation of RDRP techniques in aqueous dispersed media has been the subject or recent developments. [28, 29] More precisely in emulsion we can find several examples for NMP [30-32], reverse ATRP [33], AGET-ATRP [34], ITP [35], RITP [36] and RAFT polymerization [37-40]. Also in miniemulsion we find examples for NMP [41-43], ATRP [34], CMRP [44] and ITP polymerization [35, 45].

1.3 Nitroxide mediated polymerization (NMP)

NMP was originally initiated by a bicomponent pathway, comprising benzoyl peroxide (BPO) as a conventional thermal initiator in combination with 2,2,6,6-tetramethylpiperidinyl-1-oxy (TEMPO, Scheme 1. 8) as the stable free nitroxide. [8] This system has the advantage to use conventional radical polymerization processes with the only addition of free nitroxides, which can be also highly desirable from both economic and practical points of view. Fine-tuning the $[nitroxide]_0/[initiator]_0$ ratio is of high importance since the kinetics of the polymerization is governed by the amount of nitroxide in excess present after the initiation step. As a consequence of a high excess of free nitroxide, the reversible-deactivation equilibrium is shifted toward dormant species, which decreases the polymerization rate. All thermal

initiators suffer from the difficulty to determine precisely the efficiency of the primary radicals produced by thermal decomposition to induce the polymerization (for instance due to cage effect and induced decomposition) and also the nature of the initiating group since the majority of these primary radicals undergo rearrangement or fragmentation reactions. This usually leads to poorly reproducible polymerization kinetics and to ill-defined polymer end-groups.

However, to circumvent this issue, the group of Hawker [46, 47] developed the concept of mono-component initiator that decomposes into both the initiating radical and the nitroxide. This compound, originally termed monocomponent, is called alkoxyamine initiator. Due to its particular structure, it leads, after dissociation, to a 1:1 release of initiating radical:nitroxide. Interestingly, the structure of the initiating end-group can be tuned to perform advanced macromolecular synthesis or post-modification chemistry. Experimentally, it was observed that mono component initiators led to a better control over molar masses and molar mass distributions than bimolecular initiating systems [47].

1.3.1 Nitroxides

Many nitroxides were tested in controlled radical polymerization in homogeneous media (Scheme 1. 8). Solomon, Rizzardo and Moad were the first to note that at temperatures between 40 °C and 60 °C, nitroxides such as TEMPO (2,2,6,6-tetramethyl-1-pipieridinyloxy) (N1, Scheme 1. 8) can react with carbon radicals issued from an initiator and a vinyl monomer and act as radical traps [48, 49]. Despite of their promising work, it was Georges who was the first to propose in 1993 a system of NMP allowing to control the polymerization of styrene at 130 °C initiated by benzoyl peroxide in the presence of TEMPO as controlling agent [8]. However, TEMPO is not the ideal control agent for NMP due to two main reasons. The stability of the polystyryl-TEMPO alkoxyamines (equilibrium constant is very low K_{eq}= 1.5 $\times 10^{-11}$ mol.L^{-1} at 120 °C) [50] requires the polymerization to be conducted at high temperatures (> 130 °C) for long duration (> 24h). In NMP, the equilibrium constant K_{eq} is generally very small, so low in the presence of TEMPO, that the equilibrium becomes very strongly shifted towards the dormant species and significantly reduces the polymerization rate. Thus, only styrenic monomers can be effectively controlled by TEMPO, as acrylates exhibit a lower equilibrium constant than styrene.

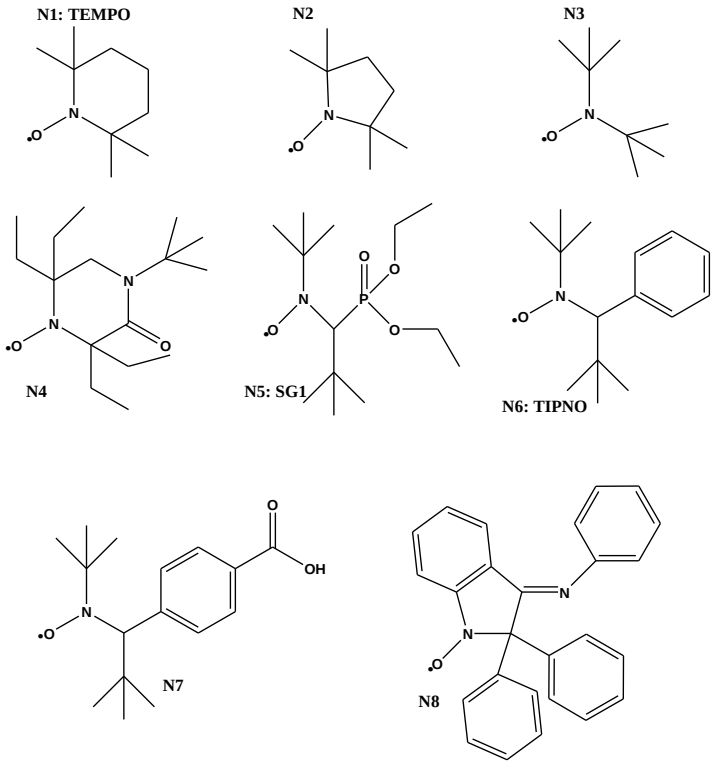

Scheme 1. 8: Main nitroxides used in NMP [51]

Therefore, to reduce the reaction time and improve the control, several research teams focused on the synthesis of new nitroxides, such as PROXYL derivative (N2) and then di-tert-butylnitroxyde derivative (N3) (Scheme 1. 8). However, no improvements were achieved, as the results remained similar to those of TEMPO, which does not allow considering NMP as an effective alternative to other CRP techniques.

A breakthrough in NMP was the development of new acyclic nitroxides with a structure completely different from that of TEMPO. In particular, they have a hydrogen atom on the carbon in α position to the nitrogen, whose function is to modulate the chemical stability. Team of Tordo [52, 53] introduced the SG1 nitroxide (*N*-tert-butyl-*N*-[1-diethylphosphono (2,2 -dimethylpropyl)] nitroxide, N5) and Hawker [54] operated TIPNO (*N*- tert-butyl-*N*-[1-phenyl-2-(methylpropyl)] nitroxide, N6). The team of Studer described the synthesis of a new TEMPO based nitroxide [55, 56] (N4), which helped to control the polymerization of styrene and n-butyl acrylate in bulk at 105 °C, or that of N-isopropylacrylamide [57]. The use of these new nitroxides allowed control of the polymerization of styrene but also new monomer families other than styrene.[58] Where TIPNO assured the control of the polymerization of 1,3-dienes [59], acrylamides [60], acrylonitrile or thermosensitive polymers based on acrylate or styrene [61, 62] while SG1 controlled polymerization of acrylic acid [63, 64], N,N-dimethylacrylamide [60, 65, 66]

and also styrene sodium sulfonate in solution in water [67]. Hydrosoluble nitroxides derived from TIPNO (N7) allowed the control of polymerization of styrene sodium sulfonate in solution in water at 95 °C [68], in addition to the monomer 4-vinylpyridine which was polymerized by NMP. [69-72]

Still, the polymerization of methacrylates remained a challenge, even when using the nitroxide SG1. This can be explained by two reasons: the reversible-deactivation equilibrium constant is very elevated [73] leading to high concentrations of propagating macroradicals, which cause irreversible termination reactions, and the presence of side reactions of abstraction of hydrogen on propagating radical [74, 75]. Recently, the team of Charleux controlled polymerization of methyl methacrylate with SG1, by adding a small amount of styrene (<10 mol %), in order to decrease the value of the reversible-deactivation equilibrium constant [76, 77] . This result was later extended to the polymerization of methacrylic derivatives such as poly (ethylene oxide), methacrylate [78] or methacrylic acid [79]. Meanwhile, the team of Bertin proposed a new nitroxide the DPAIO (N8) to control the homopolymerization of methyl methacrylate [80]. With this nitroxide, the reversible-deactivation equilibrium constant is much lower. This feature which is an advantage for methyl methacrylate, becomes an obstacle to the polymerization of other monomer families such as styrene, acrylates or acrylamides.

1.3.2 Alkoxyamines

The development of new alkoxyamines has become crucial for controlling polymerization and the final properties of the polymer (in particular the chain ends). Changing the initiator fragment or nitroxide can modulate the properties of the studied alkoxyamine. The exploitation of alkoxyamines was originally limited by a lack of efficient synthetic procedures for their preparation, procedures which often resulted in low yields and a wide range of byproducts.[46, 47, 54, 58, 77, 81, 82] However, several versatile techniques have since been developed. Alkoxyamine is characterized by its dissociation rate constant k_d, which obeys the Arrhenius law ($k_d = Ae^{\frac{-E_{a,d}}{RT}}$), and depends on the dissociation activation energy $E_{a,d}$ of the C-ON bond. Characteristics of alkoxyamines derived from the same styryl initiator fragment are totally different depending on the selected nitroxide group, styryl-TEMPO (A1), styryl-TIPNO (A2) or styryl-SG1 (A3), described in Scheme 1. 9. These characteristics are summarized in Table 1. 1 below [52, 81, 83-85]. The activation energy of the dissociation of the C-ON bond is the highest for the alkoxyamine styryl-TEMPO. NMP of styrene may therefore be

performed at lower temperatures in the presence of SG1 (115 °C) than in the presence of TEMPO, and at similar temperature the dissociation rate constant is higher in the presence of SG1. Thus, the rate of polymerization of styrene is higher in the presence of SG1.

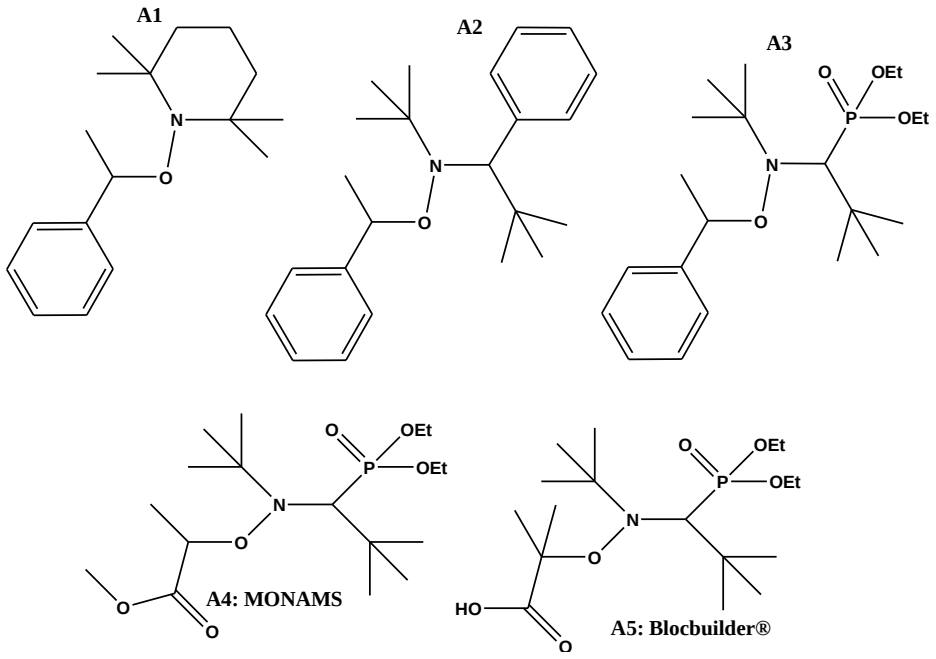

Scheme 1. 9: Important alkoxyamines used in NMP [51]

Table 1. 1: Influence of the nitroxide fragment on the activation energy $E_{a,d}$, the rate dissociation constant k_d, the half-life $t_{1/2}$ and the equilibrium constant K_{eq} at 120 °C for alkoxyamines based on styryl initiator fragment [83-85]

Alkoxyamine	Nitroxide	$E_{a,d}$ (KJ. moL^{-1})	k_d (s^{-1})	$t^{1/2}$ (min)
A1 styryl-TEMPO	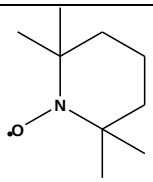	132.9	5.2×10^{-4}	22.2
A2 styryl-TIPNO	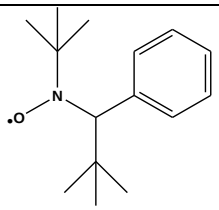	127.1	3.1×10^{-3}	3.7
A3 styryl-SG1	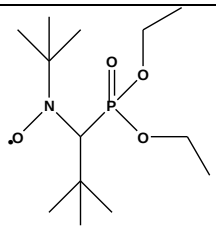	125.5	5.0×10^{-3}	2.3

SG1 based alkoxyamines

For more than fifteen years, several alkoxyamines were developed from the SG1 nitroxide. The organosoluble alkoxyamine MONAMS (A4) was first used for the bulk polymerization or miniemulsion polymerization of styrene [86] and *n*-butyl acrylate. [87] However, the addition of an excess of free SG1 (<10 mol %) is required to control the polymerization of acrylic monomers [63], which have a high propagation rate constant and a low equilibrium constant K_{eq} (few SG1 released by persistent radical effect explained later in 1.3.3). The team of Bertin and Tordo then developed more encountered [88] alkoxyamines whose radical from the initiator fragment is more stable. The most notable is the alkoxyamine BB (A5), later marketed under the name BlocBuilder® by Arkema. Because of steric hindrance, the value of the dissociation energy of the C-ON bond of BlocBuilder® is low, because the carbon radical formed during dissociation is tertiary and stable, hence the value of k_d is high (k_d, 115 °C= 0.35 s^{-1}). Accordingly, the dissociation temperature of BlocBuilder® (35 °C) is considerably lower than that of MONAMS. The persistent radical effect is so quickly established, even in the presence of monomer with high propagation rate. In addition, the BlocBuilder® is soluble in basic pH, which resulted in the successful implementation of NMP in emulsion. [32, 89]

New functional alkoxyamines have been developed, not to improve the control of the polymerization by creating new nitroxides, but rather to meet the target applications for polymers.

A primary way to synthesize functional alkoxyamine is to take advantage of the reactivity of the alkoxyamine BlocBuilder®, its 1,2 addition to an activated olefin to produce a second generation alkoxyamine with a dissociation temperature much higher than that of the BlocBuilder®. A review of Gigmes on intermolecular 1,2 addition of BlocBuilder® alkoxyamine onto activated olefins gathers the range of novel synthesized alkoxyamines. [90] The reaction occurs at moderate temperature following the reaction scheme below (Scheme 1. 10). At this temperature, the secondary alkoxyamine is stable, and the difference in reactivity between the two alkoxyamines prevents olefin polymerization. For instance, using this strategy allows the synthesis of di-functional hydrosoluble alkoxyamine [89]. Tri- and tetra-functional alkoxyamines precursors of star polymers were obtained. [91, 92] Synthesis of triethoxysilane based alkoxyamine for polymer grafting from either dense silica [93] or from ordered mesoporous silica. [94]

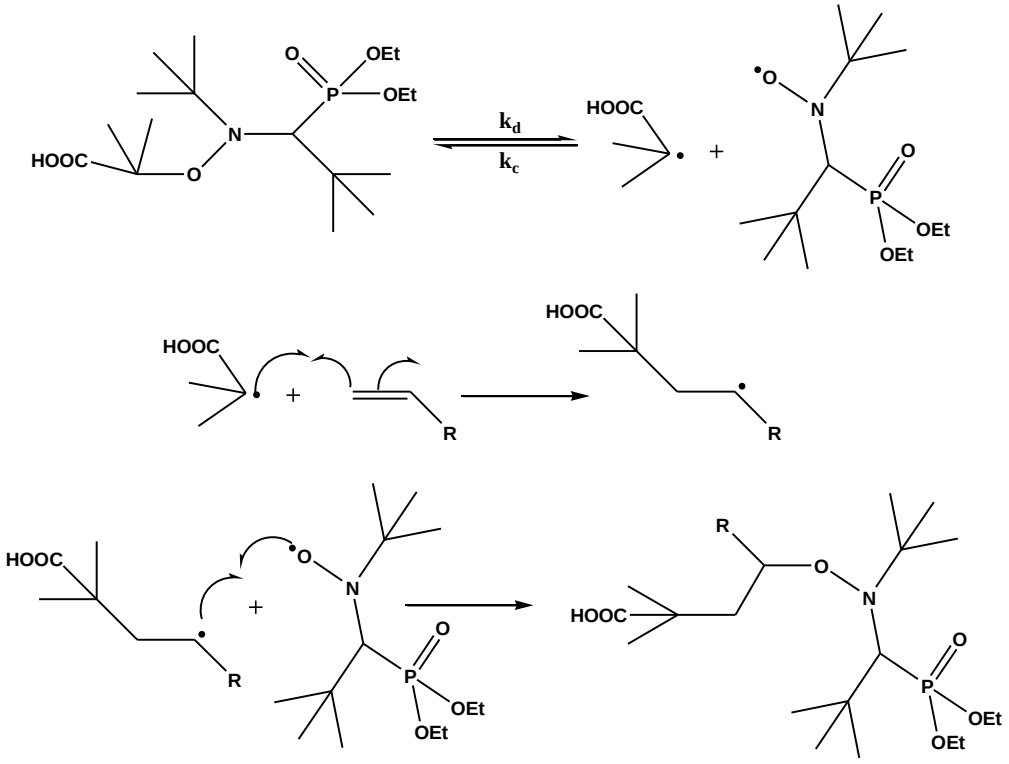

Scheme 1. 10: reactional scheme of 1,2 addition of BlocBuilder® onto activated olefins

In the literature, alkoxyamines based on TEMPO or TIPNO were modified by introducing functionality on either the initiator fragment or the nitroxide fragment. The α or ω ends of the polymer are then available for post-functionalization reactions or grafting. Thus, the teams of Hawker [95] and Braslau [96] proposed alkoxyamines based on TIPNO carrying a chlorine or a primary amine that can be used for coupling to proteins or chromophores. More recently, the popularity of "click chemistry" has led to the development of alkoxyamines bearing alkyne or azide groups on the initiator fragment [96, 97].

Few alkoxyamines are functionalized with a carboxylic acid group (displayed in Scheme 1. 9) as this function has many advantages. The A5 BlocBuilder® (Scheme 1. 9) and the A7 alkoxyamine (Scheme 1. 11) exploit the properties of solubility in water conferred by the carboxylic acid. [31] Meanwhile, the team of Braslau provides α,ω-functionalized polystyrene or poly(tert-butyl acrylate) using the A9 and A8 alkoxyamines (Scheme 1. 11). [98] Vinas et al. proposed a very performing alkoxyamine derived from BlocBuilder®, the BB-NHS (A6), after the activation of the carboxylic acid on the BlocBuilder® driven by the N-hydroxysuccinimide.[99] A peptide coupling following activation with N-hydroxysuccinimide of BlocBuilder® allows the grafting of polymers onto lysozymes where the synthesis of

amino-functionalized SG1-based alkoxyamine for polymer peptide conjugates was reported by Gigmes et al. [100]. The grafting of polymers onto aminated silica surfaces was possible thanks to the use of BB-NHS alkoxyamine. [101-104]

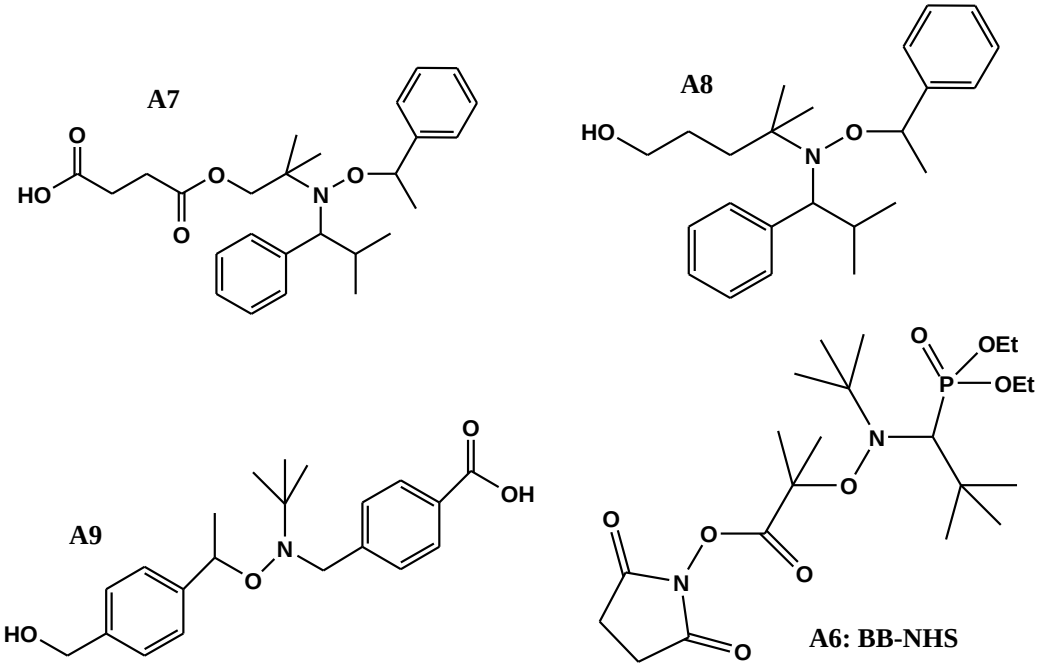

Scheme 1. 11: Examples of functional alkoxyamines; A7 [105], A8 and A9 [98] and A6 [99]

1.3.3 Persistent radical effect (PRE)

Also known as Fischer effect [6, 7, 106], it occurs in the RDRP systems based on reversible termination reaction between dormant and active species, such as NMP or ATRP. In the early stages of the polymerization, the propagating radicals can either be reversibly trapped by deactivating agent (nitroxide or copper (II)) or undergo irreversible termination reaction. However, as mentioned by Fischer, deactivating agents (persistent radicals) do not terminate, thus they cannot undergo irreversible termination reaction. Hence, the concentration of the persistent radicals progressively increases with the reaction time, shifting the equilibrium toward the dormant species. In some cases where the equilibrium constant K_{eq} is low, only a small amount of persistent radicals is produced. Thus, an excess of free deactivating agent is introduced at the beginning of the polymerization to insure good control.

PRE can be qualitatively explained as follows (Figure 1. 2). We consider a compound (RY) that decomposes into a transient (R•) and a persistent radical (Y•), with the initial concentration of radicals equals zero. At the beginning of the reaction, the concentrations of

both radical species increase linearly with time, as governed by the decomposition rate constant k_d. This period (the pre-equilibrium regime) lasts until the total radical concentration becomes large enough so that the radical species could react by bimolecular reaction (either self-termination between R• or recombination between R• and Y•). The irreversible self-termination leads to a decrease of the concentration of R• and consequently to a slow accumulation of the persistent species Y• (which cannot self-terminate).

$$R{-}Y \xrightarrow{k_d} R^{\bullet} + Y^{\bullet}$$
$$R^{\bullet} + Y^{\bullet} \xrightarrow{k_c} R{-}Y$$
$$R^{\bullet} + R^{\bullet} \xrightarrow{k_t} R{-}R$$

Therefore, the recombination of transient and persistent radicals becomes more and more favored compared to the self-reaction, which inhibits itself as it proceeds, although it never completely ceases. This is the intermediate regime. Then, after a long reaction time, the concentration of transient radicals drops to zero and the persistent radical reaches its highest concentration, which corresponds to the initial RY concentration. Two different theoretical analyses performed in parallel by Fischer and Fukuda led to the same two unusual rate laws (Equation 1. 2 and Equation 1. 3) for R• and Y• during the intermediate regime (Figure 1. 2a).

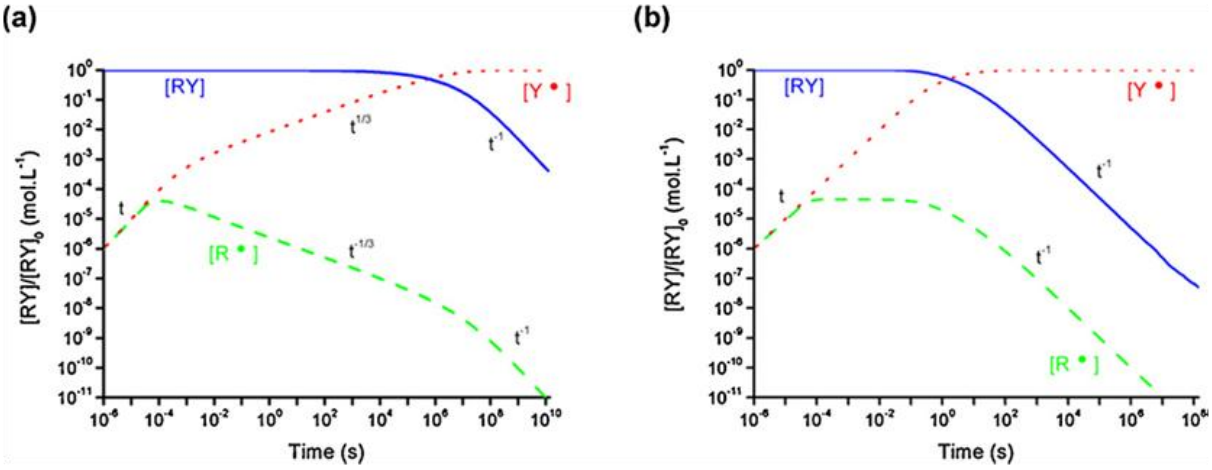

Figure 1. 2: Concentrations of RY, Y• and R• vs. time in a double logarithmic plot with $[RY]_0 = 5.0 \times 10^{-2}$ M, $k_d = 10^{-2}$ s^{-1}, $k_t = 108$ M^{-1} s^{-1}, $k_c = 10^7$ M^{-1} s^{-1} (a) and $k_c = 10^4$ M^{-1} s^{-1} (b). [7]

Equation 1. 2: $$[\mathbf{Y}\bullet] = \left(\frac{3k_t k_d^2 [RY]_0^2}{k_c^2}\right)^{1/3} t^{1/3}$$

Equation 1. 3: $$[\mathbf{R}\bullet] = \left(\frac{k_d [RY]_0}{3k_t k_c}\right)^{1/3} t^{-1/3}$$

Equation 1. 4: $$k_c[\mathbf{R}\bullet][\mathbf{Y}\bullet] = k_d[RY]_0$$

Equation 1. 5: $$\frac{k_d}{k_c} = K < \frac{[RY]_0 k_c}{4k_t}$$

The combination of Equation 1. 2 and Equation 1. 3 conducts to Equation 1. 4, showing that an equilibrium is set up even if the radical concentrations are different, with [Y•] being much larger than [R•]. Nevertheless, the equilibrium exists providing K obeys to Equation 1. 5. In case this requirement is not fulfilled, the cross reaction between the transient and the persistent radicals is not favored and Y• behaves as a spectator, meaning that [R•] reaches a steady state (similarly as with a conventional thermal initiator) and [Y•] still linearly increases with time to reach $[RY]_0$ (Figure 1. 2b). If Equation 1. 5 is satisfied, the lifetime of RY is then drastically prolonged compared with a classic irreversible first order kinetic decomposition (occurring if a radical scavenger such as oxygen is present in the medium). When conditions for Equation 1. 5 are not met (for instance when $k_c = 1.0\times10^4$ instead of 1.0×10^7 $M^{-1}s^{-1}$), the degradation of RY is very fast; of about 10 s compared to 10^5 s if Equation 1. 5 is fulfilled (Figure 1. 2b). [7]

2 Miniemulsion polymerization

2.1 Generalities and mechanism

A miniemulsion polymerization is a special case of emulsion polymerization which was studied by Smith and Ewart. [107] In emulsion, a hydrophobic monomer is dispersed or emulsified in a solution of surfactant and water forming relatively large droplets of monomer in water phase. Excess surfactant creates micelles in the water, if their concentration is higher than critical micelle concentration (CMC). A water-soluble initiator is introduced into the water phase where it reacts with the fraction of monomer soluble in water. The oligoradicals enter the monomer-swollen micelles where the polymerization takes place fed by monomer diffusion from the monomer droplet to the loci of polymerization through water phase. This is considered Smith-Ewart Interval 1. The total surface area of the micelles is much greater than the total surface area of the fewer, larger monomer droplets; therefore the fate of the oligoradicals is to enter the micelles rather than the large monomer droplets. At this point the monomer-swollen micelle has turned into a polymer particle. When both monomer droplets and polymer particles are present in the system, this is considered Smith-Ewart Interval 2. Monomer from the droplets diffuses to the growing particles. When monomer droplets disappear and all remaining monomer is located in the particles, it is considered Smith-Ewart Interval 3. The described nucleation mechanism was named “micelles nucleation” but

"homogeneous nucleation" has also been reported when self-precipitation/coagulation of hydrophobic oligoradicals creates the first particles (low content of surfactant < CMC). The final product is a colloidal dispersion of polymer particles in water, known as latex (TUPAC definition). If the monomer droplet size can be reduced to below 0.5 μm, two phenomena will occur. First, the droplets will be able to compete successfully for water-borne free radicals with any remaining micelles. Second, the huge increase in interfacial area caused by the reduction in droplet size will result in a huge increase in interfacial area. This new interface will require a monolayer of surfactant to remain stable. The surfactant necessary to support this large interfacial area will come from the break-up of surfactant micelles. In a properly formulated miniemulsion, all micelles will be sacrificed to support the droplet interfacial area. Therefore, not only do the small droplets compete effectively with micelles, but their presence causes the destruction of the micelles, leaving droplet nucleation as the dominant particle nucleation process (Figure 1. 3). Miniemulsions are not thermodynamically stable emulsions. They are produced by the combination of a high shear to break up the emulsion into submicron monomer droplets, and a surfactant/costabilizer system to retard monomer diffusion between submicron monomer droplets. [108-110]

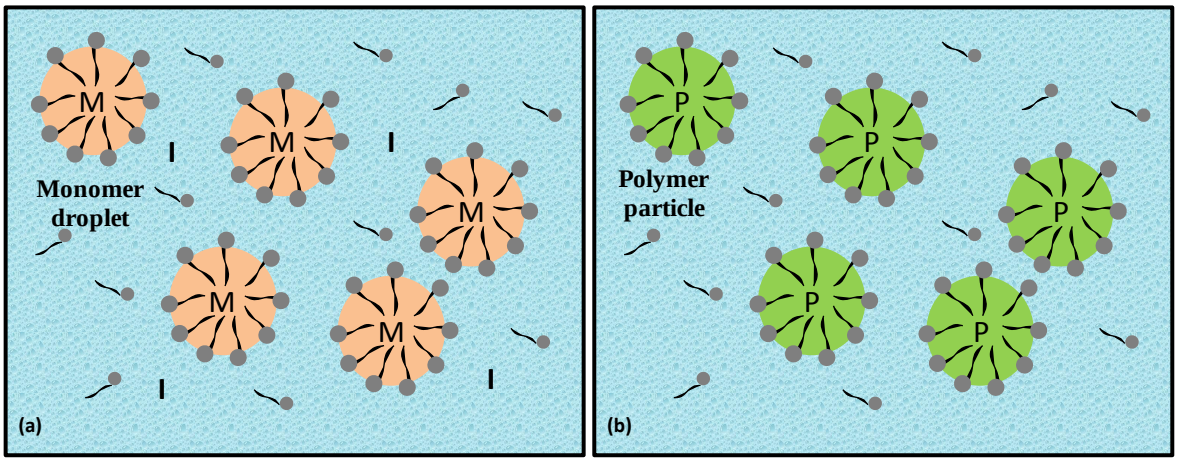

Figure 1. 3: General scheme of miniemulsion polymerization, in the initial state (a) and final state (b); M is for the monomer, P for the polymer and I for the initiator

Ugelstad et al. [111] were the first to demonstrate that under conditions in which the droplet size is small enough, nucleation of monomer droplets could account for an important part of the particles formed. It was shown in previous reports that the presence of long chain fatty alcohols drastically increased the capacity of anionic surfactants to disperse and stabilize oil-in-water emulsions. [112-115]Azad et al. [115] showed that the longer the fatty alcohol, the more stable is the liquid emulsion. Based on the work of Hallworth and Carless [112-114] and Davies

and Smith [116] who had found that the stability of light petroleum, benzene and hexane emulsions was strongly improved by small amounts of hexadecane (HD), they decided to use this compound instead of fatty alcohol to stabilize the monomer droplets. It was found that with ordinary stirring equipment, addition of hexadecane did not give the rapid emulsification that could be obtained with the long chains fatty alcohols. Therefore, a more efficient homogenization system was required.

The miniemulsion process possesses some of the same features as emulsion polymerization, but the particle nucleation mechanism is quite different. [108-110] Miniemulsion polymerization employs as a co-stabilizer a highly water-insoluble hydrophobe (e.g. hexadecane) and the initial reaction mixture is subjected to very high shear to create a dispersion of monomer droplets of ~50–200 nm in diameter. The use of sonication for the homogenization process in miniemulsions was described.[117] The term miniemulsion itself was created later by the group of El-Aasser [118]. The hydrophobe stabilizes monomer droplets against diffusional degradation (Ostwald ripening). Ideally, these monomer droplets all become polymer particles and no secondary nucleation occurs (Figure 1. 3), although in practice this ideal is often not achieved and homogeneous nucleation can occur during polymerization. Surfactant concentration in water is usually maintained below the surfactant CMC to avoid micellar nucleation. For miniemulsion polymerization, the initiator can be either oil- or water-soluble. In the case of an oil-soluble initiator, the initiator is dissolved in the monomeric phase prior to miniemulsification. Then the reaction starts within the droplets. Whereas, in the case of water-soluble initiator, initiator is dissolved in water and, therefore, the formation of free primary oligo-radicals takes place in the aqueous phase.

Monomer droplets coalescence can occur to form larger droplets. This phenomenon is generally suppressed by the surfactant provided that the surface coverage is sufficient. After passing the initial emulsion in ultrasonication, larger oil/water interface is created and must be covered by the surfactant. A usual surfactant is anionic sodium dodecyl sulfate (SDS) where it has been shown only 30 % of the particle surface was covered [119]. However, it had been shown by Landfester et al. that cationic and non-ionic surfactants can be used to create well defined miniemulsions for further miniemulsion polymerization processes, resulting in a narrow size distribution of stable cationic and non-ionic latex particles.[119] An additional point,

is that by varying the amount of the surfactant, the particle size can be varied over a wide range.[120] Thus, surfactant must be carefully selected in a miniemulsion polymerization.

Ostwald ripening phenomenon was first described by Wilhelm Ostwald in 1896 stating the diffusion of organic molecules from small monomer droplets dispersed in water toward larger ones until their disappearance. [121] Ostwald ripening is usually prevented by the addition of highly hydrophobic reagent, known as the co-stabilizer. When the diffusion of molecules from small particles to larger particles takes place, the concentration of the co-surfactant increases in the small particles and decreases in the large particles, thus compensating the Laplace pressure by the osmotic pressure. When the Laplace pressure is equal or less than the osmotic pressure, Ostwald ripening is avoided. Early work in miniemulsion polymerization used either cetyl alcohol (CA) or hexadecane (HD) to retard Ostwald ripening in submicron monomer droplets. [108] Both CA and HD, referred to here as co-stabilizers, have the requisite properties for a co-surfactant: high monomer solubility, low water solubility and low molar mass. The use of other materials as co-surfactant involved polymer which was first reported by Reimers et al. in 1995 [122], monomeric co-surfactants and other co-surfactants. [110] Miller et al. [123, 124] reported that the addition of a small amount (as small as 0.05 wt-%) of higher molar mass polystyrene (PS) to the styrene phase of a miniemulsion polymerization of styrene causes an increase in both the rate of polymerization and the number of final polymer particles.

Homogenization is the key step for miniemulsion, where miniemulsions are produced by the combination of a high shear device to break up the emulsion into submicron monomer droplets. Besides the choice of surfactant and co-stabilizer, the stability of the droplets is also affected by the homogenization process, which is responsible for the formation of the small monomer droplets acting as the nanoreactors. [110] A normal stirring is not sufficient to obtain narrow distribution of small droplets. Higher energies are necessary using homogenization devices such as rotor-stator systems, sonifiers or high-pressure homogenizers [109]. Rotor-stator systems and other shear devices (e.g. Ultra Turrax, Omni mixer) rely on turbulence to produce emulsification. The sonifier produces ultrasound waves that cause the molecules to oscillate about their main position as the waves propagate. During the compression cycle, the average distance between the molecules decreases, whilst during rarefaction the distance increases. In high-pressure homogenizers, homogenization is mainly due to extensional forces (shear) with some contribution from cavitation and impact forces. Also, during ultrasonication, the size of

the droplets decrease continuously until they reach a stable diameter, stating the diameter of the monomer nanoreactors which result in the same size of polymer particles.

A traditional way for the preparation of miniemulsion is summarized by simply mixing the surfactant in the water phase, the co-surfactant in the monomer phase. Then mixing the two phases under stirring and subjecting them to high efficient homogenization (Figure 1. 4).

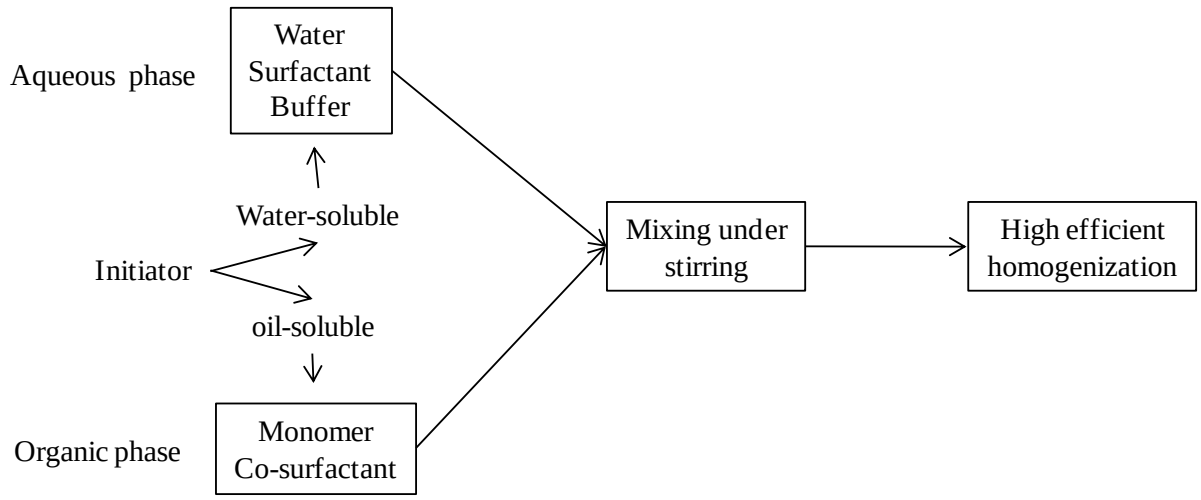

Figure 1. 4: Scheme for preparation of miniemulsion

2.2 NMP in miniemulsion

In a miniemulsion polymerization, monomer droplets are converted to polymer particles as the polymerization proceeds, and transport of nitroxide or low molar mass alkoxyamine through the aqueous phase between the monomer phase and the polymer particles is therefore not a concern. Nitroxide mediated polymerization (NMP) in miniemulsion can be divided into two categories: (i) Aqueous phase initiation [41, 86, 125-128] and (ii) oil phase initiation.[87, 125, 127-142] In aqueous phase initiation, it is possible to either use a water soluble initiator in combination with a hydrophobic nitroxide or to use a water soluble alkoxyamine.

Initiation by bi-component systems

In NMP miniemulsion polymerization, control was triggered using numerous nitroxides including TEMPO and its derivatives, TIPNO or SG1 used through bi-component systems. Using a bi-component initiating system, consisting of a nitroxide and a free-radical initiator such as benzoyl peroxide (BPO) or potassium persulfate (KPS), is a simple and reasonably effective approach to conducting nitroxide-mediated polymerizations. TEMPO-based NMP

miniemulsion of styrene has been carried out successfully for a number of different bi-component systems like: (i) TEMPO/BPO [125, 128, 131, 132], (ii) TEMPO/KPS [125, 128, 143]. Upon thermal decomposition of the initiator to yield two primary radicals, the initiation takes place to produce hydrophobic oligoradicals, hence forming the alkoxyamine by subsequent deactivation by nitroxide. In-situ formation of the alkoxyamine eliminates the need to synthesize and purify alkoxyamine, which can be a time-consuming and sometimes difficult step. However, the initiation efficiency is rather low with bi-component systems. The nitroxide-to-initiator ratio is critical to the progress of the polymerization, affecting both the kinetics and molar mass. Too much nitroxide causes long induction periods due to the excess nitroxide present at the outset of reaction, while uncontrolled polymerization results if the nitroxide/initiator ratio is too low. In a miniemulsion, nitroxide and initiator can partition between the aqueous and organic phases.

While reasonably good results have been obtained with bi-component systems in miniemulsion NMP, the sensitivity of initiation efficiency to reaction conditions and initiator/nitroxide selection makes it difficult to obtain predictable molar masses. Despite their attractive simplicity, if controlling molar mass is critical, initiation by monocomponent systems that is alkoxyamine-initiated systems are more desirable.

Initiation by monocomponent systems

Different works have explored the use of monocomponent systems in NMP miniemulsion [133, 134, 144]. First it was the teams of El-Aasser and Georges who were interested in using a PS-TEMPO previously synthesized in bulk as a macroalkoxyamine for styrene polymerization in miniemulsion [133, 145]. Pan et al. [133] used a PS-TEMPO after its isolation and purification at loadings of 5 wt-% and 20 wt-% in the organic phase for the polymerization of styrene. Experimental molar masses were lower than the theoretical ones with high dispersity values (1.8) for a final conversion of 75 %. Whereas Keoshkerian and al. [145] used PS-TEMPO after 5 % conversion in bulk directly without purification for the polymerization of styrene resulting in a 99 % conversion in six hours and low dispersity (1.15). However, in a surprising way, both studies present different singulars, which so far had not been explained. Pan et al. [139] highlighted the intervention of thermal initiation of styrene leading to molar masses slightly lower than expected ones with dispersities increasing with the conversion. Under these conditions, the authors also observed that the polymerization rate was independent of the

macroalkoxyamine PS-TEMPO concentration. On the other hand, no dependence of the polymerization rate as a function of surfactant concentration and thus, the number of particles was observed by the same authors as the effect of segregation does not apply to such systems [146]. The alkoxyamine MONAMS based on SG1 was also used for the polymerization of styrene in miniemulsion, and this alkoxyamine allows good control of the initiation step, concentration of propagating chains (thus controlling nitroxide concentration). The results obtained are similar to those obtained in bulk polymerization under similar conditions, and in comparison to the systems of bi-component the molar mass is higher with a lower dispersity. [86, 128, 129]

The monocomponent systems mentioned before were organosoluble alkoxyamines. A careful study of the work of Marestin in 1998 can highlight on hydrosoluble alkoxyamine [30]. This work, although based on the RDRP of styrene in emulsion, initiated by a TEMPO based hydrosoluble alkoxyamine, was considered by scientists as miniemulsion. The agitation rate of 900 rpm is considered important and the use of SDS as a surfactant which at high temperature can hydrolyze to dodecyl thiol and play the role of a co-stabilizer. Still, it should be more included in the part of NMP in emulsion polymerization. Miniemulsion polymerizations using SG1-based alkoxyamines have been performed for styrene [41, 86, 129, 130] and nBA [86, 87, 129, 130, 138] polymerization as reviewed by Charleux and Nicolas.[31]

Colloidal stability of NMP miniemuslion

Colloidal stability in NMP miniemulsions has frequently been a challenge and a concern, particularly for polymerizations run at temperatures above 100 °C where traditional surfactants often perform poorly. Sodium dodecyl sulfate (SDS), for example, is subject to hydrolysis at these temperatures [30]. Sodium dodecylbenzenesulfonate (SDBS) and the structurally similar DOWFAX 8390 (Scheme 1. 12) are more stable, and have shown good performance as surfactants, giving stable latexes with minimal coagulation. [31]

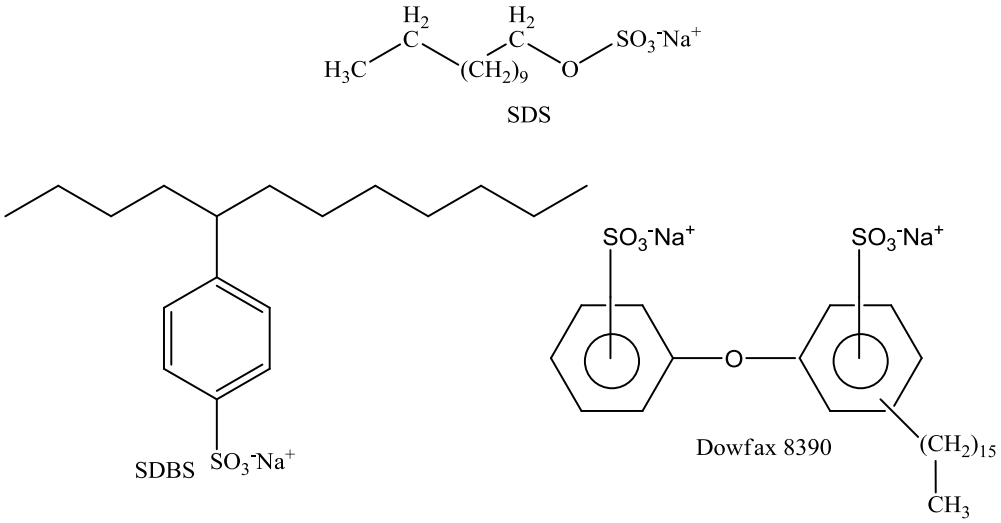

Scheme 1. 12: Scheme of different surfactants used in miniemulsion

In almost all of previous studies with bi-component initiating systems, the mean particle diameter was relatively large (> 190 nm) with a broad distribution. Given an initial droplet size of ~150 nm, this indicates that in most cases less than half of the droplets were nucleated. However for systems initiated with monocomponent system, the particle sizes are considerably smaller, typically ~120– 150 nm, indicating there are more final particles than there were droplets initially [147]. With the comparatively high solubility of styrene in water at 135 °C [143], there is a distinct possibility of homogeneous nucleation. The effects of varying surfactant concentration on particle size and number were investigated by Pan et al. [134] An unusual observation made is that low conversion samples (< 20 %) will often phase separate within a few minutes to give a milky latex with a clear liquid layer on top, presumably monomer. The final latexes did not exhibit this layer unless the final conversion was low (< 20 %).

NMP from miniemulsion to microemulsion

In conventional emulsion polymerization, segregation of the propagating radicals in different particles results in higher reaction rates and higher molar masses compared to bulk/solution processes by effectively reducing the termination rate between macro-radicals (chains terminate primarily as a result of another short radical entering from the aqueous phase). This phenomenon, known as "compartmentalization", fundamentally alters the kinetics in conventional emulsion polymerization by influencing the main chain stopping event (termination).[148-151] The relevant

question for RDRP performed in aqueous dispersed media was whether the kinetics was affected by reducing the reaction volume to that of a ~50−200 nm particle.[146]

It has been demonstrated for reversible termination systems (NMRP and ATRP) performed in polymerization in aqueous dispersed media that compartmentalization, that is the segregation of the propagating radicals in different particles which results in higher reaction rates and higher molar masses compared to bulk/solution processes by effectively reducing the termination rate between macro-radicals effects do exist under some conditions.[152] At sufficiently small particles sizes (< 80 nm), kinetic can be impacted but more importantly control and livingness are improved for linear polymers.[153-157]

It can be noted that the control of CRP in a "true" emulsion polymerization process has been a challenge for a long time. The breakthrough was provided by controlling the nucleation step via a microemulsion polymerization. [32] Indeed, polymerization of *n*-butyl acrylate using a water-soluble low molar mass alkoxyamine based on SG1 was performed under microemulsion-like conditions, whereby a very dilute aqueous emulsion of monomer (0.7 wt-%) using a high surfactant (Dowfax 8390) concentration was employed, such that most monomer and control agent were located in the monomer-swollen micelles. [32] Polymerization was taken to approximately 60 % conversion, giving number-average molar mass in the range of 1000 $g.mol^{-1}$ (oligomers), followed by introduction of monomer in one shot to swell the seed particles for further emulsion polymerization. In microemulsion the droplet size is decreased to provide a confined space, thus increasing the deactivation rate and consequently polymerization rate decreases via a decrease of radical concentration.

NMP in microemulsion was thoroughly described by the team of Okubo and Zetterlund in 2007 [158]. They performed microemulsion NMP of styrene targeting 2-5 wt-% of solids content at 125 °C in the presence of *n*-tetradecyltrimethylammonium bromide (TTAB) as a surfactant, using a bicomponent system with organosoluble (BPO, AIBN) or hydrosoluble (KPS) initiators and TEMPO or SG1 nitroxides. TEMPO-mediated polymerizations were extremely slow, that is the rates of polymerization R_p were approximately ten times lower than in the corresponding bulk polymerizations for the three initiators (organosoluble BPO, AIBN and hydrosoluble KPS). This is consistent with the confined space effect (compartmentalization) favoring fast deactivation and lowering the concentration of the propagating radicals. The lowering of R_p is also due to the increase of initial termination reactions generated by thermal

initiation of styrene due to the confined space effect. As the R_p is low, the monomer diffuses from non-nucleated monomer swollen micelles to particles, and coalescence occurs, resulting in relatively large particles (40-130 nm) in comparison to the initial monomer swollen micelles. The processes might cause a molar mass distribution with relatively broad values, that might also be caused by the alkoxyamine decomposition at elevated temperatures and long reaction times (generating a polymer chain with a terminal unsaturation and a hydroxylamine). On the other hand, polymerizations with SG1 nitroxide, which has a much higher equilibrium constant than TEMPO ($K_{eq\ PS\text{-}SG1} = 6.0 \times 10^{-9}$ M, $K_{eq\ PS\text{-}TEMPO} = 2.0 \times 10^{-11}$ at 125 °C), proceeded much more rapidly, thus leading to higher rate of polymerization R_p but comparable with bulk. The polymerization resulted in smaller particles (20-40 nm) and lower dispersity of polymers. The most likely explanation for the higher R_p in microemulsion with SG1 comparable to bulk in comparison to R_p with TEMPO, it is that the confined space effect on deactivation is counteracted by exit of SG1, increasing the concentration of the propagating radicals (the water solubility of SG1 is expected to be significantly higher than that of TEMPO). In 2012, Zetterlund studied the NMP microemulsion of styrene using a monocomponent system of PS-SG1 as organosoluble alkoxyamine with 120 wt-% of oleic acid relative to styrene. [156] Starting with droplets of 10 nm, a rate of polymerization almost 12 times higher than in bulk was observed. The control was also observed to be higher in the case of microemulsion than in bulk. Considering the rapid polymerization in microemulsion, the high level of control is quite remarkable. It was proved that the high R_p and the good control cannot be explained simply by oleic acid influencing SG1 concentration. On the basis of theoretical work on compartmentalization effects in NMP in the absence of nitroxide partitioning (exit/entry), R_p decreased with decreasing particle size, in sharp contrast to the previous results of 2012. However, if the nitroxide is able to undergo exit to a significant extent, the situation is quite different. Nitroxide exit counteracts the confined space effect on deactivation, thereby causing an increase in R_p. In such a system where the propagating radicals are segregated (reduced termination), the nitroxide is able to diffuse throughout the system, leading to an overall effect of reduced termination and thus higher R_p with control/livingness maintained. [156] Compartmentalization (confined space effect on deactivation and segregation effect on termination), nitroxide exit/entry, and a minor rate enhancing effect of oleic acid created favorable conditions in these very small particles for the polymerization to proceed very rapidly with good control/livingness. [156] Compartmentalization effects comprising of the segregation effect and the confined space

effect have been shown to operate in microemulsion for n-butyl acrylate polymerization using SG1 as a nitroxide, TTAB as surfactant and AIBN as initiator .[159] At a $[SG1]_0/[AIBN]_0$ ratio of 1.68, the polymerization rate was low, molar mass distribution shifted to higher molar mass with increasing conversion, and M_n increased linearly with the conversion close to theoretical M_n consistent with a controlled/living process, although, the molar mass distribution was relatively broad with M_w/M_n = 1.5-2.0 throughout the polymerization. In the corresponding bulk NMP, the polymerization rate was extremely high and the molar mass distribution revealed no signs of control/livingness. Although the initial diameter of the droplets was 1-2 nm, final particles showed diameters of 60-90 nm for conversion higher than 12 %. From these results, it was concluded that the superior performance of the microemulsion NMP was caused by the confined space effect explained previously. Through this study it was also shown that upon increasing the ratio of $[SG1]_0/[AIBN]_0$ the rate of polymerization decreases and so does the final particles size. In 2012, Okubo et al. [157] also reported the comparison between NMP of nBA in miniemulsion and microemulsion in order to clarify the importance of the confined space effect in the initial stage of microemulsion. In this study they used a system of SG1/AIBN nitroxide/initiator with TTAB as surfactant. The size of droplets before polymerization was ~ 50 nm in the case of miniemulsion, whereas it was 5-10 nm for microemulsion. The rate of polymerization of miniemulsion NMP was much faster than that of the microemulsion and close to the bulk NMP. Molar mass distribution of PBA obtained from miniemulsion did not shift to higher molar mass with increasing conversion, the M_n did not increase linearly with time and the dispersity was high ($M_w/M_n > 2.5$). On the other hand, M_n increased linearly with conversion and M_w/M_n was below 2 in the case of microemulsion. This indicated that NMP microemulsion proceeded under better control than miniemulsion. The confined space effect of the miniemulsion and microemulsion polymerizations can be considered as follows. In the miniemulsion NMP with initial droplets diameter of 60 nm, because the confined space effect works weakly, the deactivation between propagating radical and control agent does not occur well, thus, miniemulsion NMP proceeded in similar manner to the bulk NMP. On the other hand, in the microemulsion NMP at initial droplet diameter of 5−10 nm, because the confined space effect works strongly at the initial stage, promoting fast deactivation, PBA-SG1 oligomers were successfully formed in the initial stage, resulting in a good control of molar mass distribution. These results showed that a good control/livingness in the microemulsion NMP derived from the confined space effect due to the nanosize of the droplets in the initial stages. [156, 157]

2.3 Synthesis of composite latex by miniemulsion polymerization

Among the different heterogeneous polymerization techniques, one can first mention emulsion and dispersion polymerization, used to synthesize polymer latex. During emulsion, the polymer particles can be formed either by entry of oligo-radicals into the micelles, and/or by precipitation of growing oligomers in the aqueous phase. Therefore, it is very tough to control the structure, morphology and size of nanocomposite spheres, especially to encapsulate inorganic nanoparticles inside polymer shells. The introduction of chemical functions favoring the interaction between polymer phase and inorganic nanoparticles have an important impact on the size and stability of nanocomposite latexes.

In the field of nanocomposite latex synthesized by emulsion polymerization or aqueous dispersion polymerization, one can cite for instance the studies of S. Armes where silica nanoparticles acting as stabilizer are mainly located at the surface of the particles (Figure 1. 5). [160-162]

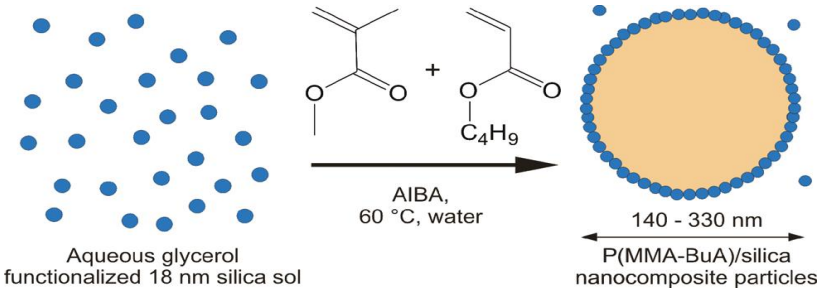

Figure 1. 5: Schematic representation of the surfactant-free synthesis of colloidal nanocomposite particles by aqueous emulsion copolymerization of methyl methacrylate with *n*-butyl acrylate at 60 °C using a cationic azo initiator (AIBA) in the presence of a commercial ultrafine glycerol-functionalized aqueous silica sol (Bindzil CC40) as the sole stabilizing agent. [161]

Emulsion and dispersion polymerization have also been implemented in the synthesis of non-spherical nanocomposite latex (called colloidal molecules) as reviewed by Duguet at al.[163]. Different parameters such as degree of monomer-grafting onto the silica particles and the ratio between number of silica and latex particles were influencing the final morphology. The use of hydrophilic polyelectrolyte reactive toward radical polymerization was also developed for the synthesis of nanocomposite latex. [164]

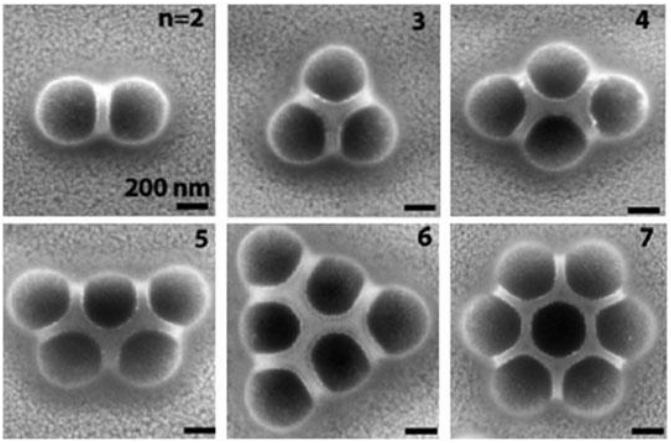

Figure 1. 6: SEM micrographs of PS/organosilicate colloidal clusters with varying the number of colloidal building blocks n. [163]

Examples of emulsion and dispersion polymerization have been given to provide a view of the literature concerning the synthesis of latex composites, though we will focus on studies concerning miniemulsion polymerization process to design nanocomposite latex. Miniemulsion is an interesting method to synthesize organic-inorganic nanocomposites latex by simplifying the nucleation step. In comparison with emulsion polymerization, the monomer droplet nucleation can provide easier encapsulation of inorganic particle. Generally, the formation of polymer-inorganic nanocomposite via miniemulsion polymerization has three steps, two dispersion and one polymerization steps (Figure 1. 7). For the present thesis, we have chosen to focus our attention on the synthesis of nanocomposite latex by miniemulsion involving the use of spherical-like nanoparticles. Precise here that a field of nanocomposite particles concerns the incorporation (or stabilization) of layered inorganic particles (clay). This field of research will not be detailed in this chapter. The development of miniemulsion for the synthesis of clay/polymer nanocomposites has been reviewed by the group of Bourgeat-Lami. [165]

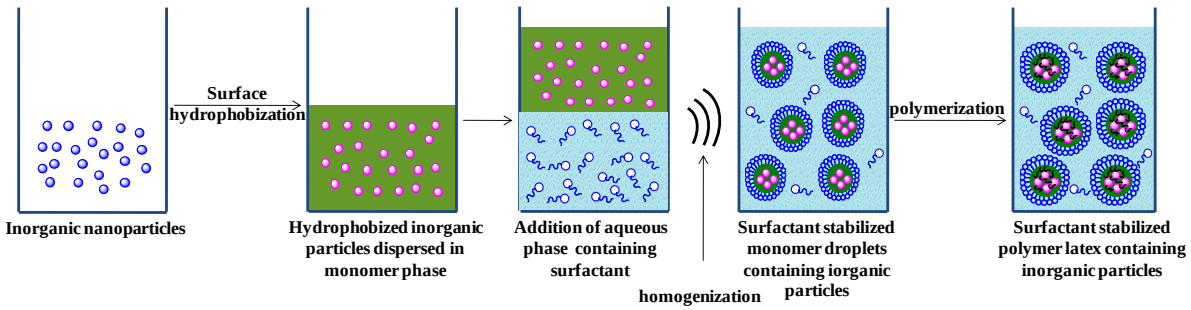

Figure 1. 7: Schematic of the synthesis of polymer-inorganic nanocomposites via miniemulsion polymerization

For the synthesis of the nanocomposite latex, the inorganic nanoparticles have to be hydrophobized. For the hydrophobization of the inorganic nanoparticles different strategies are known, including ligand adsorption or monomer/initiator covalent grafting. The different polymer-inorganic nanocomposites synthesized via miniemulsion have been the interest of scientists throughout years as reported in different reviews. [166, 167] Silica-based nanocomposite latex were paid very much attention, but we can also mention other inorganic nanoparticle-based nanocomposite latex (iron oxide, zinc oxide, gold, titanium dioxide).

Silica-based nanocomposites

Among the inorganic nanoparticles, silica SiO_2 is viewed as being very important. Therefore, polymer/silica nanocomposites have attracted substantial academic and industrial interest. Their preparation, characterization, properties, and applications have become a quickly expanding field of research. [168]. A recent review showed the important evolution in the synthesis of polymer/silica nanocomposites. [168]

Among the different polymerization techniques for the preparation of SiO_2/polymer nanocomposite latex, miniemulsion has turned out to be an attractive way to obtain these nanocomposites. In 2001, Landfester et al. [169] first reported the preparation of SiO_2/polymer nanocomposites using miniemulsion polymerization. Depending on the reaction conditions and the surfactants employed, different hybrid morphologies were obtained, comprising a "hedgehog" structure (Figure 1. 8) where the silica surrounded the latex droplet and provided stabilization even without any low molar mass surfactant. The size and morphology control of the nanocomposite particles by miniemulsion polymerization was studied by Wu and co-workers. [170-172] SiO_2/PS nanocomposite particles were synthesized through miniemulsion polymerization by using sodium lauryl sulfate (SLS) surfactant and hexadecane costabilizer in the presence of silica particles coated with methacryloxypropyltrimethoxysilane (MPS). By adjusting the size of the silica particles and the surfactant concentration employed, they were able to control the size and morphology of the nanocomposite particles.

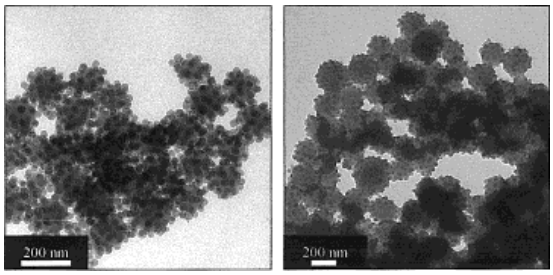

Figure 1. 8: TEM pictures of latexes using silica particles as stabilizer for monomer droplets.[169]

Very recently, asymmetric nanocomposite particle pairs of PS and silica were prepared via one-step miniemulsion polymerization by Xu et al. [173]. Nanocomposite particles with different asymmetrical morphology were obtained by controlling the concentration of styrene. When the amount of styrene was changed from 2.2 to 4.8 g (8.8 to 19.2 wt-% vs water), the shape of the nanocomposite particles varied from mushroom-like to swaddle-like (Figure 1. 9). Hence, even over this wide range of concentration, the asymmetric morphology of the nanocomposite particles could be well maintained.

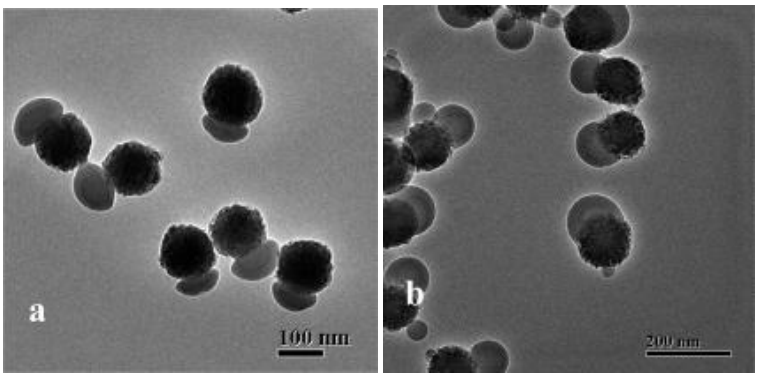

Figure 1. 9: TEM images of asymmetric silica/polystyrene nanocomposite particles: (a) 8.8 wt-% and (b) 19.2 wt-% of styrene. [173]

In 2008 Forcada et al. [174] reported the encapsulation of silica nanoparticles by miniemulsion polymerization. They managed the synthesis of monodisperse silica nanoparticles of different sizes (66-202 nm) and hydrophobized the surface of these silica with 3-(trimethoxysilyl)propyl methacrylate TPM avoiding flocculation and aggregation. Mono and multinuclear eccentric core-shell silica/polystyrene hybrid nanoparticles (Figure 1. 10) were obtained by miniemulsion polymerization. Reporting that a synergistic effect was observed using oleic acid OA and TPM as surface modifiers in the necessary compatibilization process between organic phase and inorganic nanoparticles.

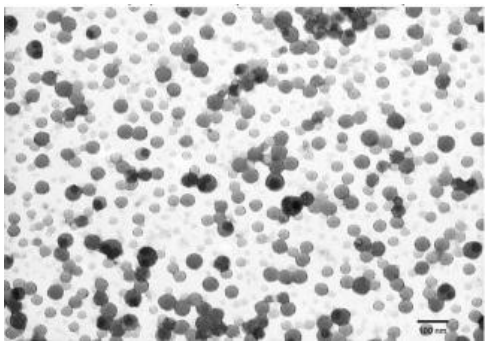

Figure 1. 10: TEM microphotographs of polystyrene/silica composite nanoparticles [174]

Matyjaszewski [175] reported for the first time the synthesis of silica/PBA by surface-initiated ATRP in miniemulsion in order to avoid cross-linking reactions and/or macroscopic gelation that occurs in bulk polymerization. 1-(chlorodimethylsilyl)propyl 2-bromoisobutyrate functionalized silica particles with diameter 20 nm were used to initiate SI-AGET ATRP in miniemulsion. In comparison to the bulk polymerization, using the same stoichiometry, miniemulsion allowed the preparation of hybrid materials with a higher yield, i.e., higher monomer conversion, and a higher polymerization rate without macroscopic gelation.

Magnetic nanoparticles-based nanocomposites

Magnetic nanoparticles have been extensively investigated due to the wide range of practical and potential applications in the biomedical fields including magnetic separation of biomolecules, magnetic resonance imaging contrast enhancement, magnetic-field induced hyperthermia therapies, etc. [176, 177] The magnetic properties of the nanoparticles allow convenient mechanical sorting, trafficking, and micromanipulation in biological systems simply by using an external magnetic field. [178] Ramirez and Landfester reported that iron oxide nanoparticles (10 nm), formed by precipitation from a ferrous and ferric chloride solution and hydrophobized by oleic acid, can be dispersed in octane and miniemulsified in water and SDS as surfactant to further conduct styrene polymerization to form polystyrene nanocomposites containing magnetic particles. [179]

Some polymerization factors such as initiator type, concentration of surfactant and dose of monomers influence the morphologies and properties of magnetic nanocomposites. With the increased applications of the magnetic nanocomposites in the biomedical fields, the magnetic nanocomposite spheres still need to be surface-functionalized. Xu et al. [180] prepared the epoxy group-functionalized magnetic polymer latex magnetic poly(styrene-divinyl benzene-glycidyl methacylate) (magnetic P(St-DVB-GMA) latex) consisting of a superparamagnetic core

coated with a polymeric shell by modified miniemulsion polymerization, and controlled the epoxy group density on the surface by a further seed polymerization of GMA monomer. With the increasing divinyl benzene (DVB) content in the monomer mixture (styrene and GMA), the thickness of shell structure increased accordingly. Forcada et al. [181] synthesized the self-stabilized magnetic polymeric nanocomposites by emulsifier-free miniemulsion polymerization using styrene as a monomer, sodium-p-styrenesulfonate as an ionic comonomer, hexadecane as a hydrophobe, and AIBN as an initiator in the presence of hydrophobized magnetite particles. Also, Gu et al. [182] developed a new process combining modified miniemulsion/emulsion polymerization with sol-gel technology to prepare monodisperse, nanoscale, superparamagnetic Fe_3O_4/polystyrene/silica nanospheres using the schematic preparation process in Figure 1. 11. The ferrofluid coated with oleic acid was added to the aqueous solution with SDS and treated ultrasonically to obtain miniemulsion A. The miniemulsion A was mixed with another miniemulsion B made of styrene monomer droplets to obtain a double-miniemulsion system. This double-miniemulsion system was carried out to form polystyrene/Fe_3O_4 nanospheres. Then the as-synthesized superparamagnetic polystyrene/Fe_3O_4 nanospheres were modified by polyoxyethylene(20) sorbitan monolaurate for dispersing the hydrophobic nanospheres into an aqueous phase. At last, polystyrene/Fe_3O_4 nanospheres were coated with a silica layer via a modified Stöber process.

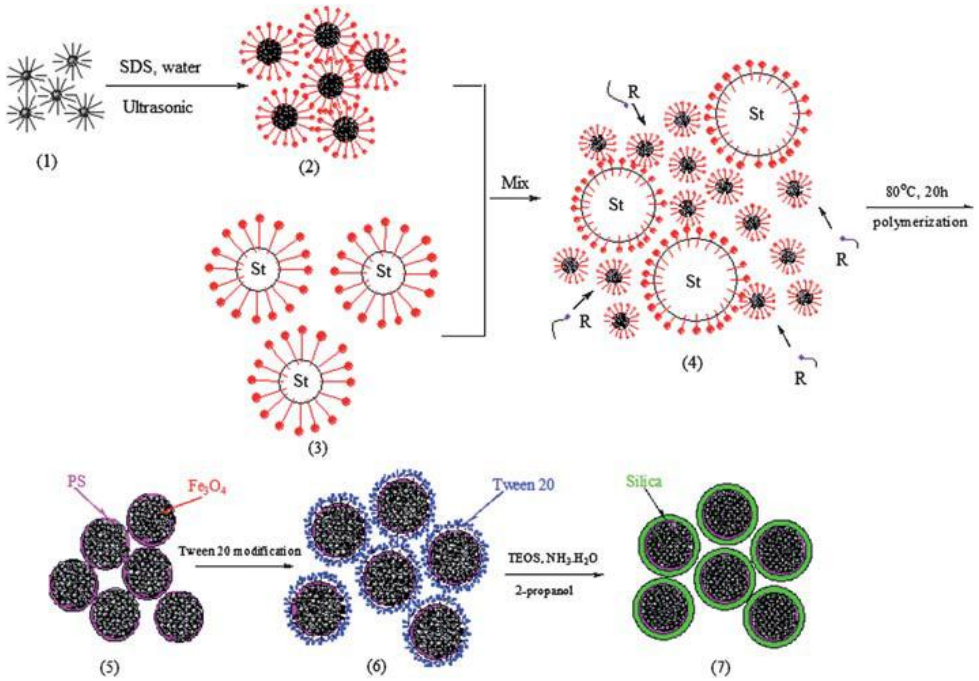

Figure 1. 11: A diagram of the preparation of hydrophilic magnetic Fe_3O_4/polystyrene/silica nanospheres with high saturation magnetization [182]

In comparison to other polymerization methods with low encapsulation of magnetic nanoparticles, such as, below 25 % for suspension polymerization and dispersion polymerization, and even below 10 % for emulsion polymerization, miniemulsion can provide more than 45 % and even as high as 80 % magnetic nanoparticle content in the nanocomposite spheres. [182]

Titanium dioxide-based nanocomposites

TiO_2 is usually applied in coatings, plastics and papers, because it has a high refractive index and possesses the ability to reflect and refract or scatter light more effectively than any other pigments. Also, it is a well-known photocatalyst for degradation of organic pollutants, medical treatment and microorganism photolysis. As other inorganic particles, TiO_2 nanoparticles tend to aggregate easily, so they need to be surface-modified. El-Asser and co-workers [183-185] modified TiO_2 nanoparticles first with polybutylene succinimide diethyl triamine and then dispersed 5 wt-% of the hydrophobized particles in styrene prior to the miniemulsion process. About 89 wt-% of TiO_2 could be encapsulated in polystyrene. In addition, multifunctional nanocomposite spheres, that is two different cores can be incorporated into polymer particles to design for instance SiO_2-PS-TiO_2 nanocomposite spheres. [186, 187]

3 Surface-initiated CRP from silica nanoparticles

3.1 Surface modification techniques

The modification of inorganic particles by a thin layer of polymer is often used to manipulate the surface properties of these materials. Although the macroscopic properties (mechanical, magnetic, optical …) of the global material (hybrid nanoparticles) are often governed by those of the inorganic substrate, modification of the inorganic surface by a polymer layer can often introduce new characteristics (such as dispersibility in an organic medium, protection against corrosion, biocompatibility …).

A number of surface grafting techniques have been used on solid surfaces. Physical adsorption (or physisorption) of functionalized homopolymers or block copolymers have been investigated. A main disadvantage is that such adsorbed layers are susceptible to removal, e.g., by exposure to a thermodynamically good solvent. In principle, adhesion between

polymer and substrate may be greatly enhanced if the chains are chemically attached (or chemisorbed) onto surfaces. Three main types of polymer grafting with surface by chemisorption are known. [188]

3.1.1 Grafting onto

The technique of "grafting onto" or "grafting to" the surface is based on the reaction of a polymer having a functionalized end, which can react with a function of the surface. In the case of silica, either the polymer presents a chain end that can react directly with surface silanols (with an alkoxysilane or chlorosilane function), or a prefunctionalisation of the surfaces by a small organic molecule is necessary to promote a chemical reaction with a functionalized polymer chain end (Figure 1. 12). A drawback for this method is the low grafting densities obtained. Indeed, the grafting density is controlled by the diffusion of the polymer towards surface, which becomes increasingly difficult as the steric hindrance increases. The more grafted chains are longer, they tend to spread on the surface and hide the remaining reaction sites. The grafting is then limited by the kinetics (diffusion of new chains more difficult) and thermodynamics (already grafted chains do not pass spontaneously from the staggered conformation to the stretched brush conformation).

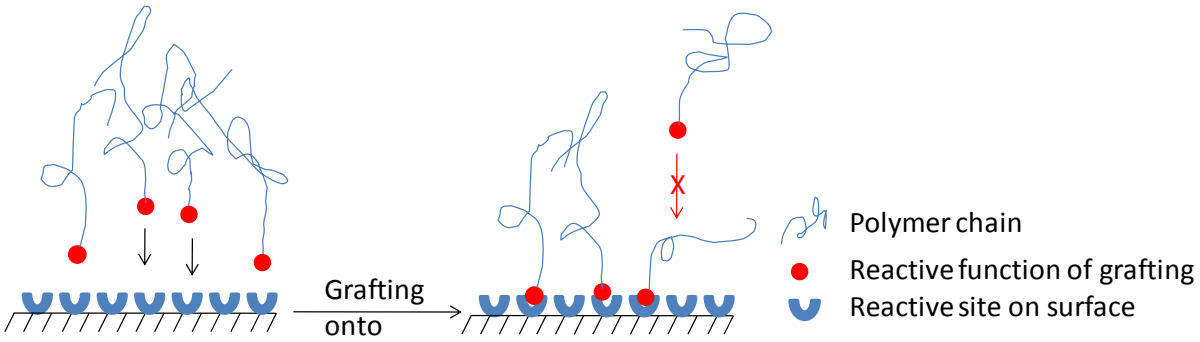

Figure 1. 12: Principle of surface functionalization by "grafting onto" method

3.1.2 Grafting through

In the "grafting through" method, monomers are covalently grafted to the surface of silica. During the polymerization of the monomer in solution, the grafted units are incorporated into the growing chain as well as the monomer units present in solution. The final polymer can be attached to the surface at several points (Figure 1. 13). The grafting densities obtained by "grafting-through" are similar to those obtained by "grafting onto".

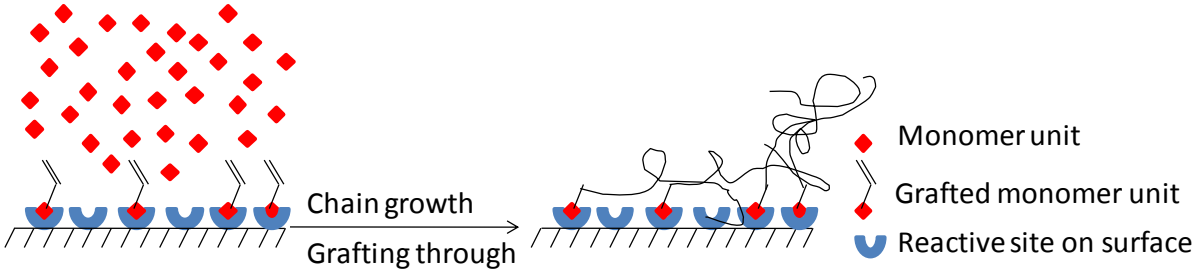

Figure 1. 13: Principle of surface functionalization by "grafting through" method

3.1.3 Grafting from

The "grafting from" method involves an initiator which is previously covalently anchored onto the surface of the inorganic particles. The polymerization reaction proceeds once the monomer becomes in contact with the functionalized inorganic particles where the polymer starts growing from the surface of the inorganic particles (Figure 1. 14). If the initiator grafting density is high (> 0.5 molecules.nm^{-2}), the combination of "grafting from" with a controlled polymerization induces simultaneous chain growth, providing a grafting density of the polymer chains far superior to that obtained with other methods of grafting.

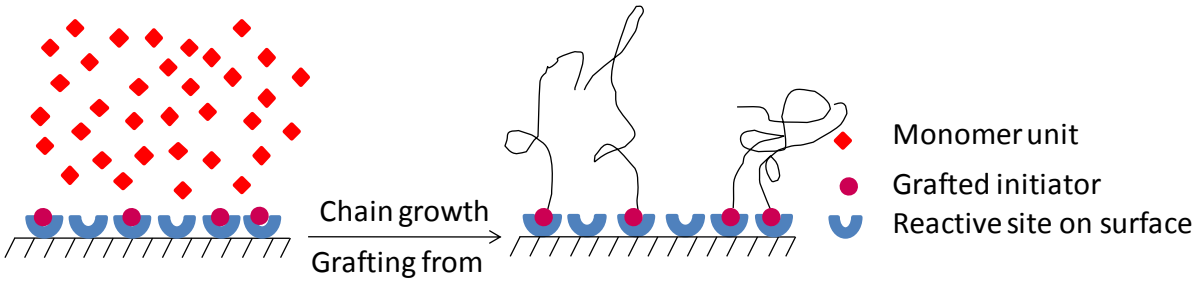

Figure 1. 14: Principle of surface functionalization by "grafting from"

When applying CRP, the method is named SI-CRP for Surface-Initiated Controlled Radical Polymerization [189]. If the grafting density is high enough, polymer brushes of controlled thickness are obtained, and the thickness of the thin layer of grafted polymer is controlled by the length of the polymer chains. These chains can reinitiate to form block copolymers with potentially interesting properties. Fukuda and al. [190] investigated by atomic force microscopy (AFM) the conformation of the polystyrene chains, poly (ethylene oxide) and poly(methyl methacrylate) on a silica surface, as a function of the density of the grafted polymer. The graph below (Figure 1. 15) summarizes the results obtained by comparing the extension of the polymer chain compared to the grafting density σ* (dimensionless grafting density, relative to the cross sectional area of the monomer). For a polymer grafting density σ* less than 0.02, the

polymer chains are in a "semi-dilute" conformation. For grafting density greater than 0.02, the polymer chain extension increases rapidly, reaching 90 % for σ* = 0.4 (which corresponds in the case of such to a grafting density of 0.7 chains/nm²). The grafted chains are then stretched to form a polymer brush tethered on the surface.

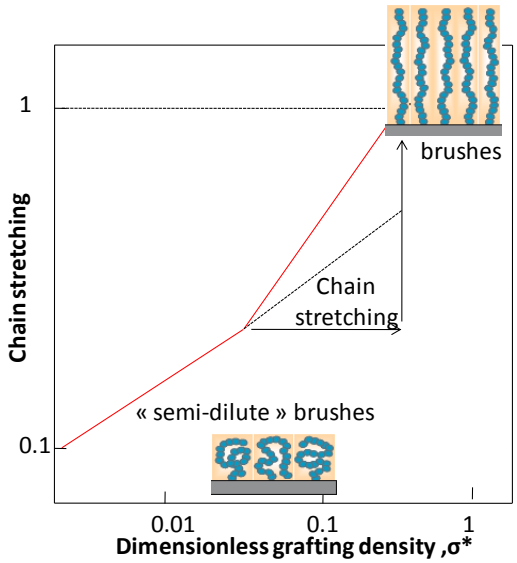

Figure 1. 15: Representation of the conformation of the grafted polymer brushes on a flat surface of silica, according to the grafting density σ * relative to the cross sectional area of the monomer.

Among the numerous inorganic–organic hybrid materials, silica–polymer hybrid materials are the most commonly reported in the literature. This may be attributed to their wide use and the ease of particle synthesis. The use of SI-CRP has proven to be a versatile approach for incorporating different types of organic polymers with varied architecture on the silica surfaces. [189] By using this technique, one can manipulate the structure of the resultant polymer shell through changes in grafting density, chemical nature, composition and molar mass. In controlled radical polymerization, the life-time of the growing radical can be controlled resulting in the synthesis of predefined molar mass, polymers with low dispersity, controlled composition, and functionality. In the following part we will describe examples of SI-CRP via different CRP methods. SI-NMP will be reviewed in more details as this method will be implemented in the present PhD work.

3.2 SI-ATRP from silica nanoparticles

An advantage of ATRP combined with “grafting from”, is its ease of use, where the reagents and the initiators used are often commercial. The first study of SI-ATRP from silica was

reported by Patten et al. [191] Their approach consisted of immobilization of the halogenated initiator molecule onto the silica particle followed by surface initiated ATRP of styrene and methyl methacrylate (MMA) under different conditions Scheme 1. 13. In this study, they described the relationship that could exist between the steric hindrance caused by the initiator and its initiator efficiency.

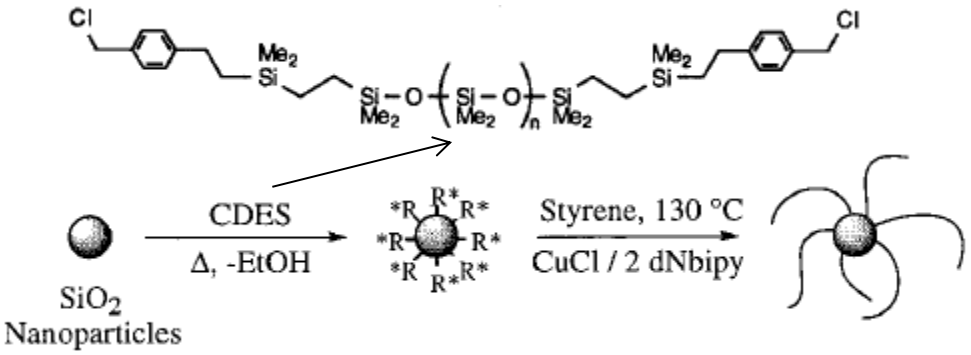

Scheme 1. 13: Synthetic scheme for structurally well-defined polymer-nanoparticle hybrids[191]

In addition, by combining their work with that of Prucker et al.[192] they could detail the modes of termination that can occur on the surface of the particle during the chain growth. Pyun et al.[193] reported similar work to Patten but they used additional Cu(II)Br_2 as the deactivating transition metal species. Styrene, n-butyl acrylate and MMA monomers were used for this study and various core–shell colloids containing tethered AB diblock copolymers were synthesized. Carrot et al. [194] studied the growth of poly(n-butyl acrylate) brushes from the surface of 12 nm silica particles by grafting a pre-formed halogenated initiator onto the silica prior polymerization (Scheme 1. 14).

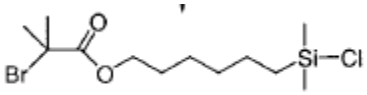

Scheme 1. 14: Halogenated initiator used by Carrot et al. for grafting onto silica surface [194]

After that, polymerization of *n*-butyl acrylate using ATRP from colloidal silica was also realized by El Harrak et al. [195] using another strategy for anchoring the initiator (Scheme 1. 15).

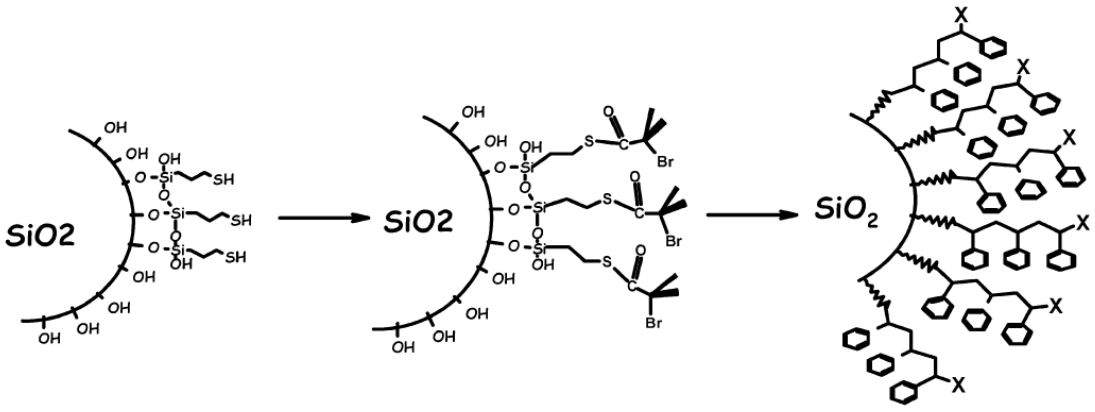

Scheme 1. 15: Grafting of the initiator molecule via "overgrafting" method used by El Harrak et. al[195]

The main challenge in SI-ATRP is the very small concentration of grafted initiator, resulting in a low concentration of deactivating agent produced in the reaction medium via PRE effect. The addition of free initiator in solution or deactivating agent allows the establishment of the ATRP equilibrium, according to the theory of persistent radical effect. Matyjaszewski [196] thus showed that adding only deactivating agent Cu (II)X_2 with activating agent Cu(I)X, without free initiator in solution, caused a linear growth of grafted polymer layer with conversion. High density PMMA brushes with molar mass near 500,000 g.mol^{-1} have been successfully grafted onto the silica nanoparticles using surface initiated ATRP. [197] A novel approach to attain environmentally responsive hairy nanoparticles was achieved by Zhao et al. [198] using a combination of surface initiated ATRP and NMP to graft mixed homopolymer brushes (Scheme 1. 16). An original work of Matyjaszewski reported the synthesis of poly(*n*-butyl acrylate) from silica surface in both bulk and miniemulsion. [175]

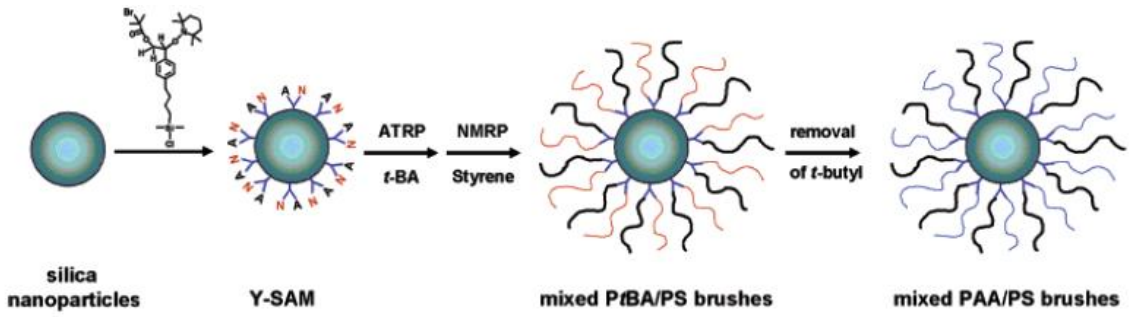

Scheme 1. 16: Synthesis of Amphiphilic Mixed Poly(acrylic acid)/Polystyrene Brushes on Silica Nanoparticles [198]

A drawback can be conferred to SI-ATRP, that is the use of aminated toxic ligands and the presence of metal complex, which is very difficult to remove from hybrid materials.

3.3 SI-RAFT from silica nanoparticles

This method is rarely used for the functionalization of inorganic surfaces, and that is due to the difficulty in the synthesis of functional RAFT agent necessary for the surface modification. Three main methods of synthesis are described in the literature, and represented in Scheme 1. 17, where the RAFT agent is grafted either by its R fragment, the initiating group or by Z fragment, the stabilizing group. Each method carries its own advantages and disadvantages in comparison to the others.

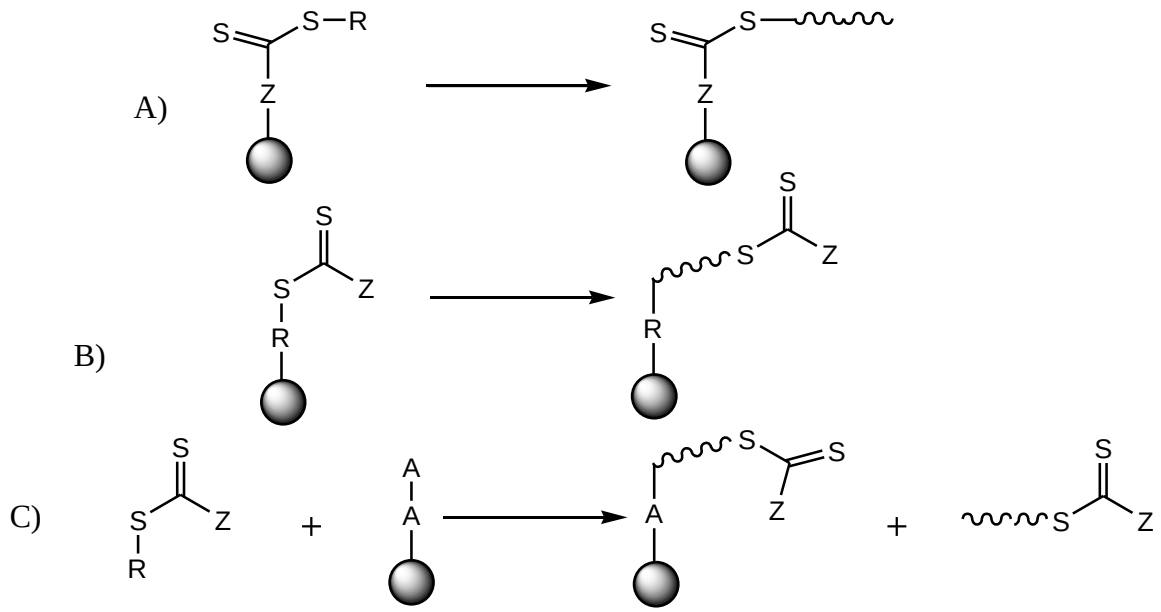

Scheme 1. 17: three modes of silica surface functionalization by RAFT: A) Z approach, B) R approach, C) grafting of radical initiator in combination with free RAFT agent

Fukuda et al. [199] were the first to describe the polymerization of styrene from dense silica nanoparticles (12 nm diameter). After grafting of the surface with an ATRP initiator and growth brushes PS oligomer, the terminal halogen group was converted to a dithiobenzoate RAFT by atom transfer radical addition (ATRA) reaction. Styrene polymerization was conducted in the presence of free RAFT agent. Upon cleaving PS chains and analysis of molar masses, Fukuda et al. [199] showed that reversible transfer reactions take place between the grafted chains, but also irreversible bimolecular termination reactions producing dead

polymer chains in a larger extent than with SI-ATRP. This phenomena is enhanced for high grafting densities (above 0.1 chains.nm^{-2}).

Baum and Brittain [200] then reported the grafting of a diazoic radical initiator on the surface of silicon wafers and silica nanoparticles. Polymerization of styrene and methyl methacrylate was then conducted in the presence of free AIBN and phenylpro-2-yl-2 dithiobenzoate RAFT agent. Cleaving the grafted polymer chains from the nanoparticles showed a good control of the polymerization (M_n free chains = M_n grafted chains and M_w/M_n <1.2). The thickness of the polymer film formed on the silicon wafers increased continuously with time. However, this technique is difficult in handling wafers functionalized by radical initiator and irreversible termination between grafted chain and a free chain in solution cannot be completely neglected.

Benicewicz [201, 202] portrayed for the first time using a dithioester RAFT agent functionalized by dimethylmethoxysilane on the R group (Scheme 1. 18), thus eliminating the multi-step process of Fukuda for the synthesis of PS and PBuA brushes by "grafting from" technique. The RAFT agent is grafted with a density of 0.15 to 0.68 molecules.nm^{-2} on silica nanoparticles (diameter 20 nm). The polymerization is controlled, block copolymers are synthesized and cleaved chains reflect a low dispersity (M_w/M_n <1.2). However, a strong retardation effect was observed.

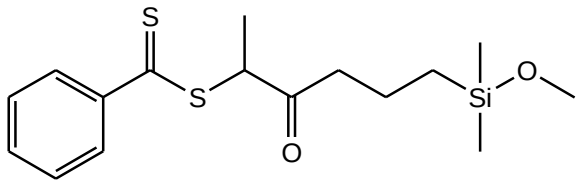

Scheme 1. 18: RAFT agent functionalized at R, used by Benicewicz [202]

Perrier et al. [203] grafted a trithiocarbonate RAFT agent onto the surface of silica particles (diameter 35-70 microns), by modifying the Z group by a trimethoxysilane. 4 - (chloromethyl) phenyltrimethoxysilane is first attached to the silica (Scheme 1. 19), and then the chlorine is substituted by the RAFT agent. The polymerization of various monomers (styrene, n-butyl acrylate, methyl methacrylate) was carried out using AIBN initiator. For the polymerization of methyl acrylate, the M_n of the free chains increased drastically above 50 % due to limited access to grafted RAFT agent. On the other hand, the M_n of grafted chains increased linearly

with conversion, being slightly below values of theoretical M_n. Various diblock copolymers were also synthesized in a controlled manner.

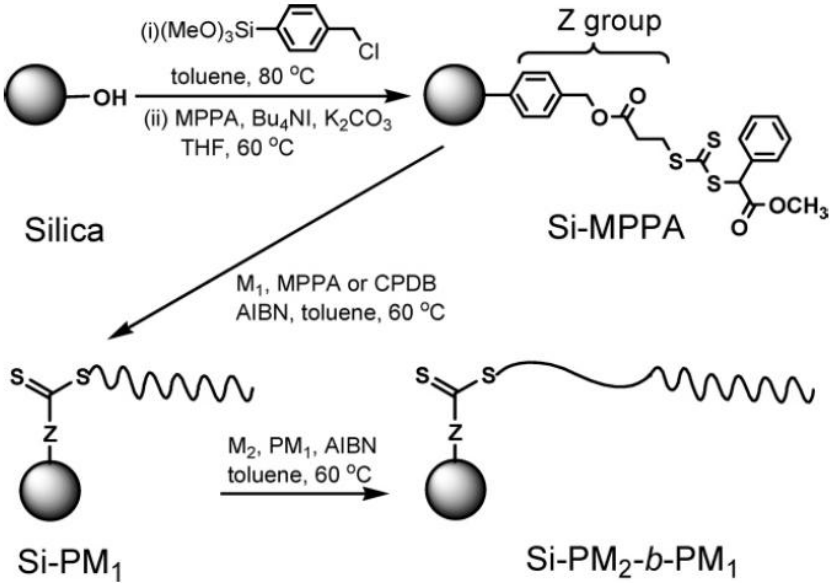

Scheme 1. 19: Grafting of RAFT agent via Z-group [203]

Grafting by the R group can often access to higher grafting densities and molar mass than the "Z" method. However, the molar mass distribution of the grafted chains is sometimes expanded due to the possibility of termination by interparticle coupling. In contrast, the grafting of the RAFT agent by Z group involves the reaction of free chains with the functionalized particles. The grafted polymer is better defined, but the grafting density may decrease because of increasing steric hindrance during the polymerization. Moreover, in case of hydrolysis of thio-carbonyl-thio function, there is a risk of chain cleavage.

Yang et al. [204] immobilized a RAFT agent on silica nanoparticles via an alternative method using a trithiocarbonate macro-RAFT agent based on 3 –methacryloxypropyltrimethoxysilane (MPS). The functional monomer was first dizomerized (n = 4) by RAFT polymerization using a trithiocarbonate RAFT agent (Scheme 1. 20). This macro-RAFT was grafted via co-condensation with the silica surface to further perform SI-RAFT of styrene in the presence of free RAFT agent in emulsion polymerization (Scheme 1. 21).

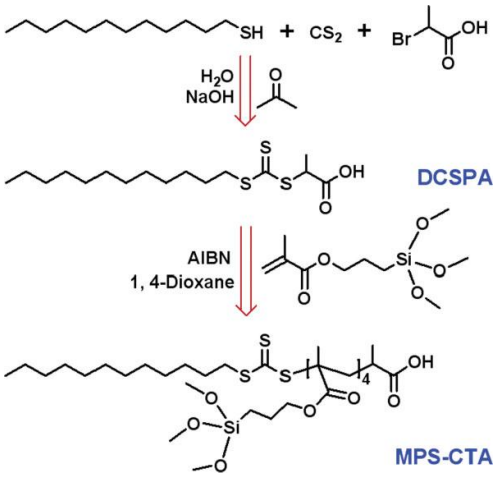

Scheme 1. 20: Synthesis of RAFT agent (DCSPA) and macro-RAFT agent (MPS-CTA)[204]

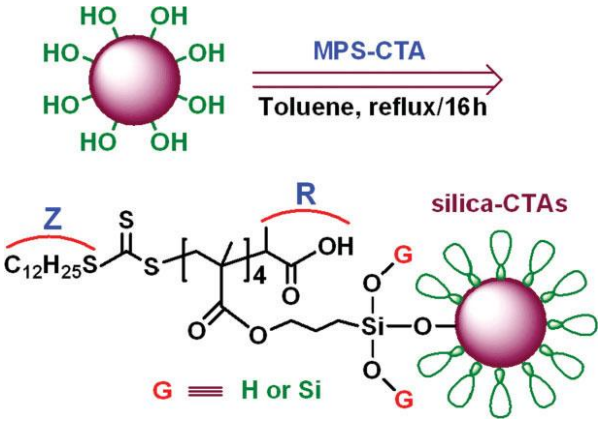

Scheme 1. 21: Preparation of silica-supported macro-RAFT chain transfer agents (silica-CTAs). [204]

Studies indicated that the effect of condensation of cleaved chains having several groups hydrolyzed methoxysilyl at one end is very likely to occur [205].

3.4 SI-NMP from inorganic surfaces

The first example of NMP initiated from inorganic surfaces was described by Hawker in 1999 [206]. A TEMPO-styryl-based alkoxyamine, functionalized with monochlorosilane was covalently attached to the surface of a silicon wafer. Controlled radical polymerization of styrene was then conducted in the presence of free alkoxyamine (Scheme 1. 22). As in ATRP the presence of a free alkoxyamine is necessary in the case of polymerization from a flat surface to retain a sufficient quantity of deactivating agent into the reaction medium to ensure a good control of the polymerization. After cleaving, analysis of the grafted chains showed similar macromolecular features to free chains present in solution. The grafted chains

displayed slightly lower dispersity than the free chains. Hawker et al. [207] adapted this technique for the synthesis of polymer brushes forming patterns on a flat surface.

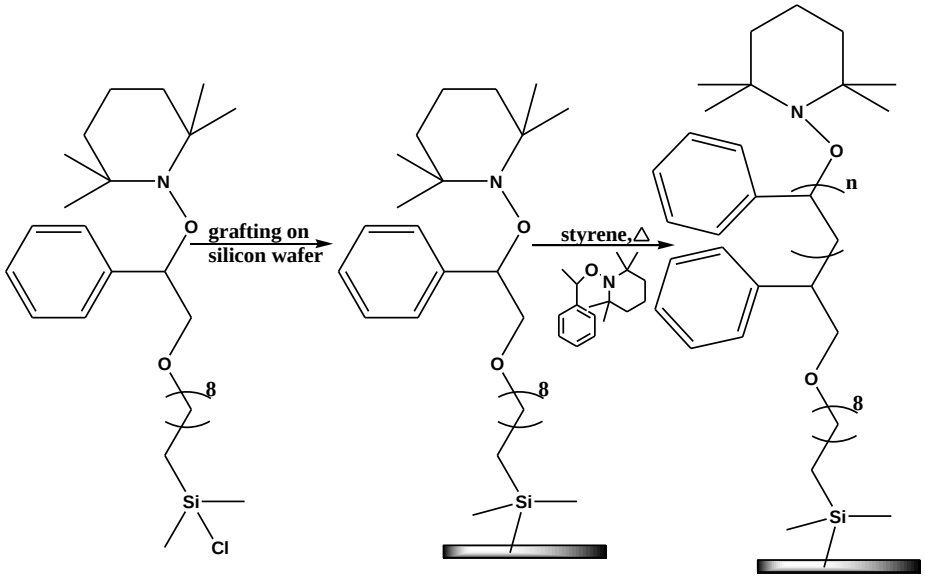

Scheme 1. 22: Principle of SI-NMP on silicon wafer proposed by Hawker et al. [207]

Although SI-NMP has been studied less than SI-ATRP for the functionalization of surfaces, it has known an interest because this technique does not require the use of metal ions, potentially polluting for the final hybrid materials. Two main reviews summarized the different studies concerning SI-NMP from different substrates.[189, 208] To summarize, SI-NMP was applied to design different hybrid particles from the following inorganic substrates: spherical silica particles [101, 103, 104, 209-219], silicon wafer [220, 221], mica pigments [222], magnetic nanoparticles [223], ordered mesoporous silica particles [94], titanium oxide nanoparticles [224]. As mentioned before upon discussing the technique of NMP, two initiating systems can be applied, mono- and bi-component systems. In the following parts, we will focus our attention on the studies reporting the synthesis of core-shell particles by SI-NMP initiated specifically from modified silica particles.

3.4.1 Bi-component initiating system

Billon et al. have demonstrated that the use of bi-component systems was adapted to the synthesis of polymer brushes in NMP from silica particles [211]. A functional diazoic initiator was used, with two trichlorosilane groups, an ester function for cleaving the chains and an initiator function (Scheme 1. 23). The free initiator AIBN was optionally added, and the polymerization of *n*-butyl acrylate was conducted in the presence of SG1 as a control agent.

The polymerization of the grafted chains was controlled (M_w/M_n <1.2) for a wide range of molar masses (4000-145000 g.mol^{-1}).

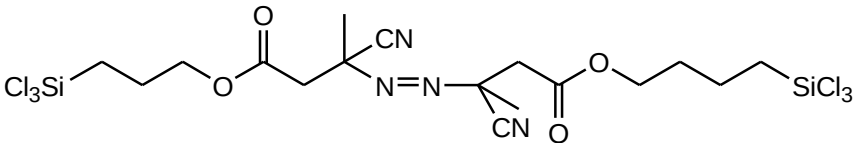

Scheme 1. 23: Symmetrical bi-functional diazoic initiator [211]

A comparison for the polymerization of *n*-butyl acrylate from the surface of silica particles (13 nm diameter) in the presence of SG1 with a mono-component system and bi-component system was studied by the same team [212]. Although in both cases the control was maintained, in the case of bi-component system it was difficult to predict the final molar mass of the grafted chains. Indeed, after the decomposition of symmetrical diazoic initiator, free fragment can migrate in solution and change the free/ grafted initiator ratio. On the contrary, the behavior of the polymerization by unimolecular system was in line with expectations, with experimental M_n values close to the theoretical ones.

The initiators used in NMP are relatively large in comparison to ATRP initiators (Scheme 1. 24). The effect of steric hindrance on the grafting density of the initiator modified particles was directly observed: an ATRP initiator may be grafted with a grafting density of 1.2 molecule.nm^{-2}, the symmetrical diazoic initiator with a density of 0.8 molecule.nm^{-2} and the hindered SG1 based alkoxyamine with a density of only 0.5 molecule.nm^{-2}. [209] This latter value is similar to those obtained by Bourgeat-Lami et al [210] with alkoxyamine described in Scheme 1. 27.

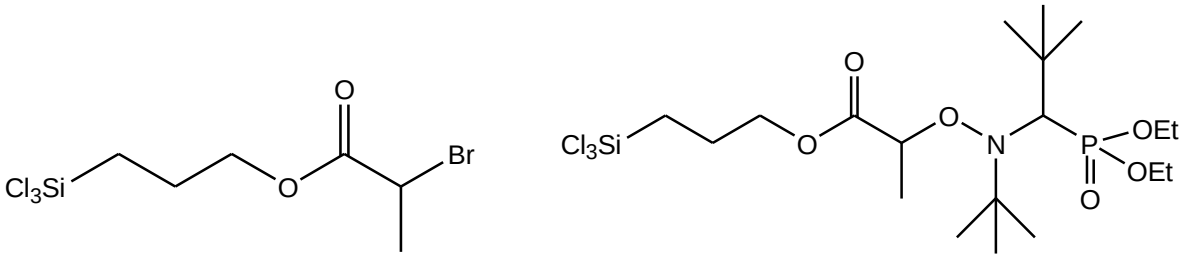

Scheme 1. 24: ATRP and NMP initiators used for comparing the grafting density [209]

3.4.2 In-situ synthesis of alkoxyamine at the surface of the silica

In 2005 both groups of Bourgeat-Lami et al. [214], and Billon et al. [215] implemented a new method for silica surface functionalization: in-situ synthesis of alkoxyamine, followed by SI-NMP polymerization.

A first method consisted of grafting silica with acryloyloxy propyltrimethoxysilane, to synthesize particles carrying acrylates functions.[214] These particles were placed in the presence of AIBN and SG1 to form the alkoxyamine on the surface of the particle, the SG1 acting as a radical scavenger (Scheme 1. 25). The one-step synthesis was successfully tested, and SI-NMP of styrene was well controlled.

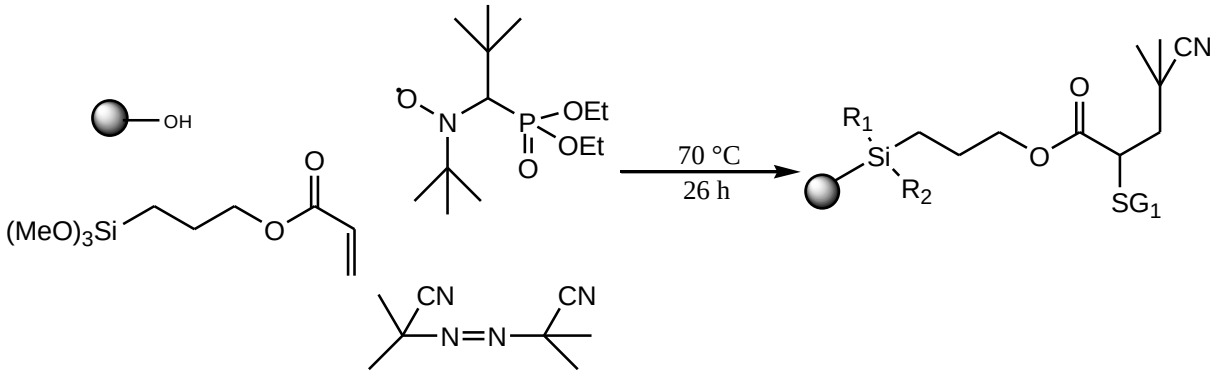

Scheme 1. 25: Synthesis of alkoxyamine in one step on the surface of silica particles [214]

A variant strategy was proposed by Billon et al. [215]: silica particles were functionalized with methacryloyloxypropyl trimethoxysilane and further reacted with an excess of MONAMS alkoxyamine (Scheme 1. 26). The polymerization of *n*-butyl acrylate was performed from these particles in a controlled manner.

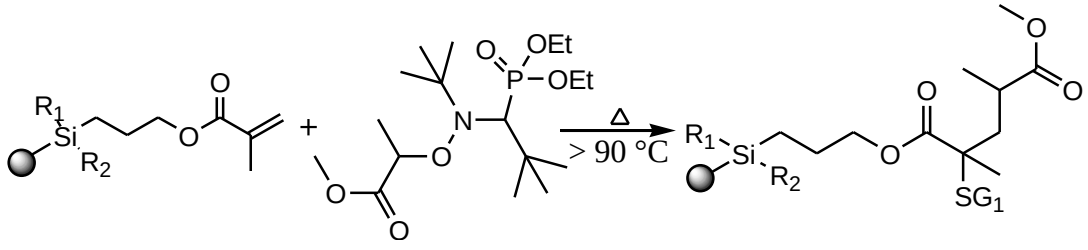

Scheme 1. 26: Addition of MONAMS on grafted methacryloyloxypropyl trimethoxysilane silica [215]

Like in the case of ATRP, NMP allows the good control of the polymer on the surface ($1.1<M_w/M_n<1.6$) and produced high grafting densities for both initiator and polymer. However, those grafting densities remain less than those obtained in SI-ATRP.

3.4.3 Mono-component initiating system

In 2003 Bourgeat-Lami et al. [210] used a pre-formed functional alkoxyamine to modify the surface of silica nanoparticles of diameter 13 nm. The alkoxyamine contained a triethoxysilane function for grafting, a hydrolyzable group to further cleave the polymer for M_n analysis and SG1 as a control agent (Scheme 1. 27). The polymerization was controlled, molar masses of grafted and free polymer chains were similar. The efficiency of initiation of the grafted alkoxyamine was about 40 %.

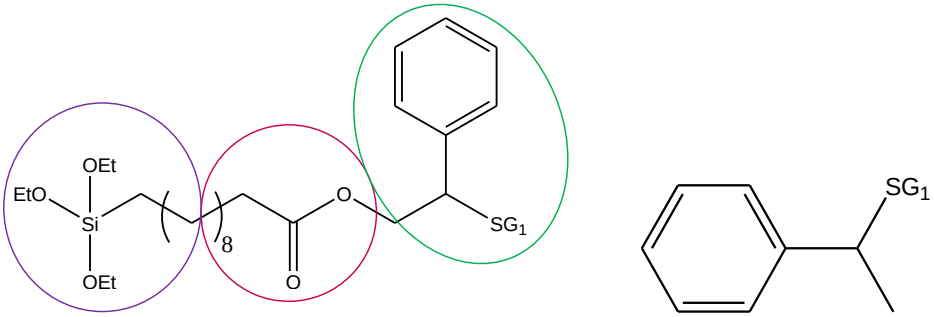

Scheme 1. 27: Grafted and free alkoxyamines used by Bourgeat-Lami [210]

Bonilla-Cruz et al. [216] reported the direct immobilization of the TEMPO nitroxide on silica particles via the formation of a peroxide (Scheme 1. 28), followed by the copolymerization of styrene and maleic anhydride acid by NMP, after thermal activation of the system. The oxoammonium salt TEMPO is brought into contact with the oxide layer on the surface of the silica particle and reacts to covalently attach the TEMPO to the surface.

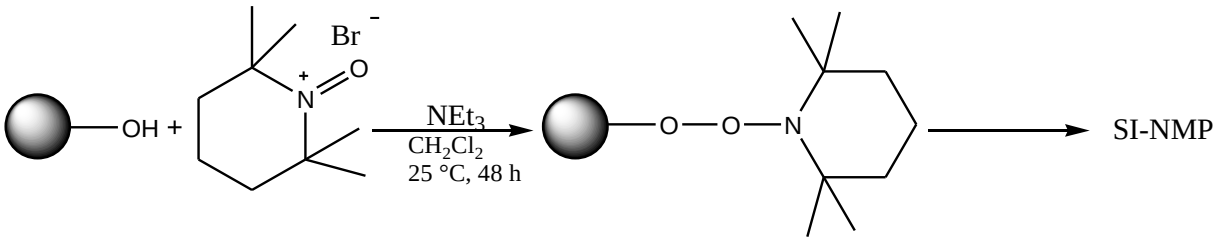

Scheme 1. 28: Direct attachment of TEMPO to silica particles surface [216]

Chevigny al. [101, 103, 104] described the direct attachment of the BB-NHS alkoxyamine to the surface of silica particles pre-functionalized by aminopropyltrimethoxysilane (Scheme 1. 29). SI-NMP of styrene was then conducted in dimethylacetamide at 120 ° C.

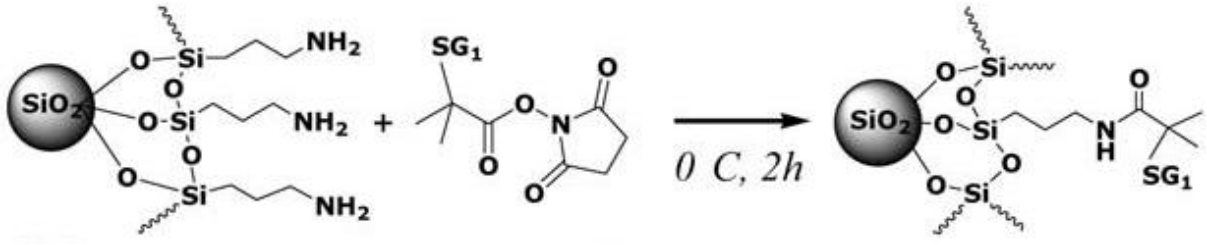

Scheme 1. 29: Overgrafting with BB-NHS to obtain the initiator-grafted silica particle [103]

Another approach was made by Inoubli [225], Billon and Deleuze [217] involving the grafting of a trifunctional alkoxyamine (synthesized by 1,2 addition of Blocbuilder® onto 3-(trimethoxysilyl)propyl acrylate (Scheme 1. 30) on silica surface, and conducting SI-NMP of styrene or *n*-butyl acrylate from the surface to design core-shell particles.

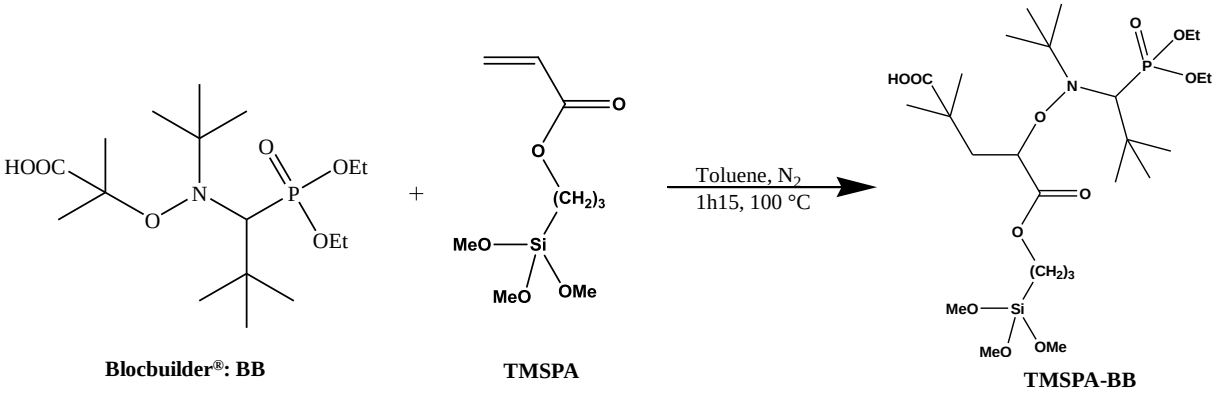

Blocbuilder®: BB **TMSPA** **TMSPA-BB**

Scheme 1. 30: Scheme of trifunctional alkoxyamine TMSPA-BB synthesis [217]

4 Conclusion

At the beginning of this PhD work in 2010, we aimed the synthesis of core@shell hybrid nanoparticles, focusing on silica particles as the core and polymer as the shell. In our work we aim to work with silica particles of diameter less than 100 nm. The process we followed is SI-NMP in miniemulsion from the silica particles in order to obtain at the end the desired particles.

The first results difficulties arose in the in-sufficient hydrophobicity of the silica particles and the control of the cleaved polymer chains. This drove us to conduct more studies and reach out to a new way for the synthesis of the core@shell nanoparticles.

In the first part of our work we focused on studying the control of the shell while targeting high molar masses upon using a new alkoxyamine. Moreover, we studied the possibility of this alkoxyamine to act as a surface-active molecule and play a role in the stabilization of the final polymer particles.

The second part of our work focused on the synthesis of the core@shell nanoparticles and studying the different aspects and characteristics of the grafted polymer chains. We managed to solve the hydrophobicity problem of the silica particles by suggesting a new way for the polymerization.

The third part of our work was addressed for the synthesis of macromolecular stabilizers based on the functionalization of dextran and polyacrylic acid by hydrophobic terpene molecules. And furthermore studying their stabilizing abilities in miniemulsion polymerization of styrene.

References

1. Odian, G., Radical Chain Polymerization, in Principles of Polymerization, Fourth Edition. *John Wiley & Sons* **2004**.
2. Jenkins, A. D.; Jones, R. G.; Moad, G., Terminology for reversible-deactivation radical polymerization previously called "controlled" radical or "living" radical polymerization (IUPAC Recommendations 2010). *Pure and Applied Chemistry* **2010,** 82, (2), 483-491.
3. Szwarc, M., Living polymers. *Nature* **1956,** 178, (4543), 1168-1169.
4. Braunecker, W. A.; Matyjaszewski, K., Controlled/living radical polymerization: Features, developments, and perspectives. *Progress in Polymer Science* **2007,** 32, (1), 93-146.
5. Fischer, H., Unusual selectivities of radical reactions by internal suppression of fast modes. *Journal of the American Chemical Society* **1986,** 108, (14), 3925-3927.
6. Fischer, H., The persistent radical effect in controlled radical polymerizations. *Journal of Polymer Science Part a-Polymer Chemistry* **1999,** 37, (13), 1885-1901.
7. Fischer, H., The persistent radical effect: A principle for selective radical reactions and living radical polymerizations. *Chemical Reviews* **2001,** 101, (12), 3581-3610.
8. Georges, M. K.; Veregin, R. P. N.; Kazmaier, P. M.; Hamer, G. K., Narrow molecular weight resins by a free-radical polymerization process. *Macromolecules* **1993,** 26, (11), 2987-2988.
9. Hawker, C. J.; Bosman, A. W.; Harth, E., New polymer synthesis by nitroxide mediated living radical polymerizations. *Chemical Reviews* **2001,** 101, (12), 3661-3688.
10. Wang, J. S.; Matyjaszewski, K., Controlled living radical polymerization-atom tranfer radical polymerization in the presence of transition-metal complexes. *Journal of the American Chemical Society* **1995,** 117, (20), 5614-5615.
11. Kato, M.; Kamigaito, M.; Sawamoto, M.; Higashimura, T., Polymerization of methyl-methacrylate with the carbon-tetrachloride dichlorotris (triphenylphosphine)ruthenium(II) methylaluminium bis(2,6-di-tert-butylphenoxide) initiating system-possibility of living radical polymerization. *Macromolecules* **1995,** 28, (5), 1721-1723.
12. Minisci, F., Free-radical additions to olefins in presence of redox systems. *Accounts of Chemical Research* **1975,** 8, (5), 165-171.
13. Matyjaszewski, K.; Xia, J. H., Atom transfer radical polymerization. *Chemical Reviews* **2001,** 101, (9), 2921-2990.
14. Jakubowski, W.; Matyjaszewski, K., Activator generated by electron transfer for atom transfer radical polymerization. *Macromolecules* **2005,** 38, (10), 4139-4146.
15. Min, K.; Gao, H. F.; Matyjaszewski, K., Preparation of homopolymers and block copolymers in miniemulsion by ATRP using activators generated by electron transfer (AGET). *Journal of the American Chemical Society* **2005,** 127, (11), 3825-3830.
16. Moad, C. L.; Moad, G.; Rizzardo, E.; Thang, S. H., Chain transfer activity of omega-unsaturated methyl methacrylate oligomers. *Macromolecules* **1996,** 29, (24), 7717-7726.
17. Chiefari, J.; Chong, Y. K.; Ercole, F.; Krstina, J.; Jeffery, J.; Le, T. P. T.; Mayadunne, R. T. A.; Meijs, G. F.; Moad, C. L.; Moad, G.; Rizzardo, E.; Thang, S. H., Living free-radical polymerization by reversible addition-fragmentation chain transfer: The RAFT process. *Macromolecules* **1998,** 31, (16), 5559-5562.
18. Moad, G.; Rizzardo, E.; Thang, S. H., Living radical polymerization by the RAFT process - A first update. *Australian Journal of Chemistry* **2006,** 59, (10), 669-692.
19. Moad, G.; Rizzardo, E.; Thang, S. H., Living Radical Polymerization by the RAFT Process - A Second Update. *Australian Journal of Chemistry* **2009,** 62, (11), 1402-1472.

20. Wayland, B. B.; Poszmik, G.; Mukerjee, S. L.; Fryd, M., Living radical polymerization of acrylates by organocobalt porphyrin complexes. *Journal of the American Chemical Society* **1994,** 116, (17), 7943-7944.
21. Arvanitopoulos, L. D.; Greuel, M. P.; Harwood, H. J., Living free-radical polymerization using alkyl cobaloximes as photoinitiators. *Abstracts of Papers of the American Chemical Society* **1994,** 208, 402-POLY.
22. Debuigne, A.; Poli, R.; Jerome, C.; Jerome, R.; Detrembleur, C., Overview of cobalt-mediated radical polymerization: Roots, state of the art and future prospects. *Progress in Polymer Science* **2009,** 34, (3), 211-239.
23. Debuigne, A.; Caille, J. R.; Jerome, R., Highly efficient cobalt-mediated radical polymerization of vinyl acetate. *Angewandte Chemie-International Edition* **2005,** 44, (7), 1101-1104.
24. Rizzardo E, C. J., Mayadunne RTA, Moad G, Thang SH. , Synthesis of defined polymers by reversible addition-fragmentation chain transfer: the raft process. In: Matyjaszewski K, editor. Controlled/ living radical polymerization. ACS Symp Ser, vol. 768. Washington, DC: Am Chem Soc; 2000. p. 278–96.
25. Stenzel, M. H.; Cummins, L.; Roberts, G. E.; Davis, T. P.; Vana, P.; Barner-Kowollik, C., Xanthate mediated living polymerization of vinyl acetate: A systematic variation in MADIX/RAFT agent structure. *Macromolecular Chemistry and Physics* **2003,** 204, (9), 1160-1168.
26. Stenzel, M. H.; Davis, T. P.; Barner-Kowollik, C., Poly(vinyl alcohol) star polymers prepared via MADIX/RAFT polymerisation. *Chemical Communications* **2004**, (13), 1546-1547.
27. Debuigne, A. J., C.; Jerome, R.; Detrembleur, C.,, Cobalt-Mediated Radical Polymerization. *Materials Science and Technology* **2013**, 67-80.
28. Save, M.; Guillaneuf, Y.; Gilbert, R. G., Controlled radical polymerization in aqueous dispersed media. *Australian Journal of Chemistry* **2006,** 59, (10), 693-711.
29. Zetterlund, P. B.; Kagawa, Y.; Okubo, M., Controlled/living radical polymerization in dispersed systems. *Chemical Reviews* **2008,** 108, (9), 3747-3794.
30. Marestin, C.; Noel, C.; Guyot, A.; Claverie, J., Nitroxide mediated living radical polymerization of styrene in emulsion. *Macromolecules* **1998,** 31, (12), 4041-4044.
31. Charleux, B.; Nicolas, J., Water-soluble SG1-based alkoxyamines: A breakthrough in controlled/living free-radical polymerization in aqueous dispersed media. *Polymer* **2007,** 48, (20), 5813-5833.
32. Nicolas, J.; Charleux, B.; Guerret, O.; Magnet, S. P., Nitroxide-mediated controlled free-radical emulsion polymerization of styrene and n-butyl acrylate with a water-soluble alkoxyamine as initiator. *Angewandte Chemie-International Edition* **2004,** 43, (45), 6186-6189.
33. Qiu, J.; Gaynor, S. G.; Matyjaszewski, K., Emulsion polymerization of n-butyl methacrylate by reverse atom transfer radical polymerization. *Macromolecules* **1999,** 32, (9), 2872-2875.
34. Min, K.; Matyjaszewski, K., Atom transfer radical polymerization in aqueous dispersed media. *Central European Journal of Chemistry* **2009,** 7, (4), 657-674.
35. Lansalot, M.; Farcet, C.; Charleux, B.; Vairon, J. P.; Pirri, R., Controlled free-radical miniemulsion polymerization of styrene using degenerative transfer. *Macromolecules* **1999,** 32, (22), 7354-7360.
36. Tonnar, J.; Lacroix-Desmazes, P.; Boutevin, B., Living radical ab initio emulsion polymerization of n-butyl acrylate by reverse iodine transfer polymerization (RITP): Use of persulfate as both initiator and oxidant. *Macromolecules* **2007,** 40, (17), 6076-6081.

37. Monteiro, M. J.; Adamy, M. M.; Leeuwen, B. J.; van Herk, A. M.; Destarac, M., A "living" radical ab initio emulsion polymerization of styrene using a fluorinated xanthate agent. *Macromolecules* **2005,** 38, (5), 1538-1541.
38. Ferguson, C. J.; Hughes, R. J.; Pham, B. T. T.; Hawkett, B. S.; Gilbert, R. G.; Serelis, A. K.; Such, C. H., Effective ab initio emulsion polymerization under RAFT control. *Macromolecules* **2002,** 35, (25), 9243-9245.
39. Freal-Saison, S.; Save, M.; Bui, C.; Charleux, B.; Magnet, S., Emulsifier-free controlled free-radical emulsion polymerization of styrene via RAFT using dibenzyltrithiocarbonate as a chain transfer agent and acrylic acid as an ionogenic comonomer: Batch and spontaneous phase inversion processes. *Macromolecules* **2006,** 39, (25), 8632-8638.
40. Charleux, B.; Delaittre, G.; Rieger, J.; D'Agosto, F., Polymerization-Induced Self-Assembly: From Soluble Macromolecules to Block Copolymer Nano-Objects in One Step. *Macromolecules* **2012,** 45, (17), 6753-6765.
41. Farcet, C.; Lansalot, M.; Charleux, B.; Pirri, R.; Vairon, J. P., Mechanistic aspects of nitroxide-mediated controlled radical polymerization of styrene in miniemulsion, using a water-soluble radical initiator. *Macromolecules* **2000,** 33, (23), 8559-8570.
42. de Brouwer, H.; Tsavalas, J. G.; Schork, F. J.; Monteiro, M. J., Living radical polymerization in miniemulsion using reversible addition-fragmentation chain transfer. *Macromolecules* **2000,** 33, (25), 9239-9246.
43. Moad, G.; Chiefari, J.; Chong, Y. K.; Krstina, J.; Mayadunne, R. T. A.; Postma, A.; Rizzardo, E.; Thang, S. H., Living free radical polymerization with reversible addition-fragmentation chain transfer (the life of RAFT). *Polymer International* **2000,** 49, (9), 993-1001.
44. Detrembleur, C.; Debuigne, A.; Bryaskova, R.; Charleux, B.; Jerome, R., Cobalt-mediated radical polymerization of vinyl acetate in miniemulsion: Very fast formation of stable poly(vinyl acetate) latexes at low temperature. *Macromolecular Rapid Communications* **2006,** 27, (1), 37-41.
45. Butte, A.; Storti, G.; Morbidelli, M., Miniemulsion living free radical polymerization of styrene. *Macromolecules* **2000,** 33, (9), 3485-3487.
46. Hawker, C. J., Molecular weight control by a living free-radical polymerization process. *Journal of the American Chemical Society* **1994,** 116, (24), 11185-11186.
47. Hawker, C. J.; Barclay, G. G.; Orellana, A.; Dao, J.; Devonport, W., Initiating systems for nitroxide-mediated "living" free radical polymerizations: Synthesis and evaluation. *Macromolecules* **1996,** 29, (16), 5245-5254.
48. Moad, G.; Rizzardo, E.; Solomon, D. H., Selectivity of the reaction of free-radicals with styrene. *Macromolecules* **1982,** 15, (3), 909-914.
49. Rizzardo, E.; Solomon, D. H., New method for investigating the mechanism of initiation of radical polymerization. *Polymer Bulletin* **1979,** 1, (8), 529-534.
50. Goto, A.; Fukuda, T., Kinetics of living radical polymerization. *Progress in Polymer Science* **2004,** 29, (4), 329-385.
51. Nicolas, J.; Guillaneuf, Y.; Lefay, C.; Bertin, D.; Gigmes, D.; Charleux, B., Nitroxide-mediated polymerization. *Progress in Polymer Science* **2013,** 38, (1), 63-235.
52. Grimaldi, S.; Finet, J. P.; Le Moigne, F.; Zeghdaoui, A.; Tordo, P.; Benoit, D.; Fontanille, M.; Gnanou, Y., Acyclic beta-phosphonylated nitroxides: A new series of counter-radicals for "living"/controlled free radical polymerization. *Macromolecules* **2000,** 33, (4), 1141-1147.

53. Grimaldi, S.; Finet, J. P.; Zeghdaoui, A.; Tordo, P., Synthesis of a new class of nitroxyl radicals and application to "living" free radical polymerization. *Abstracts of Papers of the American Chemical Society* **1997,** 213, 302-POLY.
54. Benoit, D.; Chaplinski, V.; Braslau, R.; Hawker, C. J., Development of a universal alkoxyamine for "living" free radical polymerizations. *Journal of the American Chemical Society* **1999,** 121, (16), 3904-3920.
55. Miele, S.; Nesvadba, P.; Studer, A., 1-tert-Butyl-3,3,5,5-tetraalkyl-2-piperazinon-4-oxyls: Highly Efficient Nitroxides for Controlled Radical Polymerization. *Macromolecules* **2009,** 42, (7), 2419-2427.
56. Siegenthaler, K. O.; Studer, A., Nitroxide-mediated radical polymerization/increase of steric demand in nitroxides. How much is too much? *Macromolecules* **2006,** 39, (4), 1347-1352.
57. Schulte, T.; Siegenthaler, K. O.; Luftmann, H.; Letzel, M.; Studer, A., Nitroxide-mediated polymerization of N-isopropylacrylamide: Electrospray ionization mass spectrometry, matrix-assisted laser desorption ionization mass spectrometry, and multiple-angle laser light scattering studies on nitroxide-terminated poly-N-isopropylacrylamides. *Macromolecules* **2005,** 38, (16), 6833-6840.
58. Benoit, D.; Grimaldi, S.; Robin, S.; Finet, J. P.; Tordo, P.; Gnanou, Y., Kinetics and mechanism of controlled free-radical polymerization of styrene and n-butyl acrylate in the presence of an acyclic beta-phosphonylated nitroxide. *Journal of the American Chemical Society* **2000,** 122, (25), 5929-5939.
59. Benoit, D.; Harth, E.; Fox, P.; Waymouth, R. M.; Hawker, C. J., Accurate structural control and block formation in the living polymerization of 1,3-dienes by nitroxide-mediated procedures. *Macromolecules* **2000,** 33, (2), 363-370.
60. Diaz, T.; Fischer, A.; Jonquieres, A.; Brembilla, A.; Lochon, P., Controlled polymerization of functional monomers and synthesis of block copolymers using beta-phosphonylated nitroxide. *Macromolecules* **2003,** 36, (7), 2235-2241.
61. Hua, F. J.; Jiang, X. G.; Li, D. J.; Zhao, B., Well-defined thermosensitive, water-soluble polyacrylates and polystyrenics with short pendant oligo (ethylene glycol) groups synthesized by nitroxide-mediated radical polymerization. *Journal of Polymer Science Part a-Polymer Chemistry* **2006,** 44, (8), 2454-2467.
62. Zhao, B.; Li, D. J.; Hua, F. J.; Green, D. R., Synthesis of thermosensitive water-soluble polystyrenics with pendant methoxyoligo(ethylene glycol) groups by nitroxide-mediated radical polymerization. *Macromolecules* **2005,** 38, (23), 9509-9517.
63. Couvreur, L.; Lefay, C.; Belleney, J.; Charleux, B.; Guerret, O.; Magnet, S., First nitroxide-mediated controlled free-radical polymerization of acrylic acid. *Macromolecules* **2003,** 36, (22), 8260-8267.
64. Lefay, C.; Belleney, J.; Charleux, B.; Guerret, O.; Magnet, S., End-group characterization of poly(acrylic acid) prepared by nitroxide-mediated controlled free-radical polymerization. *Macromolecular Rapid Communications* **2004,** 25, (13), 1215-1220.
65. Karaky, K.; Billon, L.; Pouchan, C.; Desbrieres, J., Amphiphilic gradient copolymers shape composition influence on the surface/bulk properties. *Macromolecules* **2007,** 40, (3), 458-464.
66. Schierholz, K.; Givehchi, M.; Fabre, P.; Nallet, F.; Papon, E.; Guerret, O.; Gnanou, Y., Acrylamide-based amphiphilic block copolymers via nitroxide-mediated radical polymerization. *Macromolecules* **2003,** 36, (16), 5995-5999.
67. Phan, T. N. T.; Bertin, D., Synthesis of water-soluble homopolymers and block copolymers in homogeneous aqueous solution via nitroxide-mediated polymerization. *Macromolecules* **2008,** 41, (5), 1886-1895.

68. Nicolay, R.; Marx, L.; Hemery, P.; Matyjaszewski, K., Synthesis and evaluation of a functional, water- and organo-soluble nitroxide for "Living" free radical polymerization. *Macromolecules* **2007,** 40, (17), 6067-6075.
69. Fischer, A.; Brembilla, A.; Lochon, P., Nitroxide-mediated radical polymerization of 4-vinylpyridine: Study of the pseudo-living character of the reaction and influence of temperature and nitroxide concentration. *Macromolecules* **1999,** 32, (19), 6069-6072.
70. Chen, Z. J.; Wang, Y.; Feng, Y.; Jiang, X. Q.; Yang, C. Z.; Wang, M., Synthesis of hydroxyl-terminated copolymer of styrene and 4-vinylpyridine via nitroxide-mediated living radical polymerization. *Journal of Applied Polymer Science* **2004,** 91, (3), 1842-1847.
71. Zaremski, M. Y.; Xin, C.; Orlova, A. P.; Blagodatskikh, I. V.; Golubev, V. B., General features and specifics of the kinetics of the pseudoliving radical polymerization of 4-vinylpyridine and styrene mediated by TEMPO. *Polym. Sci. Ser. B* **2011,** 53, (7-8), 476-483.
72. Escale, P.; Rubatat, L.; Derail, C.; Save, M.; Billon, L., pH Sensitive Hierarchically Self-Organized Bioinspired Films. *Macromolecular Rapid Communications* **2011,** 32, (14), 1072-1076.
73. Guillaneuf, Y.; Gigmes, D.; Marque, S. R. A.; Tordo, P.; Bertin, D., Nitroxide-mediated polymerization of methyl methacrylate using an SG1-based alkoxyamine: How the penultimate effect could lead to uncontrolled and unliving polymerization. *Macromolecular Chemistry and Physics* **2006,** 207, (14), 1278-1288.
74. Dire, C.; Belleney, J.; Nicolas, J.; Bertin, D.; Magnet, S.; Charleux, B., beta-hydrogen transfer from poly(methyl methacrylate) propagating radicals to the nitroxide SG1: Analysis of the chain-end and determination of the rate constant. *Journal of Polymer Science Part a-Polymer Chemistry* **2008,** 46, (18), 6333-6345.
75. McHale, R.; Aldabbagh, F.; Zetterlund, P. B., The role of excess nitroxide in the SG1 (N-tert-butyl-N- 1-diethylphosphono-(2,2-dimethylpropyl) nitroxide)-mediated polymerization of methyl methacrylate. *Journal of Polymer Science Part a-Polymer Chemistry* **2007,** 45, (11), 2194-2203.
76. Charleux, B.; Nicolas, J.; Guerret, O., Theoretical expression of the average activation-deactivation equilibrium constant in controlled/living free-radical copolymerization operating via reversible termination. Application to a strongly improved control in nitroxide-mediated polymerization of methyl methacrylate. *Macromolecules* **2005,** 38, (13), 5485-5492.
77. Nicolas, J.; Dire, C.; Mueller, L.; Belleney, J.; Charleux, B.; Marque, S. R. A.; Bertin, D.; Magnet, S.; Couvreur, L., Living character of polymer chains prepared via nitroxide-mediated controlled free-radical polymerization of methyl methacrylate in the presence of a small amount of styrene at low temperature. *Macromolecules* **2006,** 39, (24), 8274-8282.
78. Nicolas, J.; Couvreur, P.; Charleux, B., Comblike polymethacrylates with poly(ethylene glycol) side chains via nitroxide-mediated controlled free-radical polymerization. *Macromolecules* **2008,** 41, (11), 3758-3761.
79. Dire, C.; Charleux, B.; Magnet, S.; Couvreur, L., Nitroxide-mediated copolymerization of methacrylic acid and styrene to form amphiphilic diblock copolymers. *Macromolecules* **2007,** 40, (6), 1897-1903.
80. Guillaneuf, Y.; Gigmes, D.; Marque, S. R. A.; Astolfi, P.; Greci, L.; Tordo, P.; Bertin, D., First effective nitroxide-mediated polymerization of methyl methacrylate. *Macromolecules* **2007,** 40, (9), 3108-3114.
81. Bertin, D.; Gigmes, D.; Marque, S. R. A.; Tordo, P., Polar, steric, and stabilization effects in alkoxyamines C-ON bond homolysis: A multiparameter analysis. *Macromolecules* **2005,** 38, (7), 2638-2650.
82. Studer, A.; Schulte, T., Nitroxide-mediated radical processes. *Chemical Record* **2005,** 5, (1), 27-35.

83. Marque, S., Influence of the nitroxide structure on the homolysis rate constant of alkoxyamines: A Taft-Ingold analysis. *Journal of Organic Chemistry* **2003,** 68, (20), 7582-7590.
84. Marque, S.; Fischer, H.; Baier, E.; Studer, A., Factors influencing the C-O bond homolysis of alkoxyamines: Effects of H-bonding and polar substituents. *Journal of Organic Chemistry* **2001,** 66, (4), 1146-1156.
85. Marque, S.; Le Mercier, C.; Tordo, P.; Fischer, H., Factors influencing the C-O-bond homolysis of trialkylhydroxylamines. *Macromolecules* **2000,** 33, (12), 4403-4410.
86. Nicolas, J.; Charleux, B.; Guerret, O.; Magnet, S., Novel SG1-Based water-soluble alkoxyamine for nitroxide-mediated controlled free-radical polymerization of styrene and n-butyl acrylate in miniemulsion. *Macromolecules* **2004,** 37, (12), 4453-4463.
87. Farcet, C.; Nicolas, J.; Charleux, B., Kinetic study of the nitroxide-mediated controlled free-radical polymerization of n-butyl acrylate in aqueous miniemulsions. *Journal of Polymer Science Part a-Polymer Chemistry* **2002,** 40, (24), 4410-4420.
88. Beaudoin, E.; Bertin, D.; Gigmes, D.; Marque, S. R. A.; Siri, D.; Tordo, P., Alkoxyamine C-ON bond homolysis: Stereoelectronic effects. *European Journal of Organic Chemistry* **2006**, (7), 1755-1768.
89. Nicolas, J.; Charleux, B.; Guerret, O.; Magnet, S., Nitroxide-mediated controlled free-radical emulsion polymerization using a difunctional water-soluble alkoxyamine initiator. Toward the control of particle size, particle size distribution, and the synthesis of triblock copolymers. *Macromolecules* **2005,** 38, (24), 9963-9973.
90. Gigmes, D.; Dufils, P. E.; Gle, D.; Bertin, D.; Lefay, C.; Guillaneuf, Y., Intermolecular radical 1,2-addition of the BlocBuilder MA alkoxyamine onto activated olefins: a versatile tool for the synthesis of complex macromolecular architecture. *Polymer Chemistry* **2011,** 2, (8), 1624-1631.
91. Dufils, P. E.; Chagneux, N.; Gigmes, D.; Trimaille, T.; Marque, S. R. A.; Bertin, D.; Tordo, P., Intermolecular radical addition of alkoxyamines onto olefins: An easy access to advanced macromolecular architectures. *Polymer* **2007,** 48, (18), 5219-5225.
92. Paillet, S.; Roncin, A.; Clisson, G.; Pembouong, G.; Billon, L.; Derail, C.; Save, M., Combination of nitroxide-mediated polymerization and SET-LRP for the synthesis of high molar mass branched and star-branched poly(n-butyl acrylate) characterized by size exclusion chromatography and rheology. *Journal of Polymer Science Part a-Polymer Chemistry* **2012,** 50, (14), 2967-2979.
93. Inoubli, R.; Dagreou, S.; Delville, M. H.; Lapp, A.; Peyrelasse, J.; Billon, L., In situ thermo-dependant trapping of carbon radicals: a versatile route to well-defined polymer-grafted silica nanoparticles. *Soft Matter* **2007,** 3, (8), 1014-1024.
94. Blas, H.; Save, M.; Boissiere, C.; Sanchez, C.; Charleux, B., Surface-Initiated Nitroxide-Mediated Polymerization from Ordered Mesoporous Silica. *Macromolecules* **2011,** 44, (8), 2577-2588.
95. Rodlert, M.; Harth, E.; Rees, I.; Hawker, C. J., End-group fidelity in nitroxide-mediated living free-radical polymerizations. *Journal of Polymer Science Part a-Polymer Chemistry* **2000,** 38, 4749-4763.
96. Hill, N. L.; Braslau, R., Synthesis of arylethyl-functionalized N-alkoxyamine initiators and use in nitroxide-mediated radical polymerization. *Journal of Polymer Science Part a-Polymer Chemistry* **2007,** 45, (11), 2341-2349.
97. Binder, W. H.; Gloger, D.; Weinstabl, H.; Allmaier, G.; Pittenauer, E., Telechelic poly(N-isopropylacrylamides) via nitroxide-mediated controlled polymerization and "click" chemistry: Livingness and "grafting-from" methodology. *Macromolecules* **2007,** 40, (9), 3097-3107.

98. Ruehl, J.; Morimoto, C.; Stevens, D. J.; Braslau, R., Carboxylic acid- and hydroxy-functionalized alkoxyamine initiators for nitroxide mediated radical polymerization. *Reactive & Functional Polymers* **2008,** 68, (11), 1563-1577.
99. Vinas, J.; Chagneux, N.; Gigmes, D.; Trimaille, T.; Favier, A.; Bertin, D., SG1-based alkoxyamine bearing a N-succinimidyl ester: A versatile tool for advanced polymer synthesis. *Polymer* **2008,** 49, (17), 3639-3647.
100. Trimaille, T.; Mabrouk, K.; Monnier, V.; Charles, L.; Bertin, D.; Gigmes, D., SG1-Functionalized Peptides as Precursors for Polymer-Peptide Conjugates: A Straightforward Approach. *Macromolecules* **2010,** 43, (11), 4864-4870.
101. Chevigny, C.; Gigmes, D.; Bertin, D.; Jestin, J.; Boue, F., Polystyrene grafting from silica nanoparticles via nitroxide-mediated polymerization (NMP): synthesis and SANS analysis with the contrast variation method. *Soft Matter* **2009,** 5, (19), 3741-3753.
102. Parvole, J.; Ahrens, L.; Blas, H.; Vinas, J.; Boissiere, C.; Sanchez, C.; Save, M.; Charleux, B., Grafting Polymer Chains Bearing an N-Succinimidyl Activated Ester End-Group onto Primary Amine-Coated Silica Particles and Application of a Simple, One-Step Approach via Nitroxide-Mediated Controlled/Living Free-Radical Polymerization. *Journal of Polymer Science Part A-Polymer Chemistry* **2010,** 48, (1), 173-185.
103. Chevigny, C.; Gigmes, D.; Bertin, D.; Schweins, R.; Jestin, J.; Boue, F., Controlled grafting of polystyrene on silica nanoparticles using NMP: a new route without free initiator to tune the grafted chain length. *Polymer Chemistry* **2011,** 2, (3), 567-571.
104. Chevigny, C.; Dalmas, F.; Di Cola, E.; Gigmes, D.; Bertin, D.; Boue, F.; Jestin, J., Polymer-Grafted-Nanoparticles Nanocomposites: Dispersion, Grafted Chain Conformation, and Rheological Behavior. *Macromolecules* **2011,** 44, (1), 122-133.
105. Nicolas, J.; Ruzette, A. V.; Farcet, C.; Gerard, P.; Magnet, S.; Charleux, B., Nanostructured latex particles synthesized by nitroxide-mediated controlled/living free-radical polymerization in emulsion. *Polymer* **2007,** 48, (24), 7029-7040.
106. Fischer, H., The persistent radical effect in "living" radical polymerization. *Macromolecules* **1997,** 30, (19), 5666-5672.
107. Smith, W. V.; Ewart, R. H., Kinetics of emulsion polymerization. *Journal of Chemical Physics* **1948,** 16, (6), 592-599.
108. Landfester, K., Polyreactions in miniemulsions. *Macromolecular Rapid Communications* **2001,** 22, (12), 896-936.
109. Asua, J. M., Miniemulsion polymerization. *Progress in Polymer Science* **2002,** 27, (7), 1283-1346.
110. Schork, F. J.; Luo, Y. W.; Smulders, W.; Russum, J. P.; Butte, A.; Fontenot, K., Miniemulsion polymerization. In *Polymer Particles*, Okubo, M., Ed. 2005; Vol. 175, pp 129-255.
111. Ugelstad, J.; Elaasser, M. S.; Vanderho.Jw, Emulsion polymerization-initiation of polymerization in monomer droplets. *Journal of Polymer Science Part C-Polymer Letters* **1973,** 11, (8), 503-513.
112. Carless, J. E.; Hallwort.Gw, Viscosity of emulsifying agents at oil-water interfaces. *Journal of Colloid and Interface Science* **1968,** 26, (1), 75-&.
113. Hallwort.Gw; Carless, J. E., Stabilization of oil-in-water emulsion by alky sulfates-influence of nature of oil on stability. *Journal of Pharmacy and Pharmacology* **1972,** 24, P71-&.
114. Hallwort.Gw; Carless, J. E., Stabilization of oil-in-water emulsion by alky sulfates-effect of a long chain. *Journal of Pharmacy and Pharmacology* **1973,** 25, P87-P95.

115. Azad, A. R. M.; Ugelstad, J.; Fitch, R. M.; Hansen, F. K., Emulsification and Emulsion Polymerization of Styrene Using Mixtures of Cationic Surfactant and Long Chain Fatty Alcohols or Alkanes as Emulsifiers. *ACS Symposium Series* **1976,** 24, 1-23.
116. Davies SS, S. A., Theory and practice of emulsion technology. . *New York: Academic Press* **1976**, 325.
117. Durbin, D. P.; Elaasser, M. S.; Poehlein, G. W.; Vanderhoff, J. W., Influence of monomer pre-emulsification on formation of particles from monomer drops in emulsion polymerization. *Journal of Applied Polymer Science* **1979,** 24, (3), 703-707.
118. Chou, Y. J.; Elaasser, M. S.; Vanderhoff, J. W., Mechanism of emulsification of styrene using hexadecyl trimethylammonium bromide-cetyl alcohol mixtures. *Journal of Dispersion Science and Technology* **1980,** 1, (2), 129-150.
119. Landfester, K.; Bechthold, N.; Tiarks, F.; Antonietti, M., Miniemulsion polymerization with cationic and nonionic surfactants: A very efficient use of surfactants for heterophase polymerization. *Macromolecules* **1999,** 32, (8), 2679-2683.
120. Bechthold, N.; Tiarks, F.; Willert, M.; Landfester, K.; Antonietti, M., Miniemulsion polymerization: Applications and new materials. *Macromolecular Symposia* **2000,** 151, 549-555.
121. Ostwald, W., Lehrbuch der Allgemeinen Chemie, vol. 2, part 1. Leipzig, Germany. **1896**.
122. Reimers, J. L.; Skelland, A. H. P.; Schork, F. J., Monomer droplet stability in emulsion-polymerized latexes. *Polymer Reaction Engineering* **1995,** 3, (3), 235-260.
123. Miller, C. M.; Blythe, P. J.; Sudol, E. D.; Silebi, C. A.; Elaasser, M. S., Effect of the presence of polymer in miniemulsion droplets on the kinetics of polymerization. *Journal of Polymer Science Part a-Polymer Chemistry* **1994,** 32, (12), 2365-2376.
124. Miller, C. M.; Sudol, E. D.; Silebi, C. A.; Elaasser, M. S., Polymerization of miniemulsions prepared from polystyrene in styrene solutions. 2. kinetics and mechanism *Macromolecules* **1995,** 28, (8), 2765-2771.
125. Cunningham, M. F.; Tortosa, K.; Ma, J. W.; McAuley, K. B.; Keoshkerian, B.; Georges, M. K., Nitroxide mediated living radical polymerization in miniemulsion. *Macromolecular Symposia* **2002,** 182, 273-282.
126. Cunningham, M. F.; Xie, M.; McAuley, K. B.; Keoshkerian, B.; Georges, M. K., Nitroxide-mediated styrene miniemulsion polymerization. *Macromolecules* **2002,** 35, (1), 59-66.
127. Charleux, B., Nitroxide-mediated polymerization in miniemulsion: A direct way from bulk to aqueous dispersed systems. In *Advances in Controlled/Living Radical Polymerization*, Matyjaszewski, K., Ed. 2003; Vol. 854, pp 438-451.
128. Lin, M.; Cunningham, M. F.; Keoshkerian, B., Achieving high conversions in nitroxide-mediated living styrene miniemulsion polymerization. *Macromolecular Symposia* **2004,** 206, 263-274.
129. Farcet, C.; Charleux, B., Nitroxide-mediated miniemulsion polymerization of n-butyl acrylate: Synthesis of controlled homopolymers and gradient copolymers with styrene. *Macromolecular Symposia* **2002,** 182, 249-260.
130. Farcet, C.; Charleux, B.; Pirri, R., Poly(n-butyl acrylate) homopolymer and poly n-butyl acrylate-b-(n-butyl acrylate-co-styrene) block copolymer prepared via nitroxide-mediated living/controlled radical polymerization in miniemulsion. *Macromolecules* **2001,** 34, (12), 3823-3826.
131. Cunningham, M. F.; Tortosa, K.; Lin, M.; Keoshkerian, B.; Georges, M. K., Influence of camphorsulfonic acid in nitroxide-mediated styrene miniemulsion polymerization. *Journal of Polymer Science Part a-Polymer Chemistry* **2002,** 40, (16), 2828-2841.

132. Tortosa, K.; Smith, J. A.; Cunningham, M. F., Synthesis of polystyrene-block-poly (butyl acrylate) copolymers using nitroxide-mediated living radical polymerization in miniemulsion. *Macromolecular Rapid Communications* **2001,** 22, (12), 957-961.
133. Pan, G. F.; Sudol, E. D.; Dimonie, V. L.; El-Aasser, M. S., Nitroxide-mediated living free radical miniemulsion polymerization of styrene. *Macromolecules* **2001,** 34, (3), 481-488.
134. Pan, G. F.; Sudol, E. D.; Dimonie, V. L.; El-Aasser, M. S., Surfactant concentration effects on nitroxide-mediated living free radical miniemulsion polymerization of styrene. *Macromolecules* **2002,** 35, (18), 6915-6919.
135. Lin, M.; Hsu, J. C. C.; Cunningham, M. F., Role of sodium dodecylbenzenesulfonate in 2,2,6,6-tetramethy-1-piperidinyloxy-mediated styrene miniemulsion polymerization. *Journal of Polymer Science Part a-Polymer Chemistry* **2006,** 44, (20), 5974-5986.
136. Nakamura, T.; Zetterlund, P. B.; Okubo, M., Particle size effects in TEMPO-mediated radical polymerization of styrene in aqueous miniemulsion. *Macromolecular Rapid Communications* **2006,** 27, (23), 2014-2018.
137. Zetterlund, P. B.; Nakamura, T.; Okubo, M., Mechanistic investigation of particle size effects in TEMPO mediated radical polymerization of styrene in aqueous miniemulsion. *Macromolecules* **2007,** 40, (24), 8663-8672.
138. Farcet, C.; Belleney, J.; Charleux, B.; Pirri, R., Structural characterization of nitroxide-terminated poly(n-butyl acrylate) prepared in bulk and miniemulsion polymerizations. *Macromolecules* **2002,** 35, (13), 4912-4918.
139. Pan, G. F.; Sudol, E. D.; Dimonie, V. L.; El-Aasser, M. S., Thermal self-initiation of styrene in the presence of TEMPO radicals: Bulk and miniemulsion. *Journal of Polymer Science Part a-Polymer Chemistry* **2004,** 42, (19), 4921-4932.
140. Cunningham, M. F.; Ng, D. C. T.; Milton, S. G.; Keoshkerian, B., Low temperature TEMPO-mediated styrene polymerization in miniemulsion. *Journal of Polymer Science Part a-Polymer Chemistry* **2006,** 44, (1), 232-242.
141. Zetterlund, P. B.; Alam, M. N.; Minami, H.; Okubo, M., Nitroxide-mediated controlled/living free radical copolymerization of styrene and divinylbenzene in aqueous miniemulsion. *Macromolecular Rapid Communications* **2005,** 26, (12), 955-960.
142. Alam, M. N.; Zetterlund, P. B.; Okubo, M., Network formation in nitroxide-mediated radical copolymerization of styrene and divinylbenzene in miniemulsion. *Macromolecular Chemistry and Physics* **2006,** 207, (19), 1732-1741.
143. Ma, J. W.; Cunningham, M. F.; McAuley, K. B.; Keoshkerian, B.; Georges, M. K., Nitroxide partitioning between styrene and water. *Journal of Polymer Science Part a-Polymer Chemistry* **2001,** 39, (7), 1081-1089.
144. Ma, J. W.; Smith, J. A.; McAuley, K. B.; Cunningham, M. F.; Keoshkerian, B.; Georges, M. K., Nitroxide-mediated radical polymerization of styrene in miniemulsion: model studies of alkoxyamine-initiated systems. *Chemical Engineering Science* **2003,** 58, (7), 1163-1176.
145. Keoshkerian, B.; MacLeod, P. J.; Georges, M. K., Block copolymer synthesis by a miniemulsion stable free radical polymerization process. *Macromolecules* **2001,** 34, (11), 3594-3599.
146. Charleux, B., Theoretical aspects of controlled radical polymerization in a dispersed medium. *Macromolecules* **2000,** 33, (15), 5358-5365.
147. Cunningham, M. F., Recent progress in nitroxide-mediated polymerizations in miniemulsion. *Comptes Rendus Chimie* **2003,** 6, (11-12), 1351-1374.
148. Daniel, J. C.; Pichot, C., *Les latex synthétiques, Elaboration, propriétés, applications*. TEC and DOC ed.; Lavoisier: 2006.

149. Gilbert, R. G., *Emulsion Polymerization. A Mechanistic Approach*. Academic Press: New York: 1995.
150. van Herk, A., *Chemistry and Technology of Emulsion Polymerisation*. Ed.; Blackwell Publishing Ltd.: Oxford: 2005.
151. Lovell, P. A.; El-Aasser, M. S., *Emulsion Polymerization and Emulsion Polymers [*John Wiley and Sons: 1997.
152. Monteiro, M. J.; Cunningham, M. F., Polymer Nanoparticles via Living Radical Polymerization in Aqueous Dispersions: Design and Applications. *Macromolecules* **2012,** 45, (12), 4939-4957.
153. Maehata, H.; Buragina, C.; Cunningham, M.; Keoshkerian, B., Compartmentalization in TEMPO-mediated styrene miniemulsion polymerization. *Macromolecules* **2007,** 40, (20), 7126-7131.
154. Simms, R. W.; Cunningham, M. F., Compartmentalization of reverse atom transfer radical polymerization in miniemulsion. *Macromolecules* **2008,** 41, (14), 5148-5155.
155. Zetterlund, P. B.; Wakamatsu, J.; Okubo, M., Nitroxide-Mediated Radical Polymerization of Styrene in Aqueous Microemulsion: Initiator Efficiency, Compartmentalization, and Nitroxide Phase Transfer. *Macromolecules* **2009,** 42, (18), 6944-6952.
156. Guo, Y.; Zetterlund, P. B., Rate-Enhanced Nitroxide-Mediated Miniemulsion Polymerization. *Acs Macro Letters* **2012,** 1, (6), 748-752.
157. Kitayama, Y.; Tomoeda, S.; Okubo, M., Experimental Evidence and Beneficial Use of Confined Space Effect in Nitroxide-Mediated Radical Microemulsion Polymerization (Microemulsion NMP) of n-Butyl Acrylate. *Macromolecules* **2012,** 45, (19), 7884-7889.
158. Wakamatsu, J.; Kawasaki, M.; Zetterlund, P. B.; Okubo, M., Nitroxide-mediated radical polymerization in microemulsion. *Macromolecular Rapid Communications* **2007,** 28, (24), 2346-2353.
159. Tomoeda, S.; Kitayama, Y.; Wakamatsu, J.; Minami, H.; Zetterlund, P. B.; Okubo, M., Nitroxide-Mediated Radical Polymerization in Microemulsion (Microemulsion NMP) of n-Butyl Acrylate. *Macromolecules* **2011,** 44, (14), 5599-5604.
160. Dupin, D.; Schmid, A.; Balmer, J. A.; Armes, S. P., Efficient synthesis of poly(2-vinylpyridine)-silica colloidal nanocomposite particles using a cationic azo initiator. *Langmuir* **2007,** 23, (23), 11812-11818.
161. Fielding, L. A.; Tonnar, J.; Armes, S. P., All-Acrylic Film-Forming Colloidal Polymer/Silica Nanocomposite Particles Prepared by Aqueous Emulsion Polymerization. *Langmuir* **2011,** 27, (17), 11129-11144.
162. Zou, H.; Armes, S. P., Efficient synthesis of poly(2-hydroxypropyl methacrylate)-silica colloidal nanocomposite particles via aqueous dispersion polymerization. *Polymer Chemistry* **2012,** 3, (1), 172-181.
163. Duguet, E.; Desert, A.; Perro, A.; Ravaine, S., Design and elaboration of colloidal molecules: an overview. *Chemical Society Reviews* **2011,** 40, (2), 941-960.
164. Bourgeat-Lami, E.; Lansalot, M., Organic/Inorganic Composite Latexes: The Marriage of Emulsion Polymerization and Inorganic Chemistry. *Advances in Polymer Science* **2010,** 233, 53-123.
165. Faucheu, J.; Gauthier, C.; Chazeau, L.; Cavaille, J. Y.; Mellon, V.; Bourgeat-Lami, E., Miniemulsion polymerization for synthesis of structured clay/polymer nanocomposites: Short review and recent advances. *Polymer* **2010,** 51, (1), 6-17.
166. Landfester, K., Miniemulsion Polymerization and the Structure of Polymer and Hybrid Nanoparticles. *Angewandte Chemie-International Edition* **2009,** 48, (25), 4488-4507.

167. Hu, J.; Chen, M.; Wu, L. M., Organic-inorganic nanocomposites synthesized via miniemulsion polymerization. *Polymer Chemistry* **2011,** 2, (4), 760-772.
168. Zou, H.; Wu, S. S.; Shen, J., Polymer/silica nanocomposites: Preparation, characterization, properties, and applications. *Chemical Reviews* **2008,** 108, (9), 3893-3957.
169. Tiarks, F.; Landfester, K.; Antonietti, M., Silica nanoparticles as surfactants and fillers for latexes made by miniemulsion polymerization. *Langmuir* **2001,** 17, (19), 5775-5780.
170. Qiao, X. G.; Chen, M.; Zhou, J.; Wu, L. M., Synthesis of raspberry-like silica/polystyrene/silica multilayer hybrid particles via miniemulsion polymerization. *Journal of Polymer Science Part a-Polymer Chemistry* **2007,** 45, (6), 1028-1037.
171. Zhang, S. W.; Zhou, S. X.; Weng, Y. M.; Wu, L. M., Synthesis of SiO2/polystyrene nanocomposite particles via miniemulsion polymerization. *Langmuir* **2005,** 21, (6), 2124-2128.
172. Zhou, J.; Zhang, S. W.; Qiao, X. G.; Li, X. Q.; Wu, L. M., Synthesis of SiO2/poly(styrene-co-butyl acrylate) nanocomposite microspheres via miniemulsion polymerization. *Journal of Polymer Science Part a-Polymer Chemistry* **2006,** 44, (10), 3202-3209.
173. Qiang, W.; Wang, Y.; He, P.; Xu, H.; Gu, H.; Shi, D., Synthesis of asymmetric inorganic/polymer nanocomposite particles via localized substrate surface modification and miniemulsion polymerization. *Langmuir* **2008,** 24, (3), 606-608.
174. Costoyas, A.; Ramos, J.; Forcada, J., Encapsulation of Silica Nanoparticles by Miniemulsion Polymerization. *Journal of Polymer Science Part a-Polymer Chemistry* **2009,** 47, (3), 935-948.
175. Bombalski, L.; Min, K.; Dong, H. C.; Tang, C. B.; Matyjaszewski, K., Preparation of well-defined hybrid materials by ATRP in miniemulsion. *Macromolecules* **2007,** 40, (21), 7429-7432.
176. Harris, L. A.; Goff, J. D.; Carmichael, A. Y.; Riffle, J. S.; Harburn, J. J.; St Pierre, T. G.; Saunders, M., Magnetite nanoparticle dispersions stabilized with triblock copolymers. *Chemistry of Materials* **2003,** 15, (6), 1367-1377.
177. Thunemann, A. F.; Schutt, D.; Kaufner, L.; Pison, U.; Mohwald, H., Maghemite nanoparticles protectively coated with poly(ethylene imine) and poly(ethylene oxide)-block-poly(glutamic acid). *Langmuir* **2006,** 22, (5), 2351-2357.
178. Lu, A. H.; Salabas, E. L.; Schuth, F., Magnetic nanoparticles: Synthesis, protection, functionalization, and application. *Angewandte Chemie-International Edition* **2007,** 46, (8), 1222-1244.
179. Ramirez, L. P.; Landfester, K., Magnetic polystyrene nanoparticles with a high magnetite content obtained by miniemulsion processes. *Macromolecular Chemistry and Physics* **2003,** 204, (1), 22-31.
180. Xu, Y. W.; Xu, H.; Gu, H. C., Controllable Preparation of Epoxy-Functionalized Magnetic Polymer Latexes with Different Morphologies by Modified Miniemulsion Polymerization. *Journal of Polymer Science Part a-Polymer Chemistry* **2010,** 48, (11), 2284-2293.
181. Lu, S.; Ramos, J.; Forcada, J., Self-stabilized magnetic polymeric composite nanoparticles by emulsifier-free miniemulsion polymerization. *Langmuir* **2007,** 23, (26), 12893-12900.
182. Xu, H.; Cui, L. L.; Tong, N. H.; Gu, H. C., Development of high magnetization Fe3O4/polystyrene/silica nanospheres via combined miniemulsion/emulsion polymerization. *Journal of the American Chemical Society* **2006,** 128, (49), 15582-15583.
183. Erdem, B.; Sudol, E. D.; Dimonie, V. L.; El-Aasser, M. S., Encapsulation of inorganic particles via miniemulsion polymerization. I. Dispersion of titanium dioxide particles in

organic media using OLOA 370 as stabilizer. *Journal of Polymer Science Part a-Polymer Chemistry* **2000,** 38, (24), 4419-4430.
184. Erdem, B.; Sudol, E. D.; Dimonie, V. L.; El-Aasser, M. S., Encapsulation of inorganic particles via miniemulsion polymerization. II. Preparation and characterization of styrene miniemulsion droplets containing TiO2 particles. *Journal of Polymer Science Part a-Polymer Chemistry* **2000,** 38, (24), 4431-4440.
185. Erdem, B.; Sudol, E. D.; Dimonie, V. L.; El-Aasser, M. S., Encapsulation of inorganic particles via miniemulsion polymerization. III. Characterization of encapsulation. *Journal of Polymer Science Part a-Polymer Chemistry* **2000,** 38, (24), 4441-4450.
186. Zhou, J.; Chen, M.; Qiao, X. G.; Wu, L. M., Facile preparation method of SiO2/PS/TiO2 multilayer core-shell hybrid microspheres. *Langmuir* **2006,** 22, (24), 10175-10179.
187. Topfer, O.; Schmidt-Naake, G., Surface-functionalized inorganic nanoparticles in miniemulsion polymerization. *Macromolecular Symposia* **2007,** 248, 239-248.
188. Advincula, R. C., Surface initiated polymerization from nanoparticle surfaces. *Journal of Dispersion Science and Technology* **2003,** 24, (3-4), 343-361.
189. Barbey, R.; Lavanant, L.; Paripovic, D.; Schuwer, N.; Sugnaux, C.; Tugulu, S.; Klok, H. A., Polymer Brushes via Surface-Initiated Controlled Radical Polymerization: Synthesis, Characterization, Properties, and Applications. *Chemical Reviews* **2009,** 109, (11), 5437-5527.
190. Tjuji, Y. O., K.; Yamamoto, S.; Goto, A.; Fukuda, T., Structure and Properties of High-Density Polymer Brushes Prepared by Surface-Initiated Living Radical Polymerization. *Adv. Polym. Sci.* **2006,** 197, 1-46.
191. von Werne, T.; Patten, T. E., Preparation of structurally well-defined polymer-nanoparticle hybrids with controlled/living radical polymerizations. *Journal of the American Chemical Society* **1999,** 121, (32), 7409-7410.
192. Prucker, O.; Ruhe, J., Synthesis of poly(styrene) monolayers attached to high surface area silica gels through self-assembled monolayers of azo initiators. *Macromolecules* **1998,** 31, (3), 592-601.
193. Pyun, J.; Jia, S. J.; Kowalewski, T.; Patterson, G. D.; Matyjaszewski, K., Synthesis and characterization of organic/inorganic hybrid nanoparticles: Kinetics of surface-initiated atom transfer radical polymerization and morphology of hybrid nanoparticle ultrathin films. *Macromolecules* **2003,** 36, (14), 5094-5104.
194. Carrot, G.; Diamanti, S.; Manuszak, M.; Charleux, B.; Vairon, I. P., Atom transfer radical polymerization of n-butyl acrylate from silica nanoparticles. *Journal of Polymer Science Part a-Polymer Chemistry* **2001,** 39, (24), 4294-4301.
195. El Harrak, A.; Carrot, G.; Oberdisse, J.; Eychenne-Baron, C.; Boue, F., Surface-atom transfer radical polymerization from silica nanoparticles with controlled colloidal stability. *Macromolecules* **2004,** 37, (17), 6376-6384.
196. Matyjaszewski, K.; Miller, P. J.; Shukla, N.; Immaraporn, B.; Gelman, A.; Luokala, B. B.; Siclovan, T. M.; Kickelbick, G.; Vallant, T.; Hoffmann, H.; Pakula, T., Polymers at interfaces: Using atom transfer radical polymerization in the controlled growth of homopolymers and block copolymers from silicon surfaces in the absence of untethered sacrificial initiator. *Macromolecules* **1999,** 32, (26), 8716-8724.
197. Ohno, K.; Morinaga, T.; Koh, K.; Tsujii, Y.; Fukuda, T., Synthesis of monodisperse silica particles coated with well-defined, high-density polymer brushes by surface-initiated atom transfer radical polymerization. *Macromolecules* **2005,** 38, (6), 2137-2142.
198. Li, D. J.; Sheng, X.; Zhao, B., Environmentally responsive "Hairy" nanoparticles: Mixed homopolymer brushes on silica nanoparticles synthesized by living radical

polymerization techniques. *Journal of the American Chemical Society* **2005,** 127, (17), 6248-6256.
199. Tsujii, Y.; Ejaz, M.; Sato, K.; Goto, A.; Fukuda, T., Mechanism and kinetics of RAFT-mediated graft polymerization of styrene on a solid surface. 1. Experimental evidence of surface radical migration. *Macromolecules* **2001,** 34, (26), 8872-8878.
200. Baum, M.; Brittain, W. J., Synthesis of polymer brushes on silicate substrates via reversible addition fragmentation chain transfer technique. *Macromolecules* **2002,** 35, (3), 610-615.
201. Li, C.; Han, J.; Ryu, C. Y.; Benicewicz, B. C., A versatile method to prepare RAFT agent anchored substrates and the preparation of PMMA grafted nanoparticles. *Macromolecules* **2006,** 39, (9), 3175-3183.
202. Li, C. Z.; Benicewicz, B. C., Synthesis of well-defined polymer brushes grafted onto silica nanoparticles via surface reversible addition-fragmentation chain transfer polymerization. *Macromolecules* **2005,** 38, (14), 5929-5936.
203. Zhao, Y. L.; Perrier, S., Synthesis of well-defined homopolymer and diblock copolymer grafted onto silica particles by Z-supported RAFT polymerization. *Macromolecules* **2006,** 39, (25), 8603-8608.
204. Yang, Y. K.; Yang, Z. F.; Zhao, Q.; Cheng, X. J.; Tiong, S. C.; Li, R. K. Y.; Wan, X. T.; Xie, X. L., Immobilization of RAFT Agents on Silica Nanoparticles Utilizing an Alternative Functional Group and Subsequent Surface-Initiated RAFT Polymerization. *Journal of Polymer Science Part a-Polymer Chemistry* **2009,** 47, (2), 467-484.
205. BLAS, H., Université Pierre et Marie Curie. **2009**.
206. Husseman, M.; Malmstrom, E. E.; McNamara, M.; Mate, M.; Mecerreyes, D.; Benoit, D. G.; Hedrick, J. L.; Mansky, P.; Huang, E.; Russell, T. P.; Hawker, C. J., Controlled synthesis of polymer brushes by "Living" free radical polymerization techniques. *Macromolecules* **1999,** 32, (5), 1424-1431.
207. Husemann, M.; Morrison, M.; Benoit, D.; Frommer, K. J.; Mate, C. M.; Hinsberg, W. D.; Hedrick, J. L.; Hawker, C. J., Manipulation of surface properties by patterning of covalently bound polymer brushes. *Journal of the American Chemical Society* **2000,** 122, (8), 1844-1845.
208. Brinks, M. K.; Studer, A., Polymer Brushes by Nitroxide-Mediated Polymerization. *Macromolecular Rapid Communications* **2009,** 30, (13), 1043-1057.
209. Parvole, J.; Laruelle, G.; Guimon, C.; Francois, J.; Billon, L., Initiator-grafted silica particles for controlled free radical polymerization: Influence of the initiator structure on the grafting density. *Macromolecular Rapid Communications* **2003,** 24, (18), 1074-1078.
210. Bartholome, C.; Beyou, E.; Bourgeat-Lami, E.; Chaumont, P.; Zydowicz, N., Nitroxide-mediated polymerizations from silica nanoparticle surfaces: "Graft from" polymerization of styrene using a triethoxysilyl-terminated alkoxyamine initiator. *Macromolecules* **2003,** 36, (21), 7946-7952.
211. Parvole, J.; Montfort, J. P.; Billon, L., Formation of inorganic/organic nanocomposites by nitroxide-mediated polymerization in bulk using a bimolecular system. *Macromolecular Chemistry and Physics* **2004,** 205, (10), 1369-1378.
212. Parvole, J.; Laruelle, G.; Khoukh, A.; Billon, L., Surface initiated polymerization of poly(butyl acrylate) by nitroxide mediated polymerization: First comparative polymerization of a bimolecular and a unimolecular initiator-grafted silica particles. *Macromolecular Chemistry and Physics* **2005,** 206, (3), 372-382.
213. Bartholome, C.; Beyou, E.; Bourgeat-Lami, E.; Chaumont, P.; Lefebvre, F.; Zydowicz, N., Nitroxide-mediated polymerization of styrene initiated from the surface of

silica nanoparticles. In situ generation and grafting of alkoxyamine initiators. *Macromolecules* **2005,** 38, (4), 1099-1106.
214. Bartholome, C.; Beyou, E.; Bourgeat-Lami, E.; Chaumont, P.; Zydowicz, N., Nitroxide-mediated polymerization of styrene initiated from the surface of fumed silica. Comparison of two synthetic routes. *Polymer* **2005,** 46, (19), 8502-8510.
215. Inoubli, R.; Dagreou, S.; Khoukh, A.; Roby, F.; Peyrelasse, J.; Billon, L., 'Graft from' polymerization on colloidal silica particles: elaboration of alkoxyamine grafted surface by in situ trapping of carbon radicals. *Polymer* **2005,** 46, (8), 2486-2496.
216. Bonilla-Cruz, J.; Lara-Ceniceros, T.; Saldivar-Guerra, E.; Jimenez-Regalado, E., Towards controlled graft polymerization of poly styrene-co-(maleic anhydride) on functionalized silica mediated by oxoaminium bromide salt. Facile synthetic pathway using nitroxide chemistry. *Macromolecular Rapid Communications* **2007,** 28, (13), 1397-1403.
217. Deleuze, C.; Delville, M. H.; Pellerin, V.; Derail, C.; Billon, L., Hybrid Core@Soft Shell Particles as Adhesive Elementary Building Blocks for Colloidal Crystals. *Macromolecules* **2009,** 42, (14), 5303-5309.
218. Horton, J. M.; Tang, S. D.; Bao, C. H.; Tang, P.; Qiu, F.; Zhu, L.; Zhao, B., Truncated Wedge-Shaped Nanostructures Formed from Lateral Microphase Separation of Mixed Homopolymer Brushes Grafted on 67 nm Silica Nanoparticles: Evidence of the Effect of Substrate Curvature. *Acs Macro Letters* **2012,** 1, (8), 1061-1065.
219. Bao, C. H.; Tang, S. D.; Horton, J. M.; Jiang, X. M.; Tang, P.; Qiu, F.; Zhu, L.; Zhao, B., Effect of Overall Grafting Density on Microphase Separation of Mixed Homopolymer Brushes Synthesized from Y-Initiator-Functionalized Silica Particles. *Macromolecules* **2012,** 45, (19), 8027-8036.
220. Parvole, J.; Montfort, J. P.; Reiter, G.; Borisov, O.; Billon, L., Elastomer polymer brushes on flat surface by bimolecular surface-initiated nitroxide mediated polymerization. *Polymer* **2006,** 47, (4), 972-981.
221. Ostaci, R. V.; Celle, C.; Seytre, G.; Beyou, E.; Chapel, J. P.; Drockenmuller, E., Influence of nitroxide structure on polystyrene brushes "Grafted-from" silicon wafers. *Journal of Polymer Science Part a-Polymer Chemistry* **2008,** 46, (10), 3367-3374.
222. Ghannam, L.; Garay, H.; Billon, L., Sensitive Colored Hybrid Inorganic/Organic Pigments Based on Polymer-Coated Microsized Particles. *Macromolecules* **2008,** 41, (20), 7374-7382.
223. Robbes, A. S.; Cousin, F.; Meneau, F.; Dalmas, F.; Schweins, R.; Gigmes, D.; Jestin, J., Polymer-Grafted Magnetic Nanoparticles in Nanocomposites: Curvature Effects, Conformation of Grafted Chain, and Bimodal Nanotriggering of Filler Organization by Combination of Chain Grafting and Magnetic Field. *Macromolecules* **2012,** 45, (22), 9220-9231.
224. Matsuno, R.; Otsuka, H.; Takahara, A., Polystyrene-grafted titanium oxide nanoparticles prepared through surface-initiated nitroxide-mediated radical polymerization and their application to polymer hybrid thin films. *Soft Matter* **2006,** 2, (5), 415-421.
225. Inoubli, R., Thèse: Synthèse, structure et propriétés viscoélastique de polymères chargés modèles. *Université de pau et des pays de l'adour* **2005**.

Chapter 2
Synthesis of high molar mass polymer by NMP in mini(micro)emulsion

Introduction 71
2.1 Experimental Part 74
2.1.1 Synthesis of BB-BA alkoxyamine initiator 74
2.1.2 Miniemulsion polymerization 74
2.1.3 Microemulsion polymerization 75
2.2 Results and Discussion 75
2.2.1 Synthesis of BB-BA 75
2.2.2 NMP miniemulsion in the presence of surfactant 77
2.2.3 Surfactant-free miniemulsion polymerization 85
2.2.5 NMP-microemulsion of styrene 91
Conclusion 97
References 99

Introduction

In the past decades, reversible-deactivation radical polymerization (RDRP) methods have shown the possibility to design a large panel of polymers [1]. Following academic and industrial challenges, RDRP was transposed from homogenous media to polymerization in aqueous dispersed media in order to combine both advantages of macromolecular engineering via RDRP and environmental-industrial considerations of emulsion polymerization process. Several reviews summarized the controlled synthesis of polymers via RDRP in aqueous dispersed media [2-4]. RDRP was first implemented in aqueous dispersed media by miniemulsion process as the initial monomer droplets served as nanoreactors [5-6]. Several reviews summarized the process of miniemulsion with its different aspects [7-8], as we discussed in Chapter 1. Nitroxide-mediated polymerization (NMP) will be the chosen method to implement the miniemulsion polymerization, as it proved to be a robust method for the implementation of RDRP in aqueous dispersed media [9-10]. NMP is an RDRP technique that enables the design of well-defined, functional and complex macromolecular architectures. As its name indicates, it involves a nitroxide radical to establish the reversible-deactivation equilibrium known in RDRP. The evolution aspects of NMP, along with the different nitroxides and alkoxymines used throughout years, was discussed in Chapter 1 [11]. NMP has been investigated in aqueous dispersed media such as emulsion, miniemulsion, dispersion and microemulsion [3, 12].

Our next Chapter 3 will focus on the synthesis of core@shell hybrid nanoparticles in miniemulsion in the presence and absence of additional free initiator which produces free chains. Thus, the requirement of absence of free initiator alongside with the restricted content of inorganic silica versus polymer (< 10 wt-%) will impose to target a high degree of polymerization by surface-initiated NMP. The synthesis of the hybrid particles in miniemulsion in the presence of a free initiator requires the use of a free initiator with a similar structure as the grafted initiator (Scheme 1).

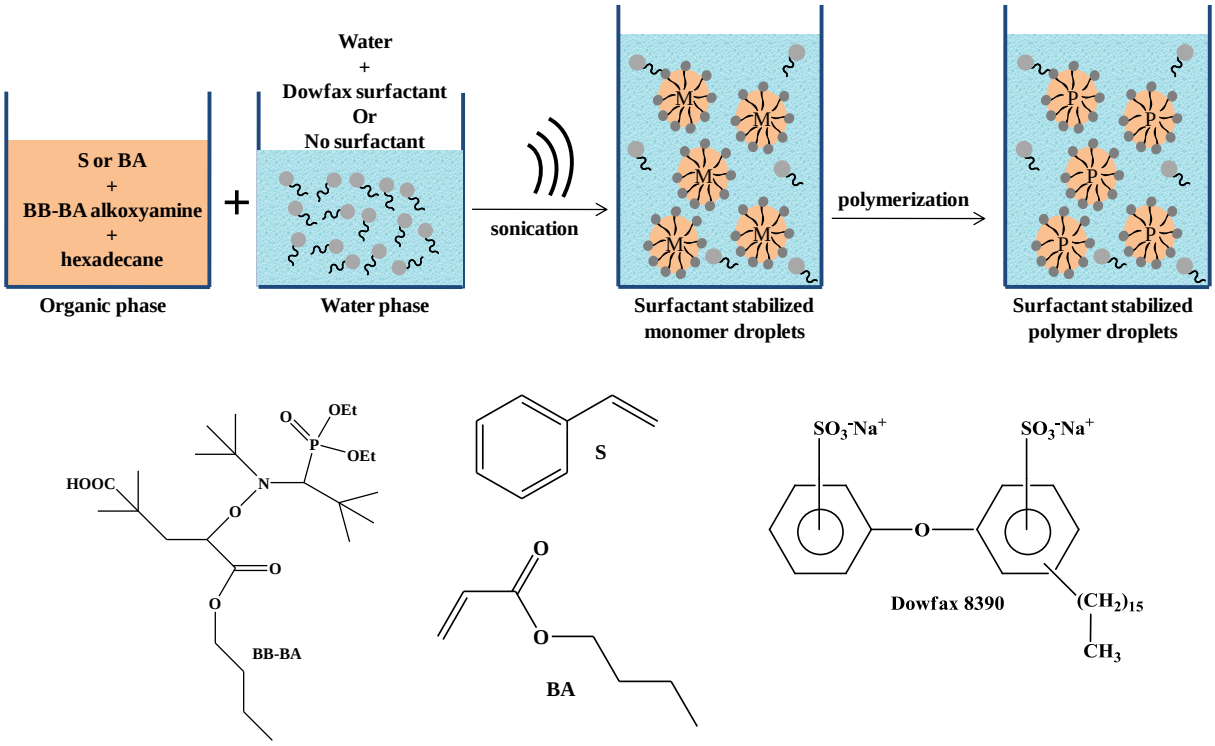

Scheme 1. Scheme of NMP in miniemulsion and molecular structures of chemicals

In that context, it was necessary to perform preliminary model NMP experiments in miniemulsion, which had not been previously described in the literature. The purpose of this chapter 2 will be to address the following issues:

1) Is it possible to maintain the control of polymerization by NMP in miniemulsion if targeting high degrees of polymerization?
2) Studies of literature reported NMP in miniemulsion with different alkoxyamines as monocomponent system (MONAMS, TEMPO-based alkoxyamine, PS-TEMPO, PS-SG1), macromolecular alkoxyamines, water soluble dialkoxyamines… This was carefully studied in the first chapter in the part concerning NMP in miniemulsion. As no studies reported the initiation of NMP in miniemulsion of styrene by BB-BA (Scheme 1, alkoxyamine based on 1,2 addition of Blocbuilder® onto *n*-butyl acrylate), we investigated NMP in miniemulsion with such alkoxyamine and assessed the control over polymerization for different targeted degrees of polymerization ranging between 200 and 1280.
3) As it appears in Scheme 1, the BB-BA alkoxyamine carrying both an alkyl chain (C4) and a carboxylic acid group, which is neutralized at pH 9 of miniemulsion polymerization, could act as a surface-active species. In order to address if a specific location of the alkoxyamine at the liquid/liquid interface could interfere with NMP

miniemulsion, we will investigate the colloidal features and stability of both initial monomer droplets and final latex while characterizing simultaneously the polymer synthesized by surfactant-free NMP miniemulsion.

4) As reported in chapter 1 (part 2.2), it has been demonstrated for reversible termination systems (NMP and ATRP) performed in polymerization in aqueous dispersed media that compartmentalization effects do exist under some conditions [4]. At sufficiently small particles sizes (which depends on the system but generally < 50 nm), kinetic can be impacted but more importantly control and livingness can be improved for linear polymers [12-16]. Thus, the last part of this Chapter 2 will be dedicated to preliminary experiments concerning microemulsion NMP but also targeting high molar masses.

2.1 Experimental Part

Materials. Styrene (S) (Sigma-Aldrich, 99 %), *n*-Butyl Acrylate (BA) (Sigma-Aldrich, 99 %) passed under inhibitor removers prior usage. Dowfax^{TM} 8390 surfactant (a mixture of mono- and dihexadecyl disulfonated diphenyloxide disodium salts, supplied by DOW company). Buffer sodium hydrogen carbonate $NaHCO_3$, co-surfactant hexadecane (Aldrich, 99 %), high molar mass polystyrene PS (300000 g.mol^{-1}), Blocbuilder® (Arkema, 99 %), *N*-tert-butyl-*N*-(1-diethylphosphono-2,2-dimethylpropyl)-*O*-(1-(methoxycarbonyl)ethyl)hydroxylamine MONAMS (95 %), sodium dodecyl sulfate (SDS) (Aldrich, 99 %).

2.1.1 Synthesis of BB-BA alkoxyamine initiator

The 1,2 radical addition of 1 equivalent of BlocBuilder® alkoxyamine BB onto BA was carried out in toluene. In a typical experiment in a 25 mL round bottom flask a mixture of BB (6 g, 1.5×10^{-2} mol), BA (2 g, 1.5×10^{-2} mol) and 15 mL of toluene was deoxygenated by nitrogen bubbling for 20 min in an ice bath. The mixture was then moved to an oil bath heated at 100 °C and stirred at 300 rpm. The reaction was proceeded for an hour and 15 min. After stopping the reaction a yellowish orange product was be observed. Toluene was evaporated using a vacuum pump and the product was re-crystallized by the minimum volume of toluene and a volume of heptane higher 5 times than toluene. After filtration and vacuum drying the final product obtained was a fine white powder, which was to be stored in the fridge. The final product was later analyzed by nuclear magnetic resonance.

2.1.2 Miniemulsion polymerization

In a typical experiment a stable aqueous emulsion of the monomer was prepared by the mixing of the organic phase containing monomer, alkoxyamine (BB-BA), high molar mass polystyrene (PS; M_w=300 kg.mol^{-1}) and hexadecane with the water phase containing the Dowfax 8930 surfactant and the buffer $NaHCO_3$. PS and hexadecane were used as hydrophobes to stabilize the monomer droplets against Ostwald ripening. The unstable emulsion was stirred in an ice bath for 10 minutes. Then, it was subjected to a high shear pressure by ultrasonication using a Vibra Cell 72408 ultrasonicator, for 15 minutes at amplitude of 30 % in an ice bath to disperse the organic phase into submicrometer droplets and to improve their stability. The stable miniemulsion was then poured into 150 mL thermostated reactor (Parr 5100) and was stirred at 300 rpm where it was deoxygenated for 30 min before heating. Afterward, a 3-bar pressure of nitrogen was applied, and the reactor was

heated to 120 °C. The time when the temperature reached 90 °C was chosen as time zero of the reaction, which was carried out for 7 hours. Samples were periodically withdrawn to monitor the monomer conversion by gravimetric study. For this purpose, the latex samples were dried under vacuum until a constant weight was obtained. The particle diameter (*D*) was measured by dynamic light scattering (DLS). After drying, the molar mass of the polymer was studied by injecting in THF size exclusion chromatography (SEC) (5 $g.mL^{-1}$).

2.1.3 Microemulsion polymerization

The aqueous phase was prepared by mixing distilled water (114 g), $NaHCO_3$ (0.114 g, 0.012 $mol.L^{-1}_{water}$) and sodium dodecyl sulfate SDS (15 g, 250 wt-% based on monomer) and then it was stirred at room temperature to the solubilization of the surfactant. The organic phase was prepared by mixing the monomer (6 g) with MONAMS and SG1 ($[SG1]_0/[MONAMS]_0$ = 5 %) and were mixed for few mins in an ice bath. The two phases were mixed and stirred for 30 min. A clear solution is obtained after the stirring was stopped. The mixture was placed in a thermostated reactor operated at 300 rpm, at room temperature. Degassing was carried out with nitrogen for 20 minutes and then the reactor was subjected to a pressure of 3 bar and the temperature was set at 120 °C for styrene polymerization and 115 °C for BA polymerization. The zero time of the reaction was noted at a temperature of 90 °C. Samples were taken every 20 minutes for 3 hours and then after an hour. Conversion was studied gravimetrically by withdrawing samples and drying under vacuum.

2.2 Results and Discussion

2.2.1 Synthesis of BB-BA

In the process of synthesis of core@shell hybrid nanoparticles later in Chapter 3, adding a free initiator in a controlled radical polymerization from a surface (SI-NMP) is sometimes necessary. In literature, the free initiator generally has a structure similar to the grafted initiator. Thus, this similarity of structure and reactivity effectively allows the comparison of the characteristics of the grafted and free polymer.

The 1, 2 radical addition of a reactive alkoxyamine (here BB®) onto an activated olefin is one way that has been exploited for the synthesis of functional alkoxyamines, including di - or tri-alkoxyamines [17-18] (see bibiliography chapter 1). This method has also been explored in the context of the SI-NMP (see bibiliography chapter 1) for the *in-situ* synthesis of

(m)ethoxysilane functionalized alkoxyamine from (meth)acryloyloxypropyltri(m)ethoxysilane [19-21]. The procedure is adapted from previous study on the 1,2 addition of BB® onto acrylates, as it was described in bibliographic part.

In the present work, we chose to synthesize a free alkoxyamine whose structure is close to that of the alkoxyamine which will be grafted onto silica (Chapter 3). This alkoxyamine, which we call BB-BA later in this manuscript, was synthesized by exploiting the reactivity of the alkoxyamine BlocBuilder® by 1,2 addition onto activated olefins (Scheme 2) as previously described in the work of Blas. [20]

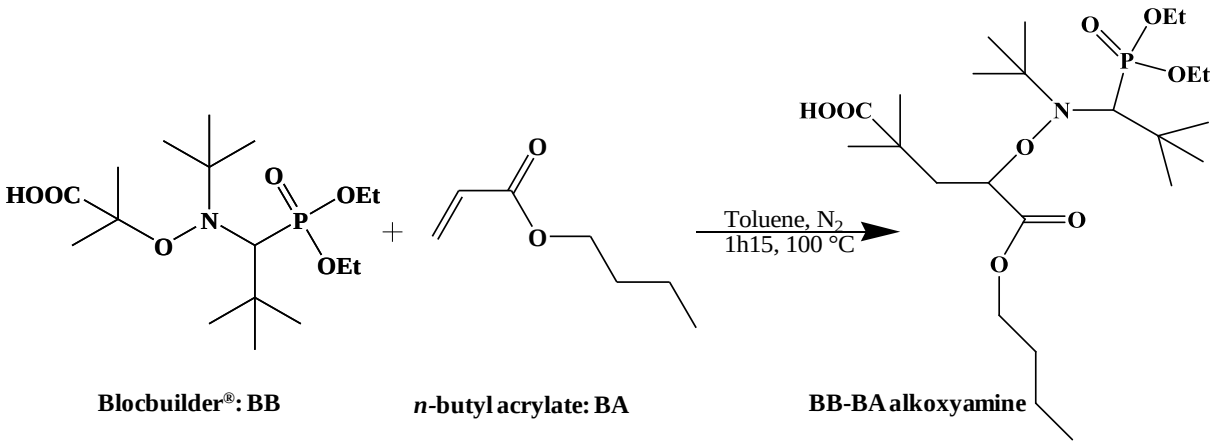

Scheme 2. Synthesis of BB-BA alkoxyamine by 1,2 addition of Blocbuilder® onto *n*-butyl acrylate,

The product of the reaction was purified and then analyzed by proton nuclear magnetic resonance NMR. In Figure 1 we see the characteristic doublet of proton H from SG1 which couples with phosphorus (with coupling constant J = 26.1 Hz), at 3.3 ppm. The appearance of peaks of protons E, F and F' along with the disappearance of the vinylic protons between 5.5 and 6.5 ppm, prove the success of the 1,2-addition of the Blocbuilder® alkoxyamine onto BA. Moreover, the good correlation between the integration of H proton with the integration of E, F and F' protons confirms the absence of BA polymerization. Because of the proximity of the ester group, the free rotation of the molecule is prevented by methylene group. The two protons F and F' are not equivalent and result in a doublet of a doublet at 2.1 and 2.5 ppm. The coupling constant between F and F' is $J_{F-F'}$=1.5 Hz and the coupling constant with E proton is J_{E-F}=12 Hz.

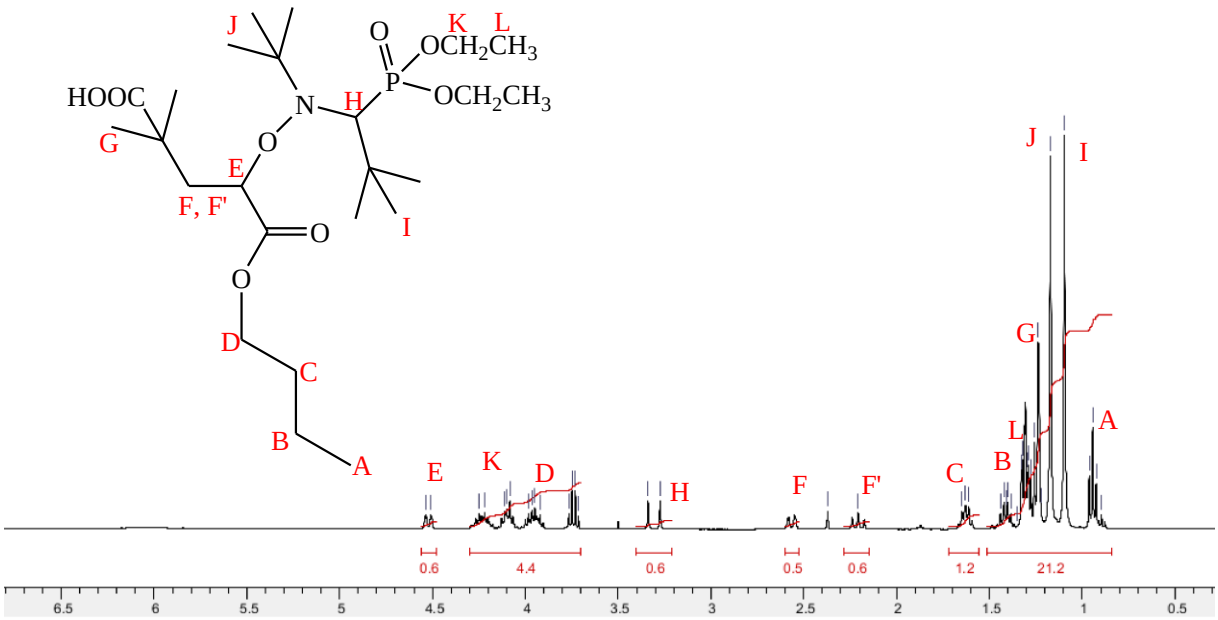

Figure 1. ^{1}H NMR spectrum of BB-BA alkoxyamine in $CDCl_3$.

2.2.2 NMP miniemulsion in the presence of surfactant

This part is dedicated to NMP of styrene in miniemulsion in the presence of surfactant targeting theoretical degree of polymerization ranging between 200 and 1280. The experimental conditions of polymerization are gathered in Table 1.

Table 1. Experimental conditions for NMP miniemulsion of styrene carried out at 120 °C in the presence of Dowfax surfactant. [a]

Expt	Exp	$[BB\text{-}BA]_0$ [b] $mol.L^{-1}_{orga}$	DP_{theo} [c]
1	HS108	4.45×10^{-2}	200
2	HS134	1.73×10^{-2}	500
3	HS113	6.85×10^{-3}	1280

[a] The polymerizations were all carried out with the following recipe: aqueous phase (H_2O, $NaHCO_3$ 0.012 $mol.L^{-1}_{water}$, at pH = 9 and Dowfax 2.2 wt-% based on styrene) and organic phase (styrene, 20 wt-% versus latex volume, hexadecane 5 wt-% based on styrene, BB-BA) were mixed and subjected to high shear pressure before polymerization, and then moved to thermostated reactor at 3 bar and 120 °C

[b] Initial concentration of BB-BA monoadduct alkoxyamine with respect to the organic phase.

[c] Theoretical degree of polymerization at 100 % conversion, $DP_{theo} = [S]_0/[BB\text{-}BA]_0$

The three NMP miniemulsions (Expt 1, 2 and 3) were performed at 120 °C with the same alkoxyamine (BB-BA) in the absence of free nitroxide and varying the concentrations of the alkoxyamine, that is various $[styrene]_0/[BB\text{-}BA]_0$ molar ratios. Dowfax surfactant had a concentration in the range of CMC (1.4×10^{-5} M), thus avoiding the existence of additional

micelles in the miniemulsion. In Figure 2, we notice that regardless of the initial concentration of the alkoxyamine, the obtained M_w/M_n values are below 1.6.

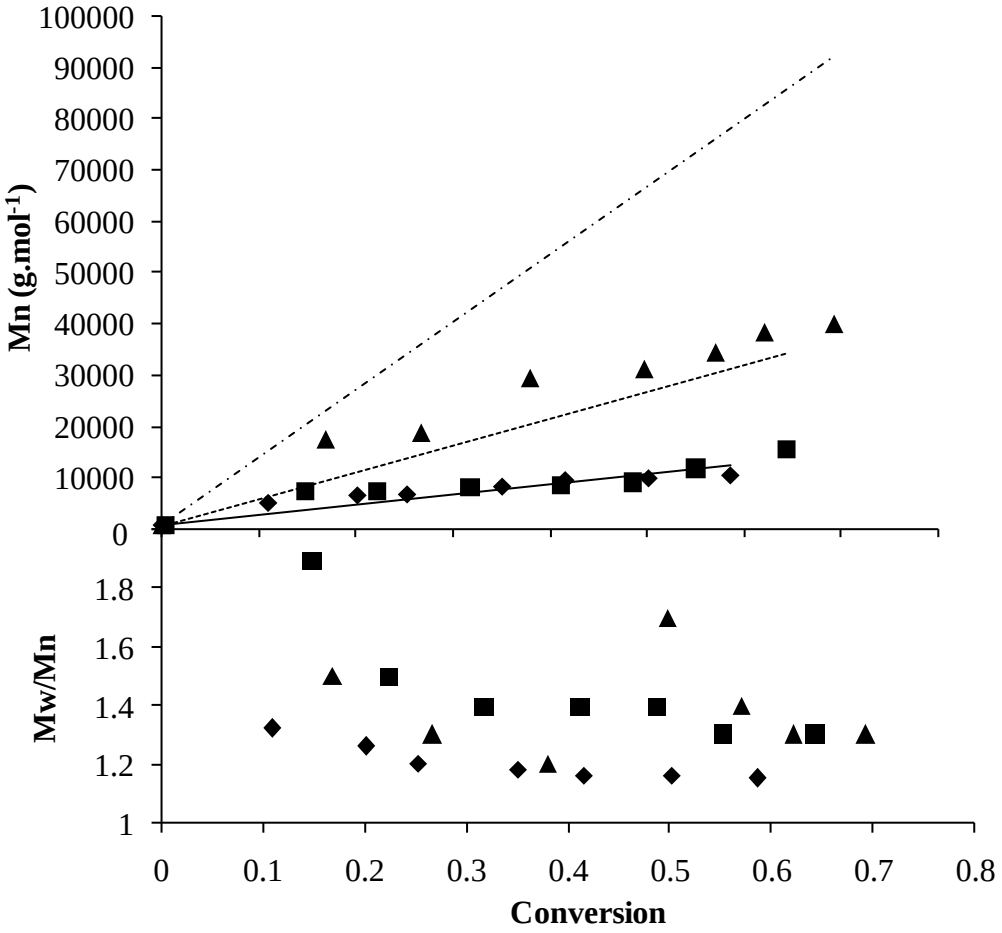

Figure 2. Plots of $M_{n,\,SEC}$ and M_w/M_n versus conversion for NMP miniemulsion of styrene with different $[BB\text{-}BA]_0$. ♦ Expt 1 (solid line) $[BB\text{-}BA]_0 = 4.45 \times 10^{-2}$ M; ■ Expt 2 (dotted line) $[BB\text{-}BA]_0 = 1.73 \times 10^{-2}$ M; and ▲ Expt 3 (dashed line) $[BB\text{-}BA]_0 = 6.85 \times 10^{-3}$ M. The lines correspond to theoretical molar masses.

The evolution of the experimental number-average molar mass with conversion is linear. However, regardless of the $[BB\text{-}BA]_0$ the experimental values are close to theoretical M_n for the highest initial alkoxyamine concentration (~ 4.4×10^{-2} M), and are inferior for initial alkoxyamine concentration below 4.45×10^{-2} M (DP higher than 500). Where the theoretical M_n can be calculated from Equation 1 below:

$$M_{n,theo} = M_{initiator} + \frac{[monomer]_0}{[initiator]_0} \times M_{monomer} \times conversion$$

Equation 1: Calculation of theoretical molar mass

The ratio between theoretical and experimental M_n ($M_{n,\,theo}/M_{n,\,exp}$) is proportional to the number of created chains in comparison with the initial alkoxyamine concentration ([polymer

chains]/$[PX]_0$). This ratio is higher for the lowest initial alkoxyamine concentration (Expt 3) of Table 2.

As shown in Table 2 and Figure 2, by decreasing the initial alkoxyamine concentration for Expt 1, 2 and 3 the ratio is $M_{n,\,theo}/M_{n,\,exp}$ is increasing from 1.2, 1.5 to 2.4 respectively.

Table 2. Results of NMP miniemulsion of styrene carried out at 120 °C in the presence of Dowfax surfactant

Expt	Conversion (time) % (h)	$[P^{\bullet}]_{exp}$ [a] mol.L^{-1}$_{orga}$	$[SG1]_{exp}$ [b] mol.L^{-1}	DPC [c] %	$M_{n,theo}$ [d] g.mol^{-1}	$M_{n,SEC}$ [e] g.mol^{-1}	M_w/M_n [e]	$\frac{M_{n,theo}}{M_{n,exp}}$
1	58 (7)	1.5×10^{-8}	1.7×10^{-2}	39	12340	10450	1.1	1.2
2	65 (7)	1.8×10^{-8}	5.9×10^{-3}	34	30400	20400	1.3	1.5
3	72 (7)	2.3×10^{-8}	1.8×10^{-3}	26	96120	39900	1.3	2.4

[a] $[P^{\bullet}] = \frac{\ln([M]_0/[M]) = f(t)}{k_p}$

[b] Concentration of released SG1calculated from Equation 4

[c] DPC corresponds to the fraction of dead polymer chains calculated from Equation 5 and Equation 4 with $[SG1]_0 = 0$

[d] The theoretical M_n was calculated from Equation 1

[e] Number-average molar mass and dispersity derived from the PS calibration (RI detector).

The higher value of the theoretical M_n indicates that higher number of created chains is formed in comparison with number of initiator; hence these chains are probably formed by thermal self-initiation of styrene. The mechanism and kinetics of styrene thermal self-initiation was previously described by Mayo.[22] Where upon heating styrene at a high temperature (up to 120 °C) reaction begins with a Diels–Alder cycloaddition between two styrene molecules to produce a styrene dimer. The styrene dimer then undergoes an electron transfer reaction with another styrene molecule to form two radicals (Scheme 3).

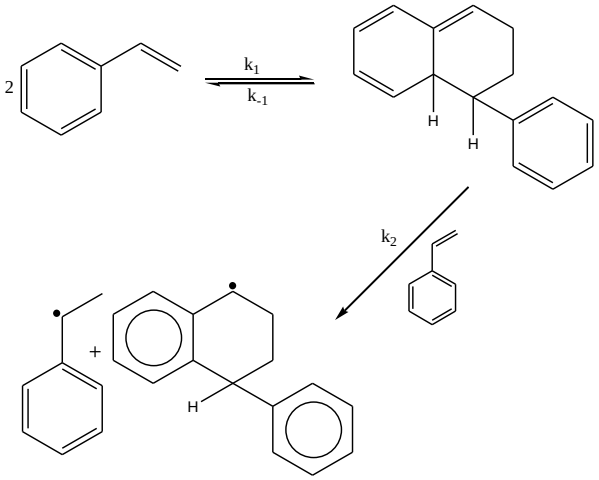

Scheme 3. Thermal self-initiation of styrene [22]

In order to assess the extent of thermal polymerization in the experimental conditions of the present work we performed a miniemulsion polymerization of styrene at 120 °C in the absence of any type of initiator. In Figure 3, we notice 33% of conversion was achieved after 7 hours of reaction and 77 % of conversion was registered after 24 hours of reaction. This result confirms the creation of additional polymer chains by thermal initiation of styrene in Expt 1, 2 and 3, leading to molar masses lower than expected. The lowest the initial alkoxyamine concentration is the most pre-dominant self-initiation is.

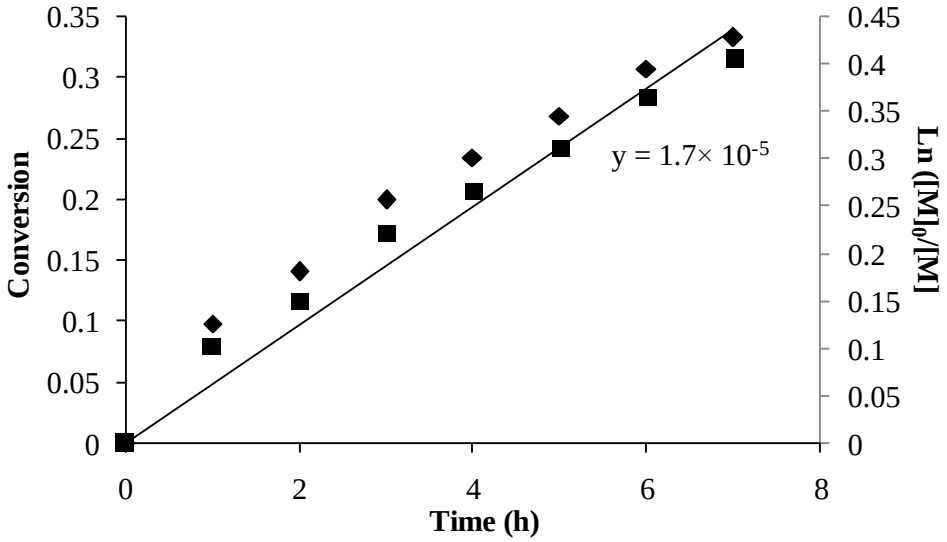

Figure 3. Conversion ♦ and logarithmic monomer concentration ■ versus time of polymerization of styrene carried out at 120 °C in miniemulsion in the absence of alkoxyamine or initiator.

It is possible to estimate the concentration of chains produced by thermal initiation ([T]) as follows: $[chains]_{exp} = [chains]_{theo} + [T]$. The theoretical number of chains corresponds to the initial concentration of alkoxyamine ($[BB\text{-}BA]_0$) and the concentration of chains produced by thermal initiation can be considered equal to the concentration of radicals produced by styrene self-initiation ($\Delta[I^\bullet]$) in bulk calculated from the rate constant of self-initiation (k_f) according to reference of Hui. *et al.* [23] (see note 1). So the experimental concentration of chains can be finally calculated as follows: $[chains]_{exp} = [BB\text{-}BA]_0 + \Delta[I^\bullet]$ (see Table 3).

[1] $k_f = 12.29\text{-}13810/T$ (T in K), $k_f = 1.21 \times 10^{-10}$ mol^{-2}.L^2.s^{-1} at T = 120 °C
$\frac{d[I^\bullet]}{dt} = 2k_f.[M]^3 = 2.42 \times 10^{-10} \times [M]^3$

Table 3. Calculation of concentration of radicals produced by styrene self-initiation (T = 120 °C)

Expt	$[BB\text{-}BA]_0$ mol.L^{-1} orga	$[chains]_{exp}$ mol.L^{-1} orga	$[T]^a$ mol.L^{-1} orga	$\frac{[T]}{[chains]_{exp}}$ (%)	$\frac{[T]}{[BB\text{-}BA]_0}{}^a$ (kinetics)	$\frac{[T]}{[BB\text{-}BA]_0}{}^b$ (molar mass)
1	4.45×10^{-2}	4.85×10^{-2}	4.05×10^{-3}	8	0.09	0.20
2	1.73×10^{-2}	2.13×10^{-2}	4.05×10^{-3}	19	0.23	0.50
3	6.85×10^{-3}	1.09×10^{-2}	4.05×10^{-3}	37	0.59	1.40

[a] $[T] = \Delta[I^\bullet] = 2k_f.\Delta[M]^3.\Delta t$

[b] $\frac{[T]}{[BB\text{-}BA]_0} = \frac{M_{n,\,theo}}{M_{n,\,exp}} - 1 = \frac{[BB\text{-}BA]_0 + [T]}{[BB\text{-}BA]_0}$

A ratio of the concentration of the produced chains by self-initiation of styrene ([T]) to the total experimental concentration of chains shows values ranging between 8 and 37 %. This ratio increases with decreasing the initial concentration of the $[BB\text{-}BA]_0$ alkoxyamine. A ratio $\frac{[T]}{[BB\text{-}BA]_0}$ calculated according to kinetics can be related to the ratio $\frac{M_{n,\,theo}}{M_{n,\,exp}}$ -1 (see calculation in Table 3). We notice that the values of $\frac{[T]}{[BB\text{-}BA]_0}$(kinetics) based on the rate of styrene thermal initiation are less than the values of $\frac{[T]}{[BB\text{-}BA]_0}$(molar mass) calculated from $\frac{M_{n,\,theo}}{M_{n,\,exp}}$ ratio, hence indicating that miniemulsion can enhanced the concentration of chains created by thermal initiation of styrene.

Nevertheless, the dispersity values remain below 1.3 even for Expt 3 which reveals that the SG1 concentration expelled by PRE is sufficient for controlling polymerization.

Next, we studied the colloidal features of the latex synthesized by NMP miniemulsion (Expt 1, 2 and 3 in Table 4). We studied the hydrodynamic diameter by dynamic light scattering (DLS) for both the initial liquid miniemulsion and the final latex. The samples were studied as in concentration mode at solids content ranging from 6 to 14 % (Table 4). The diameter of the initial liquid miniemulsion regardless of the initial concentration of the alkoxyamine ranged between 350 and 370 nm. Thus, the concentration of the alkoxyamine has no effect on the initial droplet diameter in the presence of 2.2 wt-% of Dowfax surfactant versus styrene. For different initial alkoxyamine concentrations, the diameters of the final latex are close to each other with values between ranging between 140 and 160 nm. Whether the particles are monodisperse or not, is a question that can be answered by observing the particle-diameter dispersity $\bar{d}_w/\bar{d}_n$. Distribution of diameter can be obtained automatically from the DLS,

where values below 0.1 indicate a monodisperse system, or it can be calculated according to Equation 2 and IUPAC terminology [24]:

$$\frac{\bar{d}_w}{\bar{d}_n} = \frac{\sum n_i \sum n_i d^4{}_i}{\sum n_i d_i \sum n_i d^3{}_i}$$

Equation 2. Calculation of the particle diameter dispersity

$\bar{d}_w$and $\bar{d}_n$ are the mass-average and number-average particle diameter respectively, n_i is the number of particles of a diameter d_i.

Table 4. Colloidal features of NMP miniemulsion polymerization of styrene carried out at 120 °C

Expt	Exp	Solids [a] content (%)	D_h [b] t=0 (nm)	D_h [b] t=7 h (nm)	$\bar{d}_w/\bar{d}_n$ [c]	σ [d]	N_p [e] L^{-1}_{latex}
1	HS108	6	-	160	1.01	0.1	2.5×10^{16}
2	HS134	12.6	370	140	1.01	0.3	8.5×10^{16}
3	HS113	13.6	350	160	1.05	0.2	6.3×10^{16}

[a] wt-% = $\tau_{monomer}$ × conversion
[b] hydrodynamic diameter of initial liquid miniemulsion and final latex obtained from DLS, concentrated mode
[c] particle-diameter dispersity calculated according to Equation 2.
[d] particle-diameter dispersity obtained from DLS
[e] Number of polymer particles calculated according to Equation 3.

The diameter of the final latex for all miniemulsion polymerizations ranged between 140-160 nm with a narrow particle size distribution of 1.01 for Expt. 1 and 2 and of 1.05 for Expt. 3. Upon comparing the diameter of the initial liquid miniemulsion to the diameter of the final latex, we observe that the lower diameter of the final latex (140-160 nm) in comparison with the initial droplets (350-370 nm) suggests either the formation of additional polymer particles during polymerization or slight coalescence of monomer droplets during DLS analysis.

We also calculated the number of polymer particles according to the following Equation 3:

$$N_p(L^{-1}{}_{latex}) = \frac{6\tau_{polymer}}{\rho_{polymer} \times {D_h}^3 \times \pi}$$

Equation 3. Calculation of the number of polymer particles (N_p)

With the polymer content ($\tau_{polymer} = \frac{m_{monomer}}{m_{latex}} \times conversion$), $\rho_{polymer}$ the density of polymer (ρ_{PS}= 1.05 g.cm^{-3}) and D_h the final particle diameter in cm.

In Table 4, we can notice that the number of particles is in the same range for the three NMP miniemulsion experiments.

Following, we studied the kinetics of the NMP miniemulsion polymerizations of styrene initiated by BB-BA alkoxyamine. The logarithmic concentration of monomer was plotted as a function of time (Figure 4).

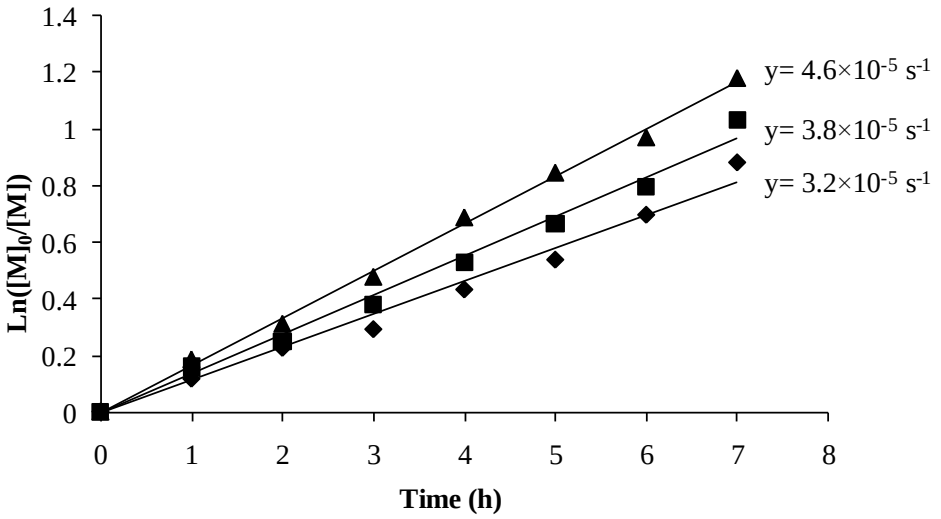

Figure 4. Logarithmic monomer concentration versus time for miniemulsion polymerizations of styrene in presence of Dowfax surfactant at different $[BB\text{-}BA]_0$, (Expt 1 ♦: $[BB\text{-}BA]_0=4.45 \times 10^{-2}$ M); (Expt 2 ■: $[BB\text{-}BA]_0=1.73 \times 10^{-2}$ M) and (Expt 3 ▲: $[BB\text{-}BA]_0=6.85 \times 10^{-3}$ M). $y = \text{slope} = k_p [P^\bullet]$

Regardless of the initial concentration of the alkoxyamine BB-BA, Figure 4 first shows a linear evolution with time, indicating that the concentration of propagating radicals remains constant during the polymerization. In Figure 4, we observe that highest slope corresponds to the polymerization of styrene starting with the lowest $[BB\text{-}BA]_0$. The slope of $Ln([M]_0/[M])$ versus time is equal to $k_p[P^\bullet]$ with k_p being the rate constant of propagation obeying Arrhenius law: $k_p = Ae^{\frac{-Ea}{RT}}$ (see Table 5).

Table 5. k_p and K_{eq} values for the polymerization of styrene at 120 °C mediated by SG1 nitroxide

A[a]	**E_a**[a]	**k_p**	**K_{eq}**[b]
$L.mol^{-1}.s^{-1}$	$kJ.mol^{-1}.s^{-1}$	$L.\ mol^{-1}.s^{-1}$	$mol.L^{-1}$
4.27×10^{7}	32.5	2.03×10^{3}	6×10^{-9}

[a] A: Arrhenius constant, Ea: activation energy [25], $k_p = Ae^{\frac{-Ea}{RT}}$

[b] Equilibrium constant [26], $K_{eq} = k_d/k_c$

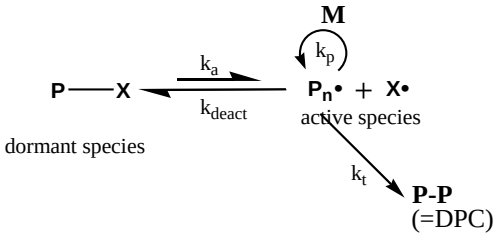

Scheme 4: scheme of NMP polymerization with alkoxyamine PX

As reported in Table 2 [P$^{\bullet}$] increases with decreasing of the initial BB-BA alkoxyamine concentration $[BB\text{-}BA]_0$, in accordance with the increasing of the slope of ln ($[M]_0/[M]$) = f(t) (Equation 4). This can be explained by the fact that the concentration of released SG1 ($[SG1]_{exp}$) by persistent radical effect (chapter 1, part 1.3.3) is higher for higher initial alkoxyamine concentration ($[BB\text{-}BA]_0$) (see Table 2 and Equation 4). In addition, the kinetic plots allow the calculation of the fraction of dead polymer chains (DPC) *via* the released concentration of SG1 (Equation 5 and Equation 4).

$$ln\frac{[M]_0}{[M]} = k_p K_{eq}\frac{[PX]_0}{[SG1]_{exp}}t$$

Equation 4

$$DPC = \frac{[SG1]_{released}}{[PX]_0} = \frac{[SG1]_{exp} - [SG1]_0}{[PX]_0} \times 100$$

Equation 5

The calculated values of DPC (26-39 %) show that a relatively large amount of SG1 is released into the reaction mixture, indicating the occurrence of substantial irreversible termination reactions at the initial stage of polymerization. This phenomenon is expected in the case of NMP of styrene as the equilibrium constant K_{eq} has a high value (see Table 5), implying a high concentration of propagating radicals P• in the reaction medium. NMP bulk polymerization of styrene with the initial concentration of alkoxyamine close to the one of Expt. 1 of Table 2 ($[BB\text{-}BA]_0 = 3.0\times10^{-2}$ mol.L^{-1}), exhibited lower DPC value (DPC = 19 %) [20] in comparison with NMP miniemulsion of styrene initiated by BB-BA showing DPC value of 39 % (see Expt 1 in Table 2, $[BB\text{-}BA]_0 = 4.45 \times 10^{-2}$ mol.L^{-1}). From the structure of the BB-BA alkoxyamine with sodium carboxylate and SG1/butyl hydrophobic groups (Scheme 2), the BB-BA alkoxyamine might exhibit surface active properties and be located at the styrene/water interface. This particular location of BB-BA alkoxyamine might explain the higher proportion of dead polymer chains observed in NMP miniemulsion of styrene (Expt. 1) in comparison with bulk polymerization of styrene [20]. We notice that the value of DPC decreases with lowering the initial concentration of alkoxyamine from 26 to 39 % (Table 2).

In order to confirm the suggested preferential location of BB-BA alkoxyamine at the particle surface, we investigated its ability to stabilize styrene droplets and final latex by performing NMP Miniemulsion polymerization of styrene in the absence of any surfactant in the next part.

2.2.3 Surfactant-free miniemulsion polymerization

In miniemulsion, the droplet nucleation being the main nucleation mechanism requires the stability of the initial liquid miniemulsion. For this purpose, before performing miniemulsion polymerizations in the absence of surfactant, it was interesting to study the ability of BB-BA to stabilize the initial liquid miniemulsion.

Table 6. Preparation of liquid miniemulsions of styrene at pH=9 with 0.012 $mol.L^{-1}_{water}$ of $NaHCO_3$

Tube	m_{H2O} (g)	m_S (g)	$m_{BB\text{-}BA}$ [a] (g)	$m_{hexadecane}$ [b] (g)	m_{Dowfax} [c] (g)	D_h [d] t = 0 h (nm)	D_h [d] t = 7 h (nm)	$\bar{d}_w/\bar{d}_n$ [e]
2	8	2	0	1.0×10^{-1}	4.4×10^{-2}	650	390	1.008
1	8	2	7.7×10^{-3}	1.0×10^{-1}	0	300	410	1.013

[a] mass of alkoxyamine ($[styrene]_0/[BB\text{-}BA]_0$=1280).
[b] hexadecane co-surfactant, 5 wt-% based on styrene
[c] 2.2 wt-% Dowfax surfactant based on styrene
[d] Hydrodynamic diameter measured by DLS with concentrated samples
[e] Particle-diameter dispersity calculated according to Equation 2.

Table 6 gathers initial recipe of two liquid miniemulsions, the first (tube 2 in Figure 5) is in the presence of Dowfax surfactant, and the second one (tube 1 in Figure 5) is in the absence of the surfactant but in the presence of BB-BA alkoxyamine.

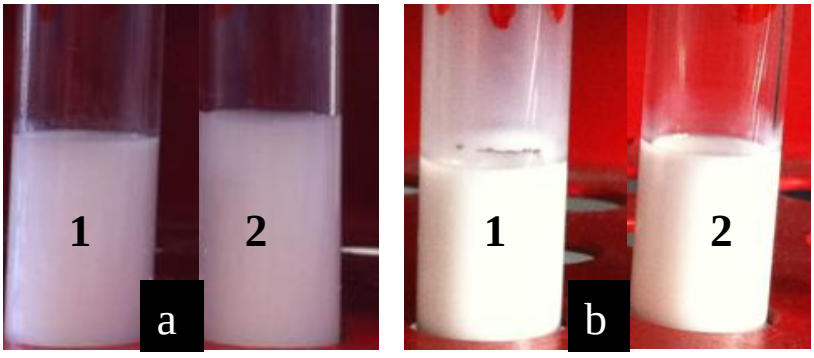

Figure 5. liquid miniemulsion, a) at time zero, b) after 7 hours

If we observe Figure 5, after the preparation of the liquid miniemulsion, at time zero we notice in both tubes the presence of only one emulsified phase, confirming the stability of the liquid droplets. In addition, after leaving the liquid miniemulsion for 7 hours, the one phase of the mixture remains stable for both tubes, *i.e.* in either the presence of Dowfax surfactant or in

the presence of BB-BA alkoxyamine. The hydrodynamic diameter of the initial liquid miniemulsion stabilized by Dowfax (tube 2 in Table 6) at time zero measured by DLS exhibited a higher diameter (D_h = 650 nm) in comparison with diameter of initial droplets stabilized with BB-BA alkoxyamine (tube 1 in Table 6) (D_h = 300 nm). However, 7 hours later, both liquid miniemulsions exhibited approximately the same diameter centered at 400 nm. The diameter dispersity is only slightly higher for droplets stabilized with BB-BA alkoxyamine but still very narrow ($\bar{d}_w/\bar{d}_n$< 1.01). These preliminary tests show the ability of BB-BA alkoxyamine to stabilize interfaces, hence confirming the hypothesis of specific location of such alkoxyamine in the initial droplets. In perspective, we should envisage to perform surface tension measurements at oil-water interface in order to determine more precisely the surface active features.

The next step of this work consisted of performing NMP miniemulsion polymerizations of styrene in the absence of surfactant, with varying the initial concentration of the BB-BA alkoxyamine (Table 7).

Table 7. Experimental conditions for NMP miniemulsion of styrene carried out at 120 °C in the absence of surfactant. [a]

Expt	Exp	$[BB\text{-}BA]_0$ [b] $mol.L^{-1}_{orga}$	DP_{theo} [c]
4	HS122	4.16×10^{-2}	200
5	HS121	6.82×10^{-3}	1280

[a] The polymerizations were all carried out with the following recipe: aqueous phase (H_2O, $NaHCO_3$ 0.012 $mol.L^{-1}_{water}$, at pH = 9) and organic phase (styrene, 20 wt-% solids content, hexadecane 5 wt-% based on styrene, BB-BA) were mixed and subjected to high shear pressure before polymerization, and then moved to thermostated reactor at 3 bar and 120 °C

[b] Initial concentration of BB-BA monoadduct alkoxyamine with respect to the organic phase.

[c] Theoretical degree of polymerization at 100 % conversion, $DP_{theo} = [S]_0/[BB\text{-}BA]_0$

The two nitroxide-mediated miniemulsion polymerizations (Expt. 4 and 5 in Table 7) were performed at 120 °C at constant styrene content with different alkoxyamine concentrations in the absence of both surfactant and free SG1 nitroxide. In Figure 6, we notice that regardless of the initial concentration of the alkoxyamine, the final M_w/M_n values are below 1.6, an indication of a controlled radical polymerization. The evolution of the experimental number-average molar mass with conversion is linear to a certain extent. However, for both Expt. 4 and 5 with $[BB\text{-}BA]_0 = 4.16\times10^{-2}$ and 6.82×10^{-3} $mol.L^{-1}$ respectively, the values of the experimental molar mass become superior to that of the theoretical molar mass. Upon

calculating the $M_{n,\,theo}/M_{n,\,exp}$ ratio, we obtain values of 0.4 and 0.6 respectively. These values of $M_{n,\,theo}/M_{n,\,exp}$ less than 1 indicate an incomplete efficiency of the initiator. However, the question which arises is why the thermal initiation is not creating additional chains like for NMP miniemulsion in the presence of surfactant when targeting the same degrees of polymerization (Expt. 1 and 3 of Table 2). The very low initiator efficiency might compensate the self-initiation of styrene to explain higher experimental M_n values in comparison with theoretical M_n. The very low alkoxyamine efficiency for surfactant-free NMP miniemulsion might be related to its specific location at styrene/water interface in the absence of Dowfax surfactant enhancing the exit of the sodium carboxylate based radical fragment to the water phase.

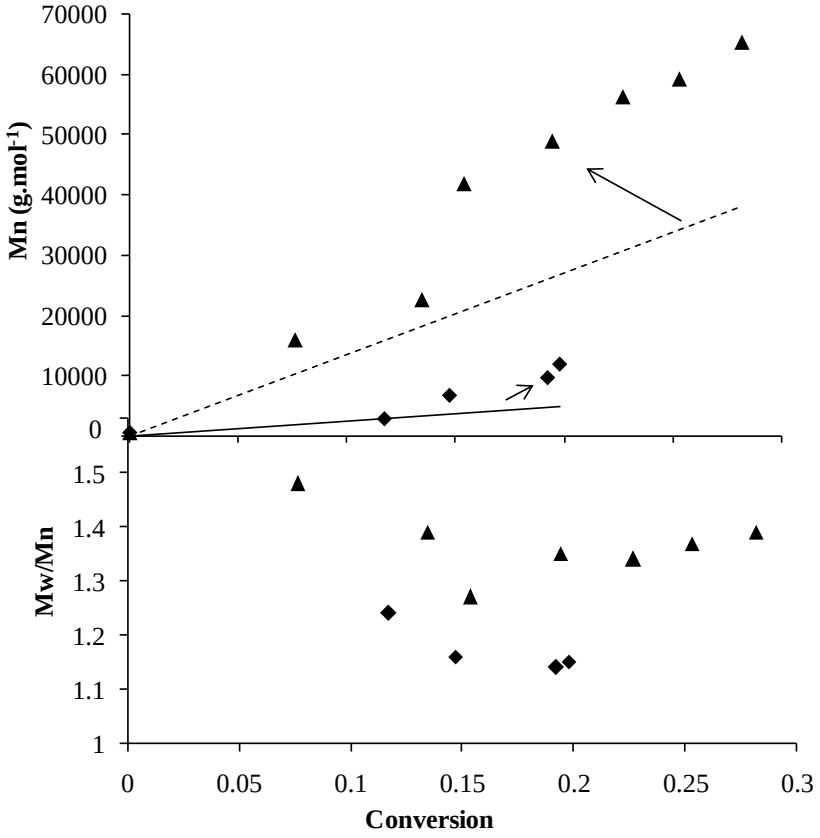

Figure 6. Plots of $M_{n,\,SEC}$ and M_w/M_n versus conversion for NMP miniemulsion of styrene in absence of surfactant with different $[BB\text{-}BA]_0$.♦ Expt 4 (solid line) and ▲ Expt 5 (dashed line), $[BB\text{-}BA]_0 = 6.82 \times 10^{-3}$ M. The lines correspond to theoretical molar masses.

Table 8. Results of NMP miniemulsion of styrene carried out at 120 °C in the absence of Dowfax surfactant

Expt	Conversion (time) % (h)	Coagulum %	$[P^{\bullet}]_{exp}$ [a] $mol.L^{-1}_{orga}$	$[SG1]_{exp}$ [b] $mol.L^{-1}_{styrene}$	DPC [c] %	$M_{n,theo}$ [d] $g.mol^{-1}$	$M_{n,SEC}$ [e] $g.mol^{-1}$	M_w/M_n [e]	$\frac{M_{n,theo}}{M_{n,exp}}$
4	20 (7)	18	4.3×10^{-9}	5.8×10^{-2}	139	4630	11860	1.1	0.4
5	30 (7)	-	9.9×10^{-9}	4.1×10^{-3}	60	38080	65430	1.3	0.6

[a] $[P^{\bullet}] = \frac{\ln([M]_0/[M]) = f(t)}{k_p}$

[b] Concentration of released SG1calculated from Equation 4

[c] DPC corresponds to the fraction of dead polymer chains calculated from Equation 5 and Equation 4 with $[SG1]_0 = 0$

[d] The theoretical M_n was calculated from Equation 1

[e] Number-average molar mass and dispersity derived from the PS calibration (RI detector).

Regardless of the initial concentration of the BB-BA alkoxyamine, Figure 7 shows a linear evolution of logarithmic monomer concentration with time, indicating that the concentration of propagating radicals remains constant during the polymerization. We notice that like in NMP miniemulsion with Dowfax surfactant for a lower initial concentration of BB-BA alkoxyamine, a higher slope is obtained, a characteristic of a higher concentration of radicals (Table 8). As in the case of presence of Dowfax, we notice that the concentration of released SG1 in Table 8 ($[SG1]_{exp}$) decreases with decreasing the $[BB\text{-}BA]_0$. The calculated values of DPC (60-140 %) show that a relatively large amount of SG1 is released into the reaction mixture, indicating the occurrence of substantial termination reactions.

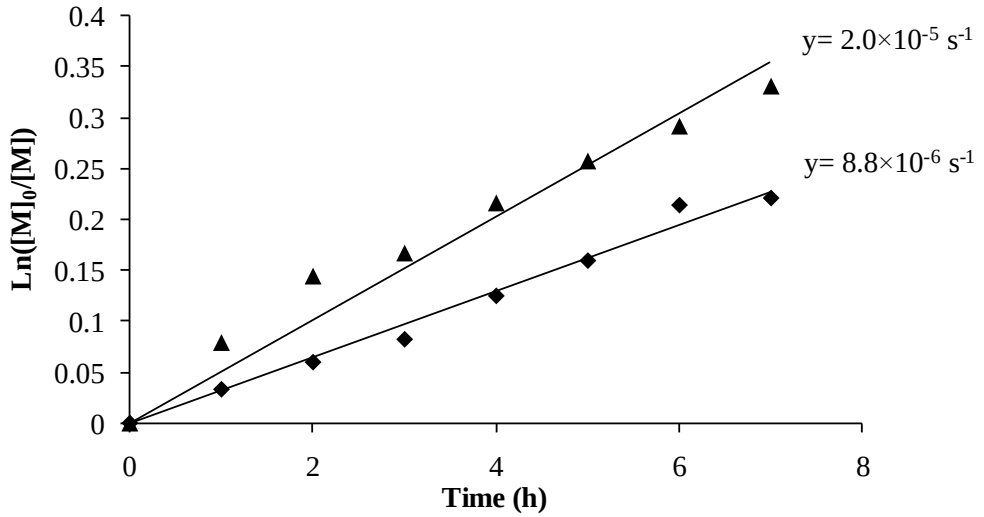

Figure 7. Logarithmic monomer concentration versus time for miniemulsion polymerizations of styrene in absence of Dowfax surfactant at different $[BB\text{-}BA]_0$; (Expt 4 ♦: $[BB\text{-}BA]_0 = 4.16 \times 10^{-2}$ M) and (Expt 5 ▲: $[BB\text{-}BA]_0 = 6.82 \times 10^{-3}$ M); y = slope = $k_p [P^{\bullet}]$

The fraction of calculated dead polymer chains is higher for the highest initial concentration of alkoxyamine. A similar trend was observed for NMP miniemulsion in the presence of Dowfax surfactant (Table 2). The highest value of DPC for surfactant free NMP polymerization mediated by BB-BA (Expt. 5 of Table 6, DPC = 60 %) in comparison with similar experiment performed in the presence of surfactant (Expt. 3 of Table 2, DPC = 26 %) confirms the loss of control by enhanced termination reactions through radical expel when BB-BA alkoxyamine is favorably placed at the styrene-water interface. This observation is in accordance with the different trends of molar masses (Figure 2 and Figure 6). Nevertheless, values of DPC above 100 % for Expt. 4 is not reasonable as the initial number of alkoxyamine cannot release a higher number of SG1. This high DPC value of 140 % might be explained by the presence of coagulum that might change the partition of SG1 and BB-BA or to the exit of BB-BA alkoxyamine to the water phase, providing lower true $[BB\text{-}BA]_0$ in the monomer droplets. The non-reasonable DPC value of 140 % is in accordance with the suggestion of the very low efficiency of the BB-BA alkoxyamine (in regard to the $M_{n,\,theo}/M_{n,\,exp}$ ratio) due to the exit of BB-BA to the water phase. In conclusion, this study reveals that the use of BB-BA alkoxyamine for NMP miniemulsion exhibiting surface active properties, induces increase in the fraction of dead polymer chains and this phenomenon is amplified in the absence of surfactant.

Following the study of kinetics, it was crucial to study the diameter of the initial liquid miniemulsion along with the diameter of the latex particles for a better understanding of the kinetics.

Table 9. Colloidal features of NMP miniemulsion polymerization of styrene carried out at 120 °C in the absence of surfactant

Expt	Exp	D_h [a] t = 0 h (nm)	D_h [a] t = 7 h (nm)	$\bar{d}_w/\bar{d}_n$ [b]	σ [c]	N_p [d] L^{-1}_{latex}
4	HS122	700	1000	1.30	0.01	7.2×10^{13}
5	HS121	355	355	1.01	0.04	2.4×10^{15}

[a] hydrodynamic diameter of initial liquid miniemulsion and final latex obtained from DLS in concentrated mode
[b] Particle-diameter dispersity calculated according to Equation 2.
[c] Particle-diameter dispersity obtained from DLS
[d] Number of polymer particles calculated according to Equation 3.

In Table 9, for Expt. 5 with the lowest initial concentration of the BB-BA alkoxyamine, the droplet size of the initial liquid miniemulsion was similar to that obtained in the presence of surfactant (Table 4). Moreover, final D_h of the final particles is higher in the absence of

surfactant (350-1000 nm) than in the presence of surfactant (~ 150 nm). For experiment carried out in the absence of surfactant, with the highest initial concentration of the alkoxyamine (Expt. 4) we obtained a high final diameter 1000 nm indicating a lower stability of the final latex (Table 9).

Next, we compared the kinetics of the NMP miniemulsion in the presence of surfactant to the miniemulsions in the absence of surfactant. For this, we plotted the logarithmic monomer concentration of the polymerization in the presence and absence of surfactant as reported in Figure 8.

Regarding Figure 8, we notice that for similar initial concentration of alkoxyamine (Expt. 3 vs Expt. 5 and Expt. 1 vs Expt. 4) the rate of polymerization systematically is higher in the presence of surfactant which is a characteristic of a lower total concentration of radicals. Both the higher fraction of irreversible termination and the lower number of particles (see $N_p < 2.4 \times 10^{15}$ L^{-1}_{latex} in Table 9 and $N_p > 2.5 \times 10^{16}$ L^{-1}_{latex} in Table 4) can explain the lower concentration of radicals in the absence of surfactant.

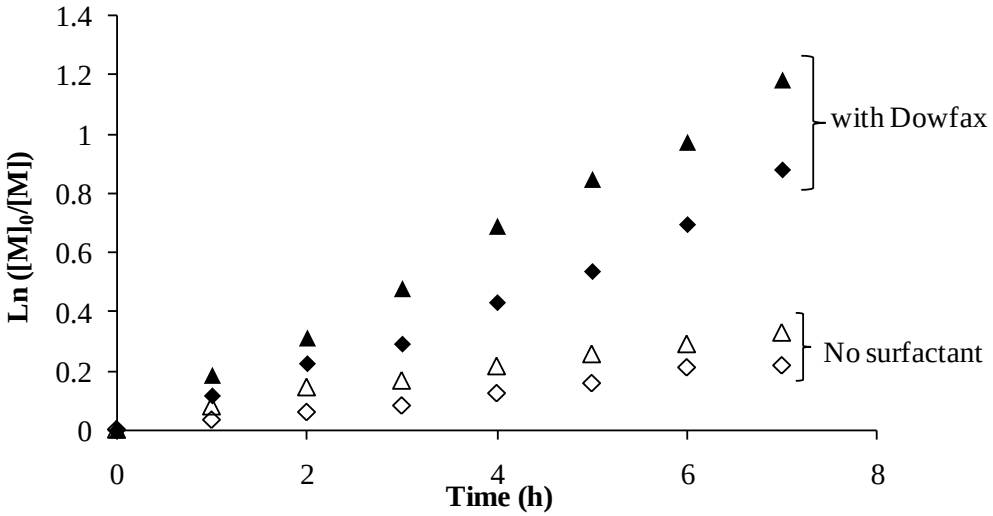

Figure 8. Comparison of logarithmic monomer concentration versus time of the styrene in the presence of Dowfax surfactant (Expt. 3 ▲: $[BB\text{-}BA]_0 = 6.85\times10^{-3}$ M; Expt. 1 ♦: $[BB\text{-}BA]_0 = 4.45\times10^{-2}$ M) and absence of surfactant (Expt. 5 Δ: $[BB\text{-}BA]_0 = 6.82\times10^{-3}$ M; Expt. 4 ◊: $[BB\text{-}BA]_0 = 4.16\times10^{-2}$ M)

If we compare the experimental values of the molar masses for similar initial concentration of alkoxyamine, they are higher in the absence of surfactant (Expt. 1 vs Expt. 4 and Expt. 3 vs Expt. 5 in Figure 9). The reason of this might be explained by the low efficiency of the alkoxyamine in the absence of surfactant which compensated the self-initiation of styrene as suggested from kinetic results. It should be noted that whatever the presence or absence of

surfactant, NMP miniemulsion of styrene initiated by BB-BA alkoxyamine is able to produce high molar mass PS ($40000 < M_n < 65000$ g.mol^{-1}) with dispersity below 1.4 (Expt. 3 and 5 in Figure 9).

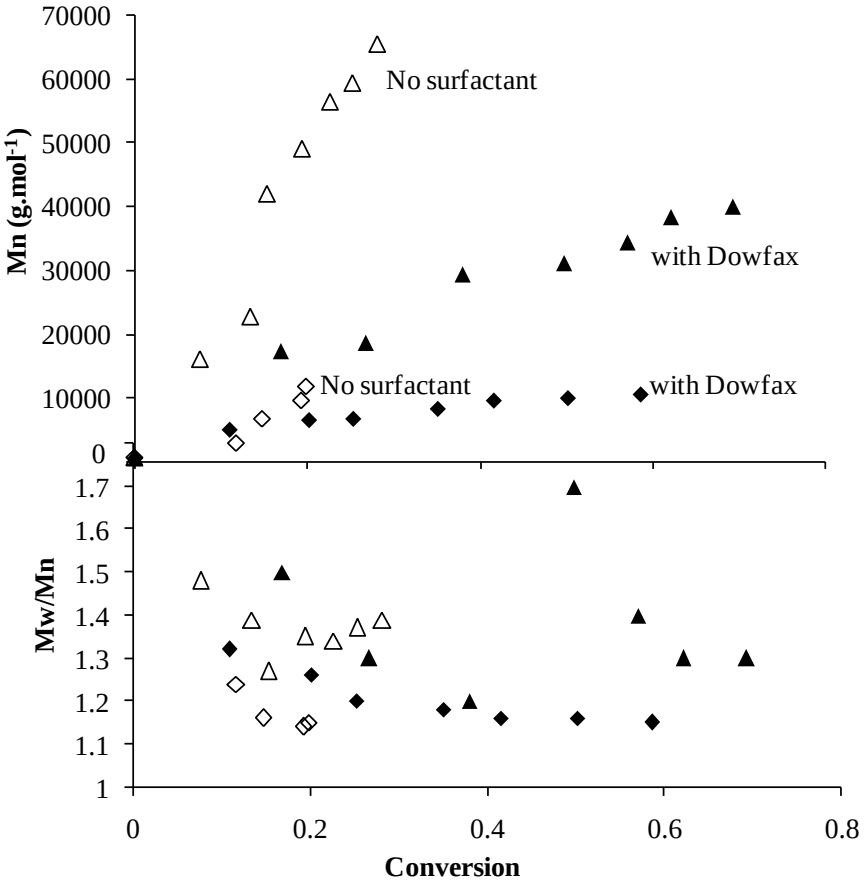

Figure 9. Comparison of $M_{n,\,SEC}$ and M_w/M_n versus conversion for the NMP miniemulsion of the styrene in the presence of Dowfax surfactant (Expt. 3 ▲: $[BB\text{-}BA]_0 = 6.85\times10^{-3}$ M; Expt. 1 ♦: $[BB\text{-}BA]_0 = 4.45\times10^{-2}$ M) and absence of surfactant (Expt. 5 Δ: $[BB\text{-}BA]_0 = 6.82\times10^{-3}$ M; Expt. 4 ◊: $[BB\text{-}BA]_0 = 4.16\times10^{-2}$ M)

2.2.5 NMP-microemulsion of styrene

As discussed in chapter 1, at sufficiently small particles sizes kinetic can be impacted but more importantly control and livingness are improved for linear polymers [12-16].

The criterion for microemulsion polymerization is that a threshold emulsifier concentration exists above which a thermodynamically stable microemulsion is formed spontaneously for a given organic and aqueous phase. Contrary to that, miniemulsions are critically stabilized and require high shear to reach a steady state. Microemulsions are thermodynamically stable with an interfacial tension at the oil/water interface close to zero, whereas in miniemulsions, the interfacial tension is much larger than zero. The high amount of surfactant, which is required for microemulsion preparation leads to a complete coverage of the droplets particles, and, therefore, the surface tension of the microemulsion reaches a minimum value. Two recent

interesting studies focused on the NMP polymerization of styrene in microemulsion which are summarized in Table 10 below.

Table 10. Studies dealing with NMP microemulsion of styrene carried out at 90 °C [15] and 100 °C [12]

Reference	Solids content [a] (%)	Surfactant [b]	Surfactant [c] (%)	Initiator	nitroxide	D_h latex (nm)
[15]	5.2	Oleic acid	120	PS-SG1	SG1	10
[12]	5.0	TTAB	250	AIBN	TIPNO or SG1	55

[a] solids content = [styrene/(styrene+ TTAB or oleic acid +water)]
[b] tetradecyltrimethylammonium bromide
[c] wt-% surfactant based on styrene

Thus, our objective in the following part is to evaluate if performing NMP of styrene in very small droplets (microemulsion conditions) can reduce the fraction of dead polymer chains while maintaining a high rate of polymerization. This question will be addressed for high targeted degree of polymerization (DP = 1000), hence for low alkoxyamine concentration. As mentioned before, such high DP will be targeted in Chapter 3 for the synthesis of core@shell particles by surface-initiated polymerization in miniemulsion.

In this context we performed styrene NMP microemulsion at 5 wt-% of solids content using a 250 wt-% of sodium dodecyl sulfate (SDS) as surfactant versus styrene. We first attempted to use Dowfax in microemulsion, however, errors with conversion measured gravimetrically were obtained due to the partial evaporation of Dowfax, which strongly impacted the conversion for such high amount of surfactant. We chose *N*-tert-butyl-*N*-(1-diethyl phosphono-2,2-dimethylpropyl)-*O*-(1-(methoxycarbonyl)ethyl) hydroxylamine (MONAMS) as an organo-soluble alkoxyamine (Scheme 1.9 in chapter 1) in order to simplify the nucleation step.

Table 11. Experimental conditions for NMP microemulsion of styrene carried out at 120 °C [a]

Expt.	Exp	Monomer	$[MONAMS]_0$ [b] $mol.L^{-1}_{styrene}$	$[SG1]_0$ $mol.L^{-1}_{styrene}$	DP_{theo} [c]
6	MK07	S	8.7×10^{-3}	0	1000

[a] The polymerizations were all carried out with the following recipe: aqueous phase (H_2O, SDS, $NaHCO_3$ 0.012 $mol.L^{-1}_{water}$, at pH = 9) and organic phase (monomer, 5 wt-% solids content, MONAMS) were mixed for 30 minutes and then moved to thermostated reactor at 3 bar, 300 rpm and 120 °C, with 250 wt-% sodium dodecyl sulfate SDS surfactant based on monomer
[b] Initial concentration of MONAMS alkoxyamine with respect to the organic phase.
[c] Theoretical degree of polymerization at 100 % conversion, $DP_{theo} = [S]_0/[MONAMS]_0$

Styrene NMP microemulsion showed a final latex diameter of 50 nm (Table 12). This diameter insures that we are in the framework of microemulsion polymerization producing nanolatex. The number of final particles is 5 times higher than miniemulsion NMP carried out with rather similar initial concentration of alkoxyamine (see Expt. 3 of Table 4). Nevertheless, the obtained value of diameter dispersity show high value, indicating a polydisperse system of particles.

Table 12. Colloidal features of NMP-microemulsion polymerization with SDS surfactant

Expt	Exp	D_h [a] t = 7 h (nm)	$\bar{d}_w/\bar{d}_n$ [b]	σ [c]	N_p [d] L^{-1}_{latex}
6	MK07	50	1.21	0.26	4.0×10^{17}

[a] hydrodynamic diameter of final latex obtained from DLS, samples concentrated, cummalnts mode
[b] Particle-diameter dispersity calculated according to Equation 2.
[c] Particle-diameter dispersity obtained from DLS
[d] Number of particles calculated according to Equation 3

In Figure 10, the evolution of the experimental number-average molar mass with conversion is linear. However, the experimental values of the molar mass are initially above theoretical M_n became inferior to that of the theoretical molar mass above 45 % of conversion. Upon calculating the final $M_{n,\,theo}/M_{n,\,exp}$ ratio we obtain a value higher than 1 (Table 13), again suggesting the creation of additional chains.

In a similar work, Zetterlund reported styrene NMP microemulsion targeting a DP of 700, using AIBN/SG1 as initiator/nitroxide and 250 wt-% of surfactant versus styrene. [12] After 4 hours of reaction, he recorded a conversion of 99 %, and experimental molar mass lower than the theoretical value ($M_{n,\,theo}/M_{n,\,exp}$ = 1.4). [12] These results are adequate with the results that we obtained, a 90 % conversion after 4 hours and $M_{n,\,theo}/M_{n,\,exp}$ = 1.6 (Table 13).

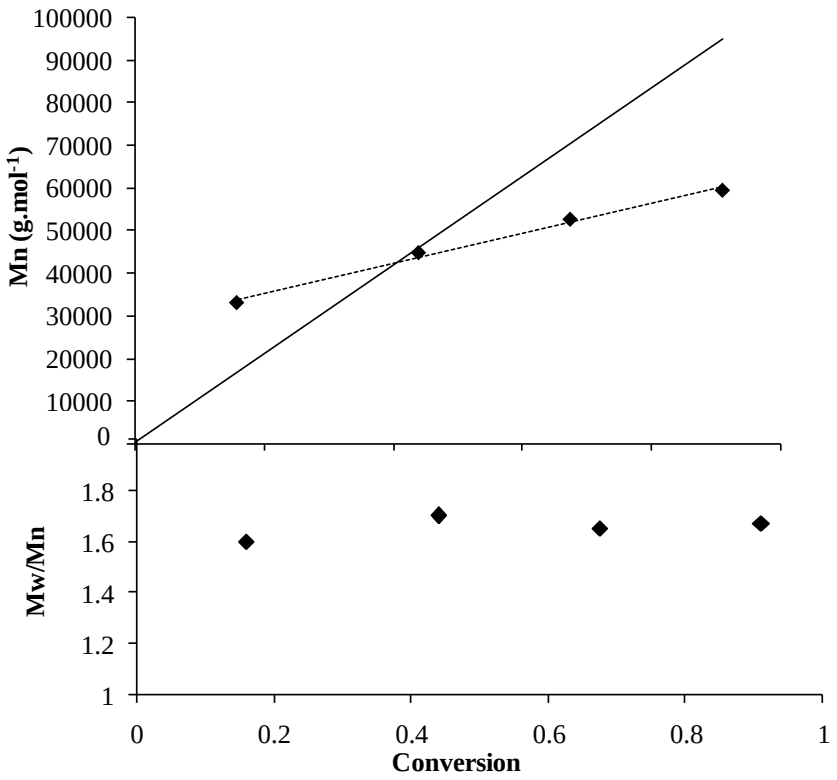

Figure 10. Plots of $M_{n,SEC}$ and M_w/M_n versus conversion of NMP microemulsion of styrene initiated by MONAMS at 120 °C; ♦ Expt 6 (solid line corresponds to theoretical M_n values) targeting a DP of 1000.

Table 13. Results of NMP microemulsion of styrene carried out with 250 wt-% of SDS surfactant versus styrene

Expt	Conversion (time) % (h)	$[P^{\bullet}]_{exp}$ [a] mol.L^{-1}	$[SG1]_{exp}$ [b] mol.L^{-1}	DPC [c] %	$M_{n,theo}$ [d] g.mol^{-1}	$M_{n,SEC}$ [e] g.mol^{-1}	M_w/M_n [e]	$\frac{M_{n,theo}}{M_{n,exp}}$
6	90 (4)	1.9×10^{-9}	6.4×10^{-4}	7.4	94880	59400	1.6	1.6

[a] $[P^{\cdot}] = \frac{\ln([M]_0/[M]) = f(t)}{k_p}$

[b] Concentration of released SG1calculated from Equation 4

[c] DPC corresponds to the fraction of dead polymer chains calculated from Equation 5 and Equation 4 with $[SG1]_0 = 0$

[d] The theoretical M_n was calculated from Equation 1

[e] Number-average molar mass and dispersity derived from the PS calibration (RI detector).

Figure 11 shows a linear evolution with time of logarithmic monomer concentration, indicating that the concentration of propagating radicals remains constant during the polymerization. The fraction of dead polymer chains DPC indicated a value of 7.4 % (Table 13). This value of DPC in NMP microemulsion of styrene was reduced in comparison to NMP miniemulsion of styrene targeting high DP of 1280 Expt. 3 of Table 2 (DPC = 26 %) while achieving a higher polymerization rate (Figure 11).

Decreasing the fraction of dead polymer chains in NMP microemulsion in comparison to NMP miniemulsion of styrene, while targeting a high DP, is an interesting result. Nevertheless, the dispersity of final polymer is higher in the case of NMP microemulsion (M_w/M_n = 1.6, Figure 10) for M_n ~ 60000 g.mol^{-1} than for NMP miniemulsion (M_w/M_n = 1.3) for 40000 g.mol^{-1} (Figure 2). Note that different alkoxyamines were involved in miniemulsion (BB-BA) and microemulsion (MONAMS) polymerization and also different surfactants due to experimental issues. Two additional experiments should be performed in a future work to distinguish effects of alkoxyamine and surfactant structures: NMP microemulsion of styrene stabilized by SDS but initiated by BB-BA and NMP miniemulsion of styrene initiated by MONAMS but stabilized by SDS. In both cases thermal initiation of styrene still leads to the creation of more chains than expected (Figure 2 and Figure 10).

Regarding the $M_{n,\ theo}/M_{n,\ exp}$ ratio for NMP microemulsion of styrene a value of 1.6 was obtained at 90 % conversion (4h), this value is lower than that obtained with NMP miniemulsion of styrene (2.4) at 72 % conversion (7h). Thus, the faster rate of polymerization achieved with microemulsion (Figure 11), induces a decrease of the fraction of chains created by thermal initiation. In conclusion, we showed that decreasing the particle size with microemulsion increased the rate of polymerization while also decreasing the fraction of dead polymer chains.

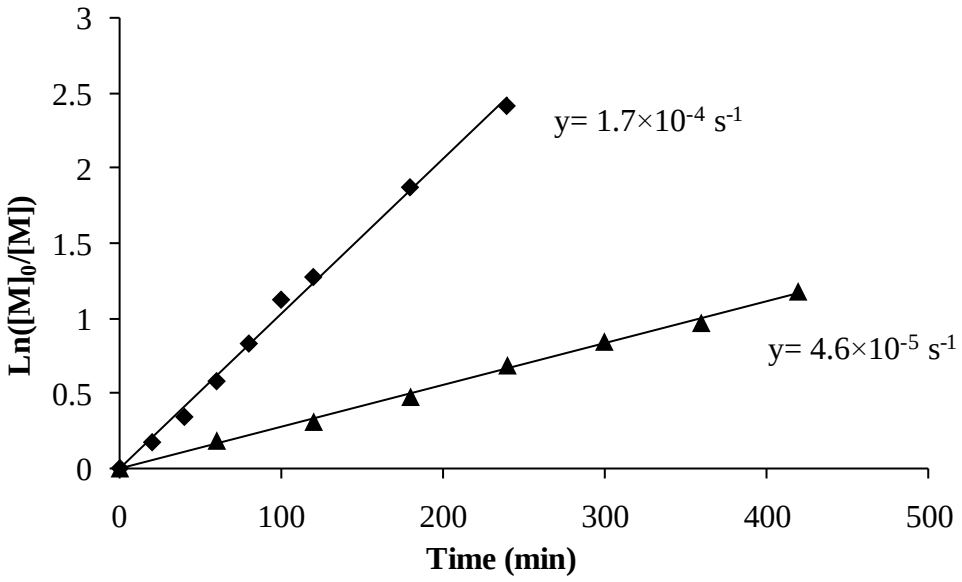

Figure 11. Logarithmic monomer concentration versus time of the styrene polymerization carried out at 120 °C in microemulsion (Expt 6 ♦; Table 11, [MONAMS] = 8.7 × 10^{-3} M) and in miniemulsion (Expt 3 ▲; Table 2, [BB-BA] = 6.8 × 10^{-3} M). y = slope.

For a more proper comparison between miniemulsion and microemulsion of styrene, further two experiments were performed. Targeting a DP of 1000 miniemulsion and microemulsion of styrene were performed using BB-BA as the initiator and SDS as the stabilizer and the results are shown in Table 14 below.

Table 14. Results of NMP microemulsion and miniemulsion of styrene carried out with 250 wt-% and 2.2 wt-% of SDS surfactant respectively, targeting a DP of 1000 and using BB-BA alkoxyamine as initiator

Expt	Type	Conversion (time) % (h)	$[P^{\bullet}]_{exp}$ [a] mol.L^{-1}	$[SG1]_{exp}$ [b] mol.L^{-1}	DPC [c] %
7	Microemulsion	82 (4)	5.7×10^{-8}	9.0×10^{-4}	10.5
8	Miniemulsion	32 (4)	1.3×10^{-8}	3.0×10^{-3}	44.0

[a] $[P^{\cdot}] = \frac{\ln([M]_0/[M]) = f(t)}{k_p}$

[b] Concentration of released SG1calculated from Equation 4

[c] DPC corresponds to the fraction of dead polymer chains calculated from Equation 5 and Equation 4 with $[SG1]_0 = 0$

Figure 12 shows a linear evolution with time of logarithmic monomer concentration, indicating that the concentration of propagating radicals remains constant during the polymerization. The fraction of dead polymer chains DPC indicated a value of 10.5 % (Table 14). This value of DPC in NMP microemulsion of styrene was reduced in comparison to NMP miniemulsion of styrene targeting high DP of 1280 Expt. 8 of Table 14 (DPC = 44 %) while achieving a higher polymerization rate (Figure 12). Decreasing the fraction of dead polymer chains in NMP microemulsion in comparison to NMP miniemulsion of styrene while using BB-BA as the alkoxyamine and SDS as the stabilizer, while targeting a high DP, is an interesting result.

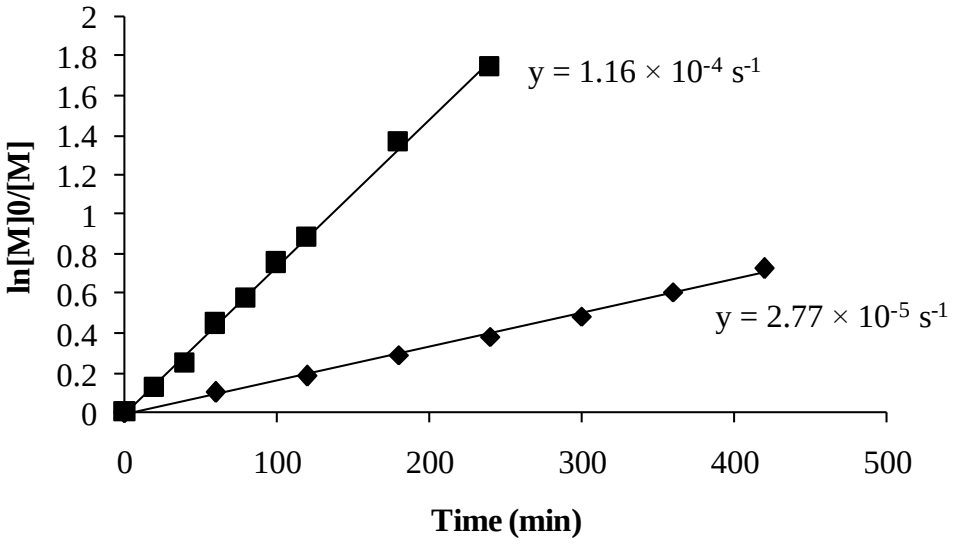

Figure 12. Logarithmic monomer concentration versus time of the styrene polymerization carried out at 120 °C in microemulsion (Expt 8 ♦; Table 14, [BB-BA] = 6.8×10^{-3} M) and in microemulsion (Expt 7 ■; Table 14, [BB-BA] = 8.7×10^{-3} M). y = slope.

Conclusion

In the study of the effect of the initial concentration of the initiator on the NMP miniemulsion polymerization of styrene in the presence of surfactant, we noticed that it was possible to control the polymerization for each experiment with linear evolution of M_n versus conversion, dispersity values decreasing with conversion and remaining below 1.4 and linear plots of ln ($[M]_0/[M]$). Thus, even upon targeting a high degree of polymerization we can still control the polymerization ($200 < DP < 1280$). Nevertheless, a ratio of $M_{n,\,theo}$ /$M_{n,\,exp}$ higher than 1 was obtained for all experiments, indicating the creation of more chains probably created by thermal initiation of styrene. The calculated values of fraction of dead polymer chains (DPC ~ 26-39 %) showed that a relatively large amount of SG1 was released into the reaction mixture by persistent radial effect. The high concentration of released SG1 is probably at the origin of the maintained polymerization control despite the high number of created chains by thermal self-initiation. Moreover, we noticed that the value of DPC decreased for lower concentration of alkoxyamine which is related to lower values of released SG1. This phenomenon explains that the rate of polymerization was faster for the polymerization conducted with lowest initial concentration of the alkoxyamine. While studying the colloidal features, we also noticed the final latex diameters recorded around 150 nm with different initial concentrations of alkoxyamines.

In comparison to bulk polymerization, miniemulsion polymerization of styrene resulted in higher values of DPC. This was explained by the fact that BB-BA alkoxyamine has a sodium carboxylate and SG1/butyl hydrophobic group (Scheme 2), hence, it can be a surface active species placed at the styrene/water interface. This particular location of BB-BA alkoxyamine might explain the higher proportion of dead polymer chains observed in NMP-miniemulsion of styrene in comparison with bulk polymerization. Indeed, the exit of SG1 or initiator fragment exit might be favored inducing occurrence of more irreversible termination reactions.

By studying surfactant free NMP polymerization of styrene targeting a high degree of polymerization via BB-BA alkoxyamine several conclusions emerged:

1. The polymerization still exhibits features of controlled radical polymerization (linearity of M_n = f(conversion)), $M_w/M_n < 1.4$, linearity of ln ($[M]_0/[M]$) = f(t). However, unlike in the presence of surfactant, the ratio M_{ntheo}/M_{nexp} recorded values lower than 1 indicating incomplete efficiency of the initiator in the absence of surfactant.
2. Stabilization of colloidal particles was still ensured by BB-BA although diameters of final latex were higher. The final latex diameters were higher than that obtained in the presence of surfactant (400-1000 nm).
3. The obvious increase of the dead polymer chain fraction for surfactant free NMP of styrene suggest a strong effect of the ability of this alkoxyamine to be located at styrene/water interface. Similar to miniemulsion in presence of surfactant the fraction of DPC decreases with decreasing initial concentration of the alkoxyamine.

When targeting high degree of polymerization above 1000, NMP microemulsion polymerization of styrene enabled us to lower the fraction of dead polymer chains from 26 % in NMP miniemulsion to 7 % in NMP microemulsion while maintaining a higher rate of polymerization. Compartmentalization effect was observed in these experiments.

This chapter was dedicated to study the kinetics of NMP miniemulsion polymerization of styrene while targeting a high degree of polymerization, which opens the door for our next chapter that involves the synthesis of core@shell hybrid nanoparticles *via* NMP polymerization while targeting a high DP (the reason is to limit the content of inorganic particles below 10 wt-%).

References

1. Braunecker, W. A.; Matyjaszewski, K., Controlled/living radical polymerization: Features, developments, and perspectives. *Progress in Polymer Science* **2007,** 32, (1), 93-146.
2. Cunningham, M. F., Controlled/living radical polymerization in aqueous dispersed systems. *Progress in Polymer Science* **2008,** 33, (4), 365-398.
3. Zetterlund, P. B.; Kagawa, Y.; Okubo, M., Controlled/living radical polymerization in dispersed systems. *Chemical Reviews* **2008,** 108, (9), 3747-3794.
4. Monteiro, M. J.; Cunningham, M. F., Polymer Nanoparticles via Living Radical Polymerization in Aqueous Dispersions: Design and Applications. *Macromolecules* **2012,** 45, (12), 4939-4957.
5. Lansalot, M.; Farcet, C.; Charleux, B.; Vairon, J. P.; Pirri, R., Controlled free-radical miniemulsion polymerization of styrene using degenerative transfer. *Macromolecules* **1999,** 32, (22), 7354-7360.
6. Li, M.; Min, K.; Matyjaszewski, K., ATRP in waterborne miniemulsion via a simultaneous reverse and normal initiation process. *Macromolecules* **2004,** 37, (6), 2106-2112.
7. Landfester, K., Polyreactions in miniemulsions. *Macromolecular Rapid Communications* **2001,** 22, (12), 896-936.
8. Asua, J. M., Miniemulsion polymerization. *Progress in Polymer Science* **2002,** 27, (7), 1283-1346.
9. Cunningham, M. F., Recent progress in nitroxide-mediated polymerizations in miniemulsion. *Comptes Rendus Chimie* **2003,** 6, (11-12), 1351-1374.
10. Charleux, B., Nitroxide-mediated polymerization in miniemulsion: A direct way from bulk to aqueous dispersed systems. In *Advances in Controlled/Living Radical Polymerization*, Matyjaszewski, K., Ed. 2003; Vol. 854, pp 438-451.
11. Nicolas, J.; Guillaneuf, Y.; Lefay, C.; Bertin, D.; Gigmes, D.; Charleux, B., Nitroxide-mediated polymerization. *Progress in Polymer Science* **2013,** 38, (1), 63-235.
12. Zetterlund, P. B.; Wakamatsu, J.; Okubo, M., Nitroxide-Mediated Radical Polymerization of Styrene in Aqueous Microemulsion: Initiator Efficiency, Compartmentalization, and Nitroxide Phase Transfer. *Macromolecules* **2009,** 42, (18), 6944-6952.
13. Maehata, H.; Buragina, C.; Cunningham, M.; Keoshkerian, B., Compartmentalization in TEMPO-mediated styrene miniemulsion polymerization. *Macromolecules* **2007,** 40, (20), 7126-7131.
14. Simms, R. W.; Cunningham, M. F., Compartmentalization of reverse atom transfer radical polymerization in miniemulsion. *Macromolecules* **2008,** 41, (14), 5148-5155.
15. Guo, Y.; Zetterlund, P. B., Rate-Enhanced Nitroxide-Mediated Miniemulsion Polymerization. *Acs Macro Letters* **2012,** 1, (6), 748-752.
16. Kitayama, Y.; Tomoeda, S.; Okubo, M., Experimental Evidence and Beneficial Use of Confined Space Effect in Nitroxide-Mediated Radical Microemulsion Polymerization (Microemulsion NMP) of n-Butyl Acrylate. *Macromolecules* **2012,** 45, (19), 7884-7889.
17. Nicolas, J.; Charleux, B.; Guerret, O.; Magnet, S., Novel SG1-Based water-soluble alkoxyamine for nitroxide-mediated controlled free-radical polymerization of styrene and n-butyl acrylate in miniemulsion. *Macromolecules* **2004,** 37, (12), 4453-4463.
18. Gigmes, D.; Dufils, P. E.; Gle, D.; Bertin, D.; Lefay, C.; Guillaneuf, Y., Intermolecular radical 1,2-addition of the BlocBuilder MA alkoxyamine onto activated olefins: a versatile tool for the synthesis of complex macromolecular architecture. *Polymer Chemistry* **2011,** 2, (8), 1624-1631.

19. Deleuze, C.; Delville, M. H.; Pellerin, V.; Derail, C.; Billon, L., Hybrid Core@Soft Shell Particles as Adhesive Elementary Building Blocks for Colloidal Crystals. *Macromolecules* **2009,** 42, (14), 5303-5309.
20. BLAS, H., Université Pierre et Marie Curie. **2009**.
21. Blas, H.; Save, M.; Boissiere, C.; Sanchez, C.; Charleux, B., Surface-Initiated Nitroxide-Mediated Polymerization from Ordered Mesoporous Silica. *Macromolecules* **2011,** 44, (8), 2577-2588.
22. Mayo, F. R., *J Am Chem Soc* **1968,** 90, 1289.
23. Hui, A. W.; Hamielec, A. E., THERMAL POLYMERIZATION OF STYRENE AT HIGH CONVERSIONS AND TEMPERATURES - AN EXPERIMENTAL STUDY. *Journal of Applied Polymer Science* **1972,** 16, (3), 749-&.
24. Slomkowski, S.; Aleman, J. V.; Gilbert, R. G.; Hess, M.; Horie, K.; Jones, R. G.; Kubisa, P.; Meisel, I.; Mormann, W.; Penczek, S.; Stepto, R. F. T., Terminology of polymers and polymerization processes in dispersed systems (IUPAC Recommendations 2011). *Pure and Applied Chemistry* **2011,** 83, (12), 2229-2259.
25. Beuermann, S.; Buback, M., Rate coefficients of free-radical polymerization deduced from pulsed laser experiments. *Progress in Polymer Science* **2002,** 27, (2), 191-254.
26. Benoit, D.; Grimaldi, S.; Robin, S.; Finet, J. P.; Tordo, P.; Gnanou, Y., Kinetics and mechanism of controlled free-radical polymerization of styrene and n-butyl acrylate in the presence of an acyclic beta-phosphonylated nitroxide. *Journal of the American Chemical Society* **2000,** 122, (25), 5929-5939.

Chapter 3
Surface-initiated NMP in miniemulsion for the design of core@shell silica@polymer nanoparticles

Introduction 102
3.1 Experimental part 104
3.1.1 Synthesis of alkoxyamine grafted colloidal silica 104
3.1.1.1 Synthesis of colloidal silica 104
3.1.1.2 Synthesis of the alkoxyamine TMSPA-BB 104
3.1.1.3 Grafting of TMSPA-BB onto silica particles 105
3.1.2 "One step" SI-NMP in miniemulsion 105
3.1.3 "Two steps" SI-NMP in miniemulsion 105
3.1.4 Cleavage of grafted chains from silica 106
3.2 Results and discussion 106
3.2.1 Synthesis of alkoxyamine grafted colloidal silica 106
3.2.1.1 Synthesis of colloidal silica 106
3.2.1.2 Synthesis of the TMSPA-BB alkoxyamine 109
3.2.1.3 Grafting of TMSPA-BB onto silica particles 111
3.2.2 "One step" SI-NMP in miniemulsion 115
3.2.3 "Two steps" SI-NMP in miniemulsion 123
Conclusion 129
References 131

Introduction

Organic/inorganic materials have been extensively studied for a long time. When inorganic phases in composites become nanosized, they are called nanocomposites. Organic/inorganic nanocomposites are generally organic polymer matrix with inorganic nanoparticles. They combine the advantages of the inorganic material (e.g., stiffness, thermal stability) and of the organic polymer (e.g., flexibility, dielectric, ductility, and processability). Nanoparticles include layered silicates (e.g., montmorillonite, saponite), nanoparticles of metals (e.g., Au, Ag), metal oxides (e.g., TiO_2, Al_2O_3), semiconductors (e.g., PbS, CdS), and so forth, among which silica (SiO_2) is viewed as being very important. Therefore, polymer/silica nanocomposites have attracted substantial academic and industrial interest. In fact, among the numerous inorganic/organic nanocomposites, polymer/silica nanocomposites are the most commonly reported in the literature. [1-3]

Nanocomposite latex particles have been synthesized by polymerization in aqueous dispersed media. Inorganic nanoparticles are either embedded in the polymeric colloidal particle or few covalent links are present through the grafting of a co-monomer function. As reported in chapter 1 (part 2), nanocomposite latex have been prepared by miniemulsion polymerization in the presence of different inorganic nanoparticles. [4-13] In this process, the hydrophobically modified inorganic particles could be dispersed in monomer phase followed by miniemulsification, then each miniemulsion droplet could indeed be treated as a small nanoreactor resulting in composite nanoparticles. The covalent grafting of monomer onto inorganic nanoparticles led to random grafting of polymer chains inside the latex particle. [14] Emulsion and dispersion polymerization have also proved to be suitable methods for the synthesis of nanocomposite latex with either spherical or anisotropic morphologies. [15-17] Different strategies were implemented to control complex nucleation step such as for instance adsorption of reactive polyelectrolyte [18] or monomer-grafted inorganic nanoparticles as nuclei of polymerization. [17]

Recently, strategies have been developed to tailor nanoparticle surfaces by the use of polymers. The purpose is to directly tether polymers from or onto the surface of these nanoparticles resulting in a core@shell type of material architecture. To construct a highly dense polymer brush, ‘‘grafting from’’ technique has been used in combination with controlled polymerization methods. In this process, the polymer chains grow from the initiator

anchored onto the surface, (named surface-initiated polymerization (SI-P)). The SI-P in conjunction with a reversible-deactivation radical polymerization (RDRP) is among the most useful synthetic routes to precisely design and functionalize inorganic surfaces with well-defined polymers and copolymers. [19-21] As reported in chapter 1 (part 3), well-defined core-shell nanoparticles have been synthesized by SI-RDRP initiated from various inorganic nanoparticles. The thickness of the polymeric shell layer can be controlled by the molar mass and the grafting density of the covalently linked polymer chains. [22, 23] Such core@shell nanoparticles were loaded into a polymer matrix in order to investigate the effect of core@shell particles dispersion state onto the mechanical properties of the final composites. [1, 2, 24] Nevertheless, most of the syntheses were performed either in bulk or in solvent and very few studies reported the synthesis of well-defined core@shell nanoparticles by implementing surface-initiated controlled radical polymerization (or surface-initiated reversible deactivation radical polymerization) in aqueous dispersed media. In 2007, the group of Matyjazsewski reported the polymerization of *n*-butyl acrylate from silica surface in miniemulsion [25] *via* surface-initiated AGET ATRP to compare both kinetic and macromolecular features with bulk SI-ATRP. They showed that in comparison to the bulk polymerization, using the same stoichiometry, miniemulsion allowed the preparation of hybrid materials with a higher yield,. *i.e.* higher monomer conversion, and a higher polymerization rate without macroscopic gelation. Esteves *et al*. synthesized CdS Quantum Dots-based core@shell nanoparticles *via* surface-initiated AGET ATRP in miniemulsion with controlled grafted polymer chains exhibiting low dispersity values. [26]

Thus, in this chapter, we will be focusing on the synthesis of core@shell hybrid nanoparticles, with silica constituting the core and polymer such as polystyrene or poly(*n*-butyl acrylate) as the shell by surface-initiated nitroxide mediated polymerization (SI-NMP) in miniemulsion. Firstly, we will report the synthesis of colloidal silica particles with diameters inferior to 100 nm, followed by the modification of the silica surface by grafting an alkoxyamine. After dispersion of the alkoxyamine grafted silica particles in the monomer droplets, the grafting of polymer chains from the surface of the modified silica particles will be performed by SI-NMP in miniemulsion, either in the presence or in the absence of free initiator. We will study the colloidal features of the formed nanocomposites, along with the molar mass of the grafted polymer chains. The interest of NMP relies with the absence of ligand and copper catalyst that needs to be removed at the end of polymerization from colloidal aqueous dispersion.

3.1 Experimental part

Materials. Styrene (S) (Sigma-Aldrich, 99 %), *n*-Butyl acrylate (BA) (Sigma-Aldrich, 99 %) passed under inhibitor removers prior usage. Dowfax^{TM} 8390 surfactant (a mixture of mono- and dihexadecyl disulfonated diphenyloxide disodium salts, supplied by DOW company). Buffer sodium hydrogen carbonate $NaHCO_3$, co-stabilizer hexadecane (Aldrich, 99 %), high molar mass polystyrene PS (300000 g.mol^{-1}), Blocbuilder® (Arkema, 99 %), Tetraethyl orthosilicate (TEOS) (98 %, Aldrich), ammonium hydroxide (NH_4OH) (28.0-30.0 % NH_3, Sigma-Aldrich), 3-(trimethoxysilyl)propyl acrylate (TMSPA), *N*-tert-butyl-*N*-(1-diethylphosphono-2,2-dimethylpropyl) nitroxide (SG1) (85 % Arkema), Toluene (VWR) dried over magnesium sulfate, tetrahydrofuran (THF) (VWR), *para*-toluene sulfonic acid (*p*-TSA) (Aldrich, 99 %), absolute ethanol.

3.1.1 Synthesis of alkoxyamine grafted colloidal silica

3.1.1.1 Synthesis of colloidal silica

Silica particles were prepared by Stöber process. [27] For preparing the 80 nm diameter particles in a 500 mL round bottom flask, 300 mL of absolute ethanol were introduced. To this 16 mL of NH_4OH were added. While the mixture was being stirred at 300 rpm at ambient temperature, 10 mL TEOS were added. The mixture was left being stirred for 7 hours before adding again the same amount of TEOS, in order to insure the condensation of silica particles. The mixture was left at ambient temperature and 300 rpm for 17 hours. For the synthesis of the 25 nm diameter silica particles, the same procedure was followed by changing the amounts used, where 250 mL absolute ethanol, 7.2 mL NH_4OH and 2*14.95 mL TEOS were used (Table 1).

3.1.1.2 Synthesis of the alkoxyamine TMSPA-BB

The synthesis of TMSPA-BB was conducted in dry toluene (passed under Na), under nitrogen. In a 25 mL round bottom flask 1.09 g (2.8×10^{-3} mol) of Blocbuilder® were introduced and degassed by nitrogen for 15 minutes. 10 mL of dry toluene were added into the flask. Then 0.51 g (2.2×10^{-3} mol) of TMSPA (n_{TMSPA}: n_{BB} = 1:1.3) were added. After that, the mixture was moved to an oil bath preheated to 100 °C. The reaction was proceeded for 75 minutes. After the reaction was stopped by cooling the solution, a sample was withdrawn for NMR characterization. The product still in toluene under nitrogen, was kept in the fridge and used later directly for the grafting step.

3.1.1.3 Grafting of TMSPA-BB onto silica particles

For modifying the surface of the silica particles, different number of molecules was grafted in order to get finally that 5 molecules.nm^{-2} of the initiator to target is the best. Two approaches were followed for grafting the silica. The first is when the initiator was synthesized in ethanol it was transferred directly to the silica in ethanol via double tipped needle and stirred at 300 rpm without any heating for 24 hrs. Whereas the second approach was when the initiator was synthesized in toluene, the silica particles were dried under vacuum, degassed for 30 minutes and re-dispersed in dry toluene (1g/30 mL). The initiator solution was then transferred to the silica dispersion under nitrogen flow via a double tipped needle. The mixture was heated to 60 °C at 300 rpm for 24 hours. For both approaches after the reaction was stopped, grafted silica particles were centrifuged (13000 rpm for 30 minutes) and washed by fresh toluene minimum 6 times in order to eliminate any free initiator.

3.1.2 "One step" SI-NMP in miniemulsion

The experiments of one step SI-NMP in miniemulsion were performed as follows (example Exp HS80). Two phases were prepared, the aqueous phase containing 80 g of water, 0.44 g (1.1×10^{-3} mol) of surfactant and 0.082 g (9.6×10^{-4} mol) of $NaHCO_3$, the organic phase containing 20 g (1.9×10^{-1} mol) of styrene, 1 g (4.4×10^{-3} mol) of hexadecane, 0.2 g (6.8×10^{-7} mol) of PS and 2 g of TMSPA-BB grafted silica (HS52) which contains 0.074 g (1.4×10^{-4} mol) of grafted initiator (TMSPA-BB). When free initiator (monoadduct) was used, it was added with the organic phase. The two phases were mixed and stirred in an ice bath for 10 min. After that, the mixture was subjected to a high shear pressure using a Vibra Cell 72408 ultrasonicator for 15 minutes at an amplitude of 30 %. The mixture was then moved to a Parr 5100 thermostated reactor, where it was degassed for 30 min before heating. The mixture was then heated to 120 °C at 3 bars, and time 0 of the reaction was taken when the temperature reached 90 °C. Table 3 shows the different "one step" SI-NMP in miniemulsion.

3.1.3 "Two steps" SI-NMP in miniemulsion

Experiments in Table 8 were carried as follow, (example Exp HS111). 20 g (1.9×10^{-1} mol) of styrene was mixed with 2 g of silica (HS52, containing 0.074 g, 1.5×10^{-4} mol grafted TMSPA-BB) and 1.09×10^{-3} g (3.71×10^{-6} mol) of SG1 in a round bottom flask and heated in an oil bath at 120 °C for one hour. The reaction mixture was removed from the oil bath, 1 g

(1.1×10^{-3} mol) of hexadecane, 0.2 g (1.1×10^{-3} mol) of PS were poured in the round bottom flask. To this mixture, the aqueous phase containing 80 g of water, 0.45 g (1.1×10^{-3} mol) of surfactant and 0.085 g of $NaHCO_3$ (9.6×10^{-4} mol), was added and the mixture was subjected to high shear pressure for 15 minutes in an ice bath. The reaction was launched again in the thermostated reactor at 3 bars at 120 °C for styrene polymerization or at 115 °C for *n*-butyl acrylate polymerization.

3.1.4 Cleavage of grafted chains from silica

The cleavage of grafted polymer chains from silica was performed via transesterification reaction using para-toluene sulfonic acid. Polymer grafted silica synthesized by bulk NMP were dissolved in THF and centrifuged 3 times at 300 000 rpm. Whereas final latex recovered after SI-NMP in miniemulsion was dried prior solubilization in THF, followed by centrifugation 3 times at 300 000 rpm. In a 100 mL round bottom flask we introduce 150 mg of polymer functionalized silica, *para*-toluene sulfonic acid (*p*-TSA) (2 equivalent with respect to the grafted initiator), 20 mL of toluene and methanol (1000 equivalent with respect to *p*-TSA). The mixture was reflux heated while being stirred at 300 rpm for 12 hours. After that, the solution was centrifuged to eliminate the residual silica particles. Toluene was evaporated under vacuum and the cleaved chains were recovered by washing 6 times with a mixture of water/dichloromethane in order to eliminate any residual *p*-TSA. Then the cleaved chains were dried before SEC analysis.

3.2 Results and discussion

3.2.1 Synthesis of alkoxyamine grafted colloidal silica

3.2.1.1 Synthesis of colloidal silica

The sol-gel method is one of the most used for the synthesis of precipitated silica. The silica particles are formed by hydrolysis-condensation of a silicon alkoxide, usually tetraethoxysilane (TEOS). This method of synthesis, performed at moderate temperature, is in the field of "chimie douce ". [28]

Hydrolysis : ≡Si-OR + H_2O → ≡Si-OH + R-OH

Condensation : ≡Si-OH + HO-Si≡ → ≡Si-O-Si≡ + H_2O

Scheme 1. Synthesis of colloidal silica by sol-gel chemistry

We followed the Stöber process, which is frequently used for synthesizing colloidal silica suspensions. This process was first introduced by Stöber and Fink in 1968, it is relatively simple to apply and based on a series of hydrolysis and condensation reactions of organosilanes. [27] The synthesis is based on the addition of tetraalkoxysilane in a mixture of absolute ethanol and ammonium hydroxide, and the stoichiometric ratio of the mixture is what controls the radius and dispersion of the final particles. Sol–gel chemistry is central in the development of hybrid materials. Typically, $M(OR)_n$, MX_n, $R'\text{-}M(OR)_{n-1}$ precursors are commonly used, where M represents a metal center, n is its oxidation state and X and RO are common ‘‘leaving groups’’ present in metallic salts or metal alkoxides. X can for example represent a chloride anion, as in metal halides. R’ is any organic functionality anchored to the metallic center via covalent bonds or via complexing ligands. [28] The sol–gel process implies connecting the metal centers with oxo- or hydroxo- bridges, therefore generating metal-oxo or metal-hydroxopolymers in solution. Hydrolysis of an alkoxy group attached to a metal center leads to hydroxyl-metal species:

$$M\text{-}OR + H_2O \longrightarrow M\text{-}OH + ROH$$

The hydroxylated metal species can react with other metal centers leading to condensation reactions, where an oligomer is formed by bridging two metal centers. In the case of oxolation, condensation leads to an oxo bridge, and water or alcohol is eliminated:

$$M\text{-}OH + XO\text{-}M \longrightarrow M\text{-}O\text{-}M + XO\text{-}H$$

X=H or R

In the case of olation, an addition reaction takes place, and a hydroxo bridge is formed. This reaction takes place when metal centers may have coordination higher than their valence, as in the case of Ti(IV), Zr(IV), or related cations,

$$M\text{-}OH + XO\text{-}M \longrightarrow M\text{-}(OH)\text{-}M\text{-}OX$$

X=H or R

For reactions catalyzed by ammonium hydroxide, after reaching a saturation threshold, silica precipitates and form germs. The later grow in parallel to progressive consuming of the hydrolyzed alkoxysilanes. During the growth step, the number of the particles in the medium remains constant. Thus, once the alkoxysilane molecules are consumed, the reaction stops and the formed medium consists of spherical particles. The obtained particles are of great interest, they carry on their surface functional silanol groups (Si-OH). The specific reactivity of these groups is important for the functionalization of the silica surface by a certain molecule or

initiator. In the present work, different batches of silica were synthesized following the recipes of reference [29], whether it was respectively for the 25 nm or 80 nm particles (Table 1).

Table 1. Experimental conditions of synthesis of silica particles and final diameter

Exp.	Solvent	[NH_4OH] mol.L^{-1}	[TEOS][a] mol.L^{-1}	Temperature °C	Time	[Si] [b] wt-%	D_h(nm) σ [c]	D_n (nm) $\bar{d}_w/\bar{d}_n$ [d]
1	Absolute ethanol	1.35	2*0.15	25	24h	4	80	1.08
2	Absolute ethanol	0.74	2*0.26	25	24h	4	25	1.02

[a] First amount of TEOS was added at the beginning of the reaction and the second amount was added 7h later
[b] Final silica content, $m_{TEOS}/3$
[c] Mean hydrodynamic diameter and particle-diameter dispersity measured by DLS of crude solution.
[d] Mean number diameter from TEM and particle-diameter dispersity obtained from Equation 2 in chapter 2.

As reported in Table 1, two batches of suspension of colloidal silica particles in ethanol were synthesized with different concentrations of ammoniac catalyst. A primary analysis of the size of the silica performed by dynamic light scattering (DLS) in ethanol, showed more than one population for each batch of silica. The mean hydrodynamic diameter was fitted from the autocorrelation curve providing D_h = 80 nm for experiment 1 and D_h = 25 nm for experiment 2 (Figure 1).

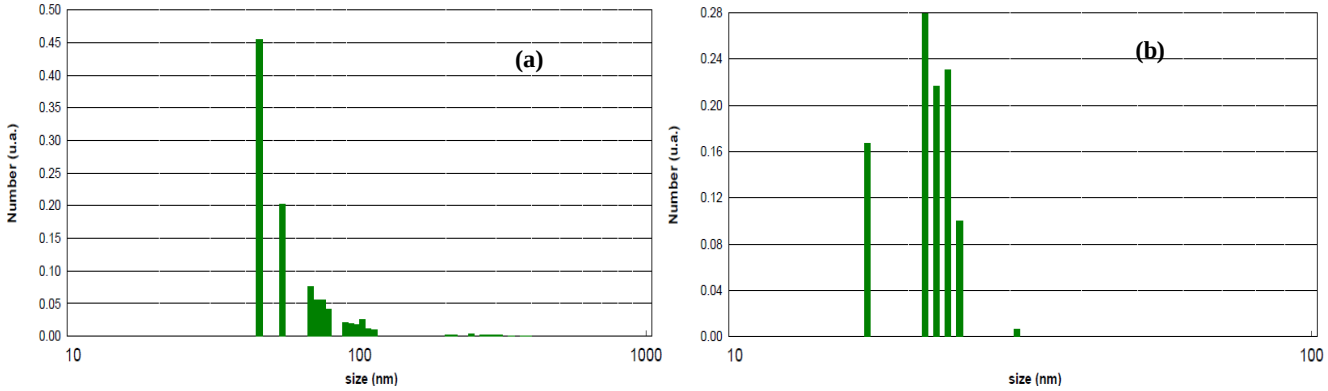

Figure 1 : Size dispersion by number of the silica particles measured by DLS in ethanol, (Exp. 1) (a) and (Exp. 2) (b)

The formed silica particles were also analyzed by Transmission Electron Microscopy TEM. From TEM analysis of both silica batches (Figure 2) we can see that silica particles were shown to be spherical in shape with monodisperse distribution. The TEM analysis allows the calculation of the number-average diameter: $D_n = \frac{\sum n_i D_i}{\sum n_i}$. A calculated value for the number-average diameter was D_n = 77 nm for experiment 1 and D_n = 24 nm for experiment 2. These values are in accordance with the values obtained from DLS, 80 nm and 25 nm respectively.

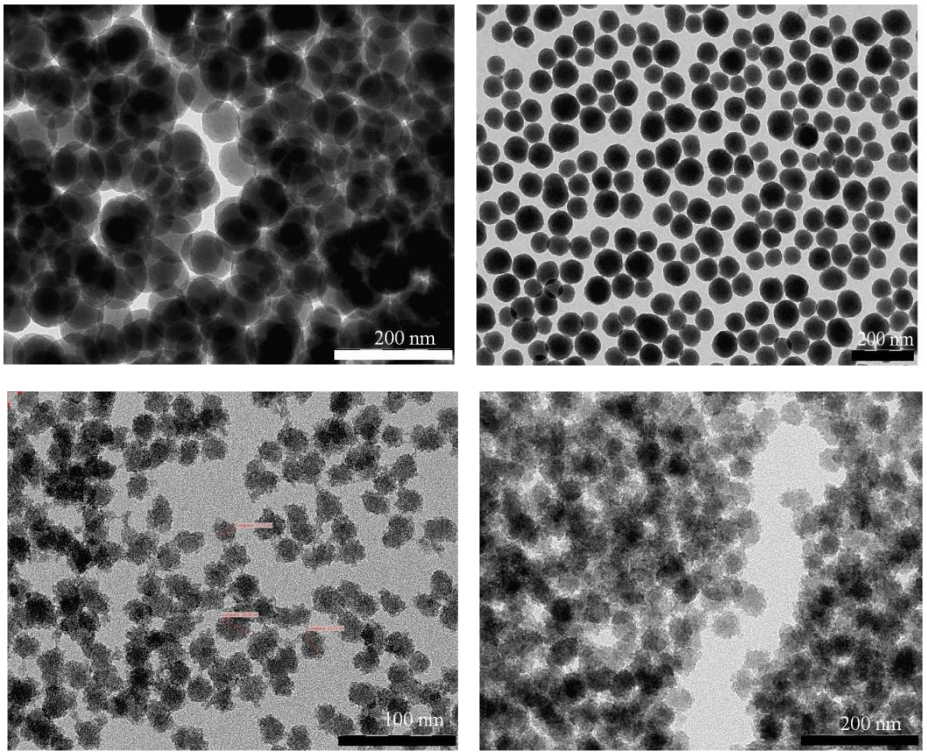

Figure 2. TEM images of Exp. 1 (top) and Exp 2. (bottom) of Table 1

3.2.1.2 Synthesis of the TMSPA-BB alkoxyamine

In the present work, the functional TMSPA-BB trialkoxysilane-based initiator was synthesized by 1,2 addition of Blocbuilder® alkoxyamine onto TMSPA acrylate according to the literature (Scheme 2). [23, 30] The principle of 1,2 radical addition onto activated olefin was previously described in chapter 2.

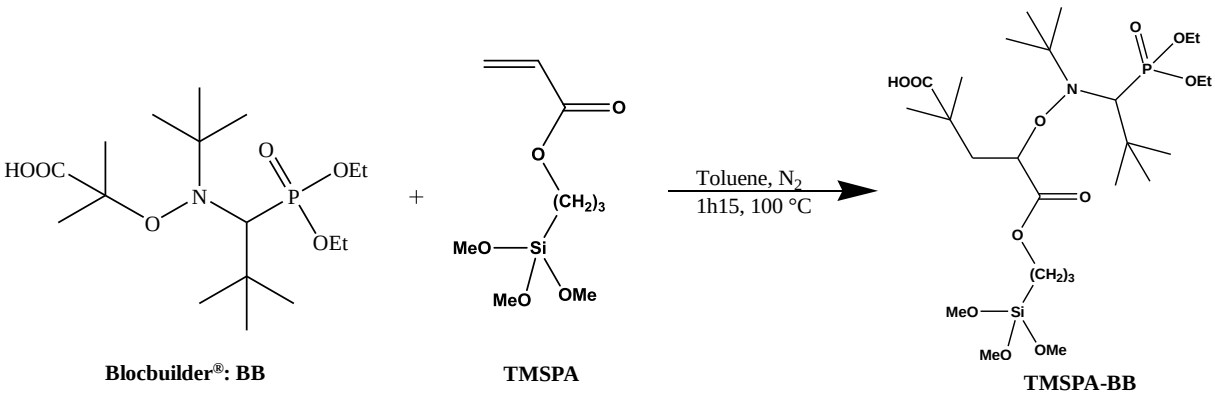

Blocbuilder®: BB **TMSPA** **TMSPA-BB**

Scheme 2. Synthesis of TMSPA-BB by 1,2 radical addition of Blocbuilder® onto TMSPA

The ^{1}H NMR spectrum of the recovered TMSPA-BB is detailed in Figure 3 below. The success of 1,2-radical addition was first proved by the appearance of F, F' and E protons characteristics of the aliphatic protons present after 1,2-addition (δ_E = 4.6 ppm, $\delta_{F,F'} \approx$ 2.5 ppm). The 1,2-addition was confirmed by the decrease of the vinylic proton of the initial

TMSPA (δ ~ 5.5 - 6.5 ppm). The ^{1}H NMR of the product of the reaction shows that the conversion is not complete, residual acrylate functions are visible on the spectrum between 6.0 and 6.5 ppm indicating 20 mol-% of residual TMSPA, ($\frac{I_{vinylic}/_{3}}{I_{vinylic}/_{3}+ I_{E}}$).

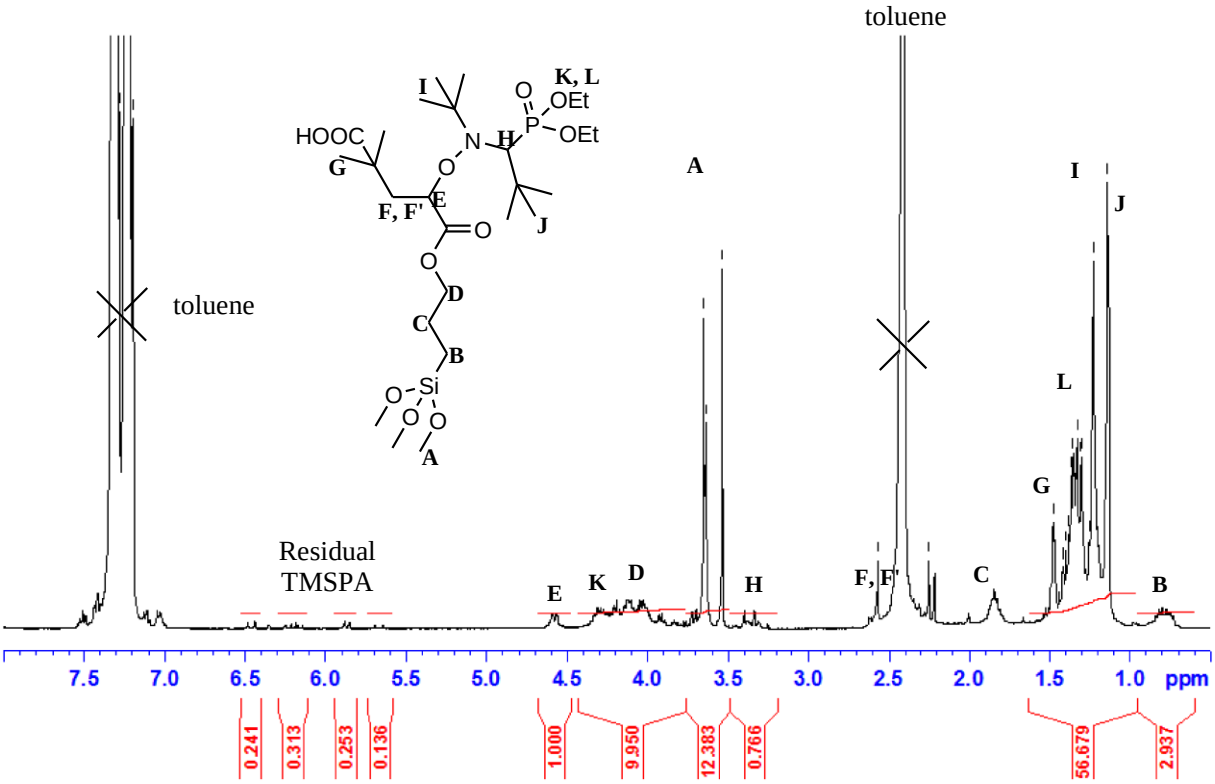

Figure 3. ^{1}H NMR spectrum of crude solution of TMSPA-BB in toluene (in $CDCl_3$)

The synthesized TMSPA-BB initiator is composed of three functional groups (Figure 4):

1. An alkoxyamine capable of dissociating and generating radicals and nitroxides by thermal dissociation, useful for polymerization.
2. An ester group cleavable by transesterification for the analysis of the grafted polymer chains.
3. A tri-alkoxysilane function, useful for the grafting with hydroxysilane groups of silica surface by hydrolysis-condensation reaction.

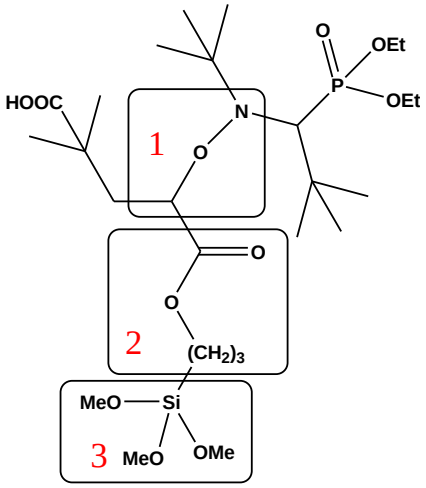

Figure 4. The molecule of TMSPA-BB initiator to be grafted on silica surface

3.2.1.3 Grafting of TMSPA-BB onto silica particles

In the case of Si-OH siliceous surfaces, grafting method commonly used consists in condensing a hybrid molecule of R-Si-X to form a siloxane bridge R-Si-O-Si. Different natures of X functions can be investigated to achieve this so-called silylation reaction. It includes the use of a chlorosilane or alkoxysilane. The condensation of a chlorosilane has an efficiency greater than alkoxysilane ones, but it requires anhydrous conditions. By using alkoxysilane function, it is however necessary to define its functionality: mono, di-or tri-functional. Mono-functional silanes or monoalkoxysilane allow the formation of a monolayer on the surface, thus avoiding side reactions occurring through vertical condensation in case of di- and tri-functional alkoxysilanes. On the other hand, trifunctional alkoxysilane produces higher grafting density. The choice comes down to promote the quality of grafting or performance of condensation.

In the present work, tri-functional alkoxysilane acrylate was available for the synthesis of the functional alkoxyamine (Figure 4). The grafting of TMSPA-BB onto colloidal silica was performed in dry toluene at 60 °C as described in the experimental part. The functionalized silica was analyzed by infrared spectroscopy. The visible characteristic bands of the initiator are shown on the FT-IR spectra (Figure 5) confirming the grafting of the alkoxyamine on the surface of the silica. Indeed, in addition to the characteristic bands of silica, new bands corresponding to the alkoxyamine molecule appear on the spectrum: ν (CH) at 2990 cm^{-1}, ν (C=O) at 1730 cm^{-1}, δ (CH) at 1480 cm^{-1}.

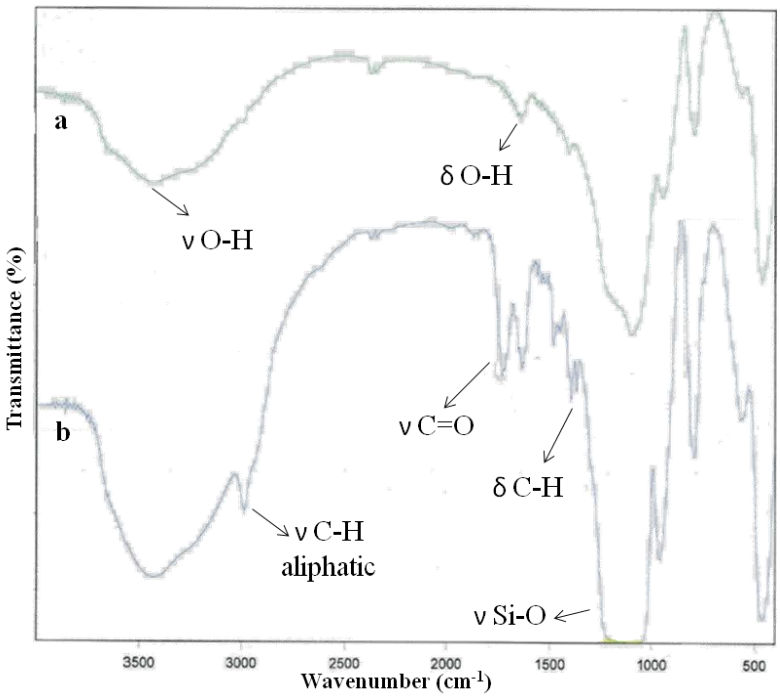

Figure 5. FT-IR spectra of (a) non-functionalized silica (HS96) and (b) alkoxyamine functionalized silica (HS98)

Thermogravimetric analysis (TGA) is used as a quantitative technique that allows the determination of the organic fraction grafted onto inorganic materials. Silica generally degrades in two stages: a first degradation in the interval 20-120 °C called "dehydration", is due to evaporation of water adsorbed on the surface; a second degradation, "de-hydroxylation" results from the release of a water molecule by rapid condensation of vicinal silanols in the interval 200-400 °C followed by slow condensation of isolated silanols in the interval 400-1000 °C.

TMSPA-BB grafted silica particles were analyzed by TGA and compared to the non-functionalized silica particles (Figure 6). Physi-sorbed water may disturb the accuracy of measurement, because the amount varies according to the hydrophilicity of the silica surface. The measurements are performed on samples previously dried under vacuum, and the mass loss is calculated between 120 and 800 °C in order not to take into account the adsorbed water. Figure 6 gives an example of thermograms obtained before and after functionalization with TMSPA-BB of the 80 nm colloidal silica.

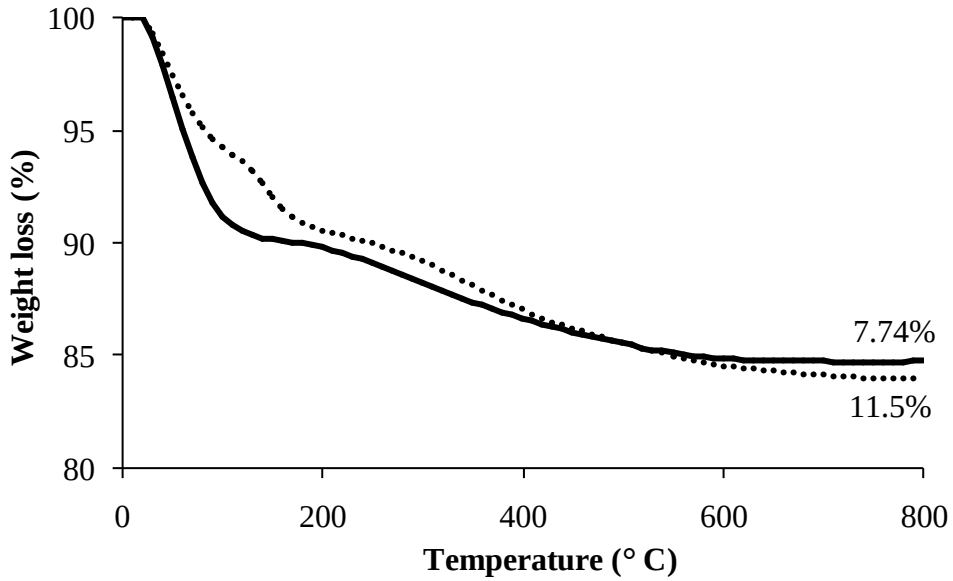

Figure 6. Weight loss of crude silica HS46 (─) and initiator grafted silica HS48 (…).

Figure 6 shows a greater final weight loss in the case of functionalized silica (11.5 %) than in the case of non-functionalized silica (7.74 %). The difference in the final weight loss is attributed to the organic initiator grafted onto the surface of the silica which is absent in non-functionalized silica.

The initiator grafting density can be calculated according to the following equation:

$$G_A = \left\{ \frac{\left[\left(\frac{W\%_{120-800(modified\ silica)}}{100 - W\%_{120-800(modified\ silica)}} \right) - \left(\frac{W\%_{120-800(crude\ silica)}}{W\%_{120-800(crude\ silica)}} \right) \right]}{M_{initiator} \times specific\ surface\ area} \right\} \times N_A$$

G_A (molecules.nm^{-2}) the grafting density, % $W_{120\text{-}800}$ is the weight loss obtained by TGA between 120 and 800 °C, and the specific surface area (S_{spe}) (nm^2.g^{-1}) is the one of the silica particles. The specific surface area (S_{spe}) of the 80 nm and 25 nm was calculated to be 3.4×10^{19} nm^2.g^{-1} and 1.05×10^{20} nm^2.g^{-1} respectively, it was theoretically calculated according to the following equation:

$$S_{spe} = \frac{surface\ area\ of\ silica\ (S)}{mass\ of\ silica}\ , \quad S = 4\pi r^2 \times N_p\ , \quad N_p = \frac{volume\ of\ silica}{volume\ of\ 1\ Np} = \frac{m_{silica}/\rho_{SiO2}}{\frac{4}{3}\pi r^3}$$

S (nm^2) representing the surface area, r (nm) the radius of silica particles, N_p the number of silica particles, $\rho = 2.2$ g.cm^{-3} the density of silica.

The initiator grafting density of the different TMSPA-BB grafted silica particles is represented in Table 2 along with the specific surface area. We observe that even for the same

size of silica we obtained different grafting densities for different batches, HS45 and HS98 with G_A 0.5 and 2.0 molecules.nm^{-2} respectively. The much lower G_A in HS45 may be due to that the grafting took place in absolute ethanol whereas in the two other experiments the grafting was performed in dry toluene. For the 80 nm particles, (HS48, HS52) the grafting density displays value of G_A = 1.6 molecules.nm^{-2}.

Table 2. Grafting density of alkoxyamine-grafted silica particles

Crude silica	**Diameter nm**	**S_{spe} nm^2.g^{-1} crude silica**	**%$W_{loss\ (120°C-800°C)}$, non-functionalized silica**	**Initiator grafted silica**	**Solvent**	**%$W_{loss\ (120°C-800°C)}$, functionalized silica**	**G_A molecules.nm^{-2}**
HS43	25	1.05×10^{20}	19.70	**HS45**	Ethanol	22.2	0.5
HS71	25	1.05×10^{20}	7.65	**HS79**	Toluene	16.5	1.3
HS96	25	1.05×10^{20}	12.45	**HS98**	Toluene	24.0	2.0
HS46	80	3.41×10^{19}	7.75	**HS48**	Toluene	11.5	1.6
HS64	80	3.41×10^{19}	5.50	**HS66**	Toluene	9.0	1.2
HS51	80	3.41×10^{19}	7.75	**HS52**	Toluene	11.5	1.6

In order to check the efficiency of the washing process to confirm that TGA analysis refer only to the grafted initiator, TGA analysis was performed after 4, 5 and 6 cycles of centrifugation. Figure 7 indeed shows a decrease of final weight loss (from 10.3 % to 9.0 %) between the fourth and the sixth centrifugation cycles. The weight loss remains constant after that showing the complete removal of free alkoxyamine.

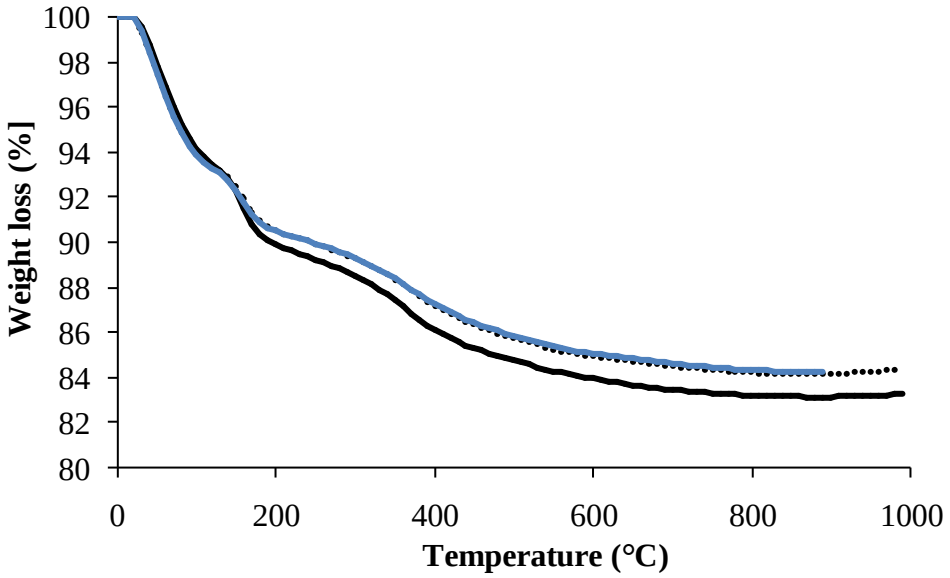

Figure 7. % Weight loss of (HS66) alkoxyamine grafted silica versus temperature after 4 cycles (−), after 5 cycles (…) and after 6 cycles (−)

3.2.2 "One step" SI-NMP in miniemulsion

In the present work, we aim to synthesize core@polymer particle in miniemulsion from the surface of TMSPA-BB grafted silica. We first used the 80 nm silica particles and started miniemulsion polymerization by introducing TMSPA-BB grafted silica into the monomer prior emulsification step, forming the initial droplets miniemulsion. We will name this procedure "one step" SI-NMP miniemulsion (Scheme 3) in contrast to the "two steps" SI-NMP procedure described in the next part 3.2.3.

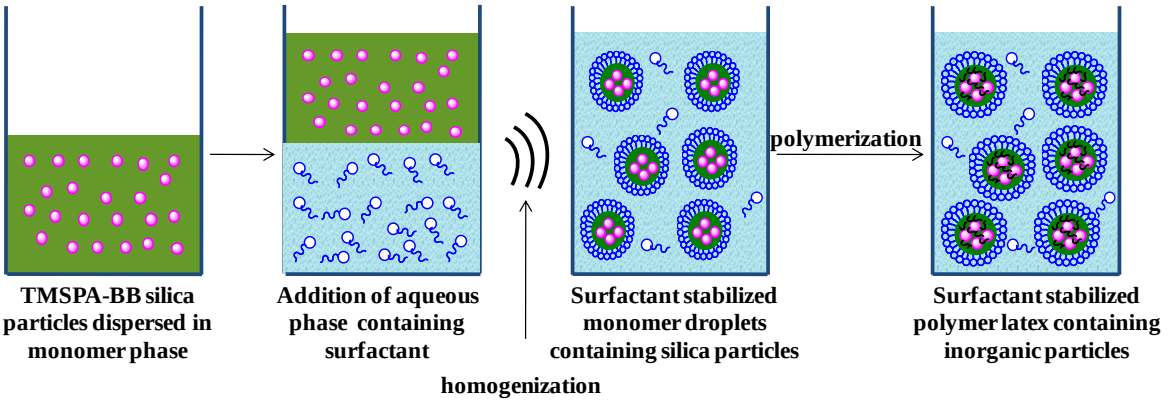

Scheme 3 : « one step » SI-NMP in miniemulsion from TMSPA-BB grafted silica

A maximum weight percentage of silica set at 10 % imposed a low concentration of alkoxyamine [PX], so high degree of polymerization was targeted. Table 3 shows the conditions of the experiments performed with "one step" SI-NMP miniemulsion performed with various content of free alkoxyamine BB-BA.

Table 3. Experimental conditions of "one step" SI-NMP miniemulsion of styrene initiated by 80 nm TMSPA-BB silica particles (batch HS52 Table 2) [a] carried out at 120 °C

Expt	Exp	wt-% silica [b]	mol-% free alkoxyamine [c]	DP $_{theo}$ [d]	wt-% monomer fraction [e]
1	HS49b	0.0	100	1280	20
2	HS61	2.7	80	1280	10
3	HS63	4.8	50	1280	10
4	HS53	10.0	0	1280	20

[a] 2.2 wt-% disponil surfactant based on styrene, 5 wt-% hexadecane based on styrene; 0.012 mol.L$^{-1}_{water}$ of $NaHCO_3$; 1 wt-% PS based on styrene; $[initiator]_0 = 6.83\times10^{-3}$ mol.L^{-1};

[b] wt-% based on styrene

[c] $n_{BB\text{-}BA}/(n_{BB\text{-}BA}+n_{TMSPA\text{-}BB}) \times 100$

[d] degree of polymerization DP = $[styrene]_o/([grafted\ alkoxyamine]+[free\ alkoxyamine])_o$

[e] monomer fraction = $m_{monomer}/(m_{monomer}+m_{water})$

Figure 8 shows an overlay of the evolution of the logarithmic monomer concentration as function of time. The plots reveal a decrease of the slope within time, showing that the concentration of propagating radicals was not constant throughout the polymerization. Moreover, an obvious decrease of the slope was observed with decreasing the molar ratio of the free alkoxyamine from 100 to 0 % (Figure 8). Note that the overall initial alkoxyamine concentration was similar for all experiments (see Table 3).

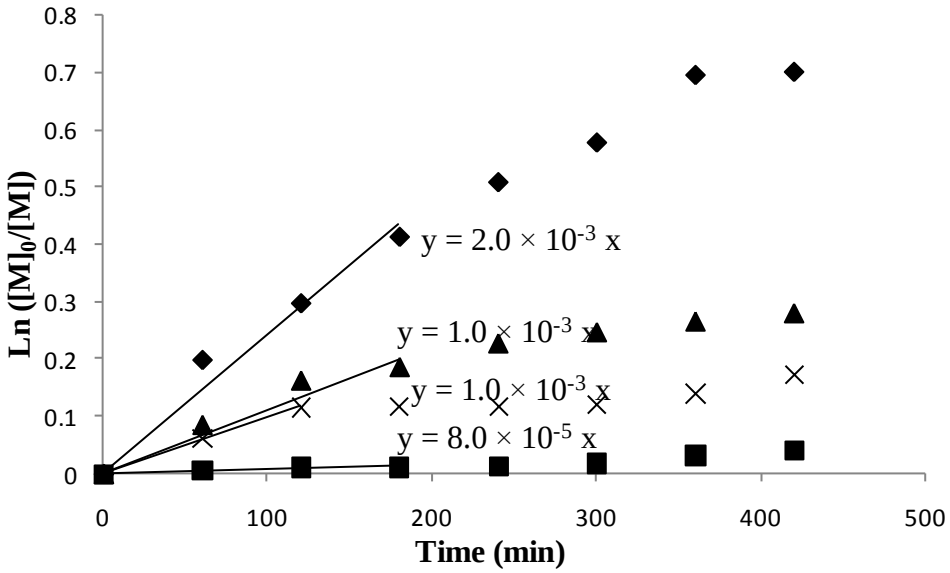

Figure 8. Logarithmic monomer concentration versus time of "one step" SI-NMP miniemulsion of styrene with different ratios of free initiator (Table 3), (♦) (100 mol-% free initiator) Expt. 1; (▲) (80 mol-% free initiator) Expt. 2; (×) (50 mol-% free initiator) Expt. 3; (■) (0 mol-% free initiator) Expt. 4

In Table 4 we reported values of the concentrations of radicals of released SG1 calculated from Equation 1 and the fraction of the dead polymer chains (DPC) calculated from the slope of ln ($[M_0]/[M]$) = f(t) and Equation 1 and Equation 2. The calculation of released SG1 and DPC was based on the total concentration of free and grafted alkoxyamine.

Table 4. Results of "one step" SI-NMP miniemulsion of styrene carried out at 120 °C in the presence of disponil surfactant

Expt	Conversion % (time) (h)	% coagulum	$[PX]_{0,\ free}$	$[SG1]_{exp}$ mol.L^{-1}	$[P^{\bullet}]^{a}$ mol.L$^{-1}_{styrene}$	DPC ^{a} (%)
1	50.0 (7)	0	6.8×10^{-3}	2.5×10^{-3}	1.60×10^{-8}	38
2	24.0 (7)	22	5.7×10^{-3}	4.8×10^{-3}	7.86×10^{-9}	76
3	15.7 (7)	0	3.4×10^{-3}	4.8×10^{-3}	7.86×10^{-9}	76
4	3.5 (7)	20	0	6.0×10^{-2}	6.40×10^{-10}	940

[a] calculated according to Equation 1 and Equation 2, with $[PX]_0 = [PX]_{0,\ free} + [PX]_{0,\ grafted}$.

$$ln\frac{[M]_0}{[M]} = k_p K_{eq}\frac{[PX]_0}{[SG1]_{exp}}t$$

Equation 1

$$DPC = \frac{[SG1]_{released}}{[PX]_0} = \frac{[SG1]_{exp} - [SG1]_0}{[PX]_0}$$

Equation 2

We first observe that the radical concentration, related to slope of the ln ($[M_0]/[M]$) = f (t) is strongly impacted by the molar fraction of free and grafted initiator. Indeed, an increase of the molar ratio of grafted alkoxyamine, at constant total amount of alkoxyamine, induces a high decrease of radical concentration (see Expt 1 to 4 in Tables 3 and 4). This suggests that the dissociation of grafted alkoxyamine is very low for producing radicals in the monomer droplets, the loci of polymerization in miniemulsion polymerization. The very low efficiency of the grafted alkoxyamine might be explained by the exit of TMSPA-BB grafted silica to water phase. Indeed, the pH of water phase (pH = 9) was above the pKa of the carboxylic acid group and despite the hydrophobic SG1 group the neutralized form of grafted alkoxyamine might promote transfer of grafted silica particles to the water phase. This pH was chosen in order to prevent SG1 degradation. [31] A test involving the solubilization of TMSPA-BB grafted silica in styrene and water at a pH = 9 ($NaHCO_3$) showed after phase separation the presence of the silica in the water phase.

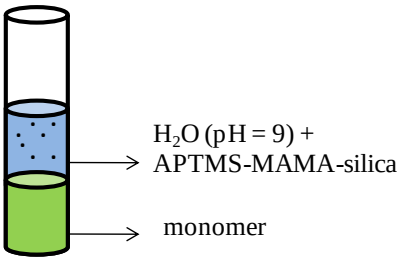

In the presence of free alkoxyamine in Expt 1 to 3, we notice that upon increasing the percentage of grafted alkoxyamine from 0 to 50 %, the concentration of released SG1 increases and so does the percentage of dead polymer chains DPC (from 38 to 76 % for Expt. 1 and 3 respectively; see Table 4). However, upon increasing the percentage of grafted alkoxyamine to 100 %, the concentration of releases SG1 increases to a high value which is almost 10 times higher than the initial concentration of the alkoxyamine (see Expt. 4 in Table 4). A calculation for the concentration of the released SG1 $[SG1]_{exp} = \frac{K_{eq}[PX]_0}{[P\bullet]}$ relates it to

the initial concentration of the alkoxyamine. The high value obtained of SG1 is an artifact because the real experimental concentration of the alkoxyamine participating to reaction is probably lower due to exit of the TMSPA-BB grafted silica to the water phase.

SEC analysis of free and grafted polystyrene chains

After separating free chains from grafted silica, the grafted chains were cleaved by *p*-TSA. As described in the experimental part, the cleavage of the grafted polymer chains from the surface of the silica occurs by transesterification reaction between the ester function of the initiator and methanol. This method was used by Bourgeat-Lami *et al.* [32] and Billon *et al.* [33] to collect the grafted polymer from the surface of spherical silica. Table 5 gathers the macromolecular features of the cleaved and free polymer chains analyzed by size exculsion chromatrography on the basis of PS calibration.

Table 5. SEC analysis of "one step" SI-NMP miniemulsion of styrene carried out at 120 °C in the presence of disponil surfactant

Exp	$M_{n,theo}$ ($g.mol^{-1}$)	Free polymer chains			Grafted polymer chains		
		$M_{n,\,SEC}$ ($g.mol^{-1}$)	M_w/M_n	$M_{n,theo}/M_{n,SEC}$ free chains	$M_{n,\,SEC}$ ($g.mol^{-1}$)	M_w/M_n	$M_{n,theo}/M_{n,SEC}$ free chains
1	67820	61230	1.3	1.1	---	---	---
2	30520	36630	1.3	0.8	38670	1.2	0.78
3	21620	37990	1.7	0.6	32540	1.5	0.70
4	5660	---	---	---	60190	2.3	0.09

$M_{n,\,theo}$ in this case takes into consideration both free and grafted alkoxyamines, $f = M_{n,\,theo}/M_{n,\,SEC\ free\ chains}$

We can first conclude that targeting a high degree of polymerization in the absence of grafted silica (Expt. 1 of Tables 3, 4 and 5), the low dispersity value together with the matching of theoretical and experimental $M_{n,\,SEC}$ both confirm control of NMP miniemulsion initiated by BB-BA alkoxyamine in miniemulsion. The dispersity of free chains is low (M_w/M_n = 1.3 Expt 1 and 2 in Table 5) for 100 and 80 mol-% of free alkoxyamine, but starts to increase to 1.7 for Expt. 3 in the presence of 50 mol-% of grafted alkoxyamine. We also observe an increase of dispersity of grafted chains with an increase of grafted alkoxyamine ratio (M_w/M_n = 1.2 for Expt. 2 with 20 mol-% grafted alkoxyamine, and M_w/M_n = 1.5 for Expt. 3 with 50 mol-% of grafted alkoxyamine in Table 5. For SI-NMP miniemulsion carried out with 100 mol-% of grafted alkoxyamine, both the high value of dispersity (M_w/M_n = 2.3) of the grafted chains and the discrepancy between $M_{n,\,exp}$ and $M_{n,\,theo}$ show the loss of polymerization control. This last result is in accordance with the literature which showed that control of surface-initiated

RDRP requires either the presence of sacrificed free initiator [34] or the presence of additional controlled agent [25].

Nevertheless, the rate of polymerization being particularly low in the present experiments, adding free SG1 cannot be considered (3.5 % conversion in 7 h for Expt. 4 in Table 4). The ratio between the experimental $M_{n,\,SEC}$ chains and the theoretical M_n is characteristic of the overall efficiency of alkoxyamine (*f*).

$$f = \frac{M_{n,theo}}{M_{n,SEC}} = \frac{[PX]_{exp}}{[PX]_{0,free} + [PX]_{0,grafted}}$$

The results of Expt. 1 highlights a high efficiency of free alkoxyamine ($f \sim 1$) while Expt. 4 shows a very low efficiency of 9 % for the grafted initiator (Table 5). On the basis of experimental M_n of free chains, the global efficiency decreases with increasing the fraction of grafted initiator (f = 0.8 for Expt. 2 with 20 mol-% grafted alkoxyamine, f = 0.6 for Expt. 3 with 50 mol-% of grafted alkoxyamine).

Figure 9 below shows an overlay of the free chains and the cleaved chains in the case of Expt. 2 with 80 mol-% of free alkoxyamine. The chromatograms of the grafted polymer chains superimpose perfectly with the free chains, where it is obvious that the free chains are of almost the same molar mass as the cleaved chains. This result agrees with the results of literature showing similar molar masses of free and grafted chains for SI-NMP in the presence of free initiator. [30]

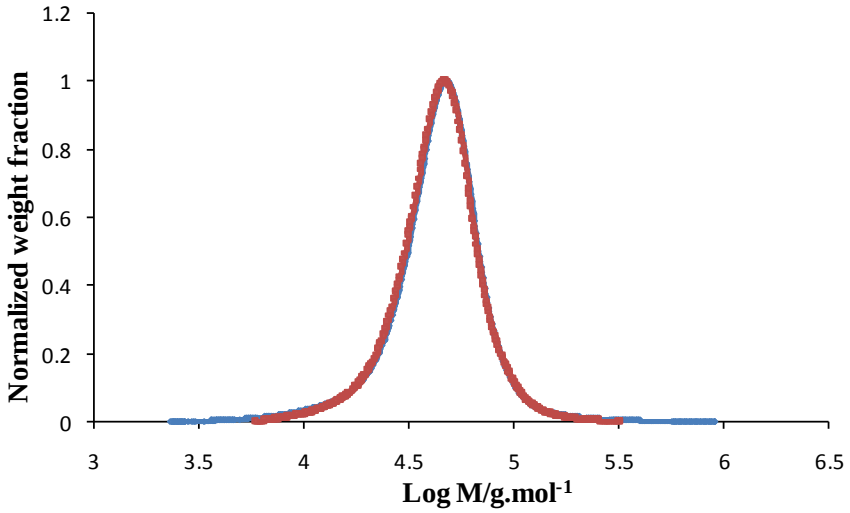

Figure 9. Normalized weight fraction versus logarithmic molar mass of (—) free and (—) grafted chains of SI-NMP miniemulsion of styrene carried out with 80 mol-% of free initiator (Expt. 2 of Tables 3, 4 and 5)

The SEC trace of grafted chains also overlays the SEC trace of free chains for the case of Expt. 3 with 50 mol-% of free alkoxyamine but a small shoulder at higher molar mass is observed in Figure 10 ($M_{p,1}$ = 43740 g.mol^{-1}, $M_{p,2}$ = 162600 g.mol^{-1}).

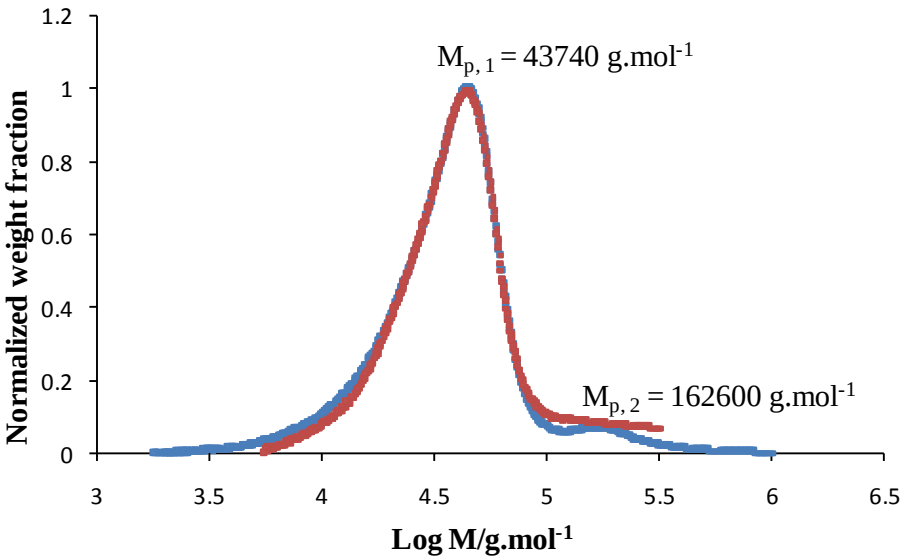

Figure 10. Normalized weight fraction versus logarithmic molar mass of (—) grafted and (—) free chains of SI-NMP miniemulsion of styrene carried out with 50 mol-% of free initiator (Expt. 3 of Tables 3, 4 and 5)

In Figure 11, we observe the chromatogram of the grafted PS chains of SI-NMP miniemulsion of styrene in the presence of 100 % of grafted alkoxyamine (Expt. 4 of Table 5). A monomodal chromatogram is observed but also accompanied with a small shoulder at high molar mass ($M_{p,1}$ = 90220 g.mol^{-1}, $M_{p,2}$ = 579160 g.mol^{-1}).

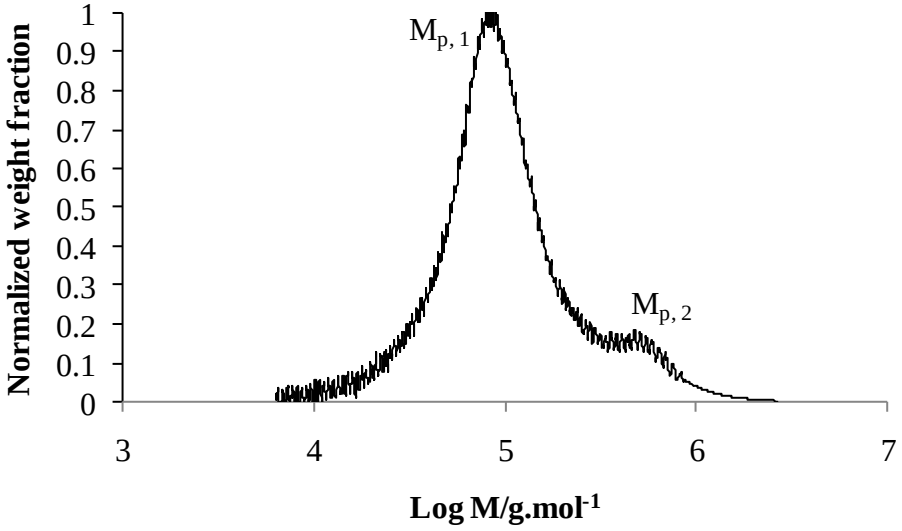

Figure 11. Normalized weight fraction versus logarithmic molar mass of grafted PS chains of SI-NMP miniemulsion of styrene carried out with 100 mol-% of grafted initiator (Expt. 4 of Tables 3, 4 and 5)

The conclusions of the molar mass analysis are in accordance with the conclusions of kinetic data of SI-NMP in miniemulsion. The efficiency of the grafted alkoxyamine initiator is very poor and not in favor with the synthesis of hybrid core@shell particles in the absence of free chains.

When synthesizing latex particles, it is also important to assess the colloidal features and stability of the dispersion. The hydrodynamic diameter of the latex was measured by DLS and results are shown in Table 6. Coagulum was observed in the case of 20 and 100 mol-% of grafted alkoxyamine with a 20 wt-% according to styrene.

Table 6. Colloidal characterization of the final latex of "one step" SI-NMP in miniemulsion of styrene

Exp	mol-% free alkoxyamine	wt-% silica	D_h [a] t=7 h (nm)	$\bar{d}_w/\bar{d}_n$ [b]	σ [c]	$N_{p,\,Silica}$ [d] L^{-1}_{latex}	$N_{p,\,polymer}$ [d] L^{-1}_{latex}	$\frac{N_{p,SiO2}}{N_{p,polymer}}$
1	100	0.0	110	1.05	0.34	---	---	---
2	80	2.7	135	1.01	0.22	4.50×10^{15}	3.50×10^{16}	0.12
3	50	4.8	140	1.02	0.22	8.30×10^{15}	8.50×10^{16}	0.09
4	0	10.0	245	1.02	0.22	3.30×10^{16}	1.20×10^{16}	2.75

[a] hydrodynamic diameter of final latex obtained from DLS, samples concentrated, cummalnts mode

[b] particle-diameter dispersity calculated from Equation 2 in chapter 2.

[c] particle-diameter dispersity obtained from DLS

[d] Number of silica and polymer particles calculated according to Equation 3 in chapter 2

The final hydrodynamic diameter of latex was found to be in the range of 110-250 nm. Furthermore, TEM analysis for Expt. 2 and 3 showed the co-existence of silica particles embedded into polymer particles with latex particles free of silica (Figure 12). The experimental content of silica was fixed at 10 wt-% of silica versus monomer for the experiment in the absence if free initiator. This ratio was based on the article of Matyjazewski *et al.* concerning SI-AGET ATRP in miniemulsion. [25]. The silica content was not increased to more than 10 wt-% to limit the risk of irreversible termination reactions between different particles. For the other set of experiments (Expt. 1, 2 and 3 of Table 4) in the presence of free alkoxyamine, the overall alkoxyamine concentration ($[PX]_{0,\,free} = [PX]_{0,\,grafted} = 6.8 \times 10^{-3}$ $mol.L^{-1}$) was kept constant in order to compare kinetics, molar masses and efficiency. Consequently, the initial weight fraction of silica ranged between 2.7 and 10 wt-%. On the basis of these experimental conditions, the ratios between initial number of silica particles and the final number of latex particles was calculated to be as low as 0.1 with 20 and 50 mol-% of grafted TMPSA-BB alkoxyamine, and this value increases to reach 2.7 when the mol-% of

the grafted alkoxyamine is 100 % (see Expt. 2, 3 and 4 in Table 6). The TEM images of Expt. 2 and Expt. 3 indeed highlight the presence of both silica@PS composite particles and PS particles free of silica (Figure 12). The TEM images show a higher dipersity of particle size for Expt. 2 in comparison to Expt. 3 which is in accordance with the dispersity values of DLS (Table 6). The case where we had no free initiator (Expt. 4) was not analyzed by TEM due to the high quantity of the styrene monomer which was still present.

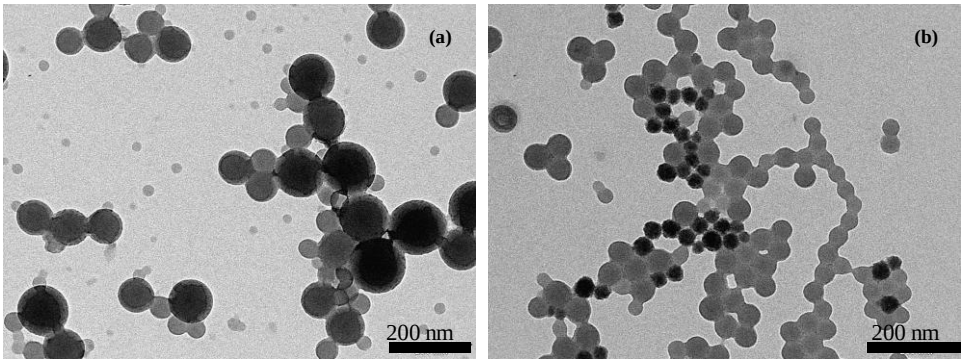

Figure 12. PS-silica latex particles, (a) Expt. 2 and (b) Expt. 3 in Table 4

The very low monomer conversion (3 %) obtained in the absence of free initiator (Expt. 4) was a reason for performing SI-NMP of styrene in bulk instead in order to compare results and understand the effect of dispersed state. For this purpose, 10 wt-% of TMSPA-BB grafted silica (80 nm) was mixed with styrene to conduct a SI-NMP in bulk at 120 °C targeting high degree of polymerization of DP = 1280 (Expt. 5 of Table 7).

Table 7. Macromolecular features of PS grafted polymer chains synthesized by SI-NMP of styrene in miniemulsion (Expt. 4) and in bulk (Expt. 5) carried out at 120 °C

Exp	Expt.	Conversion (%) time (h)	$M_{n,\ theo}$ ($g.mol^{-1}$)	$M_{n,\ SEC}$ ($g.mol^{-1}$)	M_w/M_n	$M_{n,\ theo}/M_{n,\ SEC}$
HS53	4	3 (7)	5660	60190	2.3	0.09
HS50	5	74 (5)	100000	158000	1.9	0.63

The grafted polymer chains of SI-NMP conducted in bulk and miniemulsion exhibit high values of dispersity (M_w/M_n > 1.9) which was expected when targeting a high degree of polymerization in the absence of free SG1. The final monomer conversion after 5 hours was higher for SI-NMP of styrene in bulk (74 %, Expt. 5) than in miniemulsion (3 %, Expt. 4). Moreover, the M_n of the grafted chains recovered from SI-NMP of styrene in bulk were in the range of the theoretical M_n ($M_{n,\ theo}/M_{n,\ SEC}$ = 0.63), whereas a high discrepancy between theoretical and experimental molar mass of grafted chains was observed for SI-NMP in miniemulsion. The low value of the later ratio highlights a very low efficiency of the grafted

initiator to create polymer chains in miniemulsion, probably due to the diffusion of the alkoxyamine to the water phase as suggested by kinetic results.

3.2.3 "Two steps" SI-NMP in miniemulsion

As it appeared in the previous part with "one step " SI-NMP, the silica were not hydrophobic enough to reside in the organic phase and initiate adequately NMP from silica surface in miniemulsion. Our goal was to synthesize core@shell hybrid nanoparticles in the absence of free initiator in order to avoid synthesis of mixed nanocomposites. In the following part we propose an approach in order to hydrophobize the silica particles to a certain extent that keeps them in the organic phase. Thus, we decided first to implement SI-NMP in bulk up to low monomer conversion, and then continuing the polymerization in miniemulsion (see experimental part for exact procedure) (Scheme 4).

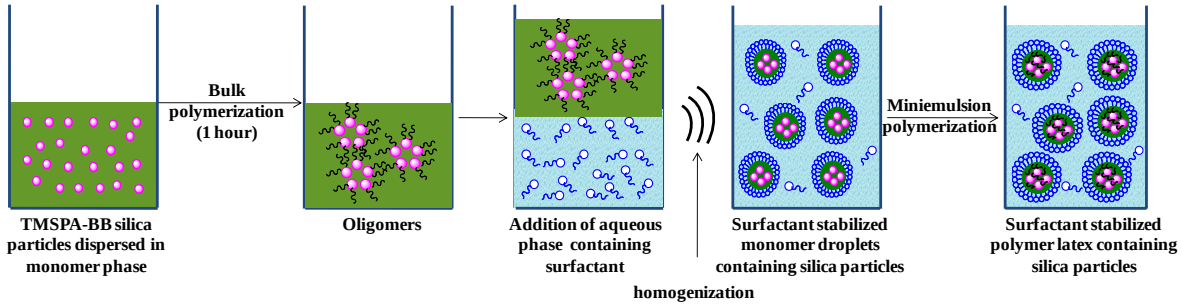

Scheme 4. « two steps » SI-NMP in miniemulsion from TMSPA-BB grafted silica

We used two TMSPA-BB-grafted silica with different diameters (80 and 25 nm), for SI-NMP of styrene and *n*-butyl acrylate (BA) targeting two different degrees of polymerization (200 or 1280). The experimental conditions are gathered in Table 8 and the results in Table 9.

Table 8. "two steps" SI-NMP in miniemulsion carried out at 120 °C for S and 115 °C for *BA* [a]

Exp (Expt.)	Monomer	TMSPA-BB SiO_2	wt-% monomer [b]	$[TMSPA\text{-}BB]_0$ ($mol.L^{-1}_{monomer}$)	$[Monomer]_0/[TMSPA\text{-}BB]_0$	Silica (nm)	wt-% silica [c]	mol-% SG1 [d]
111 (6)	S	HS66	20	6.79×10^{-3}	1280	80	11	2.5
99 (7)	S	HS79	10	4.10×10^{-2}	205	25	20	0
105 (8)	BA	HS98	10	3.40×10^{-2}	210	25	11	2.5
112 (9)	BA	HS66	20	5.50×10^{-3}	1280	80	9	2.5

[a] 2.2 wt-% of Dowfax based on monomer; 5 wt-% of hexadecane based on monomer; 0.012 $mol.L^{-1}_{water}$ of $NaHCO_3$; 1 wt-% of PS based on monomer.

[b] wt-% of monomer versus total latex

[c] wt-% of silica versus monomer

[d] molar % of SG1 versus alkoxyamine = $n_{SG1}/n_{alkoxyamine}$

Table 9. Results of "two steps" SI-NMP in miniemulsion carried out at 120 °C for S and 115 °C for *BA*

Exp (Expt.)	% conversion at 1 h	% conversion at 7 h	% conversion at 24 h	% coagulum	Latex		N_p silica[c] /L_{latex}	N_p [c] polymer /L_{latex}	N_p silica/N_p polymer
					D_h[a] (nm)	σ [b]			
111 (6)	3	40	66	17	150	0.05	3.60×10^{16}	6.80×10^{16}	0.52
99 (7)	9	58	-	26	245	0.2	1.00×10^{18}	7.00×10^{15}	142
105 (8)	5	37	-	11	340	0.2	5.90×10^{17}	1.70×10^{15}	350
112 (9)	6	32	61	0	310	0.06	2.90×10^{16}	7.13×10^{15}	4.00

[a] hydrodynamic diameter of final latex obtained from DLS, samples concentrated, cummalnts mode

[b] particle-diameter dispersity (σ) obtained from DLS in cumulants mode

[c] Number of silica and polymer particles calculated according to Equation 3 in chapter 2

Table 10. Results of kinetics of "two steps" SI-NMP in miniemulsion carried out at 120 °C for S and 115 °C for *BA*

Exp (Expt.)	Monomer	$[PX]_0$	$[SG1]_0$	$[P^\bullet]$[a]	$[SG1]_{exp}$	DPC[a] (%)
			mol.L^{-1}	mol.$L^{-1}{}_{styrene}$	mol.L^{-1}	
111 (6)	S	6.79×10^{-3}	1.74×10^{-4}	1.08×10^{-8}	3.54×10^{-3}	52
99 (7)	S	4.10×10^{-2}	0	5.30×10^{-9}	4.64×10^{-2}	113
105 (8)	BA	3.40×10^{-2}	8.48×10^{-4}	5.16×10^{-9}	1.22×10^{-2}	33
112 (9)	BA	5.50×10^{-3}	1.40×10^{-4}	5.40×10^{-9}	1.90×10^{-3}	31

[a] Concentration of radicals and fraction of dead polymer chains (DPC) calculated according to Equation 1 and Equation 2

"Two steps" SI-NMP in miniemulsion from 80 nm TMSPA-BB grafted silica particles

Starting with the experiments concerning the 80 nm TMSPA-BB-grafted silica particles, both monomers styrene or *n*-butyl acrylate were polymerized while targeting a high degree of polymerization (Expt. 6 and 9 of Table 8). We notice that the "two steps" process enabled us to increase the final conversion in the absence of free alkoxyamine. Where in comparison of a "one step" SI-NMP (Expt. 4 in Table 4), "two steps" SI-NMP (Expt. 6 of Table 9) conversion was increased from 3 to 40 % after 7 hours of reaction, respectively. The increase in conversion in comparison with "one step" SI-NMP in miniemulsion led to the conclusion that after starting the reaction for 1 h in bulk giving a conversion less than 10, we were able to hydrophobize the silica and nucleate monomer droplets.

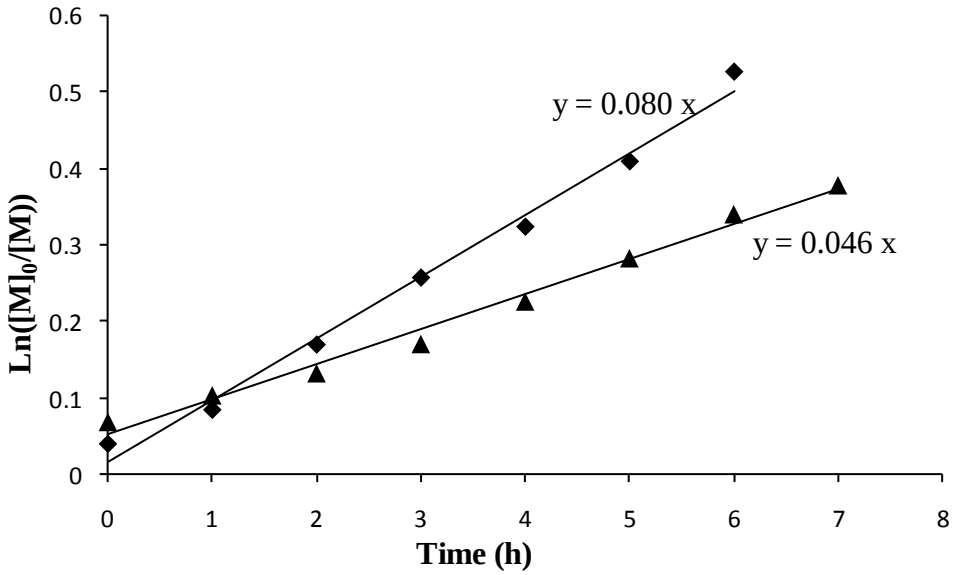

Figure 13. Logarithmic monomer concentration versus time of "two steps" SI-NMP miniemulsion of styrene at 120 °C (♦) Expt. 6 and BA at 115 °C (▲) Expt. 9, from 80 nm TMSPA-BB-grafted silica particles

Figure 13 shows the logarithmic monomer concentration versus time for "two steps" SI-NMP in miniemulsion of both styrene (Expt. 6) and BA (Expt. 9) monomers. A linearity of $\ln([M]_0/[M]) = f(t)$ was observed for BA polymerization (Expt. 9) indicating a constant concentration of free radicals with time, while an increase of slope is observed for styrene (Expt. 6) above 60 % of conversion. A longer polymerization time of 24 h conducted to 60 - 66 % of conversion (Expt. 6 and 9 of Table 9). In Table 10 we reported values of the concentration of radicals calculated from the slope of $\ln([M]_0/[M]) = f(t)$, the concentration of released SG1 calculated from Equation 1 and the fraction the dead polymer chains (DPC) calculated from Equation 1 and Equation 2. The calculation of released SG1 and DPC was based on the total concentration of grafted alkoxyamine. Concerning first SI-NMP of styrene targeting high degree of polymerization initiated from 80 nm TMSPA-BB-silica, the value of DPC is much lower in the "two steps" method (Expt. 6 of Table 10, DPC = 52 %) in comparison to "one pot" method carried out in the absence of free initiator (Expt. 4 of Table 4, DPC = 940 %) but also lower in comparison to "one pot" method carried out in the presence of 20 to 50 mol-% of free initiator (Expt. 2-3 of Table 4, DPC = 76 %). This can be explained by the lower value of released SG1, as the grafted silica remained in the organic phase.

Figure 14 shows the TEM images of Expt. 6 for "two steps" SI-NMP of styrene from 80 nm TMSPA-BB grafted silica. It displays PS-silica particles of various diameters ranging

between 150 nm and 300 nm while DLS provided an average hydrodynamic diameter of 150 nm (Expt. 6 of Table 9). TEM also reveals the presence of free polymer particles which can be attributed to thermal initiation of styrene monomer as no free initiator was added to nucleate droplets. This observation can be correlated to the ratio of the initial number of silica particles ($N_{p,\ silica}$) to the final number of latex particles ($N_{p,\ polymer}$), which is below 1 for Expt. 6 (Table 9). The black dots of higher contrast in Figure 14 corresponding to silica particles are in the range of 60-80 nm which is in good correlation of the initial silica particle diameter (see Figure 2). PBA@silica particles were not observed by TEM because of low PBA glass transition temperature and the flow of particles under electron beam.

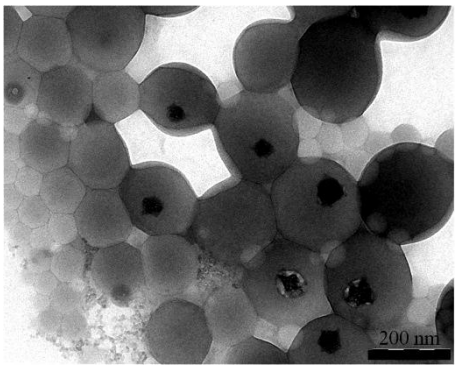

Figure 14. PS@silica latex particles, Expt. 6 of Table 8

"Two steps" SI-NMP in miniemulsion from 25 nm TMSPA-BB grafted silica particles

Two experiments of SI-NMP in miniemulsion were performed with TMSPA-BB grafted silica of 25 nm. The degree of polymerization was equal to 200 for both styrene (Expt. 7) and BA (Expt. 8) polymerizations. The final conversion after 7 hours was 58 % for styrene and 37 % for BA polymerizations. Upon plotting the logarithmic monomer concentration versus time of Expt. 7 and 8 (Figure 15) we observe a linear evolution for both S and BA polymerizations. The "two steps" SI-NMP of styrene initiated from 25 nm TMSPA-BB-silica exhibits high DPC values of 113 % (see Table 10) but it should noticed from Table 8 that this experiment was carried out in the absence of free SG1. The reason of this choice of initial experimental conditions of expt 7 was driven by the fact that the first step of bulk polymerization showed very low conversion at 1h. Concerning SI-NMP of BA, the value of dead polymer chains is lower (DPC = 33 %) for both polymerizations initiated from 25 nm and 80 nm TMSPA-BB grafted silica particles.

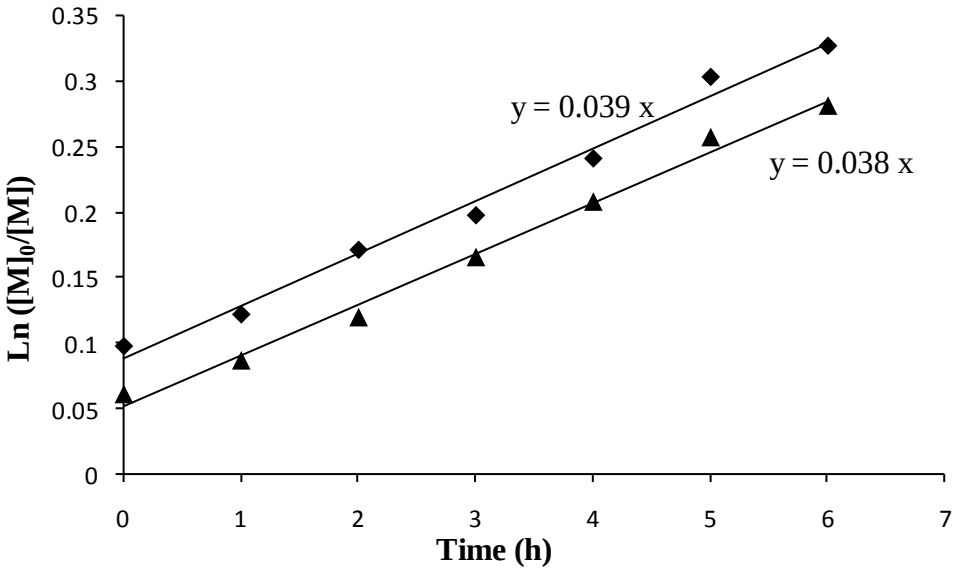

Figure 15. Logarithmic monomer concentration versus time of "two steps" SI-NMP miniemulsion of styrene at 120 °C (♦) Expt. 7 and BA at 115 °C and (▲) Expt. 8, from 25 nm TMSPA-BB-grafted silica particles

TEM image of Expt. 7 shows monodisperse latex particles of average diameter of 150 nm which is below the hydrodynamic diameter measured by DLS (D_h = 245 nm, Table 9) (Figure 16). Normally contrast between polymer and silica nanoparticles in TEM is high enough,[13] but in the present case for small 25 nm they are not easy to distinguish. (see Figure 2 showing TEM of 25 nm silica).

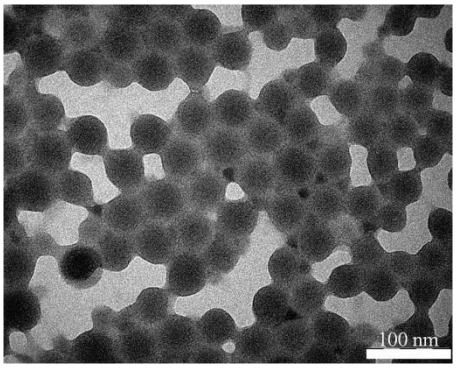

Figure 16. PS-silica latex particles (Expt. 7 of Tables 8 and 9)

For these smaller 25 nm silica, the ratio of the initial number of silica particles ($N_{p,\ silica}$) to the final number of latex particles ($N_{p,\ polymer}$) is higher than 100, suggesting that several small core@shell particles can be embedded in the latex particles.

The polymer@silica core@shell particles were recovered by centrifugation in organic solvent and the grafted chains were further cleaved to be analyzed by size exclusion chromatography (SEC). Nevertheless, the values of the molar mass and dispersity were not provided in Table 9

as all chromatograms were multimodal, such as the example of Expt. 9 of Table 8 displayed in Figure 17.

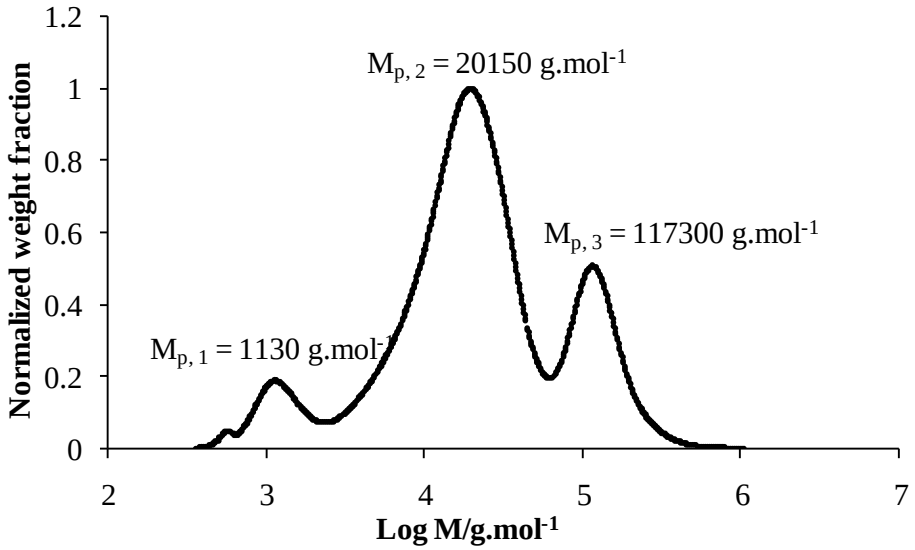

Figure 17 : Normalized weight fraction versus logarithmic molar mass of grafted PBA of SI-NMP in miniemulsion from 80 nm TMSPA-BB grafted silica, Expt 9 of Table 8

In the case of experiments carried out from 25 nm silica targeting a low degree of polymerization of 200, two peaks were observed in the chromatogram, such as the example of Expt. 7 of Table 8 displayed in Figure 18.

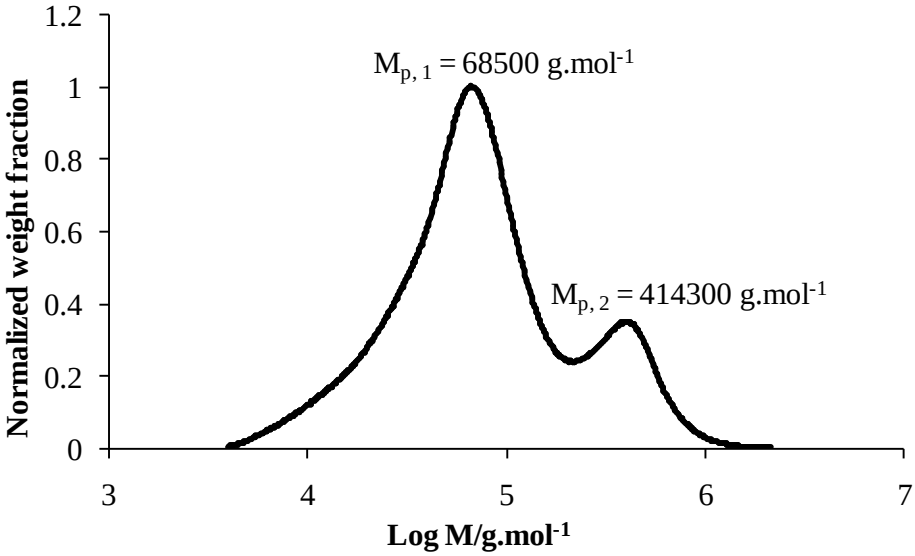

Figure 18 : Normalized weight fraction versus logarithmic molar mass of grafted PS of SI-NMP in miniemulsion from 25 nm TMSPA-BB grafted silica of Expt 7 of Table 8

In conclusion of this part, we showed that hydrophobization of silica surface by short polymer chains was required to enhance polymerization rate by favoring the location of grafted silica

inside the monomer droplets, hence of grafted initiator promoting droplet nucleation. This method enables us to synthesize polymer@silica core@shell particles in the absence of free initiator in miniemulsion polymerization.

Conclusion

During our work in this chapter, we aimed to synthesize core@shell hybrid nanoparticles by surface-initiated nitroxide mediated polymerization implemented in miniemulsion. The first step consisted in the synthesis of grafted alkoxyamine silica from two batches of silica with different diameters (D_h = 25 or 80 nm). For the synthesis of the core@shell nanoparticles we developed two strategies to implement the polymerization step by SI-NMP in miniemulsion.

The first strategy which we called "one step" method, consisted of dispersing the alkoxyamine grafted silica into the monomer droplets, and starting the polymerization in directly miniemulsion whether in presence or absence of free initiator. Targeting a high degree of styrene polymerization (1280) from 80 nm alkoxyamine grafted silica in the absence of any free initiator, a primary result led to very low polymerization rate (conversion = 3 %). However, it was possible to increase the conversion by adding a free alkoxyamine to the medium. By increasing the molar fraction of free alkoxyamine from 0 to 80 % while keeping constant $[alkoxyamine]_0$, we managed to increase the conversion from 3 to 24%. It was also possible to control the polymerization in the presence of free initiator with dispersity values less than 1.7 for both grafted and free polymer chains, whereas in the absence of free initiator, controlling the polymerization was difficult with a value of 2.3. Thus, showing the low efficiency of the grafted alkoxyamine, which might be possible to the exit of the alkoxyamine grafted silica to the water. Colloidal characterization of the "one step" experiments showed diameters of PS-silica particles within the range of 100-250 nm.

After concluding the insufficient hydrophobicity of the silica from the first strategy, we developed the second strategy called "two steps" method, which requires two steps. The first step consisted of SI-NMP carried out in bulk up to low conversion of styrene (< 10 %) followed by the second step that is adding water and surfactant to create the initial state of liquid miniemulsion, followed by miniemulsion polymerization. In the "two steps" method we avoided the use of free alkoxyamine in order to avoid synthesis of mixed nanocomposites. Targeting two different degrees of polymerization (DP = 200) from 25 nm alkoxyamine grafted silica and (DP = 1280) from 80 nm alkoxyamine grafted silica polymerizing two

monomers (styrene and *n*-butyl acrylate), we managed to obtain a final conversion in the range of 30-66 %. Hence, in the absence of free alkoxyamine, we managed to increase the conversion for synthesizing PS@silica from 3 % in "one step" to more than 30 % in "two steps". Nevertheless, after cleaving the grafted polymer chains in the "two steps" strategy, no information can be retrieved from the SEC analysis as the chromatograms were muti-modal in each case unlike the monomodal chromatogram which was obtained in the case of "one step" method with no free initiator. Still colloidal features showed particles of diameters around 150 nm with one silica particle enclosed in polymer shell. It was possible to synthesize polymer@silica particles via SI-NMP in miniemulsion in the absence of free alkoxyamine, but cleaving the polymer chains showed impossible to analyze.

References

1. Inoubi, R.; Dagreou, S.; Lapp, A.; Billon, L.; Peyrelasse, J., Nanostructure and mechanical properties of polybutylacrylate filled with grafted silica particles. *Langmuir* **2006,** 22, (15), 6683-6689.
2. Chevigny, C.; Dalmas, F.; Di Cola, E.; Gigmes, D.; Bertin, D.; Boue, F.; Jestin, J., Polymer-Grafted-Nanoparticles Nanocomposites: Dispersion, Grafted Chain Conformation, and Rheological Behavior. *Macromolecules* **2011,** 44, (1), 122-133.
3. Kumar, S. K.; Jouault, N.; Benicewicz, B.; Neely, T., Nanocomposites with Polymer Grafted Nanoparticles. *Macromolecules* **2013,** 46, (9), 3199-3214.
4. Tiarks, F.; Landfester, K.; Antonietti, M., Silica nanoparticles as surfactants and fillers for latexes made by miniemulsion polymerization. *Langmuir* **2001,** 17, (19), 5775-5780.
5. Zhang, S. W.; Zhou, S. X.; Weng, Y. M.; Wu, L. M., Synthesis of SiO2/polystyrene nanocomposite particles via miniemulsion polymerization. *Langmuir* **2005,** 21, (6), 2124-2128.
6. Zhou, J.; Zhang, S. W.; Qiao, X. G.; Li, X. Q.; Wu, L. M., Synthesis of SiO2/poly(styrene-co-butyl acrylate) nanocomposite microspheres via miniemulsion polymerization. *Journal of Polymer Science Part a-Polymer Chemistry* **2006,** 44, (10), 3202-3209.
7. Bailly, B.; Donnenwirth, A. C.; Bartholome, C.; Beyou, E.; Bourgeat-Lami, E., Silica-polystyrene nanocomposite particles synthesized by nitroxide-mediated polymerization and their encapsulation through miniemulsion polymerization. *Journal of Nanomaterials* **2006**.
8. Topfer, O.; Schmidt-Naake, G., Surface-functionalized inorganic nanoparticles in miniemulsion polymerization. *Macromolecular Symposia* **2007,** 248, 239-248.
9. Qiao, X. G.; Chen, M.; Zhou, J.; Wu, L. M., Synthesis of raspberry-like silica/polystyrene/silica multilayer hybrid particles via miniemulsion polymerization. *Journal of Polymer Science Part a-Polymer Chemistry* **2007,** 45, (6), 1028-1037.
10. Crespy, D.; Landfester, K., Synthesis of polyvinylpyrrolidone/silver nanoparticles hybrid latex in non-aqueous miniemulsion at high temperature. *Polymer* **2009,** 50, (7), 1616-1620.
11. Landfester, K., Miniemulsion Polymerization and the Structure of Polymer and Hybrid Nanoparticles. *Angewandte Chemie-International Edition* **2009,** 48, (25), 4488-4507.
12. van Herk, A. M., Historical Overview of (Mini)emulsion Polymerizations and Preparation of Hybrid Latex Particles. In *Hybrid Latex Particles: Preparation With*, VanHerk, A. M.; Landfester, K., Eds. 2010; Vol. 233, pp 1-18.
13. Hu, J.; Chen, M.; Wu, L. M., Organic-inorganic nanocomposites synthesized via miniemulsion polymerization. *Polymer Chemistry* **2011,** 2, (4), 760-772.
14. Ge, X. P.; Ge, X. W.; Wang, M. Z.; Liu, H. R.; Fang, B.; Li, Z.; Shi, X. J.; Yang, C. Z.; Li, G., One-Pot Synthesis of Colloidal Nanobowls and Hybrid Multipod-like Nanoparticles by Radiation Miniemulsion Polymerization. *Macromolecular Rapid Communications* **2011,** 32, (20), 1615-1619.
15. Charleux, B.; D'Agosto, F.; Delaittre, G., Preparation of Hybrid Latex Particles and Core-Shell Particles Through the Use of Controlled Radical Polymerization Techniques in Aqueous Media. *Advances in Polymer Science* **2010,** 233, 125-183.
16. Bourgeat-Lami, E.; Lansalot, M., Organic/Inorganic Composite Latexes: The Marriage of Emulsion Polymerization and Inorganic Chemistry. *Advances in Polymer Science* **2010,** 233, 53-123.
17. Duguet, E.; Desert, A.; Perro, A.; Ravaine, S., Design and elaboration of colloidal molecules: an overview. *Chemical Society Reviews* **2011,** 40, (2), 941-960.

18. Nguyen, D.; Zondanos, H. S.; Farrugia, J. M.; Serelis, A. K.; Such, C. H.; Hawkett, B. S., Pigment encapsulation by emulsion polymerization using macro-RAFT copolymers. *Langmuir* **2008,** 24, (5), 2140-2150.
19. Advincula, R. C., Surface initiated polymerization from nanoparticle surfaces. *Journal of Dispersion Science and Technology* **2003,** 24, (3-4), 343-361.
20. Tsujii, Y.; Ohno, K.; Yamamoto, S.; Goto, A.; Fukuda, T., Structure and properties of high-density polymer brushes prepared by surface-initiated living radical polymerization. In *Surface-Initiated Polymerization I*, Jordan, R., Ed. 2006; Vol. 197, pp 1-45.
21. Barbey, R.; Lavanant, L.; Paripovic, D.; Schuwer, N.; Sugnaux, C.; Tugulu, S.; Klok, H. A., Polymer Brushes via Surface-Initiated Controlled Radical Polymerization: Synthesis, Characterization, Properties, and Applications. *Chemical Reviews* **2009,** 109, (11), 5437-5527.
22. Ohno, K.; Morinaga, T.; Koh, K.; Tsujii, Y.; Fukuda, T., Synthesis of monodisperse silica particles coated with well-defined, high-density polymer brushes by surface-initiated atom transfer radical polymerization. *Macromolecules* **2005,** 38, (6), 2137-2142.
23. Deleuze, C.; Delville, M. H.; Pellerin, V.; Derail, C.; Billon, L., Hybrid Core@Soft Shell Particles as Adhesive Elementary Building Blocks for Colloidal Crystals. *Macromolecules* **2009,** 42, (14), 5303-5309.
24. Zou, H.; Wu, S. S.; Shen, J., Polymer/silica nanocomposites: Preparation, characterization, properties, and applications. *Chemical Reviews* **2008,** 108, (9), 3893-3957.
25. Bombalski, L.; Min, K.; Dong, H. C.; Tang, C. B.; Matyjaszewski, K., Preparation of well-defined hybrid materials by ATRP in miniemulsion. *Macromolecules* **2007,** 40, (21), 7429-7432.
26. Esteves, A. C. C.; Bombalski, L.; Trindade, T.; Matyjaszewski, K.; Barros-Timmons, A., Polymer grafting from Cds quantum dots via AGET ATRP in miniemulsion. *Small* **2007,** 3, (7), 1230-1236.
27. Stöber, W.; Fink, A.; Bohn, E., Controlled growth of monodisperse silica spheres in the micron size range. *Journal of Colloid and Interface Science* **1968,** 26, (1), 62-69.
28. Sanchez, C.; Rozes, L.; Ribot, F.; Laberty-Robert, C.; Grosso, D.; Sassoye, C.; Boissiere, C.; Nicole, L., "Chimie douce": A land of opportunities for the designed construction of functional inorganic and hybrid organic-inorganic nanomaterials. *Comptes Rendus Chimie* **2010,** 13, (1-2), 3-39.
29. Inoubli, R., Thèse: Synthèse, structure et propriétés viscoélastique de polymères chargés modèles. *Université de pau et des pays de l'adour* **2005**.
30. Blas, H.; Save, M.; Boissiere, C.; Sanchez, C.; Charleux, B., Surface-Initiated Nitroxide-Mediated Polymerization from Ordered Mesoporous Silica. *Macromolecules* **2011,** 44, (8), 2577-2588.
31. Farcet, C.; Lansalot, M.; Charleux, B.; Pirri, R.; Vairon, J. P., Mechanistic aspects of nitroxide-mediated controlled radical polymerization of styrene in miniemulsion, using a water-soluble radical initiator. *Macromolecules* **2000,** 33, (23), 8559-8570.
32. Bartholome, C.; Beyou, E.; Bourgeat-Lami, E.; Chaumont, P.; Zydowicz, N., Nitroxide-mediated polymerizations from silica nanoparticle surfaces: "Graft from" polymerization of styrene using a triethoxysilyl-terminated alkoxyamine initiator. *Macromolecules* **2003,** 36, (21), 7946-7952.
33. Parvole, J.; Laruelle, G.; Guimon, C.; Francois, J.; Billon, L., Initiator-grafted silica particles for controlled free radical polymerization: Influence of the initiator structure on the grafting density. *Macromolecular Rapid Communications* **2003,** 24, (18), 1074-1078.
34. Gigmes, D.; Dufils, P. E.; Gle, D.; Bertin, D.; Lefay, C.; Guillaneuf, Y., Intermolecular radical 1,2-addition of the BlocBuilder MA alkoxyamine onto activated

olefins: a versatile tool for the synthesis of complex macromolecular architecture. *Polymer Chemistry* **2011,** 2, (8), 1624-1631.

Chapter 4
Terpene based amphiphilic copolymer as stabilizers for latex functionalization via styrene miniemulsion polymerization

Introduction 135
Experimental Section 139
Synthesis of amphiphilic terpene grafted copolymers 139
Synthesis of Dextran grafted with DHM terpene 139
Synthesis of PAA grafted with THG terpene 140
Miniemulsion polymerization using amphiphilic copolymer as stabilizer 140
Results and discussion 141
1. Synthesis of amphiphilic terpene grafted copolymers 141
1.1. Synthesis of Dextran grafted with DHM terpene 141
1.2. Synthesis of PAA grafted with THG terpene 149
2. Miniemulsion polymerization using amphiphilic copolymers as stabilizer 152
2.1. Stabilization with Dext-g-DHM 152
2.2. Stabilization with PAA-g-THG 156
2.3. Comparison between Dext-g-DHM and PAA-g-THG stabilizers 159
2.4. Particle morphology 163
Conclusion 167
References 168

Introduction

The present PhD work is focused on the synthesis of colloids by polymerization in miniemulsion. We showed in the previous chapters that this point had proven to be interesting either to implement NMP in aqueous dispersed media or to encapsulate nanoparticles in the final polymer colloids. As in emulsion, the monomer droplets and the polymer particles are stabilized against coalescence by the surfactant molecules. The present chapter will not focus on the core of the latex particles but on the shell of polymeric particles synthesized by miniemulsion polymerization *via* the design of novel macromolecular stabilizers.

Surfactants are usually organic compounds that are amphiphilic, meaning they contain both hydrophobic and hydrophilic groups. Surfactants will diffuse in water and adsorb at interfaces between air and water or at the interface between oil and water, in the case where water is mixed with oil. In miniemulsion polymerization the surfactant must prevent droplet coalescence during the emulsification step and particle aggregation over time needed for polymerization so as to maintain the size of the particles close to the one of the droplets produced by the emulsification step. Polymerization in aqueous dispersed media and especially in emulsion and miniemulsion generally involve the use of molecular surfactants. With molecular surfactants composed of a lipophilic hydrocarbon tail and a charged hydrophilic head, the particles' stability is ensured by electrostatic repulsion.[1] When nonionic stabilizers with a hydrophilic block (such as poly(ethylene oxide) for instance) instead of the ionic head are used, a steric effect operates and is particularly efficient against electrolyte, high shear, and/or freeze-thaw induced destabilizations. [2] Polyelectrolyte stabilizers gather both electrostatic and steric stabilization to provide electrosteric stabilization, from here arouse the interest in polymeric surfactant for polymerization in aqueous dispersed media (emulsion and miniemulsion). [3]

The interest of amphiphilic copolymers, and especially in block copolymers with well-defined structure, molar mass, and composition, arises mainly from their unique solution and associative properties. [3] Block copolymers, consisting in the simplest case of hydrophilic and hydrophobic blocks, behave similarly to low-molecular-weight surfactants; however, polymeric surfactants have much lower diffusion coefficients and critical micelle concentrations than molecular surfactants in general. [3] Polymeric surfactants have been used in emulsion and miniemulsion polymerization for several reasons related to the characteristics

of the resulting lattices: a) macromolecules physically or chemically anchored onto the surface of the particles provide specific properties to the dispersion in terms of colloidal stability b) the adsorption of polymeric surfactants at interfaces, contrary to that of molecular surfactants, is kinetically irreversible (especially for multi-anchored polymers) c) macromolecular engineering provides efficient methods for preparing multi-functional polymeric surfactants which can act not only as stabilizers but also as initiators, chains transfer agents, co-surfactants [4] and d) functionalization of the particle via the outer layer through the hydrophilic part of the polymeric stabilizer.

Apart of block copolymers, grafted copolymers are also an interesting class of polymeric surfactants which have been previously used as stabilizers for miniemulsion polymerization. Whether it was by using synthetic polymers,[4, 5] or by the use of grafted polymer with natural polysaccharide backbone. [6] The modification of polysaccharide backbone for the synthesis of surfactants was first pioneered by Landoll [7], as he mainly dealt with the preparation of hydrophobically modified cellulose derivatives by reacting the polymer with aliphatic epoxides. The interfacial properties of these hydrophobically modified polysaccharides were considered with more interest, especially in the preparation of polymeric suspensions containing particles with well-defined surface characteristics [8-10]. Durand *et al.* reported the synthesis of dextran-based amphiphilic copolymers to further study their emulsifying properties for liquid miniemulsions [11, 12] and stabilization of polymer particles by miniemulsion polymerization. [6, 13] Dextran polysaccharide was hydrophobized either by grafting biodegradable hydrophobic polylactide [11] or by grafting hydrophobic small molecules. [6, 12, 13] It was shown that a dextran-based stabilizer can replace the conventional molecular surfactants for miniemulsion polymerization [6, 13]. Poly(acrylic acid) PAA has been also used as hydrophilic part of amphiphilic copolymers acting as stabilizer for miniemulsion [14] and emulsion polymerization.[15, 16]

The fossil resources depletion is leading to a growing interest toward materials derived from sustainable resources. Polysaccharides and terpenes are two interesting classes of materials issued from renewable biomass. Polysaccharides are mainly hydrophilic and terpenes belong to hydrocarbon-rich biomass. Terpenes are an interesting class of molecules as they can represent an alternative to fossil molecules but also to hydrocarbon-rich biomass feedstock such as oilseeds and palm oil. Different terpene molecules are distilled from either turpentine or from paper oil, a by-product of the paper-making industry. Some terpene building blocks

have been used for the synthesis of different hydrophobic polymers as recently reviewed in the literature.[17-19] Among the examples of terpene-based polymers,[17, 18, 20-24] the synthesis of amphiphilic polymers were limited to the design of terpene end-modified poly(ethylene oxide) polymers by anionic ring-opening polymerization of ethylene oxide from terpene-based initiator.[25, 26] To the best of our knowledge, the synthesis of amphiphilic dextrans hydrophobically modified by terpenes has never been reported.

Our aim in the following chapter is first to present the synthesis of amphiphilic terpene grafted dextran and terpene grafted poly(acrylic acid) copolymers to further assess the stabilizing properties of these amphiphilic copolymers in miniemulsion polymerization. The synthesis of the amphiphilic copolymers from functional terpenes was carried out in collaboration with Marie Hélène Alvès, a postdoc researcher working at the IPREM-EPCP in the framework of BIOPOLYSURF project funding by DRT and LVMH. Thus, the originality of our work lies in the fact that the grafted hydrophobic groups are therefore terpene units from renewable resources.

Here we will describe the synthesis of the dextran and PAA grafted with terpene units (Scheme 1). Note that the structures of terpenes used for preparation of both hydrophobically modified dextran and PAA are different. Tetrahydrogeraniol (THG) terpene, supplied by DRT was used to modify PAA because it contained the primary alcohol group required for esterification reaction (Scheme 1). However, no available terpene with a carboxylic acid function for the esterfication of dextran was available, thus it was important to implement thiol-ene chemistry to synthesize the functional carboxylic acid based terpene (Scheme 1). For that reaction, dihydromyrcenol (DHM) terpene was chosen as a non toxic terpene containing a mono-substituted vinylic function suitable for applying the chosen thiol-ene addition chemistry.

The stabilizing properties of the synthesized copolymers were assessed through colloidal features of PS latex synthesized by miniemulsion polymerization. For a miniemulsion of styrene we used as a surfactant different terpene-grafted dextarn Dext-*g*-$(DHM)_n$ (Scheme 1), prepared by grafting a certain number of DHM-COOH terpene units onto dextran (Scheme 1). Also, in parallel, miniemulsion of styrene was performed by using different terpene-grafted poly(acrylic acid) PAA-*g*-$(THG)_n$, prepared by grafting different amounts of THG units onto poly(acrylic acid) (Scheme 1).

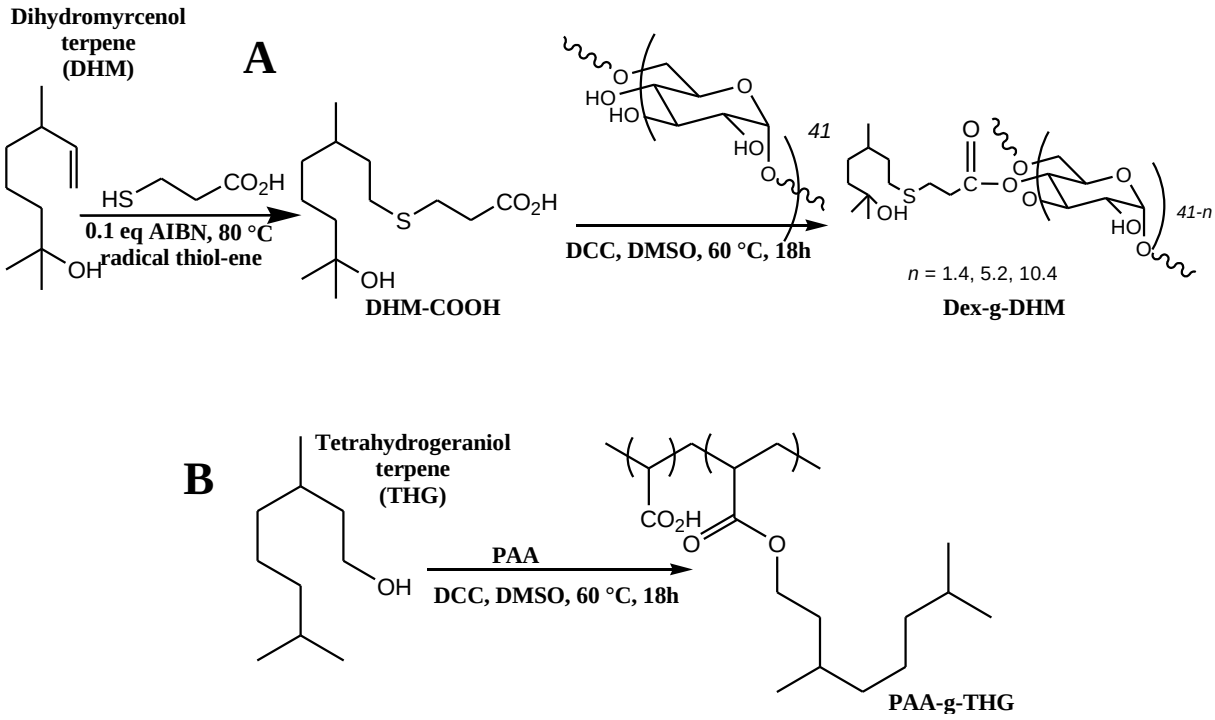

Scheme 1. Preparation of the amphiphilic surfactants A) Dext-*g*-DHM and B) PAA-*g*-THG

Experimental Section

Materials

Styrene (Sigma-Aldrich, 99 %) passed under inhibitor removers, acrylic acid (AA, Aldrich, 99 %), hexadecane (Aldrich, 99 %), 4,4'-azobis(4-cyanopentanoic acid) (ACPA, Fluka, ≥ 98 %), dibenzyltrithiocarbonate (CTA=DBTTC), trimethylsilyl diazomethane (TMS, Aldrich, 2M in diethyl ether), tetrahydrogeraniol (THG),6-Dimethyloct-7-ene-2-ol also named dihydromyrcenol (DHM) was supplied by Dérivés Résiniques Terpéniques (DRT company),2 2'-azobis(2-methylpropionitrile) (AIBN, Aldrich,98 %), N-dicyclocarbodiimide (DCC, Aldrich, 99 %), diethyl ether (Sigma-Aldrich, ≥ 99,8 %), tetrahydrofuran (THF, Technical grade, VWR), dimethyl sulfoxide (DMSO, Technical grade, VWR) was dried over molecular sieves which were previously dried under vacuum at 100 °C), commercial ethanol, distilled water.

Synthesis of amphiphilic terpene grafted copolymers

Synthesis of Dextran grafted with DHM terpene

Synthesis of DHM-COOH by thiol-ene chemistry. The terpene DHM-COOH displayed in Scheme 2 was synthesized as follows: 20 g of DHM (1.3×10^{-1} mol), 13.6 g of 3-mercaptopropionic acid (1.3×10^{-1} mol) and 210 mg of AIBN (1.3×10^{-3} mol) were mixed in a round bottom flask sealed with a rubber septum prior degassing 15 minutes with nitrogen flow. The reaction was carried out at 80 °C for 4 hours and the final product (non colored oil, quantitative product, Scheme 2) was used without purification.

Grafting of DHM-COOH for the synthesis of hydrophobically modified Dextran. Dextran 8 (1 g, M_n = 6600 g.mol^{-1}, 1.5×10^{-4} mol) were mixed with 6 mL of dried DMSO heated at 60 °C before adding N,N′-Dicyclohexylcarbodiimide (3.7 g, 1.8×10^{-2} mol). A solution of DHM-COOH terpene (3.9 g, 1.5×10^{-2} mol) was prepared with 2 mL of DMSO and subsequently poured into the round bottom flask containing the Dextran 8 and DCC solution. The initial number of moles of DHM terpene over the number of moles of anhydroglucose units (AGU), $x = (m_{DHM,0}/FW_{DHM})/(m_{Dextran,0}/M_{n,AGU})$, is equal to 0.24, 1.22 and 2.44 respectively for the synthesis of Dext-graft-DHM_1, Dext-graft-DHM_5 and Dext-graft-DHM_{10} grafted copolymers. After 18 hours at 60 °C, the modified Dextran was precipitated three times into methanol in order to eliminate free terpene. The final amphiphilic polymer was recovered as a white powder after drying process.

Synthesis of PAA grafted with THG terpene

Synthesis of PAA. The synthesis of this polymer was carried out by reversible addition fragmentation transfer (RAFT) polymerization according to the literature [27] (Scheme 4), in ethanol, ([Monomer]= 2,92 mol.L^{-1}) at 80°C using 4,4'-azobis(4-cyanopentanoic acid) (ACPA) as initiator with a molar ratio [CTA]/[ACPA]=10.10 g of acrylic acid (AA) (13.8 $x10^{-2}$ mol), 19.4 mg of ACPA (1.4 $x10^{-4}$ mol), 201 mg of (tri)thiocarbonic acid dibenzyl ester (DBTTC) (1.4 $x10^{-3}$ mol) and 30 g of ethanol (3.3 $x10^{-1}$ mol) were introduced into a round bottom flask sealed with a septum. The solution was degassed by purging nitrogen for 30 min, and then placed in an oil bath heated to 80 °C for 90 min. The polymer was precipitated in diethyl ether (cooled with liquid nitrogen), re-dissolved in ethanol and re-precipitated in diethyl ether. The re-precipitation was repeated three times to remove any residual monomer. The polymer was dried in a vacuum oven and recovered as a yellow powder. PAA-TTC was then characterized by ^{1}H NMR and THF SEC (after methylation). For THF SEC analysis, the PAA must first be methylated (Scheme 4). To do this, 10 mg of PAA was dissolved in 1 ml of a water / THF (1/1), and a yellow solution of trimethylsilyldiazomethane (solution of 2M TMS in diethyl ether) was added dropwise in the reaction medium and an off-gas (N_2) occurs instantly. The yellow color of the medium then fades little by little and it is necessary to add TMS to maintain the yellow color of methylation reagent and stop gassing. The solution was stirred at room temperature for 4 h and then allowed to evaporate under the hood. The dried residue was then diluted with THF and analyzed by SEC.

Grafting of THG terpene for the synthesis of PAA-g-THG. For the synthesis of PAA-g-$(THG)_7$, 1 g of PAA-TTC (7995 g.mol^{-1}) is solubilized in 5 mL of dry DMSO at 60 °C. The coupling agent DCC (477 mg, 18 molar equivalent to PAA) was then added. Then, a solution of THG (305 mg, 15 molar equivalent to PAA) in 1 mL of DMSO was added. The mixture was heated to 60 °C for 18 h. The modified PAA was precipitated in diethyl ether, redissolved in ethanol and reprecipitated in diethyl ether to remove the non reacted terpene. This process was repeated three times. The grafted copolymer was dried in vacuum oven and recovered in the form of brown powder.

Miniemulsion polymerization using amphiphilic copolymer as stabilizer

All the miniemulsion experiments carried out in this chapter were carried out in the following manner: the aqueous phase was prepared by dissolving 100 mg of the copolymer as surfactant

(2.2 wt-% vs monomer) in 20 g of distilled water. The organic phase was prepared by mixing 5 g of styrene (4.8×10^{-2} mol), 0.25 g of hexadecane (1.1×10^{-3} mol, 5 wt-% vs monomer), 25 mg of AIBN (1.5×10^{-4} mol). The two phases were then mixed, placed in an ice bath and stirred for 10 minutes at 300 rpm. The mixture still in the ice bath, was then subjected to high shear pressure using a Vibra Cell 72408 ultrasonicator for 6 minutes at amplitude of 30 %. After sonication, a white liquid emulsion is obtained, which is then poured into a 50 mL round bottom flask and sealed with a septum. The latex was then degassed by purging nitrogen for 20 min. The flask was placed in an oil bath preheated to 70 °C. The reaction was proceeded for 6 h, at which the reaction was stopped by introducing oxygen and fast cooling. Samples were withdrawn each 2 h for conversion and analysis of colloidal features.

Results and discussion

1. Synthesis of amphiphilic terpene grafted copolymers

1.1. Synthesis of Dextran grafted with DHM terpene

Synthesis of DHM-COOH by thiol-ene chemistry. As introduced in this chapter, in the present work the synthesis of carboxylic-acid based terpene is required for further dextran modification (Scheme 1), the synthesis of the functional terpene was performed by thiol-ene chemistry thermally initiated with AIBN initiator (Scheme 2). As reported in literature,[28, 29] the first step of thiol–ene radical reaction is the formation of thiyl radicals ($RS^{\bullet}$) obtained from transfer reaction of the carbon-centered radicals which are generated by the initiator decomposition. The reaction proceeds then *via* addition of the thiyl radical through the ene functional group to form a carbon radical. For ideal thiol-ene reactions, no homopolymerization is observed and chain transfer of the carbon radical to another thiol functional group follows the addition step, regenerating the thiyl radical and forming the thiol-ene addition product (Scheme 2). For alkyl thiols and alkenes, the reaction is chain-transfer-limited and first order in thiol functional group concentration.[29, 30] The DHM-COOH molecule functionalized by carboxylic acid was synthesized from the initial dihydromyrcenol (DHM) terpene (Scheme 2).

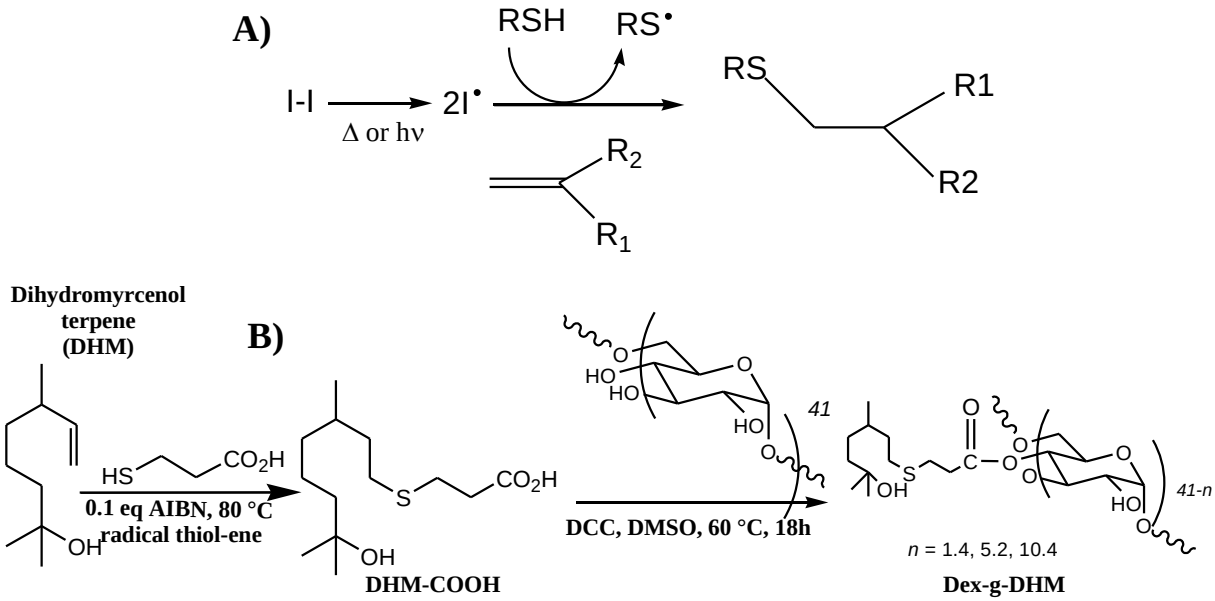

Scheme 2. (A) general principle of radical thiol-ene chemistry using an initiator (I-I) and a thiol transfer agent (RSH); (B) Derivatization of dihydromyrcenol DHM terpene by thiol-ene chemistry to produce functional DHM-COOH terpene

The analysis of the proton NMR spectra of the DHM-COOH (Figure 1B) confirmed the success of the thiol-ene reaction performed with 3-mercaptopropionic acid acting as transfer agent for the coupling reaction (Scheme 2). Indeed, the disappearance of the alkene signals of dihydromyrcenol between 4.8 and 5.6 ppm (Figure 1A) along with the chemical shift from 2.1 ppm to 1.5 ppm of the *c* proton in α position of the alkene group (Figure 1B) proves the complete addition reaction.

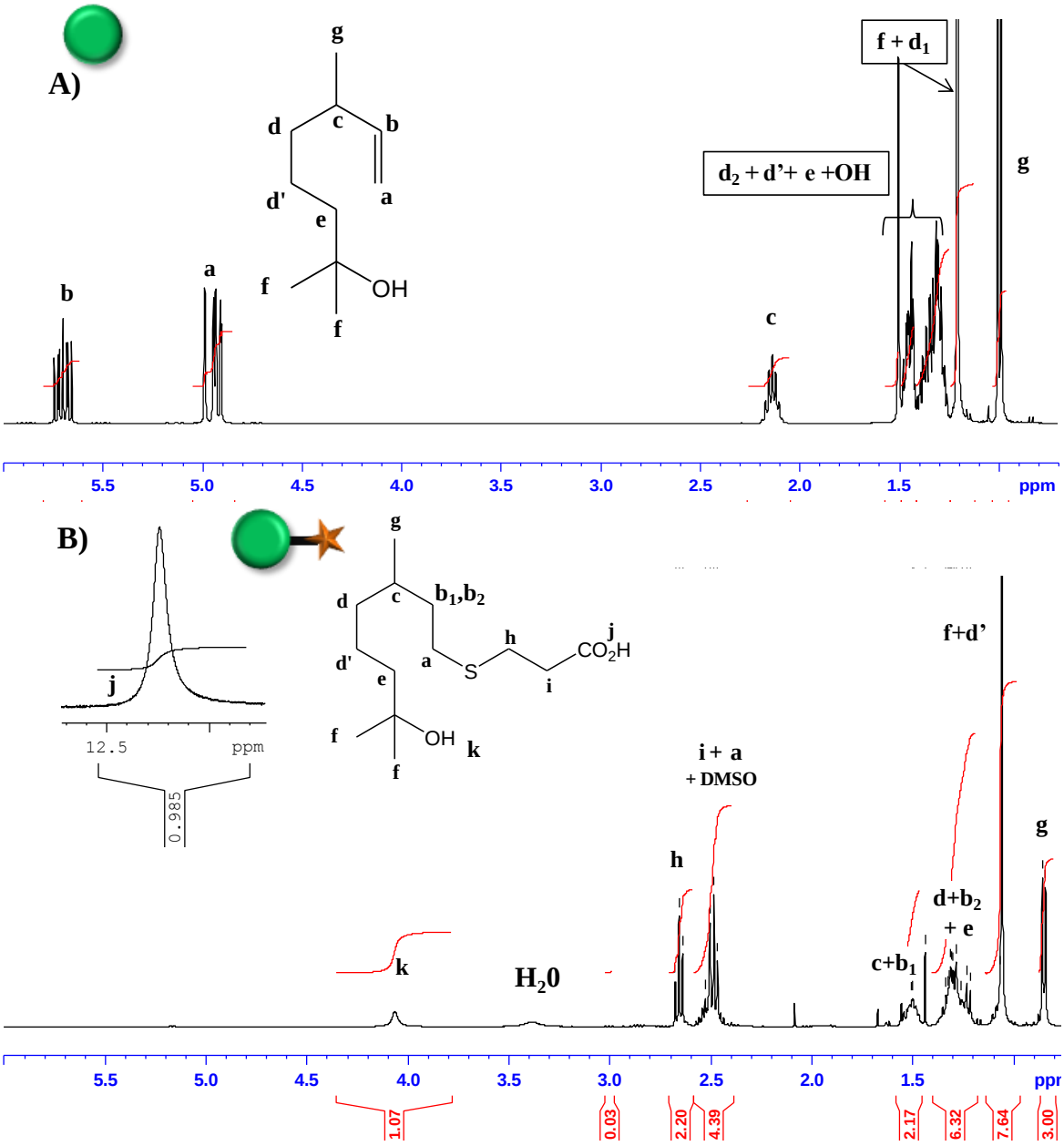

Figure 1. [1]H NMR spectra of (A) DHM and (B) DHM-COOH terpene

Complete disappearance of the alkene signals (Figure 1) was observed for the synthesis of DHM-COOH performed in stoichiometric amounts of DHM and 3-mercaptopropionic acid, but the NMR integrations of the thiol moiety peak (I_h = 2.20 (2H)) exhibits 10 % excess in comparison with the NMR integration of the terpene peak (I_g = 3.00 (3H)) (Figure 1B). However, the good agreement between the integration values of the carboxylic acid proton (I_j = 0.985 (1H)) and the terpenic protons (I_g = 3.00 (3H)) along with the single carboxylic acid peak at 173.3 ppm were observed respectively in the proton (Figure 1B) and the carbon (Figure 2B and Figure 3) NMR spectra of terpene DHM-COOH. These observations support

the absence of either residual 3-mercaptopropionic acid or oligomers issued from polyesterification between the tertiary alcohol group and the carboxylic acid group.

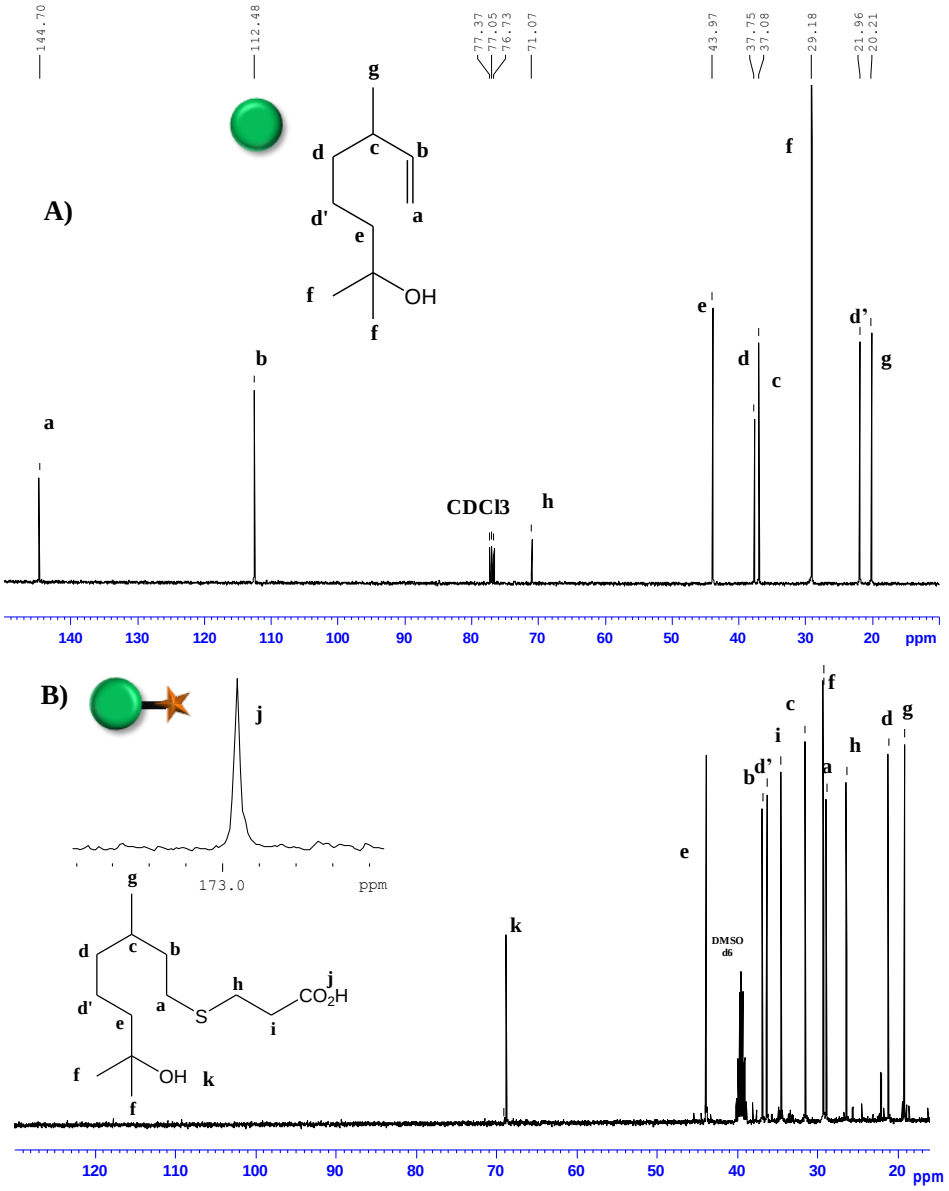

Figure 2. ^{13}C spectra of (A) DHM and (B) DHM-COOH terpene in DMSO-*d6*

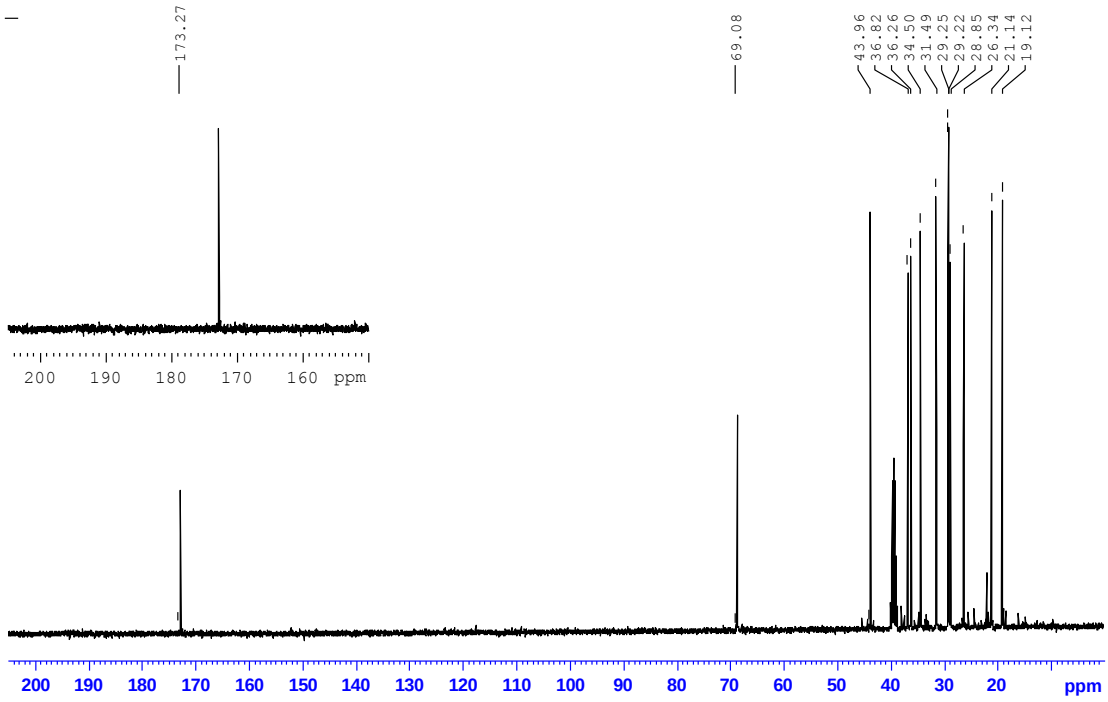

Figure 3. complete ^{13}C NMR spectrum of DHM-COOH terpene in DMSO-*d*6

The analysis of DHM-COOH terpene by two dimensional heteronuclear single quantum coherence (HSQC) NMR (Figure 4A) enabled us to accurately ascribe the chemical shifts of all protons and carbons. The plot of HSQC NMR analysis confirms the expected structures of DHM-COOH terpene obtained predominantly by the anti-Markovnikov[31] addition (Scheme 2). A zoom of HSQC NMR spectrum (Figure 4B) displays additional methyne (δ = 39.0 ppm) and methyl (δ = 19.4 ppm) groups suggesting the presence of a small amount of the Markovnikov addition product. From the integration of the doublet at 1.10 ppm, this secondary structure corresponds to only 5 mol-% of the DHM-COOH terpene. Finally, the absence of additional signal of any thioester group between 170 and 210 ppm (Figure 3) excludes transesterification side reaction between acid-based terpene and 3-mercaptopropionic acid.[32]

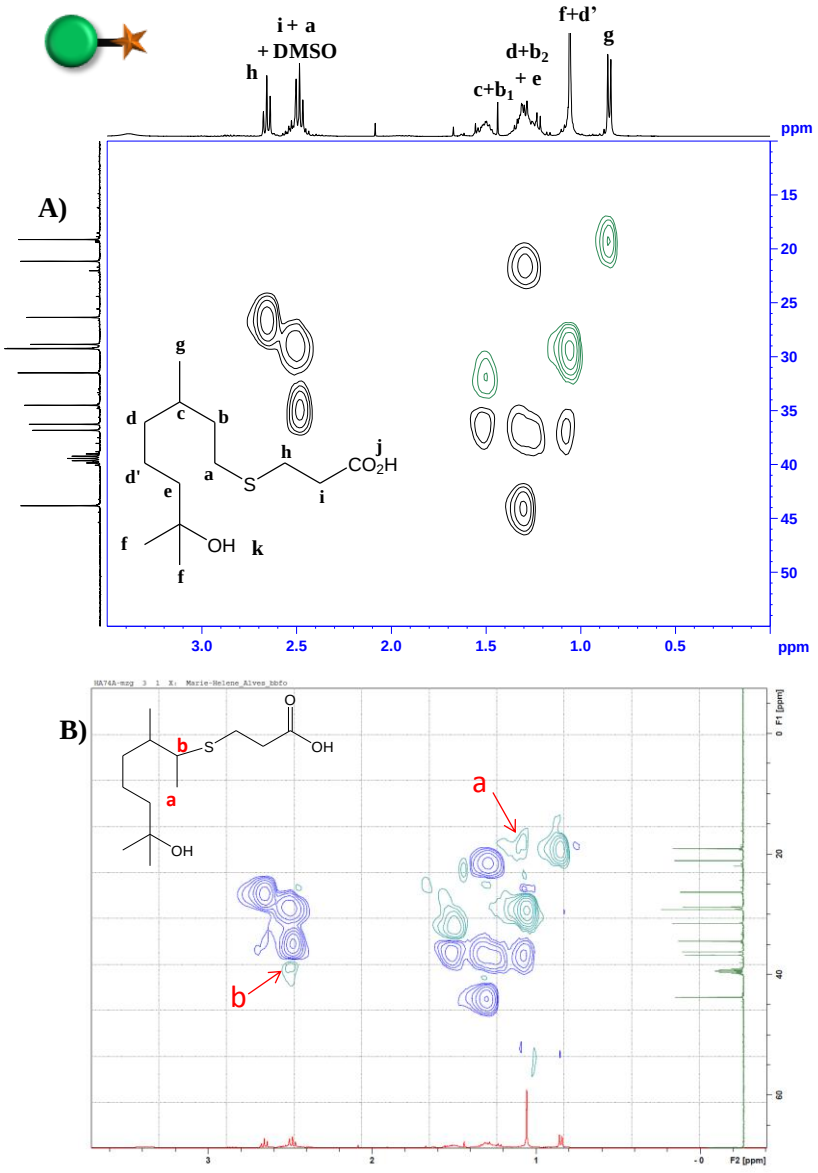

Figure 4. HSQC spectrum of A) DHM-COOH terpene in DMSO-*d*6, B) Zooming

The influence of the initiator concentration on the double bond conversion was investigated and the results are reported in Table 1. The 3-mercaptopropionic acid being initially soluble in DHM, the stoichiometry between thiol and vinylic groups was sufficient to provide 100 % of coupling efficiency. As we increased the [RSH]/[AIBN] ratio from 10 to 100 (Entry 1 to 2), the conversion remained the same, showing no effect of decreasing the amount of initial concentration of initiator.

Table 1. Thiol-ene chemistry reaction between dihydromyrcenol (DHM) terpene and thiol carried out at T = 80 °C in bulk.[a]

Entry	R-SH	$[DHM]_0$ *mol.L^{-1}*	$[R\text{-}SH]_0$ *mol.L^{-1}*	$[AIBN]_0$ *mol.L^{-1}*	Time *h*	conversion[a] *%*
1	3-mercaptopropionic acid	3.6	3.6	3.6×10^{-1}	4	100
2	3-mercaptopropionic acid	3.6	3.6	3.6×10^{-2}	4	100

[a] Coupling efficiency determined by ^{1}H NMR using the integrations of initial DHM and final terpene (Figure 1): conversion = $[1-(I_{g,DHM}/(I_{g,DHM}+I_{e,terpene\ 1}))] \times 100$.

Grafting of DHM-COOH for the synthesis of hydrophobically modified Dextran. The strategy of grafting the hydrophobic terpene group onto the dextran backbone focuses on tuning the hydrophobic content of the amphiphilic modified dextran *via* the number of grafted terpene molecules. DHM-COOH terpene derivatized with carboxylic acid group was covalently grafted onto the polysaccharide by esterification reaction carried out in dimethylsulfoxide (DMSO) at 60 °C in the presence of *N*,*N*′-dicyclohexylcarbodiimide (DCC) catalyst (Scheme 3). The number average molar mass of dextran was 6600 g.mol^{-1} corresponding to a degree of polymerization of 41 (N_{AGU} = 41).

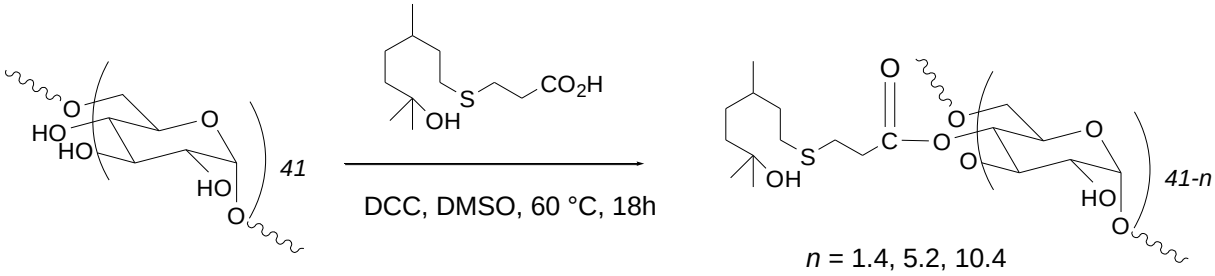

Scheme 3. Synthesis of hydrophobically modified dextran (Dext-*graft*-DHM) by esterification reaction between dextran and DHM-COOH.

The efficient grafting of DHM-COOH terpene was evidenced by the presence of characteristic peaks of protons *f* and *g* in the NMR spectrum of the amphiphilic copolymer (Figure 5). The number of grafted DHM units per chain of dextran polymer was calculated from equation (1) using the NMR integrations of both DHM methylic protons (I_g) and dextran anomeric protons ($I_{(a+a')}$). Prior NMR analysis, the hydrophobically modified dextran was carefully precipitated three times into methanol to remove any unreacted DHM-COOH terpene.

$$y = \frac{N_{\text{DHM}}}{N_{\text{Dextran}}} = \frac{(I_c)/3}{(I_{a+a'})/41}$$

Equation 1. Calculation of the average final number of DHM units per dextran polymer chain

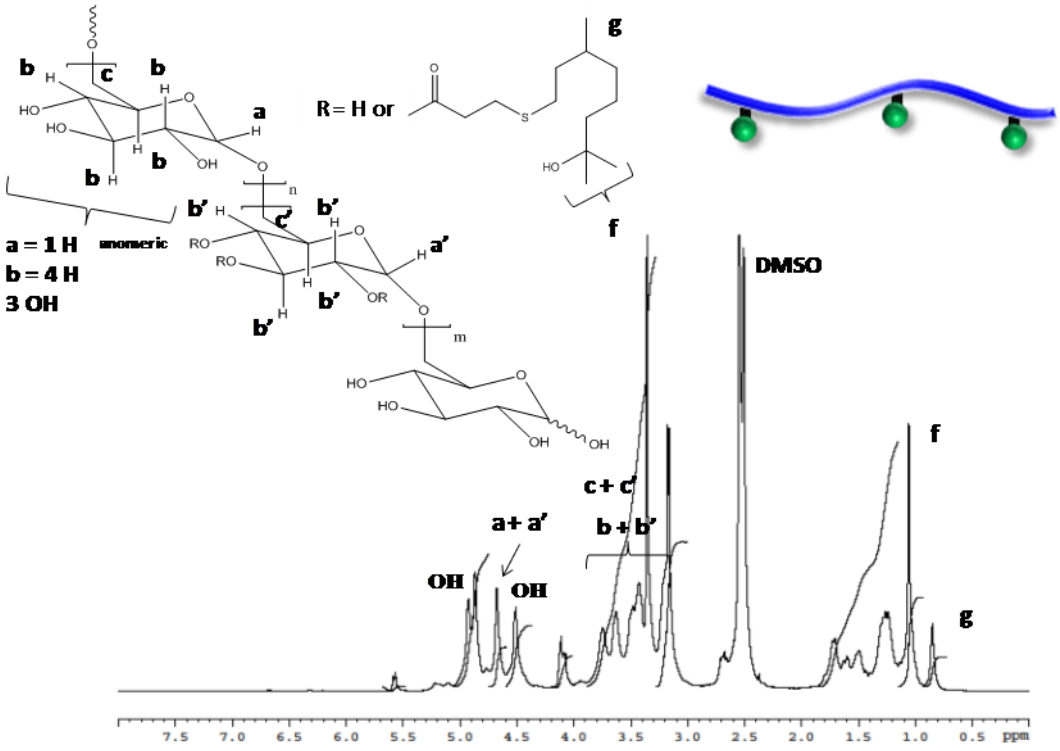

Figure 5. ^{1}H NMR spectrum of Dext-*graft*-DHM$_{10.4}$ in DMSO-*d*6.

As depicted in Table 2, we successfully synthesized three different terpene modified dextrans exhibiting respectively 1.4, 5.2 and 10.4 grafted terpene molecules per polysaccharide chain. It corresponds to a degree of substitution (DS), *ie*. the percentage of terpene functions per glucosidic unit, ranging between 3.4 and 25.4 %. By applying the simplified Griffin method,[33] (Equation 2) the hydrophilic lipophilic balance (HLB) values of these amphiphilic copolymers ranged between 15 and 19, where HLB can be simply defined as a measure of the degree to which a surfactant is hydrophilic or lipophilic.

Equation 2: $$HLB = 20 \times \frac{M_h}{M}$$

Where M_h is the molar mass of the hydrophilic portion of the molecule, and M is the molar mass of the whole molecule, giving a result on a scale of 0 to 20. A HLB value of 0 corresponds to a completely lipophilic molecule, and a value of 20 corresponds to a completely hydrophilic molecule.

Table 2. Synthesis of dextran-*graft*-DHM by esterification of dextran[a] with DHM-COOH terpene carried out at 60°C for 18 h in DMSO.

Exp	Polymer	$x = \frac{n_{DHM,0}}{n_{Dextran,0}}$ [b]	$y = \frac{N_{DHM}}{N_{Dextran}}$ [c]	DS [d] (%)	HLB
1	Dext-*graft*-$DHM_{1.4}$	10	1.4	3.4	19
2	Dext-*graft*-$DHM_{5.2}$	50	5.2	12.7	16.5
3	Dext-*graft*-$DHM_{10.4}$	100	10.4	25.4	14

[a] Dextran 8 polymer from Serva Electrophoresis®: $M_{n,Dext}$ = 6600 g.mol^{-1}, M_w/M_n = 2.2, N_{AGU} = 41

[b] Initial number of moles of DHM terpene over number of moles of Dextran polymer chains, $x = (m_{DHM,0}/M_{n,DHM})/(m_{Dextran,0}/M_{n,Dext})$

[c] Average final number of DHM units per Dextran polymer chain analyzed by proton NMR of the precipitated of Dext-*graft*-DHM (Figure 1 and Equation 1).

[d] Degree of substitution of the Dext-*graft*-DHM, *ie*. number of DHM functions per glucosidic unit .

1.2. Synthesis of PAA grafted with THG terpene

Synthesis of PAA by RAFT polymerization

The synthesis of poly(acrylic acid) (PAA) was carried out by reversible addition fragmentation chain transfer (RAFT) polymerization according to the literature [27]. The transfer agent was the dibenzyltrithio carbonate (DBTTC, Scheme 4) supplied by Arkema company. After the synthesis of the polymer PAA-TTC, the polymer was methylated (Scheme 4) in order to be characterized by THF-SEC. The results are shown in Table 4.

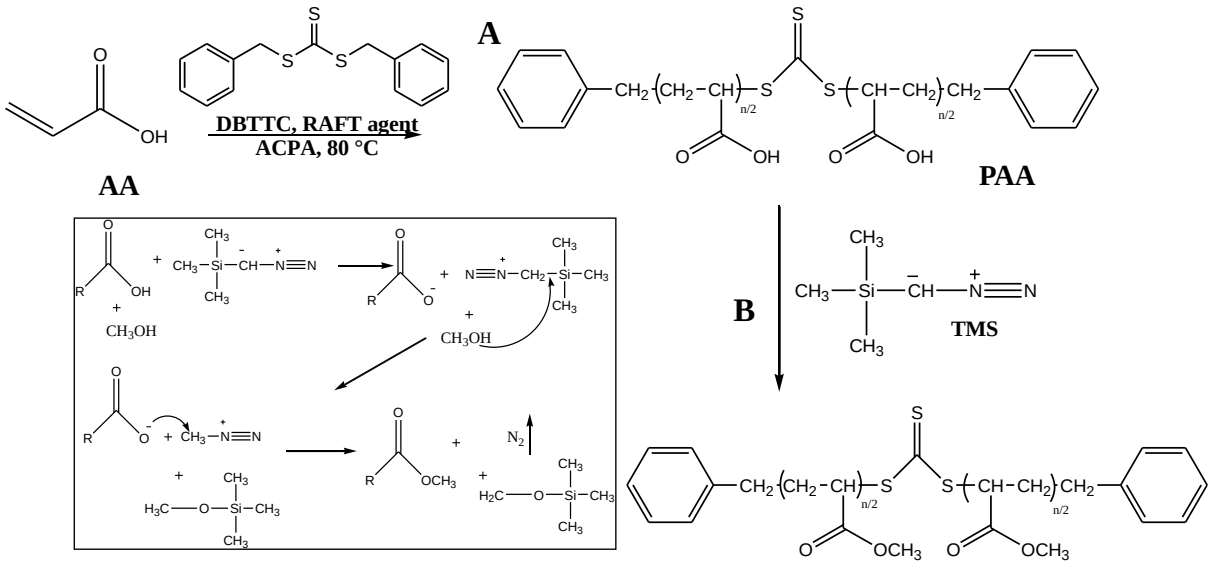

Scheme 4. A) Synthesis of PAA by RAFT polymerization using DBTTC as RAFT agent; B) methylation of PAA

SEC analysis of methylated PAA (poly-(methyl acrylate), PMA) showed an experimental M_n of 9470 g.mol^{-1} indicating a number average degree of polymerization (DPn) of 107. On this basis the experimental molar mass ($M_{n,\ exp}$) of PAA was calculated to be 7995 g.mol^{-1}. The low dispersity (Đ = 1.25) and the correct matching between the theoretical molar mass $M_{n(theo)}$ (7400 g.mol^{-1}) and experimental one showed a good control of the RAFT polymerization of AA carried out in ethanol.

Table 3: PAA-TTC characteristics

Polymer	$[AA]_0/[DBTTC]_0$	$M_{n,\ PMA}$ [a] g.mol^{-1}	$M_{n,\ PAA\ (exp)}$ [b] g.mol^{-1}	$DP_{n,\ SEC}$ [a]	$DP_{n,\ NMR}$ [c]	M_w/M_n [a]
PAA-TTC	200	9470	8000	107	140	1.25

[a] $M_{n\ (exp)}$ of PMA determined by THF-SEC analysis, [b] calculated molar mass of PAA, [c] number average degree of polymerization calculated by ^{1}H NMR

Grafting of THG terpene for the synthesis of PAA-g-THG

An esterification reaction between the PAA and the THG terpene takes place in order to graft the terpene onto the PAA (Scheme 4). Upon varying the stoichiometry of terpene (THG), it was possible to graft between 2 and 15 terpene units per chain of PAA, thus modulating the HLB of the synthesized surfactants. The results of grafting are shown in Table 4.

Table 4: Results of the esterfication in DMSO of PAA with tetrahydrogeraniol (THG) terpene

Polymer	$x = \frac{n_{THG,0}}{n_{PAA,0}}$ [a]	$y = \frac{N_{THG}}{N_{PAA}}$ [b]	Efficiency (%) = y/x*100	DS [c] (%)	HLB [d]
PAA-*g*-$(THG)_2$	7.7	2.3	30	1.8	18
PAA-*g*-$(THG)_7$	15.0	7.0	45	6.5	17
PAA-*g*-$(THG)_{15}$	20.0	15.0	75	14	14

[a] Initial number of moles of THG terpene over number of moles of PAA polymer chains, $x = (m_{THG,0}/M_{n,THG})/(m_{PAA,0}/M_{n,PAA})$

[b] Average final number of THG units per PAA polymer chain analyzed by proton NMR of the precipitated of PAA-*graft*-THG

[c] Degree of substitution of the PAA-*graft*-THG, *ie*. Number of THG functions per PAA unit

[d] Calculated from Equation 2.

The grafting degree of the terpene grafted poly(acrylic acid) (PAA-*g*-THG) was determined by ^{1}H NMR, by comparing the intensity of grafted terpene signal (δ_{Ia} = 0.8 ppm) to the benzyl chain ends of the polymer (*Ph*CH_2) (δ_{Ic} = 7.3 ppm) (Figure 6). Nevertheless, as revealed by the discrepancy observed between the degree of polymerization of PAA calculated by either

SEC or NMR (see Equation 3 and Table 3) a fraction of PAA chains are probably not functionalized by benzyl groups due to irreversible chains transfer reactions to ethanol. [27] Therefore, the grafting degree of terpene was calculated according to Equation 4 by introducing a correction-factor (f)

$$\frac{DP_{SEC}}{DP_{RMN}} = \frac{(\frac{n_{AA}}{n_{chains}})}{\frac{n_{AA}}{n_{benzyl}})} = \frac{n_{benzyl}}{n_{chains}} = \frac{107}{140} = f = 0.76$$

Equation 3

$$\frac{N_{terpene}}{N_{chain}} = \frac{n_{terpene}}{n_{benzyl}} \times f = \frac{I_{terpene}}{I_{benzyl}} \times f$$

Equation 4

The degree of esterification of PAA-*g*-THG was calculated from ^{1}H NMR integrations (Figure 6), that is by comparing the intensity of peak **c** (10H protons of benzyl chains *Ph*CH_2 = I_{benzyl} of Equation 4) to that of peak **a** (C*H*, 9H of THG = $I_{terpene}$ of Equation 4). The efficiency of the esterification ranges between 30 % and 70 %. As reported in Table 4 the ^{1}H spectrum also reveals remaining functions of the non-modified acrylic acid units (I_b at 12 ppm in Figure 6).

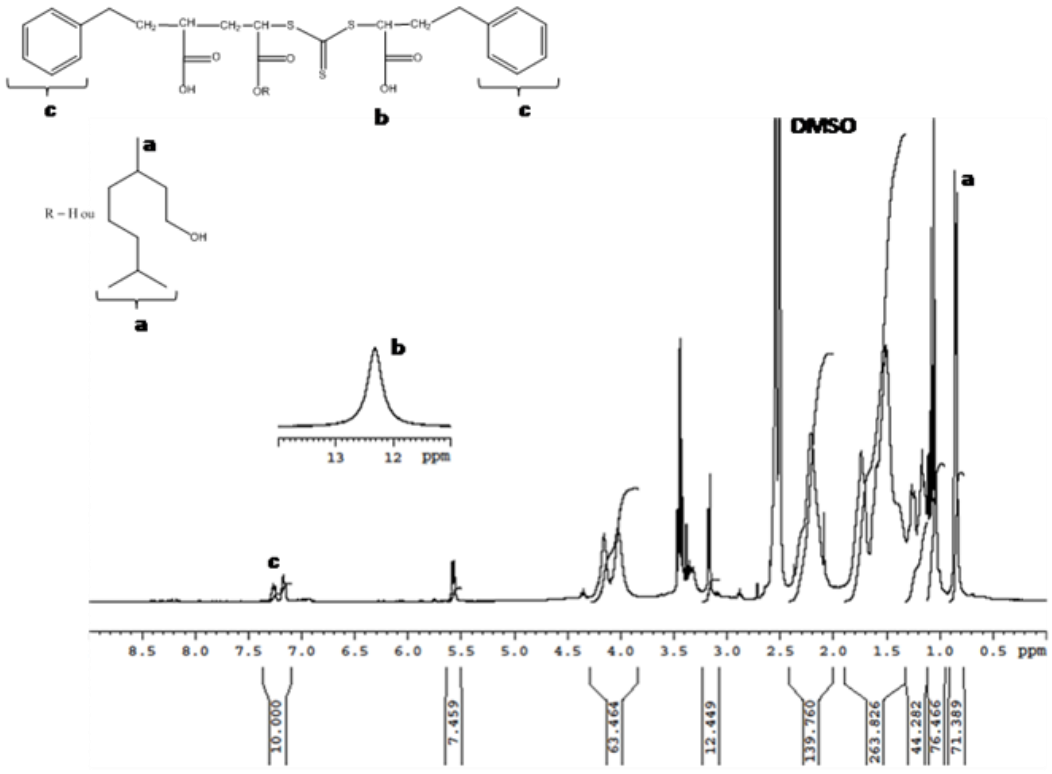

Figure 6: 1H NMR spectrum of purified PAA-*g*-$(THG)_7$, (in DMSO-d^6).

2. Miniemulsion polymerization using amphiphilic copolymers as stabilizer

2.1. Stabilization with Dext-g-DHM

The Dext-*g*-DHM amphiphilic grafted copolymers based on dextran backbone, (see synthesis in part 1.1) differing by their degree of substitution of DHM functions per glucosidic unit, will be used as stabilizers for free radical miniemulsion polymerization of styrene (Table 2). The experimental conditions of polymerization are gathered in notes of Table 5 along with final conversion and colloidal features obtained by dynamic light scattering (DLS).

Table 5: Summary of the results of miniemulsion polymerization of styrene stabilized by Dext-*g*-DHM copolymers

Exp	Expt.	Surfactant	% grafted terpene	Final conversion [a] (%)	D_h [b] (nm)	$\bar{d}_w/\bar{d}_n$ [c]	σ [e]	N_p [f] (L^{-1}_{latex})
HS130	1	Dext-*g*-$(DHM)_{1.4}$	3.4	53	234/390 (0.51/0.37)[d]	1.012	0.47	8.6×10^{15}
HS131	2	Dext-*g*-$(DHM)_{5.2}$	12.7	63	170/390 (0.2/0.55)[d]	1.104	0.05	8.8×10^{15}
HS132	3	Dext-*g*-$(DHM)_{10.4}$	25.4	48	245	1.007	0.05	1.2×10^{16}

[a] Determined gravimetrically; [b] Hydrodynamic diameter of final latex measured by DLS after dilution by a factor of 100; [c] particle-diameter dispersity calculated from Equation 5; [d] proportion in intensity; [e] particle-diameter dispersity obtained from DLS; [f] Number of particles calculated from Equation 6. $[AIBN]_0 = 3\times10^{-2}$ moL.$L^{-1}_{styrene}$, 5 wt-% hexadecane co-stabilizer vs styrene, 2 wt-% stabilizer vs styrene, 20 wt-% styrene vs total volume, T = 70 °C at pH ~ 9

Before performing the polymerization reactions, we first studied the ability of these copolymers to stabilize initial liquid miniemulsions. Regarding Figure 7, one population centered at 355 nm is viewed for styrene liquid miniemulsion stabilized by Dex-*g*-$(DHM)_{1.4}$. However, two populations appeared upon increasing the number of grafted DHM per chain. The presence of a population with smaller diameter is a characteristic of a higher number of droplets.

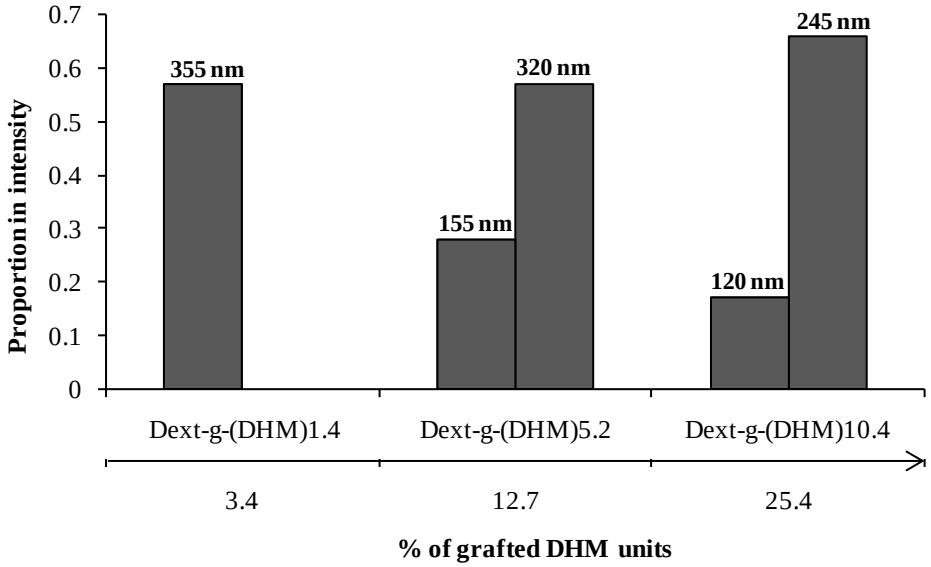

Figure 7. Proportion in intensity and average hydrodynamic diameters of the initial styrene liquid miniemulsion stabilized by different Dext-*g*-(DHM), studied by DLS in diluted mode.

We studied the size of the final latex by the DLS, where the samples were diluted in distilled water by a factor of 100. Figure 8 shows the size of the final particles stabilized by Dext-*g*-DHM copolymers. We notice that two populations (235 nm/390 nm and 170 nm/390 nm) existed with 3.4 % and 12.7 % of grafted DHM units respectively, whereas it was just one population centered at 245 nm in the case with 25.4 % of grafted units. Thus, only Dext-*g*-$(DHM)_{10.4}$ provides one population of PS particles, corresponding to one of the initial population of droplets. Along with the diameters given by the DLS, we calculated the particle size distribution $\bar{d}_w/\bar{d}_n$, according to Equation 5.

$$\frac{\bar{d}_w}{\bar{d}_n} = \frac{\sum n_i \sum n_i D^4{}_i}{\sum n_i D_i \sum n_i D^3{}_i}$$

Equation 5. Calculation of the particle size distribution, n_i the number of particles with diameter D_i

The values of $\bar{d}_w/\bar{d}_n$ in Table 5 show monodispersed latexes obtained with Dext-g-$(DHM)_{1.4}$ and Dext-*g*-$(DHM)_{10.4}$ ($\bar{d}_w/\bar{d}_n$ < 1.02) whereas $\bar{d}_w/\bar{d}_n$=1.10 for Dext-*g*-$(DHM)_{5.2}$ shows a polydispersed latex.

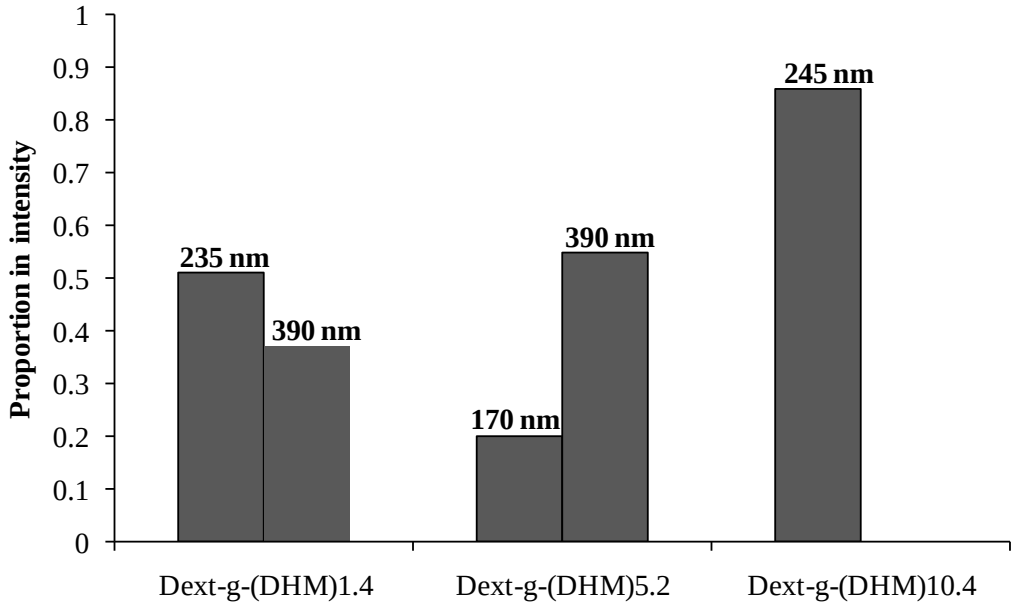

Figure 8. Proportion in intensity and average hydrodynamic diameters of the final latex particles stabilized with different Dext-*g*-(DHM) copolymers, studied by DLS after dilution with a factor of 100.

Stable latexes were recovered after 6 hours and the final diameters of latex particles (Figure 8) are compared to the initial diameters of liquid droplets reported in Figure 7. We notice that the diameters are in the same range for all cases, but the disappearance of the small droplet population existing when analysis in concentrated mode (D_h ~ 20 nm) with Dext-*g*-$(DHM)_{10.4}$ might reveal monomer diffusion while secondary nucleation might explain the presence of a secondary latex population with Dext-*g*-$(DHM)_{1.4}$ and Dext-*g*-$(DHM)_{5.2}$. The conclusions should be carefully considered from the difficulty to measure accurately the droplet diameter by DLS (effect of monomer diffusion).

We reported in Figure 9 the kinetics of miniemulsion polymerization of styrene performed with different Dext-*g*-DHM stabilizers. The final conversions at 6 hours ranged between 47 % and 63 %. The highest conversion was achieved with the Dext-*g*-$(DHM)_{5.2}$ grafted with 12.7 % of terpene units. Thus, regardless of the number of grafted DHM terpene, incomplete conversion was obtained when Dext-*g*-DHM was used a stabilizer.

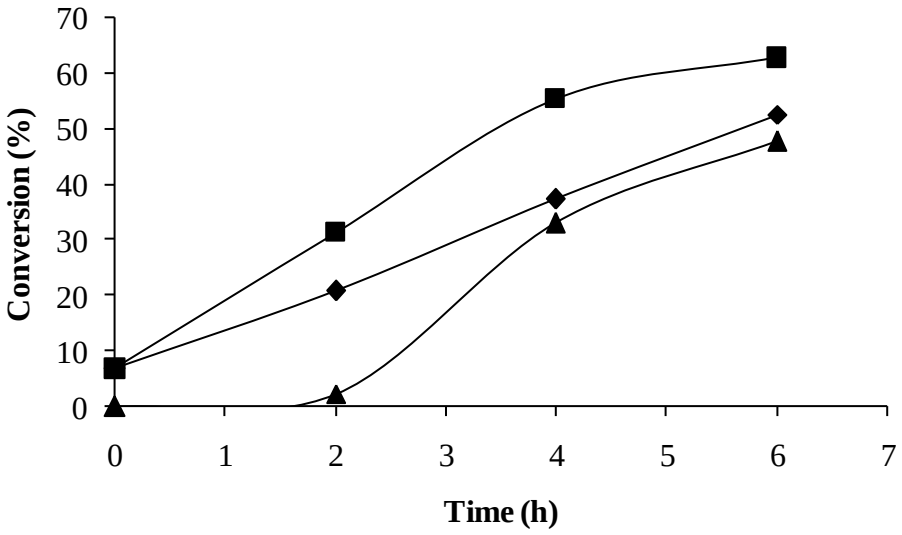

Figure 9. Conversion versus time for miniemulsion polymerization of styrene performed at 70 °C, with 2 wt-% of Dext-*g*-(DHM) vs styrene; ♦ Dext-*g*-$(DHM)_{1.4}$, ■ Dext-*g*-$(DHM)_{5.2}$, ▲ Dext-*g*-$(DHM)_{10.4}$.

In order to correlate the kinetics with the colloidal features of the PS particles, we calculated the number of particles according to Equation 6.

$$N_p = \frac{6\tau_{polymer}}{\rho_{polymer} \times {D_h}^3 \times \pi}$$

Equation 6. Calculation of the number of polymer particles (N_p)

With ($\tau_{polymer} = \frac{m_{monomer}}{m_{latex}} \times conversion$), $\rho_{polymer}$ the density of polystyrene 1.05 g.cm^{-3}, D_h the final diameter of particles in cm.

When two populations of diameter are obtained, one should take into consideration the percentage in volume of each population. Two values of N_p (N_{p1} and N_{p2}) are calculated according to each diameter obtained depending on the volumic fraction of each population provided by DLS.

$Np_1 = \frac{6V_{P1}}{{D_1}^3 \times \pi}$ with $Vp_1 = \frac{\tau_{polymer}}{\rho_{polymer}} \times V_1\%$, $Np_2 = \frac{6V_{P2}}{{D_2}^3 \times \pi}$ with $Vp_2 = \frac{\tau_{polymer}}{\rho_{polymer}} \times V_2\%$ and $Np=Np_1+Np_2$.

For the Dext-*g*-DHM miniemulsion polymerizations, the values of N_p are reported in Table 5.We observed that the final N_p values were in the range of 8.7×10^{15} particles per liter of latex for both Dext-*g*-$(DHM)_{1.4}$ and Dext-*g*-$(DHM)_{5.2}$ stabilizers. However, although a lower conversion was obtained with Dext-*g*-$(DHM)_{10.4}$ copolymer (Figure 9), the calculated N_p was

higher for such dextran hydrophobically modified with 25 % of grafted terpene units. The slight difference might be explained by the uncertainty of calculation in the later case only one population was measured, whereas in the others two diameters were obtained by DLS.

2.2. Stabilization with PAA-g-THG

We also performed miniemulsion polymerization of styrene with different PAA-*g*-THG copolymers exhibiting different amounts of grafted THG units (Table 6). Figure 10 shows that regardless of the percentage of grafted THG units only a single population of droplets was formed after sonication step. We notice that the diameter of the initial liquid miniemulsion increases from 155 nm to 280 nm as the percentage of the grafted THG units increases from 1.8 to 14.

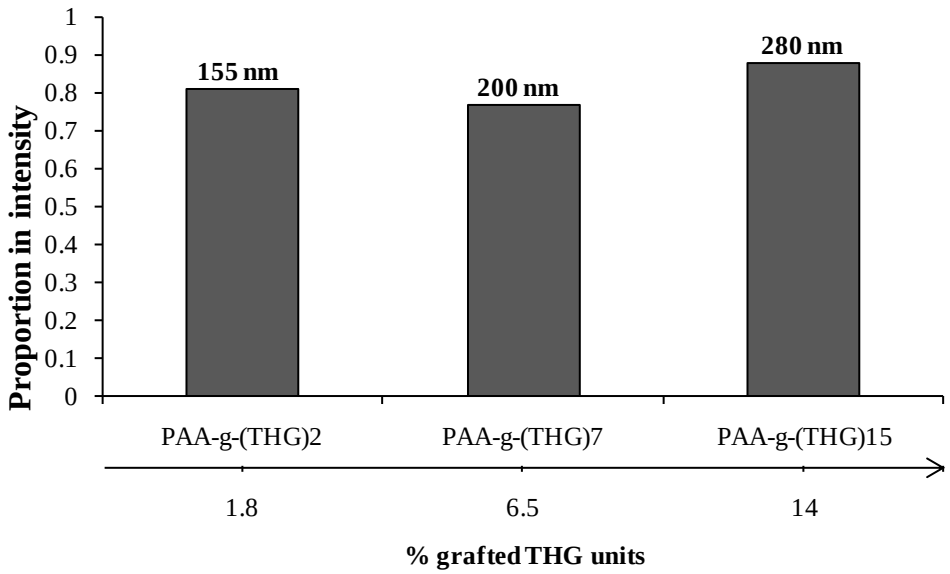

Figure 10. Proportion in intensity and average hydrodynamic diameters of the initial styrene liquid miniemulsion stabilized by different PAA-*g*-THG, studied by DLS in diluted mode

We also studied the kinetics of the miniemulsion polymerizations of styrene stabilized with 2 wt-% of PAA-*g*-THG containing different percentages of grafted THG chains (Table 6). Upon regarding the kinetic overlay of the miniemulsions performed with PAA-*g*-(THG) as stabilizer (Figure 11), a final high conversion in monomer of 96 % and 100 % is obtained in the respective cases of PAA-*g*-$(THG)_2$ and PAA-*g*-$(THG)_7$ in contrast to the lower monomer conversion obtained in the case of PAA-*g*-$(THG)_{15}$ (45 %). Thus, as we increased the percentage of the THG grafted chains we decreased the polymerization rate. In a free radical polymerization the propagation rate depends on the concentration of the active growing chains [$P^\bullet$] ($v_p=k_p[M][P^\bullet]$). In miniemulsion polymerization, the concentration of $P^\bullet$ is affected by ñ, the average number of radicals per particle ($[P^\bullet]= ñ \times Np$) with N_p being the

number of particles. [1] In miniemulsion polymerization, the droplet nucleation mechanism suggests that the monomer droplets formed during the emulsification step are polymerized directly *via* a radical that enters these monomer droplets and reacts with the monomer present there. For controlling ñ, one can change the initiator to change the flux of radicals. The number of particles N_p also influences the concentration of the propagating radicals [$P^{\bullet}$]. The stabilizer is an important factor in order to control the number of droplets of particles. As calculated in Table 6, the number of particles is 10 times lower for miniemulsion polymerization stabilized by PAA-*g*-$(THG)_{15}$ (Expt. 6) in comparison with N_p obtained in miniemulsion polymerization stabilized by PAA-*g*-$(THG)_2$ and PAA-*g*-$(THG)_7$ (Expt. 4-5).

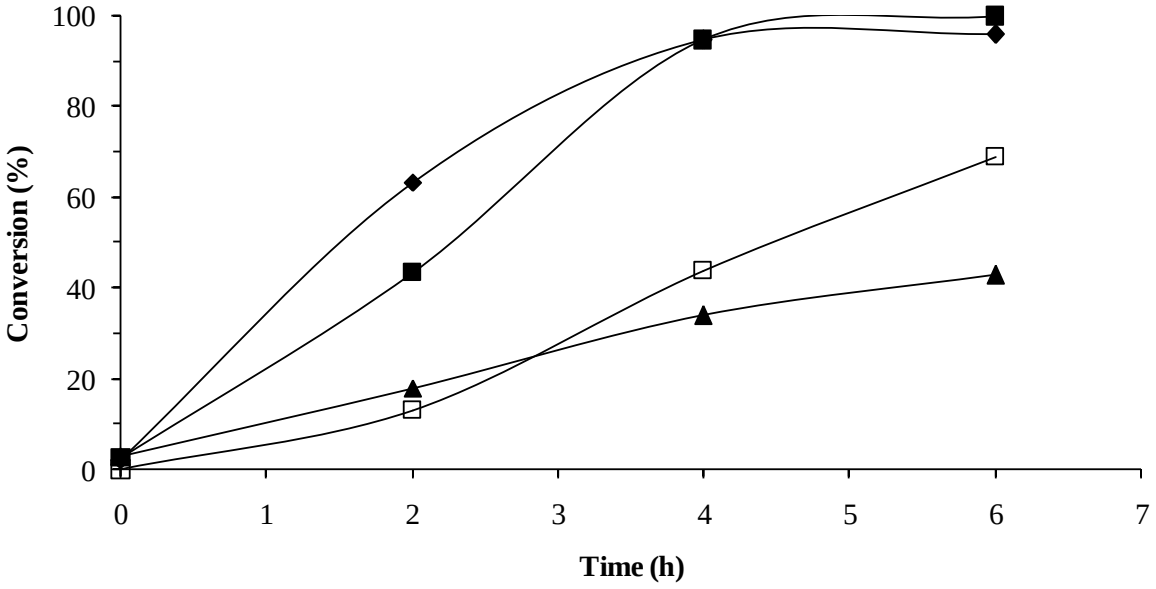

Figure 11. Miniemulsion polymerization of styrene at 70 °C, with 2 wt-% vs styrene of PAA-*g*-(THG) as surfactant differeing in the number of grafted THG units,♦ PAA-*g*-$(THG)_2$, ■ PAA-*g*-$(THG)_7$, □ PAA-*g*-$(THG)_7$ no hexadecane, ▲ PAA-*g*-$(THG)_{15}$

Table 6: Summary of the results of miniemulsion polymerization of styrene stabilized by different PAA-*g*-THG copolymers

Exp	Expt.	Surfactant	% grafted terpene	Final conversion [a] (%)	Final D_h [b] (nm)	$\bar{d}_w/\bar{d}_n$ [c]	σ [d]	N_p [e] (L^{-1}_{latex})
HS127	4	PAA-*g*-$(THG)_2$	1.8	96	170	1.077	0.03	7.0×10^{16}
LE22	5	PAA-*g*-$(THG)_7$	6.5	100	186	1.008	0.04	5.2×10^{16}
LE59	6	PAA-*g*-$(THG)_{15}$	14	45	295	1.016	0.14	6.2×10^{15}
LE58*	7	PAA-*g*-$(THG)_7$	6.5	70	135	1.003	0.08	1.0×10^{17}

[a] Determined gravimetrically; [b] hydrodynamic diameter measured by DLS after dilution by a factor of 100; [c] particle-diameter dispersity calculated from Equation 5; [d] particle-diameter dispersity obtained from DLS; [e] Number of particles calculated from Equation 6. $[AIBN]_0 = 3\times10^{-2}$ moL.$L^{-1}_{styrene}$, 5 wt-% hexadecane vs styrene, 2 wt-% stabilizer vs styrene, 20 wt-% styrene vs total volume, T= 70 °C; * performed without hexadecane.

The final particle diameters of latex stabilized with PAA-*g*-THG are shown in the histogram of Figure 12. All of the latexes stabilized by PAA-*g*-(THG) regardless of the percentage of grafted THG units, showed a single population of particle diameter. This population is within the range of 130-190 nm when the percentage of grafted THG units is below 6.5 % and entered at 300 nm for the highest percentage of grafted terpene units (14 %, see Figure 12). Thus, as number of grafted terpene units increase above 7 % the stabilization efficiency decreases.

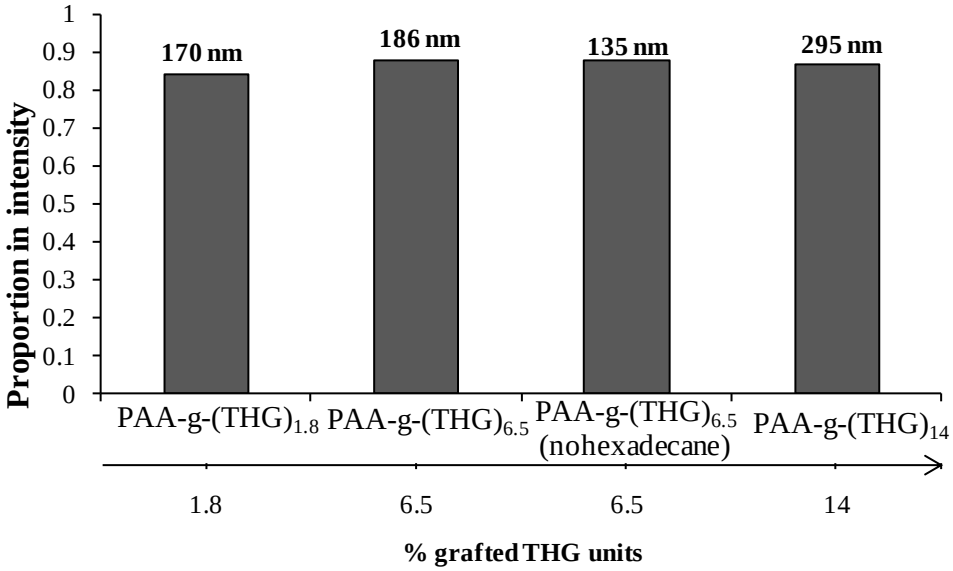

Figure 12. Proportion in intensity and average hydrodynamic diameters of the final polystyrene latex particles stabilized different PAA-*g*-(THG), studied by DLS after dilution by a factor of 100.

One of the miniemulsion polymerization with PAA-*g*-$(THG)_7$ was conducted in the absence of hexadecane to study the ability of the grafted alkyl chains to act as an hydrophobe, i.e. to prevent Ostwald ripening. Indeed, it is reported in the literature [4, 5] that amphiphilic comblike copolymers with dodecyl or hexadecyl alkyl chains demonstrated their ability to act as sole stabilizers in the absence of co-surfactant (*i.e.* hydrophobe). For this reason, we chose PAA-*g*-$(THG)_7$ which achieved a full conversion to try if it can replace hexadecane. A stable latex was indeed recovered with a narrow particle size distribution and average PS particle diameter of 135 nm (see Expt. 7 in Table 6), but we noticed that a lower monomer conversion (70 %) was obtained in the absence of hexadecane in comparison to its analogous with hexadecane (100 %). Upon calculating the number of particles in the absence of hexadecane (Expt. 7 of Table 6) a higher N_p was obtained than in the presence of hexadecane although a lower

polymerization rate was observed for Expt. 7 in comparison to Expt. 5. Such behavior has not been well understood yet.

2.3. Comparison between Dext-g-DHM and PAA-g-THG stabilizers

Miniemulsion polymerization of styrene stabilized with Dext-*g*-DHM and PAA-*g*-THG exhibiting approximately the same percentage of grafted terpene units were chosen for comparison and are shown in Table 7.

Table 7. Miniemulsion polymerization of styrene with 2 wt-% of amphiphilic copolymers vs monomer (T= 70 °C)

Expt	Surfactant	% grafted terpene	Final conversion [a] (%)	Initial D_h [b] (nm) t = 0	k_{app} [d] (s^{-1})	Final Diameter (nm)[b]	N_p [e] (L^{-1}_{latex})
1	Dext-*g*-$(DHM)_{1.4}$	3.4	53	355	3.2×10^{-5}	234/390 (0.51/0.37)[c]	8.6×10^{15}
4	PAA-*g*-$(THG)_2$	1.8	96	155	2.0×10^{-4}	170	7.0×10^{16}
5	PAA-*g*-$(THG)_7$	6.5	100	280	2.0×10^{-4}	186	5.2×10^{16}
2	Dext-*g*-$(DHM)_{5.2}$	12.5	63	155/320 (0.28/0.57) [c]	4.5×10^{-5}	170/390 (0.2/0.55)[c]	8.8×10^{16}
6	PAA-*g*-$(THG)_{15}$	14.0	45	204	2.7×10^{-5}	295	6.2×10^{15}

[a] Determined gravimetrically; [b] measured by DLS after dilution by a factor of 100; [c] proportion in intensity; [d] slope $k_{app} = k_p [P^\bullet]$; [e] Number of particles calculated from Equation 6. $[AIBN]_0 = 3\times10^{-2}$ moL.$L^{-1}_{styrene}$, 5 wt-% hexadecane vs styrene, 2 wt-% surfactant vs styrene, 20 wt-% styrene vs total volume, T= 70 °C at pH~ 9

Taking into consideration the same percentage of grafted terpene units, we can compare between the diameters of liquid miniemulsion stabilized by PAA-*g*-(THG) and Dext-*g*-(DHM). In Table 7, with 2-3 % of grafted terpene units (Expt. 1 and 4), the initial diameter recorded lower value with PAA-*g*-$(THG)_2$ (D_h = 155 nm) in comparison to Dext-*g*-$(DHM)_{1.4}$ (D_h = 355 nm). Also with 13-14 % of grafted terpene units, PAA-*g*-$(THG)_{15}$ produces a monopopulation of droplets (D_h ~ 200 nm), whereas Dext-*g*-$(DHM)_{5.2}$ showed the presence of two populations (D_h = 155 nm and 320 nm) (Expt. 2 and 6 in Table 7). Thus, PAA-*g*-THG copolymer showed a better stabilizing efficiency of the liquid miniemulsion than Dext-*g*-DHM copolymer. This can be explained by the fact that PAA-*g*-$(THG)_n$ shows an electrostatic stabilisation in addition to the steric stabilization due to the carboxylate groups of the polymer chains (pH of reaction = 8 > $pK_{A,\,PAA}$). However, Dext-*g*-(DHM) provides only steric stabilization. In addition to that, the rigid backbone of the dextran and not in PAA, can modify the properties of the interface stabilization, although Durand[12, 34] demonstrated the ability of dextran grafted with alkyl chains to stabilize liquid miniemulsions.

In order to compare the polymerization rates of styrene miniemulsion polymerization stabilized with PAA-*g*-THG and Dext-*g*-DHM with almost similar percentage of grafted terpene units we plotted the logarithmic monomer concentration versus time $Ln\frac{M_0}{M} = k_p[P^{\cdot}]t$. The initial concentration of AIBN initiator was similar for all experiments and set at $[AIBN]_0 = 3.0 \times 10^{-2}$ mol.L^{-1} $_{styrene}$.

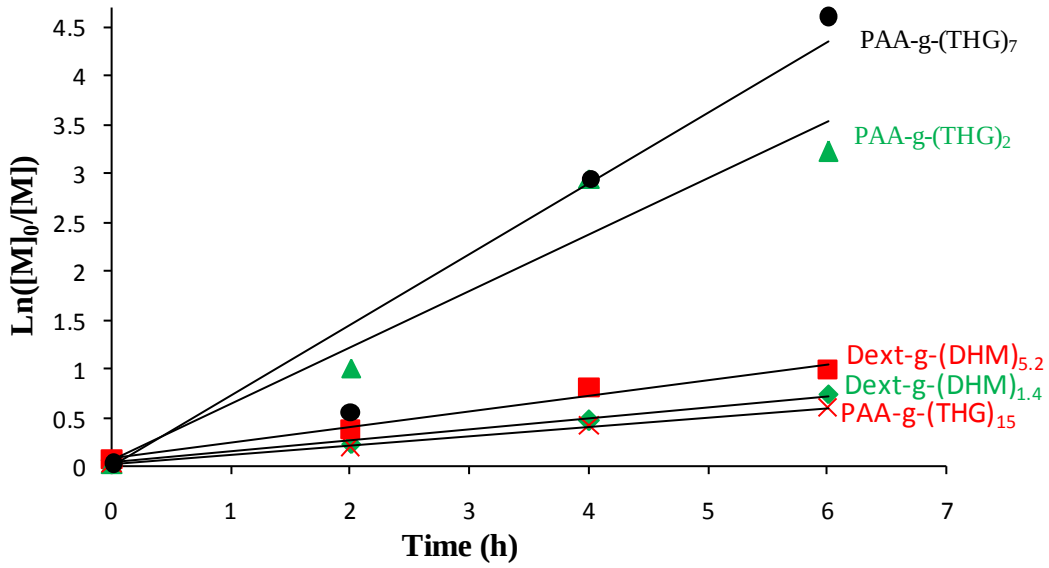

Figure 13. Logarithmic monomer concentration versus time for miniemulsion polymerization of styrene with 2 wt-% of stabilizer vs styrene (♦ Expt. 1; ▲ Expt. 4), (■ Expt. 2; × Expt. 6) and (● Expt. 5)

In Figure 13, we observe for low percentage of grafted terpene units (2-3 %), that PAA-*g*-(THG)$_2$ shows a higher rate of polymerization with a higher slope (Expt. 4, $k_{app} = 2.0 \times 10^{-4}$ s^{-1}) than with Dext-*g*-(DHM)$_{1.4}$ (Expt. 1, $k_{app} = 3.2 \times 10^{-5}$ s^{-1}) (Table 7). On the other hand, with a 13-14 % of grafted terpene units, the apparent rate constant was in a similar range for both PAA-*g*-(THG)$_{15}$ (Expt. 6) and Dext-*g*-(DHM)$_{5.2}$ (Expt. 2) stabilizers. We calculated the N_p, where with 2-3 % of grafted terpene chains we obtained a higher number of particles with PAA-*g*-(THG)$_2$ (7.0×10^{16}.L^{-1}$_{latex}$) versus Dext-*g*-(DHM)$_{1.4}$ (8.6×10^{15}.L^{-1}$_{latex}$). This explains the faster kinetics with PAA-*g*-(THG)$_2$ in comparison to Dext-*g*-(DHM)$_{1.4}$.Whereas with 13-14 % of grafted terpene units, the rate of miniemulsion polymerizations stabilized by either Dext-*g*-(DHM)$_{5.2}$ or PAA-*g*-(THG)$_{15}$ were in the same range (Figure 13). As the final conversion is strongly linked with N_p, hence it is linked to the stabilization efficiency. The highest number of particles ($N_p \sim 8 \times 10^{16}$ and 5.2×10^{16}.L^{-1}$_{latex}$) is obtained for polymerization exhibiting full conversion (Expt. 4 and 5), with the lowest diameter in the range of 170-180 nm. Whereas a final monomer conversion below 70 % at 6 hours, when the N_p is below 8.8 ×

10^{15} L^{-1}_{latex} (Table 7) corresponding to diameters of the final latex diameter ranging between 300-350 nm.

Regardless of the terpene grafting percentage we never obtained a high styrene conversion when using Dext-*g*-DHM as stabilizer. As mentioned before, by varying the amount of the stabilizer, the particle size can be varied over a wide range. Thus, we tried to manipulate the size of the droplet, hence the N_p, by varying the amount of Dext-*g*-DHM in order to increase the final conversion. For this purpose, we chose Dext-*g*-$(DHM)_{5.2}$ which gave the highest conversion among the other Dext-*g*-DHM when using 2 wt-% of this copolymer versus styrene (Figure 9).

Table 8 summarizes the results obtained with polymerization upon changing the amount of polymeric stabilizer.

Table 8. Miniemulsion polymerization of styrene with varying amounts of Dext-*g*-$(DHM)_{5.2}$ stabilizer.

Exp (Expt.)	wt-% [a] Dext-g-$(DHM)_{5.2}$	Final conversion [b] (%)	% coagulum [a]	Initial D_h [c] (nm) t=0	Final D_h [c] (nm)	$\bar{d}_w/\bar{d}_n$ [e]	N_p [f] (L^{-1}_{latex})
HS131 (2)	2	63	0	155/320 (0.28/0.57)[d]	170/390 (0.2/0.55)[d]	1.104	8.8×10^{15}
LE67 (8)	3	73	0	195/355 (0.26/0.61)[d]	260	1.007	1.5×10^{16}
LE62 (9)	4	84	38	185/325 (0.45/0.43)[d]	235	1.020	2.3×10^{16}

[a] wt-% based on monomer; [b] Determined gravimetrically; [c] measured by DLS after dilution by a factor of 100; [d] proportion in intensity; [e] particle-diameter dispersity calculated from Equation 5; [f] Number of particles calculated from Equation 6. $[AIBN]_0 = 3.0 \times 10^{-2}$ $moL.L^{-1}_{styrene}$, 5 wt-% hexadecane vs styrene, 20 wt-% styrene vs total volume, T = 70 °C at pH~9

Regardless of the amount of Dext-*g*-$(DHM)_{5.2}$ copolymer, we notice that the initial diameter of the liquid miniemulsion shows two populations of diameters between 150 and 350 nm (Table 8). Thus, the amount of Dext-*g*-$(DHM)_{5.2}$ has no effect on the stabilization of the initial monomer droplets. Figure 14 shows the conversion of styrene miniemulsion polymerizations stabilized by the different weight fraction of Dext-*g*-$(DHM)_{5.2}$ copolymer. We notice that upon increasing the amount of stabilizer the final conversion slightly increases. However, when increasing the amount of Dext-*g*-$(DHM)_{5.2}$ to 4 wt-% versus styrene a coagulum (38 wt-%) was recovered at the end of the polymerization. The best results were obtained with 3 wt-% of Dext-*g*-$(DHM)_{5.2}$, as 73 % of monomer conversion lead to stable latex free of coagulum

exhibiting monodisperse latex of average hydrodynamic diameter of 260 nm (Expt. 8 in Table 8).

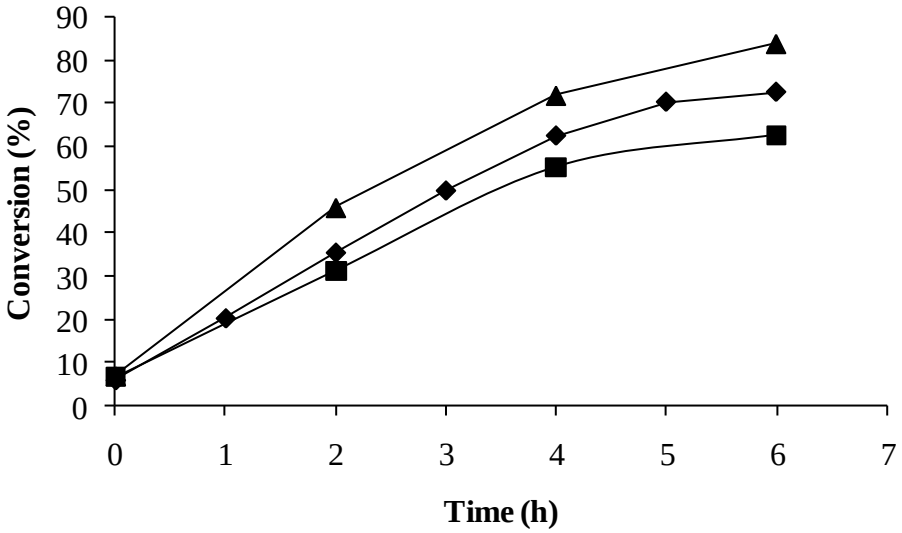

Figure 14. Miniemulsion polymerization of styrene at 70 °C stabilized by varying amounts of Dext-*g*-$(DHM)_{5.2}$: ■ Expt. 2 (2 wt-%), ♦ Expt. 8 (3 wt-%), ▲ Expt. 9 (4 wt-%) (see Table 8)

As expected, the polymerization rate was increased with an increase of the final N_p, which was equal to 8.8×10^{15}, $1.5 \times 10^{16}.L^{-1}_{latex}$ and $2.3 \times 10^{16}.L^{-1}_{latex}$ for miniemulsion polymerizations with 2 wt-%, 3 wt-% and 4 wt-% of Dext-*g*-$(DHM)_{5.2}$ respectively.

After successfully increasing the conversion from 63 % with 2 wt-% of Dext-*g*-$(DHM)_{5.2}$ to 73 % with 3 wt-% free of coagulum, we tried to increase the conversion by manipulating another parameter which might affect the rate of polymerization, that is the initial concentration of the initiator. While maintaining a 3 wt-% of Dext-*g*-$(DHM)_{5.2}$ we increased the initial concentration of the initiator $[AIBN]_0$.

Table 9. Miniemulsion polymerization of styrene stabilized by 3 wt-% of Dext-*g*-$(DHM)_{5.2}$ vs styrene

Exp (Expt.)	$[AIBN]_0$ ($mol.L^{-1}_{styrene}$)	τ coagulum [a]	Final conversion [b] (%)	Initial D_h [c] (nm) t=0	Final D_h [c] (nm)	$\bar{d}_w/\bar{d}_n$ [e]	N_p [f] (L^{-1}_{latex})
LE67 (8)	3.0×10^{-2}	0	73	195/355 (0.26/0.61)[d]	260	1.007	1.5×10^{16}
LE70 (10)	8.0×10^{-2}	24	86	270	260	1.014	1.6×10^{16}

[a] fraction of coagulum based on monomer; [b] Determined gravimetrically; [c] Hydrodynamic diameter measured by DLS after dilution by a factor of 100; [d] proportion in intensity; [e] particle-diameter dispersity calculated from Equation 5; [f] Number of particles calculated from Equation 6. 5 wt-% hexadecane vs styrene, 3 wt-% surfactant vs styrene, 20 wt-% styrene vs total volume, T = 70 °C at pH~ 9

In Table 9 above we observe that conversion was increased up to 86 % when increasing the initial concentration of the inititaor $[AIBN]_0$ by a factor of 2.5, but this increase in conversion was accompanied by a 24 wt-% of coagulum. A similar final particle diameter was obtained for both AIBN concentrations, but the diameter dispersity is clearly lower with lower AIBN concentration. As we compare N_p between Expt. 8 and 10 (Table 9), an increase of AIBN concentration by a factor 2.5 induces only 7 % of increase of N_p showing a limited impact of the concentration of the initiator. It is noteworthy to mention that in the purpose of increasing the conversion with maintaining 2 wt-% of surfactant, a water soluble initiator was also used (2,2'-Azobis(2-methylpropionamidine dihydrochloride) of molecular formula $[=NC(CH_3)_2C(=NH)NH_2]_2.2HCl$, Vazo-56), however a viscous solution was obtained within the first hour of the polymerization, not allowing us to study nor kinetics neither the diameter of the latex.

Apart from the different stabilization efficiency, a suggestion for reason of low conversion observed in the polymerizations stabilized with Dext-*g*-DHM in comparison to polymerizations stabilized with PAA-*g*-THG is as follows. DHM terpene grafted on Dextran exhibits a hydroxyl group whereas this group is not present in the THG terpene grafted on PAA (Scheme 1). If transfer reactions to the OH group occur during the polymerization, the alkoxyl radical $O^{\bullet}$ is not as reactive as the alkyl radicals, thus causing a decrease in the radical concentration and so to a decrease of polymerization rate in the cases of Dext-*g*-DHM in comparison to PAA-*g*-THG. But, a low conversion was also obtained with the case of PAA-*g*-$(THG)_{15}$ leading to a perspective of synthesizing PAA grafted with DHM of a similar grafting density as PAA-*g*-$(THG)_{15}$ in order to distinguish between effect of hydrophobe content and hydroxyl groups on the styrene miniemulsion. For that purpose, thiol-ene addition of 3-mercaptoethanol onto terpene could provide a terpene molecule with primary alcohol for esterfication of PAA.

2.4. Particle morphology

After studying the kinetics of the miniemulsion polymerization and colloidal features of latex stabilized with both PAA-*g*-THG and Dext-*g*-DHM copolymers, we investigated the morphology of the final latex particles.

Images of the final latex of the miniemulsion polymerizations of styrene stabilized with Dex-*g*-$(DHM)_n$ and PAA-*g*-$(THG)_n$ were obtained by Scanning electron microscopy (SEM) and

Atomic force microscopy (AFM). The height channel displays topographical images of the samples and the peak force below the baseline shows an adhesion map of sample.

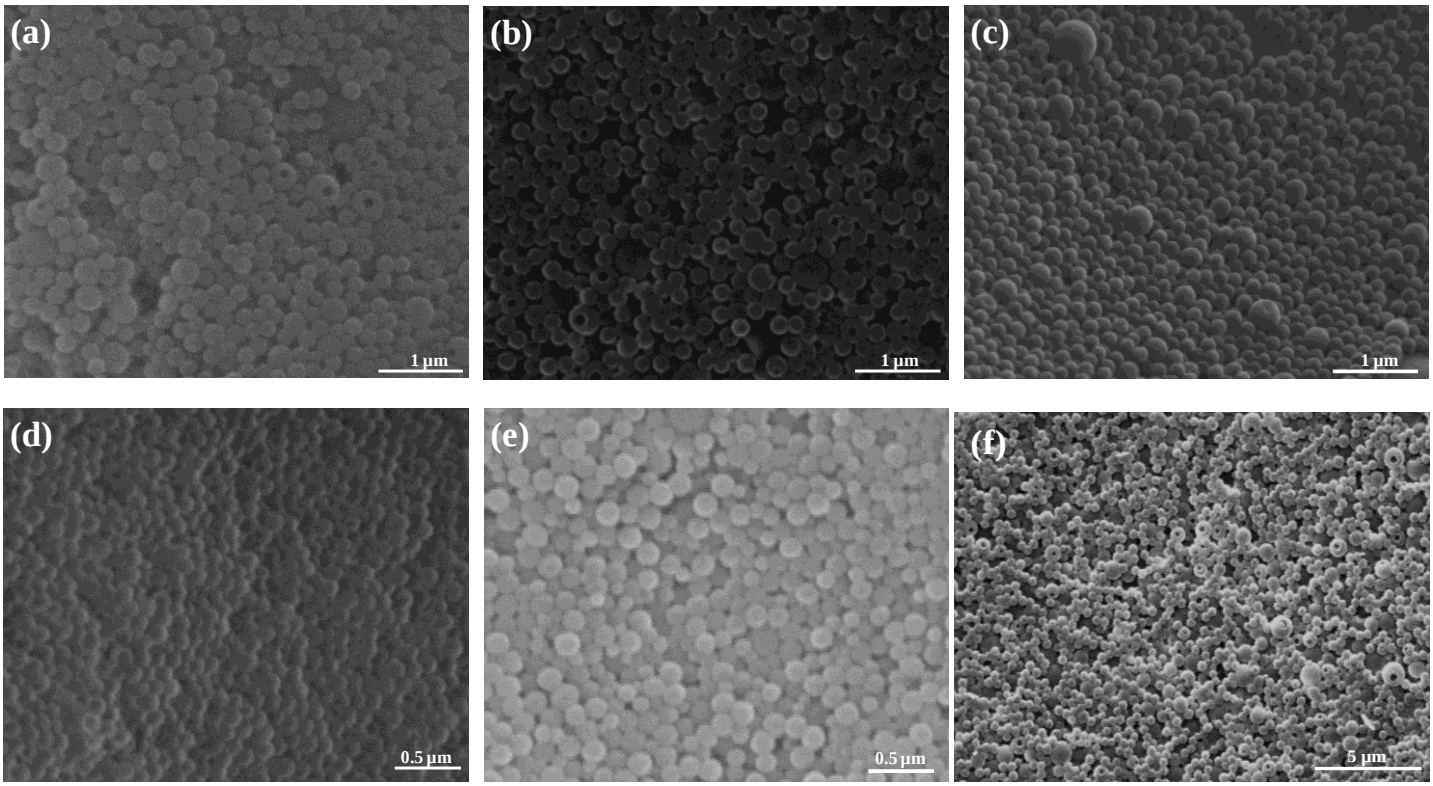

Figure 15. SEM images of the latex of miniemulsions with (a) Dext-*g*-$(DHM)_1$, (b) Dext-*g*-$(DHM)_{5.2}$, Dext-*g*-$(DHM)_{10.4}$, (d) PAA-*g*-$(THG)_{2.4}$, (e) PAA-*g*-$(THG)_7$ and (f) PAA-*g*-$(THG)_{15}$.

Upon analyzing images (a), (b) and (c) in Figure 15 which correspond to latex synthesized by polymerization stabilized respectively by Dext-*g*-$(DHM)_{1.4}$, Dext-*g*-$(DHM)_{5.2}$ and Dext-*g*-$(DHM)_{10.4}$, it is obvious that the synthesized particles are spherical. For the two miniemulsion polymerization carried out with Dext-*g*-$(DHM)_{1.4}$ and Dext-*g*-$(DHM)_{5.2}$ more than one population of particles appears comprised between 200 and 400 nm. These results are consistent with the results given by the DLS (Table 5). However, upon using Dext-*g*-$(DHM)_{10.4}$, SEM showed the presence of few large particles not observed by DLS which fitted only one population of D_h ~ 245 nm with a diameter dispersity of 1.007.

For the PAA-*g*-(THG), images (d), (e) and (f) in Figure 15 represent the latex morphology for the miniemulsion polymerizations stabilized respectively by PAA-*g*-$(THG)_2$, (PAA-*g*-$(THG)_7$ and PAA-*g*-$(THG)_{15}$. Images (d), (e) and (f) also show spherical particles, that can be considered monodispersed with diameters less than 250 nm and in well accordance with the diameter and the D_w/D_n obtained from the DLS (Table 6). Some hollow particles are observed

in Fig (a), (b), (c) and (f) of Figure 15 corresponding to experiments showing incomplete monomer conversion. This is probably due to monomer removal during drying process for conversion study.

Further analysis of latex particles were performed by atomic force microscopy (AFM). The images of particles stabilized by PAA-*g*-$(THG)_2$ and Dext-*g*-$(DHM)_{1.4}$, two copolymers grafted by 2-3 % of terpene molecules versus the degree of polymerization, are displayed in Figure 16 and Figure 17.

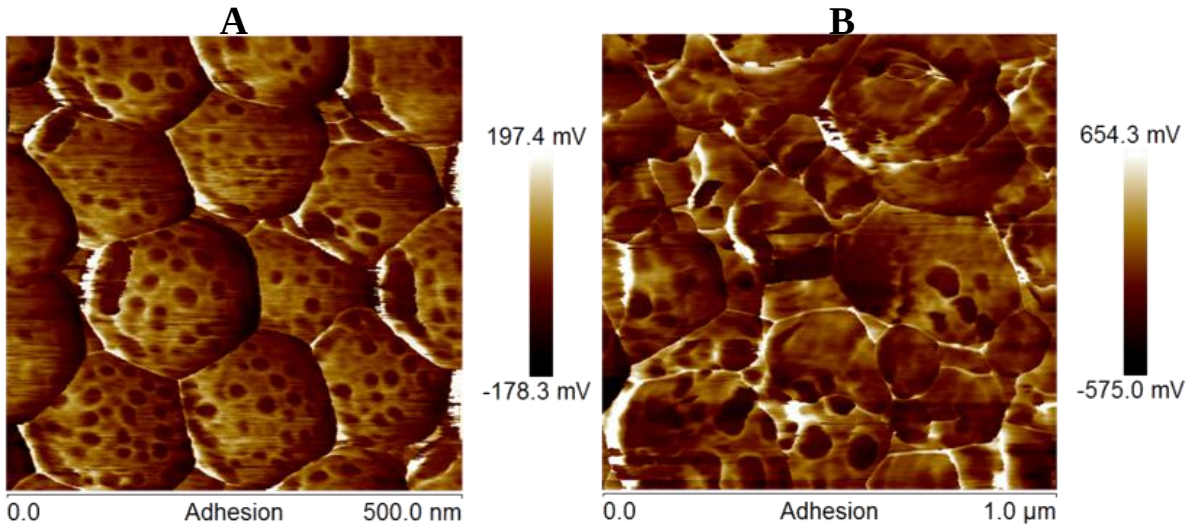

Figure 16. AFM images in adhesion mode of the latex stabilized with (A) PAA-*g*-$(THG)_2$, (B) Dext-*g*-$(DHM)_{1.4}$

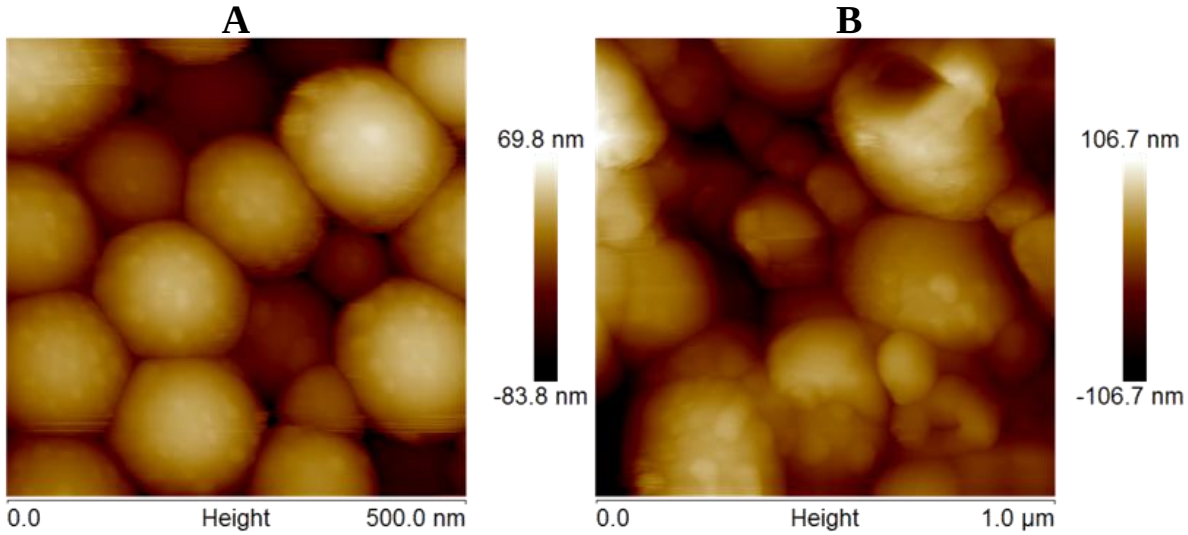

Figure 17. AFM images in topography mode of the latex stabilized with (A) PAA-*g*-$(THG)_2$, (B) Dext-*g*-$(DHM)_{1.4}$

The AFM images reveal that small nodules of about 20 nm diameter are systematically observed on the surface of the synthesized particles. The adhesion of the nodules is lower than

the latex particles surface but in the nanometer scale (probe scale), we had observed an artifact of AFM recording systematically a lower apparent adhesion for nano-pillar and higher apparent adhesion for nano-holes. The amphiphilic copolymer was used at 2 wt-% based on monomer, corresponding to a weight concentration of copolymer regarding to water phase of 4 $g.L^{-1}_{latex}$. The small nodules of 20 nm diameter can be rendered to intramolecular interactions between terpene molecules of a grafted copolymer, intrachain self-assembly at the surface of PS particles. A study of Hao et al. [35] showed the occurrence of intrachain association in unimer micelles of about 10-20 nm for dodecyl molecules grafted onto PAA above 40 %. Although we did not show all the AFM images for all the latexes by the different terpene grafted copolymers, the nodules existed in each case.

Conclusion

As a conclusion, amphiphilic copolymers synthesized from renewable resources were studied as stabilizers for styrene miniemulsion polymerization. This study included two types of the macromolecular stabilizers: one based on dextran and one on PAA backbone, both modified by terpene units. Dextran and PAA were modified by different amounts of hydrophobic terpene. In the case of Dext-*g*-(DHM), while maintaing a 2 wt % of stabilizer vs monomer, regardless of the percentage of grafted terpene units the conversion was below 70 % and polydisperse latex was obtained except with Dext-*g*-$(DHM)_{10.4}$ We investigated the impact of increasing weight fraction of stabilizer on kinetics and colloidal features. The best result was observed for 3 wt-% of Dext-*g*-$(DHM)_{5.2}$ versus monomer with AIBN concentration of 3.0×10^{-2} M. Under such conditions, a final conversion of 73 % was attained producing monodisperse latex of average hydrodynamic diameter of 260 nm.

In the case of PAA-*g*-(THG), we obtained a full monomer conversion when the percentage of grafted terpene units was below 6.5. Concerning colloidal stability, we noticed that all of the latexes stabilized by PAA-*g*-THG copolymer exhibited one population of particles with average hydrodynamic diameter ranging between 170 and 300 nm. We also investigated the ability of PAA-*g*-$(THG)_7$ to act as a hydrophobe instead of hexadecane. Despite lower conversion in the absence of hexadecane, both polymerization stabilized by PAA-*g*-$(THG)_7$ with C10 alkyl side chains is able to act as both hydrophobe and stabilizer of colloidal particles against Ostwald ripening.

We discussed the comparison of stabilization efficiency between PAA-*g*-THG and Dext-*g*-DHM for similar percentage of grafted terpene units. We found that regardless of the percentage of grafted terpene units, PAA-*g*-THG copolymers show better stabilizing properties than Dext-*g*-DHM copolymers.

Finally no matter of the type or percentage of grafted terpene units, particles exhibit spherical shape accompanied with the presence of small nodules of 20 nm in diameter on the surface of the particles which might be due to intramolecular interactions occurred within the grafted terpene copolymers.

References

1. Landfester, K., Polyreactions in miniemulsions. *Macromolecular Rapid Communications* **2001,** 22, (12), 896-936.
2. Lazaridis, N.; Alexopoulos, A. H.; Chatzi, E. G.; Kiparissides, C., Steric stabilization in emulsion polymerization using oligomeric nonionic surfactants. *Chemical Engineering Science* **1999,** 54, (15-16), 3251-3261.
3. Riess, G.; Labbe, C., Block copolymers in emulsion and dispersion polymerization. *Macromolecular Rapid Communications* **2004,** 25, (2), 401-435.
4. Manguian, M.; Save, M.; Chassenieux, C.; Charleux, B., Miniemulsion polymerization of styrene using well-defined cationic amphiphilic comblike copolymers as the sole stabilizer. *Colloid and Polymer Science* **2005,** 284, (2), 142-150.
5. Baskar, G.; Landfester, K.; Antonietti, M., Comblike polymers with octadecyl side chain and carboxyl functional sites: Scope for efficient use in miniemulsion polymerization. *Macromolecules* **2000,** 33, (25), 9228-9232.
6. Durand, A.; Marie, E., Macromolecular surfactants for miniemulsion polymerization. *Advances in Colloid and Interface Science* **2009,** 150, (2), 90-105.
7. Landoll, L. M., Non ionic polymer surfactants. *Journal of Polymer Science Part a-Polymer Chemistry* **1982,** 20, (2), 443-455.
8. Durand, A.; Marie, E.; Rotureau, E.; Leonard, M.; Dellacherie, E., Amphiphilic polysaccharides: Useful tools for the preparation of nanoparticles with controlled surface characteristics. *Langmuir* **2004,** 20, (16), 6956-6963.
9. Marie, E.; Landfester, K.; Antonietti, M., Synthesis of chitosan-stabilized polymer dispersions, capsules, and chitosan grafting products via miniemulsion. *Biomacromolecules* **2002,** 3, (3), 475-481.
10. Rouzes, C.; Leonard, M.; Durand, A.; Dellacherie, E., Influence of polymeric surfactants on the properties of drug-loaded PLA nanospheres. *Colloids and Surfaces B-Biointerfaces* **2003,** 32, (2), 125-135.
11. Raynaud, J.; Choquenet, B.; Marie, E.; Dellacherie, E.; Nouvel, C.; Six, J. L.; Durand, A., Emulsifying properties of biodegradable polylactide-grafted dextran copolymers. *Biomacromolecules* **2008,** 9, (3), 1014-1021.
12. Durand, A.; Dellacherie, E., Neutral amphiphilic polysaccharides: chemical structure and emulsifying properties. *Colloid and Polymer Science* **2006,** 284, (5), 536-545.
13. Wu, M.; Dellacherie, E.; Durand, A.; Marie, E., Poly(n-butyl cyanoacrylate) nanoparticles via miniemulsion polymerization (1): Dextran-based surfactants. *Colloids and Surfaces B-Biointerfaces* **2009,** 69, (1), 141-146.
14. Lefay, C.; Save, M.; Charleux, B.; Magnet, S., Miniemulsion polymerization stabilized by a well-defined, amphiphilic gradient poly(styrene-co-acrylic acid) copolymer. *Australian Journal of Chemistry* **2006,** 59, (8), 544-548.
15. Burguiere, C.; Pascual, S.; Bui, C.; Vairon, J. P.; Charleux, B.; Davis, K. A.; Matyjaszewski, K.; Betremieux, I., Block copolymers of poly(styrene) and poly(acrylic acid) of various molar masses, topologies, and compositions prepared via controlled/living radical polymerization. Application as stabilizers in emulsion polymerization. *Macromolecules* **2001,** 34, (13), 4439-4450.
16. Thickett, S. C.; Gilbert, R. G., Rate-controlling events for radical exit in electrosterically stabilized emulsion polymerization systems. *Macromolecules* **2006,** 39, (6), 2081-2091.
17. Yao, K. J.; Tang, C. B., Controlled Polymerization of Next-Generation Renewable Monomers and Beyond. *Macromolecules* **2013,** 46, (5), 1689-1712.

18. Wilbon, P. A.; Chu, F. X.; Tang, C. B., Progress in Renewable Polymers from Natural Terpenes, Terpenoids, and Rosin. *Macromol. Rapid Commun.* **2013,** 34, (1), 8-37.
19. Zhao, J. P.; Schlaad, H., Synthesis of Terpene-Based Polymers. In *Bio-Synthetic Polymer Conjugates*, Schlaad, H., Ed. Springer-Verlag Berlin: Berlin, 2013; Vol. 253, pp 151-190.
20. Sharma, S.; Srivastava, A. K., Alternating copolymers of limonene with methyl methacrylate: Kinetics and mechanism. *Journal of Macromolecular Science-Pure and Applied Chemistry* **2003,** A40, (6), 593-603.
21. Sharma, S.; Srivastava, A. K., Radical copolymerization of limonene with acrylonitrile: Kinetics and mechanism. *Polymer-Plastics Technology and Engineering* **2003,** 42, (3), 485-502.
22. Sharma, S.; Srivastava, A. K., Synthesis and characterization of copolymers of limonene with styrene initiated by azobisisobutyronitrile. *European Polymer Journal* **2004,** 40, (9), 2235-2240.
23. Sharma, S.; Srivastava, A. K., Synthesis and characterization of a terpolymer of limonene, styrene, and methyl methacrylate via a free-radical route. *Journal of Applied Polymer Science* **2004,** 91, (4), 2343-2347.
24. Firdaus, M.; de Espinosa, L. M.; Meier, M. A. R., Terpene-Based Renewable Monomers and Polymers via Thiol-Ene Additions. *Macromolecules* **2011,** 44, (18), 7253-7262.
25. Zhao, J. P.; Jeromenok, J.; Weber, J.; Schlaad, H., Thermoresponsive Aggregation Behavior of Triterpene-Poly(ethylene oxide) Conjugates in Water. *Macromolecular Bioscience* **2012,** 12, (9), 1272-1278.
26. Zhao, J. P.; Schlaad, H.; Weidner, S.; Antonietti, M., Synthesis of terpene-poly(ethylene oxide)s by t-BuP4-promoted anionic ring-opening polymerization. *Polymer Chemistry* **2012,** 3, (7), 1763-1768.
27. Loiseau, J.; Doerr, N.; Suau, J. M.; Egraz, J. B.; Llauro, M. F.; Ladaviere, C., Synthesis and characterization of poly(acrylic acid) produced by RAFT polymerization. Application as a very efficient dispersant of CaCO3, kaolin, and TiO2. *Macromolecules* **2003,** 36, (9), 3066-3077.
28. Hoyle, C. E.; Bowman, C. N., Thiol-Ene Click Chemistry. *Angewandte Chemie-International Edition* **2010,** 49, (9), 1540-1573.
29. Hoyle, C. E.; Lee, T. Y.; Roper, T., Thiol-enes: Chemistry of the past with promise for the future. *Journal of Polymer Science Part a-Polymer Chemistry* **2004,** 42, (21), 5301-5338.
30. Cramer, N. B.; Reddy, S. K.; O'Brien, A. K.; Bowman, C. N., Thiol-ene photopolymerization mechanism and rate limiting step changes for various vinyl functional group chemistries. *Macromolecules* **2003,** 36, (21), 7964-7969.
31. Posner, T., Information on unsaturated compounds II The addition of mercaptan to unsaturated hydrocarbon. *Berichte Der Deutschen Chemischen Gesellschaft* **1905,** 38, 646-657.
32. Jaillet, F.; Desroches, M.; Auvergne, R.; Boutevin, B.; Caillol, S., New biobased carboxylic acid hardeners for epoxy resins. *Eur. J. Lipid Sci. Technol.* **2013,** 115, (6), 698-708.
33. Griffin, W. C., Classification of surface-active agents by HLB. *Cosmet. Chem. J. Soc.* **1949,** 1, 311–326.
34. Durand, A., Viscosity of dilute colloidal dispersions involving polysaccharide-based stabilizers. *Colloid and Polymer Science* **2008,** 286, (13), 1505-1510.
35. Hao, J.; Li, Z.; Cheng, H.; Wu, C.; Han, C. C., Kinetically Driven Intra- and Interchain Association of Hydrophobically and Hydrophilically Modified Poly(acrylic acid) in Dilute Aqueous Solutions. *Macromolecules* **2010,** 43, (22), 9534-9540.

General Conclusion

The first challenge of the present work was to transpose the synthesis of hybrid core@shell nanoparticles by surface-initiated nitroxide mediated polymerization (SI-NMP) from bulk to an aqueous dispersed medium via the miniemulsion process. For that purpose, alkoxyamine grafted silica particles should be designed to initiate and control the growth of polymer chains from the surface of the particles dispersed in monomer droplets. Before to develop such syntheses, a preliminary study developed in chapter 2 was dedicated to the investigation of NMP of styrene in miniemulsion initiated from an alkoxyamine that mimics the chemical structure of the grafted alkoxyamine. While targeting high degree of polymerization using the BB-BA alkoxyamine based on 1,2 addition of Blocbuilder® onto n-butyl acrylate, NMP miniemulsion of styrene was controlled. Despite the features of a controlled polymerization, the degree of dead polymer chains produced by the persistent radical effect was higher in miniemulsion than in bulk. This suggested an exit of the carboxylate-based initiating fragment due to the ability of the BB-BA alkoxyamine to be located at the styrene/water interface. Indeed, in the absence of surfactant we showed the ability of BB-BA alkoxyamine to stabilize liquid miniemulsion, and its ability to control polymerization of styrene in miniemulsion. However, in the absence of surfactant a lower efficiency of the BB-BA alkoxyamine was noticed as higher experimental molar masses were obtained compared to the theoretical ones. Moreover, the higher fraction of dead polymer chains observed for NMP miniemulsion polymerization of styrene in the absence of surfactant in comparison to the presence of surfactant confirmed that the specific localization of this alkoxyamine at the interface impacted the control of polymerization. The final part of this chapter 2 showed that percentage of dead polymer chains which was obtained in the NMP miniemulsion of styrene even in the presence of surfactant was decreased moving to microemulsion conditions to implement NMP of styrene through an organosoluble alkoxyamine and offered the possibility to decrease the fraction of dead polymer chains while maintaining a high polymerization rate.

Chapter 3 described the synthesis of silica@polymer nanocomposite particles via SI-NMP in miniemulsion. For that purpose, we first synthesized well dispersed spherical silica particles with two diameters of 25 and 80 nm, modified with the TMSPA-BB alkoxyamine synthesized by 1,2 addition of Blocbuilder® onto trimethylsilylpropylacrylate (TMSPA). We developed two strategies to implement the polymerization step by SI-NMP in miniemulsion. The first

strategy consisted of the direct dispersion of the alkoxyamine grafted silica particles into the monomer droplets prior to start miniemulsion polymerization in the absence or in the presence of free initiator ("one step" method). The second strategy required two steps and was named "two step" miniemulsion. A first step of SI-NMP carried out in bulk up to low conversion of styrene (< 10 %) was performed prior adding water and surfactant to create the initial state of liquid miniemulsion followed by miniemulsion polymerization. The results of the first strategy revealed very low polymerization rate in the absence of free alkoxyamine whereas an increasing molar fraction of free BB-BA alkoxyamine in the medium insured the increase of monomer conversion. This result suggested a low efficiency of the grafted alkoxyamine which was confirmed by the high molar mass of the grafted chains. Such low efficiency was ascribed to the diffusion of the silica particles to the water phase, thus inhibiting the polymerization. Thus, it was crucial to hydrophobize the alkoxyamine grafted silica particles to keep them in the monomer phase to initiate more efficiently SI-NMP miniemulsio. In order to address this issue, the second "two steps" miniemulsion procedure described above was investigated. Such method was interesting as it allowed the increase of monomer conversion for NMP initiated from the sole TMSPA-BB grafted alkoxyamine in the absence of free alkoxyamine. It is noteworthy that for the "one step" miniemulsion procedure carried out in the presence of free alkoxyamine, it was possible to control the features of the grafted chains with experimental molar masses close to theoretical ones. Nevertheless, throughout the several SI-NMP of styrene and BA performed in "two steps" miniemulsion in the absence of free initiator, the cleaved polymer chains systematically exhibited bi- or multi-modal SEC chromatograms showing a loss of control.

The work of Chapter 4 was focused on the synthesis of amphiphilic macromolecular stabilizers based on reneawable resources to investigate their ability to stabilize styrene miniemulsion polymerization. This study included two types of the macromolecular stabilizers, one based on dextran as natural polysacharide and the other one on the synthetic poly(acrylic acid) (PAA). Both hydrophilic backbones were modified by hydrophobic functional terpene molecules. Such functional terpenes were supplied by an industrial partner and synthesized from basic terpenes issued from wood feedstock (paper oil). We synthesized different hydrophobically modified dextrans or poly(acrylic acid) copolymers by varying the percentage of grafted terpene units. It was shown that regardless of the percentage of grafted terpene units, stable lattices were synthesized but PAA-g-THG copolymers showed better stabilizing properties than Dext-g-DHM copolymers. Also, no matter of the type or

percentage of grafted terpene units, we obtained spherical particles accompanied with the presence of small nodules of 20 nm in diameter on the surface of the particles which might be due to intramolecular interactions occurred within the grafted terpene copolymers.

In conclusion, this PhD work was focused on the design of latex particles by miniemulsion polymerization. Macromolecular engineering enabled us to investigate two different aspects: the design of nanocomposite latex containing hybrid core-shell nanoparticles and the synthesis of new renewable amphiphilic copolymers as efficient polymeric stabilizer for producing colloidal particles by miniemulsion polymerization.

Analytical techniques:

Thermal gravimetric analysis (TGA) was used to determine the density of initiator grafted onto silica particles. It is a simple analytical technique that measures the weight loss of a material as a function of temperature. As materials are heated, they can lose weight from a simple process such as drying, or from chemical reactions that liberate gasses. Some materials can gain weight by reacting with the atmosphere in the testing environment. Since weight loss and gain are disruptive processes to the sample material or batch, knowledge of the magnitude and temperature range of those reactions are necessary in order to design adequate thermal ramps and holds during those critical reaction periods. The test results are a graph of the TGA signal (actual weight loss or gain converted to percent weight loss) on the Y-axis plotted versus the sample temperature in °C on the X-axis. Samples were analyzed using TGA Q50 (TA Instruments) at a scan rate of 10 °C.min^{-1} under air.

Dynamic light scattering (DLS) was used to determine the size of the silica particles or the size of the droplets and particles. It is a technique in physics, which can be used to determine the size distribution profile of small particles in suspension (chemistry) or polymers in solution. It can also be used to probe the behavior of complex fluids such as concentrated polymer solutions. When light hits small particles the light scatters in all directions (Rayleigh scattering) so long as the particles are small compared to the wavelength (below 250 nm). If the light source is a laser, and thus is monochromatic and coherent, then one observes a time-dependent fluctuation in the scattering intensity. The machine used is Vasco DL135.

Nuclear magnetic resonance (NMR). NMR spectroscopy is one of the principal techniques used to obtain physical, chemical, electronic and structural information about molecules due to either the chemical shift, Zeeman effect, or the Knight shift effect, or a combination of both, on the resonant frequencies of the nuclei present in the sample. Samples were analyzed by Bruker 400 MHz at 25 °C in $CDCl_3$, DMSO…

Size exclusion chromatography (SEC). It is a chromatographic method in which molecules in solution are separated based on their size (more correctly, their hydrodynamic volume). It is usually applied to large molecules or macromolecular complexes such as proteins and industrial polymers. Typically, when an aqueous solution is used to transport the sample through the column, the technique is known as gel filtration chromatography, versus the name gel permeation chromatography which is used when an organic solvent is used as a mobile phase. SEC is a widely used polymer characterization method because of its ability to provide

good M_w results for polymers. Characterizations of the polymers were performed at 30 °C with THF as eluent at a flow rate of 1 $mL.min^{-1}$. The SEC system was equipped with three Waters Styragel columns HR 0.5, 2, 4 working in series (separation range 1×10^2 to 3×10^6 g mol^{-1}) and a refractive index detector ERC 7515-A. Number-average molar mass (M_n) and the dispersity ($D = M_w/M_n$) were derived against a calibration derived from PS standards. All polymers samples were prepared at 1 to 5 $g.L^{-1}$ concentrations and filtered through PVDF 0.45 mm filters.

Transmission electron microscopy (TEM). It is a microscopy technique in which a beam of electrons is transmitted through an ultra-thin specimen, interacting with the specimen as it passes through. An image is formed from the interaction of the electrons transmitted through the specimen; the image is magnified and focused onto an imaging device, such as a fluorescent screen, on a layer of photographic film, or to be detected by a sensor such as a CCD camera. Images were taken with a JEOL JEM 100CXII (100 kV) instrument. The samples dispersed in ethanol were dropped onto a carbon-coated copper grid and dried before TEM analysis. TEM analysis were performed by Patricia Beaunier at UPMC, Paris 6.

Atomic Force Microscopy (AFM). Measurements were performed with an Innova AFM (Veeco Instrument Inc.). The images were scanned in tapping mode under ambient conditions and recorded either as phase images or in topography. Rectangular silicon cantilevers from Veeco-probes (MMP-12100-10) with a resonance frequency of about 150 kHz were used.

Scanning electron microscope (SEM). The surface morphology of the latex samples is observed, without metallization by scanning electron microscope Electroscan E3, for an acceleration voltage of 25 keV. Electron micrographs were recorded at different magnifications ranging from 500-3000.

Fourier-transform infrared (FT-IR). IR spectra were recorded in transmission, from KBr pellets at room temperature using a an Alpha-T FT-IR from bruker.